

**CRANIOFACIAL INTEGRATION, PLASTICITY AND
BIOMECHANICS IN THE MOUSE MASTICATORY SYSTEM**

HESTER BAVERSTOCK

PhD

University of Hull

Hull York Medical School

February 2014

ABSTRACT

The craniomandibular skeleton is a complex, dynamic structure, housing many vital tissues and required to perform critical functions. This region is however subject to substantial morphological change during development, and required to adapt to its environment and individual variance. The capacity of this region to maintain correlated form and appropriate functional performance despite these challenges is not fully understood. The sample consists of three strains of mice; a wild-type strain and two mutant strains from the same genetic background strain. Both mutations selectively affect chondrocranial growth, and thus influence of both are limited to the crania. The brachymorph mutant phenotype is characterised by a shortened cranium, while the pten is elongated. This sample therefore allows exploration of a potential plastic response in terms of the mandible, the masticatory lever system, and in turn mechanical advantage, when cranial length and the out-lever are varied. Three dimensional landmarks were applied to micro-CT scans and partial-least-squares analysis carried out to determine covariance between crania and mandibles. Mechanical advantage was calculated as a ratio of muscle in-lever and jaw out-lever for three key masticatory muscles. A common pattern of both variance and covariance was found among all three strains, with mandibular morphology in each strain covarying with cranial phenotypes. Jaw out-lever lengths were found to be significantly different in all three strains, and yet little significant difference between strains was found in mechanical advantage for any muscles. This maintenance of mechanical advantage is attributed to plastic adaptation in regions influencing muscle in-lever length, the latter which were found to be significantly different in the three strains. These results show the potential of the craniomandibular complex to plastically adapt to maintain both correlated form and functionality when variation occurs in one region, and thus these results have significant implications for the evolvability of the complex.

LIST OF CONTENTS

ABSTRACT.....	2
LIST OF CONTENTS	3
CHAPTER 1 INTRODUCTION AND LITERATURE REVIEW	16
1.1 INTRODUCTION.....	16
1.2 MAMMALIAN AND RODENT CRANIOFACIAL MORPHOLOGY	23
1.3 EVOLUTION OF COMPLEX MORPHOLOGIES, TRAITS AND SYSTEMS	31
1.3.1 Modularity.....	31
1.3.2 Integration	36
1.3.3 Plasticity.....	37
1.3.4 Modularity as plasticity.....	38
1.3.5 Hierarchical organisation	38
1.3.6 Evolvability.....	39
1.4 BONE BIOLOGY	41
1.4.1 Bone Architecture	41
1.4.2 Bone Modelling and Remodelling	43
1.4.3 Formation of the Bones of the Cranium and Mandible.....	45
1.4.4 Mechanical Stimuli and Bone Plasticity	50
1.5 MUSCLE BIOLOGY	54
1.5.1 Fibre Architecture	54
1.5.2 Length Tension Relationships.....	56
1.5.3 Cross Sectional Area.....	61
1.5.4 Fibre Orientation	63
1.5.5 Myofibril Composition	65
1.5.6 Trade-off Between Gape and Muscle Force Capacity	66
1.5.7 Muscle Plasticity	70
1.6 MASTICATORY BIOMECHANICS.....	71
1.7 CONCLUSION TO INTRODUCTION.....	82
CHAPTER 2 MATERIALS AND METHODS.....	85
2.1 MATERIALS	85

2.1.1	Sample details	85
2.1.2	Sample exploration.....	90
2.2	METHODS.....	116
2.2.1	Geometric Morphometric and Statistical Methods	117
2.2.2	Pre-processing for Geometric Morphometric Methods	122
2.2.3	Biomechanical Methods.....	130
2.2.4	Comparison with other Biomechanical Methods.....	145
2.2.5	Visualisations	153
2.3	CONCLUSIOION TO MATERIALS AND METHODS.....	153
CHAPTER 3 THE MORPHOLOGY OF THE MOUSE MASTICATORY		
MUSCULATURE.....		
		156
3.1	INTRODUCTION	156
3.2	MATERIALS AND METHODS	160
3.2.1	Dissection.....	160
3.2.2	3D Skull and Muscle Reconstruction.....	160
3.2.3	Nomenclature	163
3.3	RESULTS.....	165
3.3.1	Superficial masseter	167
3.3.2	Deep Masseter.....	171
3.3.3	Zygomaticomandibularis.....	173
3.3.4	Temporalis.....	179
3.3.5	Pterygoids.....	181
3.4	DISCUSSION	183
CHAPTER 4 CRANIOMANDIBULAR INTEGRATION AND ADAPTIVE		
PLASTICITY IN THE MURINE SKULL		
		188
4.1	INTRODUCTION	188
4.2	MATERIALS AND METHODS	195
4.2.1	Sample.....	195
4.2.2	Data Acquisition.....	197
4.2.3	Geometric Morphometric Methods.....	203
4.2.4	Principal Component Analysis.....	204
4.2.5	Partial least squares analysis	204
4.2.6	Vector direction comparison	205

4.2.7	Calculation of percentage of overall variance.....	206
4.2.8	Visualisation.....	207
4.2.9	Analyses addressing whether patterns of mandibular morphology in the three mouse strains correspond to patterns of observed variance in their respective crania.	207
4.2.10	Analyses addressing whether shared common patterns of covariance between crania and mandibles exist between the three strains.....	207
4.3	RESULTS.....	209
4.3.1	Do patterns of mandibular morphology in the three mouse strains correspond to patterns of observed variance in their respective crania?	212
4.3.2	Do shared common patterns of covariance between crania and mandibles exist between the three strains?	217
4.4	DISCUSSION	224
CHAPTER 4 SUPPLEMENTARY MATERIAL.....		233
CHAPTER 5 FUNCTIONAL MAINTENANCE AND VARIATION IN CRANIAL LENGTH OF THE MOUSE MASTICATORY SYSTEM		256
5.1	INTRODUCTION.....	256
5.2	MATERIALS AND METHODS	262
5.2.1	Sample.....	262
5.2.2	Data Acquisition	263
5.2.3	Statistical analyses	270
5.2.4	Shape analysis	270
5.3	RESULTS.....	277
5.3.1	Jaw Out Lever Lengths	277
5.3.2	Muscle In Lever Lengths	279
5.3.3	Mechanical Advantage.....	284
5.3.4	Assessing the Mechanism of Maintenance of Mechanical Advantage	284
5.3.5	Scaling of Lever-Arm System with Centroid Size.....	285
5.4	DISCUSSION	293
CHAPTER 6 DISCUSSION		304
6.1	DISCUSSION	304
6.2	LIMITATIONS AND NEED FOR FUTHER INVESTIGATION.....	312
REFERENCES.....		315

LIST OF FIGURES

CHAPTER 1: INTRODUCTION

Figure 1.2.1: Rodent Anatomy

Figure 1.2.2: Rodent Conditions.

Figure 1.2.3: Rodent Phylogeny

Figure 1.3.1: Types Of Modularity And Integration

Figure 1.4.1: Bone Remodelling

Figure 1.4.2: Development Of The Craniofacial Skeleton

Figure 1.4.3: Development Of The Craniofacial Skeleton In Context Of Mutant Strains

Figure 1.4.4: Influence Of Exogenous Forces On Macroscopic Bone Morphology

Figure 1.5.1: Organisation Of Skeletal Muscle

Figure 1.5.2 Relaxed And Contracted State Of A Myofibril

Figure 1.5.3: Relationship Of Muscle Length To Tension

Figure 1.5.4: Muscle Force Is Proportional To Cross-Sectional Area

Figure 1.5.5: Parallel And Pinnate Muscles

Figure 1.5.6: Trade-Off Between Gape And Muscle Force Capacity

Figure 1.6.1: Biomechanical Trade-Offs Between Speed And Force Generation

Figure 1.6.2: Influence Of In- And Out- Lever Lengths On Mechanical Advantage

Figure 1.6.3: Different Jaw Shapes With Equivalent Functional Consequences

Figure 1.6.4: Effect Of Gape And Muscle Stretch On Force Production

CHAPTER 2: MATERIALS AND METHODS

Figure 2.1.1: Sample: Crania And Mandibles Of Three Mouse Strains

Figure 2.1.2: Cranial Linear Measurements

Figure 2.1.3: Mandibular Linear Measurements

Figure 2.1.4: Cranial Length Comparison

Figure 2.1.5: Mandibular Length Comparison

Figure 2.1.6: Sample: Linear Measurements Comparison

Figure 2.1.7: Cranial Landmarks

Figure 2.1.8: Mandibular Landmarks

Figure 2.1.9: Inter-Strain Cranium

Figure 2.1.10: Inter-Strain Mandible

Figure 2.1.11: Brachymorph Cranium

Figure 2.1.12: C57 Cranium

Figure 2.1.13: Pten Cranium

Figure 2.1.14: Brachymorph Mandible

Figure 2.1.15: C57 Mandible

Figure 2.1.16: Pten Mandible

Figure 2.2.1: Thresholding Comparison

Figure 2.2.2: PCA Of Cranial Landmarks - Thresholding Comparison

Figure 2.2.3: PCA Of Mandibular Landmarks - Thresholding Comparison

Figure 2.2.4: Jaw Out Lever Calculation

Figure 2.2.5: Depiction Of Landmark Positions For Jaw Out-Lever Calculation

Figure 2.2.6: Attachment Curves Methodology

Figure 2.2.7: Attachment Areas Methodology

Figure 2.2.8: Attachment Muscle Force Vectors

Figure 2.2.9: Method Comparison

Figure 2.2.10: Alternative In- And Out- Lever Measurements

Figure 2.2.11: Comparison With Traditional (Alternative) Methods

CHAPTER 3: MORPHOLOGY OF THE MOUSE MASTICATORY MUSCULATURE

Figure 3.3.1: Key Anatomical Regions On The Cranium And Mandible

Figure 3.3.2: Dissection

Figure 3.3.3: Three Dimensional Reconstruction Of Masticatory Apparatus

Figure 3.3.4: Masticatory Muscle Attachment Areas

Figure 3.3.5: Micro-Ct Slices Highlighting Masticatory Musculature

Figure 3.3.6: Cross-Sections Of Masticatory Musculature

CHAPTER 4: CRANIOMANDIBULAR INTEGRATION AND ADAPTIVE PLASTICITY IN THE MURINE SKULL

Figure 4.2.1: Cranial Landmarks

Figure 4.2.2: Mandibular Landmarks

Figure 4.3.1: Inter-Strain Cranium - Principal Component Analysis

Figure 4.3.2: Inter-Strain Mandible - Principal Component Analysis

Figure 4.3.3: Inter-Strain - Partial Least Squares Analysis

Figure 4.3.4: Inter-Strain - Partial Least Squares Analysis; Pooled By Group

Figure 4.3.5: PLS Analysis - Vector And Warp Comparison

Figure 4.3.6: PLS Analysis - Vector And Warp Comparison

CHAPTER 4: SUPPLEMENTARY MATERIAL

Figure S4.3.1: Inter-Strain Cranium - Principal Component Analysis

Figure S4.3.2: Inter-Strain Mandible - Principal Component Analysis

Figure S4.3.3: Interstrain - Partial Least Squares Analysis

Figure S4.3.4: Interstrain - Partial Least Squares Analysis

Figure S4.3.5: Interstrain - Partial Least Squares Analysis

Figure S4.3.6: Interstrain - Partial Least Squares Analysis; Pooled By Group

Figure S4.3.7: PLS Analysis - Vector And Warp Comparison

Figure S4.3.8: Brachymorph - Partial Least Squares Analysis

Figure S4.3.9: Brachymorph - Partial Least Squares Analysis

Figure S4.3.10: Pten - Partial Least Squares Analysis

Figure S4.3.11: Pten - Partial Least Squares Analysis

Figure S4.3.12: PLS Analysis - Vector And Warp Comparison

Figure S4.3.13: Interstrain - Partial Least Squares Analysis

Figure S4.3.14: Interstrain - Partial Least Squares Analysis

Figure S4.3.15: Brachymorph - Partial Least Squares Analysis

Figure S4.3.16: Brachymorph - Partial Least Squares Analysis

Figure S4.3.17: C57 - Partial Least Squares Analysis

Figure S4.3.18: C57 - Partial Least Squares Analysis

Figure S4.3.19: Pten - Partial Least Squares Analysis

Figure S4.3.20: Pten - Partial Least Squares Analysis

CHAPTER 5: FUNCTIONAL MAINTENANCE AND VARIATION IN CRANIAL LENGTH OF THE MOUSE MASTICATORY SYSTEM

Figure 5.2.1: Attachment Muscle Force Vectors

Figure 5.2.2: Muscle In Lever Calculation

Figure 5.2.3: Jaw Out Lever Calculation

Figure 5.2.4: Depiction Of Landmark Positions

Figure 5.3.1: Comparison Of Jaw Out-Lever In Three Mouse Strains

Figure 5.3.2: Comparison Of Muscle In-Lever Length And Mechanical Advantage In Three Mouse Strains

Figure 5.3.3: Comparison Of Muscle In-Lever Length And Mechanical Advantage In Three Mouse Strains

Figure 5.3.4: Comparison Of Muscle In-Lever Length And Mechanical Advantage In Three Mouse Strains

Figure 5.3.5: Relationship Of Jaw Out-Lever Length To Muscle In-Lever Length

Figure 5.3.6: Relationship Of Jaw Out-Lever Length To Muscle In-Lever Length (Logarithmic Scale)

Figure 5.3.7: PCA Of Lever Arm System Landmarks

Figure 5.3.8: Modularity Hypothesis

LIST OF TABLES

CHAPTER 2: MATERIALS AND METHODS

Table 2.1.1: Definitions Of Lengths Compared Between Strains

Table 2.1.2: Cranial Landmarks Definitions

Table 2.1.3: Mandibular Landmark Definitions

Table 2.2.1: Comparison Of In-Lever Variance Between Methodologies

Table 2.2.2: Comparison Of In-Lever Measurements Between Methodologies

Table 2.2.3: Comparison Of In- And Out-Lever Lengths Determined Via Three Different Methodologies

CHAPTER 3: THE MORPHOLOGY OF THE MOUSE MASTICATORY MUSCULATURE

Table 3.3.1: Volumes, Masses And Percentages Of Masticatory Muscles

CHAPTER 4: CRANIOMANDIBULAR INTEGRATION AND ADAPTIVE PLASTICITY IN THE MURINE SKULL

Table 4.2.1: Cranial Landmark Definitions

Table 4.2.2: Mandibular Landmark Definitions

Table 4.3.1: RV Coefficients, Singular Values And Pairwise Correlations Of PLS Scores Between Cranial And Mandibular Blocks

Table 4.3.2: Vector Comparison Between Individual PLS Scores And Inter-Strain PLS Scores For Cranial Block

Table 4.3.3: Vector Comparison Between Individual PLS Scores And Inter-Strain PLS Scores For Mandibular Block

CHAPTER 4; SUPPLEMENTARY MATERIAL

Table S4.3.1: RV Coefficients, Singular Values And Pairwise Correlations Of PLS Scores Between Cranial And Mandibular Blocks

Table S4.3.2: Vector Comparison Between Individual PLS Scores And Inter-Strain PLS Scores For Cranial Block

Table S4.3.3: Vector Comparison Between Individual PLS Scores And Inter-Strain PLS Scores For Mandibular Block

CHAPTER 5: FUNCTIONAL MAINTENANCE AND VARIATION IN CRANIAL LENGTH OF THE MOUSE MASTICATORY SYSTEM

Table 5.2.1: Lever Arm System Landmarks (Right Side)

Table 5.2.2: Cranial Landmarks (Right Side)

Table 5.3.1: Anova Significances Between Strains In Muscle In-Levers

Table 5.3.2: Anova Significances Between Strains In Mechanical Advantage

Table 5.3.3: Slopes Intercepts And Correlations For RMA Regression Of Muscle In-Lever And Jaw Out-Lever Lengths

DEDICATION

This thesis is dedicated to the memory of Ted Jack Cole.

ACKNOWLEDGEMENTS

Dr Samuel Cobb - for his sage advice when asked, shrewd criticisms when needed, and encouragement and friendship throughout.

My parents Bernard and Sarah - for their unwavering love and support tempered with a healthy dose of neglect and folly.

Andy Green and Ben Osborne - for their immeasurable tolerance and love.

Prof. Paul O'Higgins; Dr. Sarah Elton; Dr. Laura Fitton; Dr. Philip Cox; Dr. Jason Dunn; Dr. Miguel Proa; Dr. Eline Van Asperen-Smith; Viviana Toro Ibacache; Andrew McIntosh; Karen Swan; Ricardo Miguel Godinho; Olivia Smith; Thomas Puschel; Han Cao; Philip Morris.

Prof. Benedikt Hallgrímsson; Dr. Heather Jamniczky; Dr. Nathan Jeffery; Prof. Chris Klingenberg; Dr. Carlo Meloro; Dr. Andrea Cardini; Dr. Jesus Marugan.

AUTHORS DECLARATION

I confirm that this work is original and that if any passage(s) or diagram(s) have been copied from academic papers, books the internet or any other sources these are clearly identified by the use of quotation marks and the reference(s) is fully cited. I certify that, other than where indicated, this is my own work and does not breach the regulations of HYMS, the University of Hull or the University of York regarding plagiarism or academic conduct in examinations. I have read the HYMS Code of Practice on Academic Misconduct, and state that this piece of work is my own and does not contain any unacknowledged work from any other sources.

CHAPTER 1 INTRODUCTION AND LITERATURE REVIEW

1.1 INTRODUCTION

Since Darwin proposed a concept of natural selection via adaptive variation (Darwin, 1859), biologists have investigated correlations between skeletal form and function (Metzger and Herrel, 2005). In this regard, focus on the craniomandibular complex is prevalent, and thus examination of the relationship between the craniofacial form and feeding behaviour is common (van Cakenberghe et al., 2002, Metzger and Herrel, 2005, Measey et al., 2011, Herrel and Holanova, 2008, Dumont et al., 2009, Aerts et al., 2002, Dumont, 1997, Pérez-Barbería and Gordon, 1999, Sacco and Van Valkenburgh, 2004, Emerson, 1985, Grine et al., 2010, Fitton et al., 2009, Taylor, 2006, Daegling and McGraw, 2007, Koyabu and Endo, 2009, Curtis et al., 2011a, Schaerlaeken et al., 2012, Herrel et al., 2003). Feeding is undoubtedly one of the most fundamental functions of the cranium and mandible, and as such selective pressures on the feeding apparatus are in theory likely to be high, leading to optimisation of the form-function relationship of this complex. This has resulted in the investigation of masticatory apparatus as an explanation of the diversity of form found in both extinct and extant skulls.

While the craniofacial complex is the morphological structure upon which the masticatory muscles and other soft tissues act, in turn the action of such muscles influences skeletal growth and development, with bone deposition occurring in regions of high muscle activity (Moss and Salentijn, 1971, Moore, 1967). As a result not only is the form of the complex sculpted through millions of years of evolution such that the individual may function to an optimal or near optimal level within its niche; but in addition the skull is remodelled during post-natal life through interactions with the applied loads of its own soft tissues such that its mechanical properties and morphology are able to allow optimal function of those muscles (Currey, 2002, Curtis et al., 2011b, Preuschoft and Witzel, 2002, Currey, 2005). This fundamental interlacing of form and function of skeletal elements has captured

the attention of generations of scientists in a bid to understand the diversity of form of the skull.

The craniofacial skeleton is a dynamic structure not only in that its function is dependent on its form and in-turn its form remodelled by its own functional loads, but also due to the continual requirement of the complex to adapt to changes in its form. The cranium and mandible are both subject to an elaborate pattern of morphological changes during development, are required to respond and adapt to numerous external as well as internal stimuli, and have the potential for developmental variants to occur early on via individual mutation. As a consequence, the viability of this complex and thus the individual or species is reliant on an ability to manage any regional modifications.

Two key challenges exist in the presence of regional variance or modification. First the complex must remain cohesive, such that parts correspond suitably in terms of their form. A key example of this is the need for appropriate occlusion of the cranium and mandible, such that as modification in cranial form occurs, corresponding proportionate modification is required to take place in the mandible. Second the complex must remain cohesive and maintain integrity in terms of functional performance. Regional variance or modification to skeletal or muscular components could have significant impact on the functional performance of the complex in terms of masticatory ability. It might therefore be expected that in response to regional modification correlated compensatory changes would occur in functionally linked skeletal or muscular elements such that functional performance of the complex and thus fitness of the organism was maintained.

In recent years understanding of how the vertebrate form is correlated with function has soared, alongside the rise in development of modern-day analytical methods, imaging techniques and computing power. From coordinate and measurement data assessing the functional potential of the craniomandibular skeleton (Radinsky, 1985a, Radinsky, 1981a, Radinsky, 1981b, Radinsky, 1982, Sharon and Radinsky, 1980, Vinyard et al., 2003, Swiderski and Zelditch, 2010, Throckmorton and Throckmorton, 1985, Fitton, 2007, Ravosa, 1990, Dechow and Carlson, 1990); to comparative studies of morphology and bite force, both estimated (O'Connor et al.,

2005, Demes and Creel, 1988, Davis et al., 2010, Christiansen, 2007, Christiansen and Wroe, 2007, Christiansen and Adolfssen, 2005, Kiltie, 1982, Thomason, 1991a, Dumont and Herrel, 2003, Herrel et al., 2008, Williams et al., 2009, Ellis et al., 2008, Wroe et al., 2005) and by means of *in vivo* measurements (Erickson et al., 2003, Herrel and Holanova, 2008, Aguirre et al., 2002, Dumont et al., 2009, Hylander et al., 1992, Santana and Dumont, 2009, Williams et al., 2009), and via functional analyses utilising computational techniques such as finite element analysis (Ross et al., 2005, Kupczik et al., 2009, Kupczik et al., 2007, Strait et al., 2007, Strait et al., 2009, Wroe et al., 2010, Wroe et al., 2007, Curtis et al., 2010a, Dumont et al., 2011, Wang et al., 2010, Cox et al., 2012, O'Higgins et al., 2011).

One approach to examining the form and functional integrity of the skull in response to changing components is to assess these parameters during ontogeny. From the earliest post-natal stages the mammalian skull is subject to remarkable changes in both shape and the size. Even a small change in an individual's morphology can have a profound effect on its functional capability (Koehl, 1996), and yet the craniomandibular complex must remain cohesive, meeting and maintaining the functional needs of the developing individual such that the juvenile may process food, the latter which may often be comparable to the diet of mature individuals of the species (Monteiro et al., 1999, Herrel and Gibb, 2006, La Croix et al., 2011a, La Croix et al., 2011b, Wainwright and Reilly, 1994). Ontogenetic studies of craniofacial development and performance have been carried out in the spotted hyena (Tanner et al., 2010, La Croix et al., 2011a, Binder and Van Valkenburgh, 2000); coyote (La Croix et al., 2011a); American alligator (Erickson et al., 2003) and in carnivores (Christiansen and Adolfssen, 2005). While La Croix et al. (2011) found decreased bite force capacity and poor biomechanical abilities in coyote juveniles when compared to adults of the same species they also report early achievement of adult mechanical advantage measurements. Throughout a development period where dramatic changes in the size and shape of the cranium and mandible occur, a maintenance of the proportions of jaw in- and out-levers and thus mechanical advantage is reported. Additionally this maintenance of mechanical advantage was not found to be due to isometric growth, with the jaw out-lever reaching adult size at 12 weeks in comparison to the jaw in-lever which attained adult lengths at 21 weeks.

The authors suggest that such early maturity of mechanical advantage is likely to assist feeding performance in juveniles, such that functional disadvantage in juveniles is not exacerbated (La Croix et al., 2011b). Similarly Tanner et al., (2010) found that the mechanical advantage of the masseter muscle was maintained throughout ontogeny, and while the mechanical advantage of the temporalis muscle shows some increase during ontogeny this ceased at 22 months of age, long before skull shape maturity was reached at 34 months.

While some such studies have shown a degree of functional performance maintenance despite the considerable changes in size and shape of the craniofacial complex imposed by post-natal ontogeny, little literature exists regarding the underlying processes and means by which such maintenance could be achieved. Focus on underlying arrangements of skeletal morphology in terms of integration and modularity may help address the ability of a complex skeletal structure to respond to variation in form.

The craniofacial skeleton is a highly dynamic region, housing the brain, major sensory organs and masticatory apparatus, the latter of which can impose significant forces on vast and diverse regions of the complex. An arrangement of individual compartments surrounding organs, spaces and tissues, with many of these regions sharing bony walls and thus the necessity to maintain functional associations between each other throughout development makes the craniofacial skeleton one of the most complex regions of the mammalian skeleton, (Hallgrímsson et al., 2009). Any complex structure such as the skull can be viewed as being composed of semi-independent parts or regions, and with a hierarchical arrangement of these parts, where there is greater connectivity between and within certain semi-independent regions than within and between others. The partial dissociation between semi-independent regions is termed modularity, whilst the coordinated variation of functionally and developmentally related modules is termed integration (Olson and Miller, 1958, West-Eberhard, 2003, Pigliucci and Preston, 2004). In developmental terms an integrated bony complex shows a tendency to produce covariation, that is, there is a group of potential connections or interactions between developmental modules or components that, in the presence of variation, produce covariation between such semi-independent regions (Hallgrímsson et al., 2009). Such integrated

variation between modular parts which are functionally related may result in the coordinated and appropriate adaptation of the craniofacial complex in response to change in one region so as to maintain morphological and thus functional integrity of the whole. Simultaneously, the modular nature of regions of the overall structure may allow for distinct skeletal elements to adapt semi-independently permitting population specific solutions to the same functional requirements such that morphological diversity is present despite functional similarity (Alfaro et al., 2005, Young et al., 2007, Young et al., 2010).

The past decade has seen much emphasis placed upon patterns of integration, modularity and covariation in the craniofacial complex. Patterns of integration and modularity have been investigated in hominoid crania (Bastir, 2008, Bastir and Rosas, 2005, Bastir and Rosas, 2006, Bastir et al., 2005a, Ackermann, 2005, Bookstein et al., 2003, Gómez-Robles and Polly, 2012, González-José et al., 2003, Martínez-Abadías et al., 2012, Mitteroecker and Bookstein, 2008, Polanski, 2011, Roseman et al., 2011, Strait, 2001); primates in general (Cheverud, 1995, Cheverud et al., 2004, Cobb and Baverstock, 2009b, Hlusko and Mahaney, 2009, Lieberman et al., 2000b, Makedonska et al., 2012, Polanski and Franciscus, 2006, Shirai and Marroig, 2010, Singh et al., 2011) the mouse (Burgio et al., 2009, Hallgrímsson et al., 2006, Hallgrímsson et al., 2004a, Hallgrímsson et al., 2009, Hallgrímsson et al., 2004b, Jovic et al., 2007, Jović et al., 2012, Klingenberg and Leamy, 2001, Leamy, 1993, Leamy et al., 1999, Willmore et al., 2009); rodents in general (Roth, 1996, Monteiro et al., 2005, Zelditch, 1988, Zelditch et al., 2008, Zelditch and Carmichael, 1989) and carnivores (Goswami, 2006, Goswami and Polly, 2010, Drake and Klingenberg, 2010, Meloro et al., 2011).

Assessing such patterns of modularity and integration can give insight into both the plastic ability (West-Eberhard, 2003, West-Eberhard, 2005) and the evolvability of an organism (Raff and Sly, 2000, Griswold, 2006, Jones et al., 2007, Wagner et al., 2007a, Hansen and Houle, 2008, Hallgrímsson et al., 2009). The expression of phenotypic variation upon which natural selection acts is structured through development (Alberch, 1982, Raff and Kaufman, 1991, Hall, 1999, Hallgrímsson et al., 2009), and thus such structuring is in part determined via the integrated and/or modular arrangement of parts (Cheverud, 1996b, Wagner, 1996). Modularity may

allow mutations within a specific region or group of traits to occur and accumulate, with such variance only affecting sets of developmentally or functionally related traits without deleterious effects on other regions of the whole. Additionally a modular arrangement of parts may result in semi-independent regions possessing the ability to plastically adapt in response to variance with relatively little influence on other regions. Conversely integration may produce coordinated variation, resulting in a correlated response and adaptation to mutation, directing evolutionary change in preferential directions (Hallgrímsson et al., 2009, Raff and Sly, 2000, Raff, 1996, Wagner and Mezey, 2004).

This thesis aims to explore the capacity of the craniofacial skeleton to adapt in reaction to changes in components of its form, and the implication of any such adaptation for the functional ability of the complex. Using a cranial length model that reflects morphological variation that occurs both during development and evolution, the ability of the craniofacial complex to respond to regional variance is tested. The sample consists of three strains of mice, one wild-type strain and two mutant strains. Both brachymorph and pten mutant strains have the same genetic background as the 'wild-type' strain (C57) alongside a known genetic mutation that specifically influences chondrocranial growth early on in development. Consequently, length of the craniofacial skeleton is altered without direct genetic effect on development of either the masticatory musculature or the greater part of mandibular morphology. The pten mutation results in a cranium that is increased in length, while the brachymorph mutation results in a cranium that is decreased in length. A sample has therefore been constructed that is made up of three strains differing in cranial length, where differences in mandibular morphology in the two mutant strains when compared to the wild-type strain can be reasonably assumed to be due to epigenetic, plastic influences. Using these mouse strains as a model for variance potentially occurring during vertebrate evolution and development, this sample is employed to address two broad questions.

Firstly the cohesion of the craniofacial complex in terms of form when cranial length alone is altered is investigated. By assessing patterns and strengths of covariance between cranial and mandibular morphology in the three strains of mice, the potential of the complex to plastically adapt in order to retain a cohesive overall

structure may be examined. In a highly integrated and adaptive complex, isolated changes in cranial length could result in mandibular morphology that corresponds closely with cranial morphology despite the presence of differing genetic patterns in these two semi-independent structures. A strong covariance between cranial and mandibular morphology in this sample would indicate the potential for a high level of plasticity and epigenetic patterning in the mandible.

Secondly the functional integration of the craniofacial complex and plastic capacity of the masticatory system is investigated. By measuring the mechanical advantage of the masticatory system, the ability of the craniofacial complex to plastically adapt regions pertaining to and therefore able to modify the lever-arm system is assessed. In a highly integrated and adaptive complex a change in craniomandibular length and thus out-lever length could be compensated for by plastic adaptation in relative masticatory muscular attachments sites such that a maintenance of functional performance was achieved.

By addressing these two broad aims through this mouse model, the plastic potential and evolvability of the craniofacial complex are assessed. A highly integrated and plastic response in the mandible when faced with altered cranial length could show the potential for substantial capacity for epigenetic patterning the craniomandibular complex. Such a finding could indicate that the skull is a highly evolvable structure that can readily adapt, such that a mutation occurring within a specific region would not necessarily have deleterious effects on the whole, but instead could be compensated for by correlated and plastic changes in other regions of the complex. Appropriate plastic adaptation in the masticatory and lever arm system, resulting in maintenance of mechanical advantage in response to largely isolated changes in cranial length would again indicate a highly evolvable craniomandibular complex. A complex in which mutation in one region led to plastic, epigenetic adaptation in other functionally linked regions such that performance and this fitness of the whole was maintained could for allow rapid evolution. Such parsimonious plastic adaptation in response to variance would contrast with a requirement of individual genetically determined adaptation in multiple regions within the complex in order to produce a functioning phenotype.

1.2 MAMMALIAN AND RODENT CRANIOFACIAL MORPHOLOGY

Rodents are recognised as the most successful and abundant mammalian order (Wood, 1965), defined by their unique open rooted, enlarged and continuously growing incisors, alongside associated distinct and specialised masticatory apparatus (Wood, 1965, Cox et al., 2012, Cox and Jeffery, 2011, Nowak and Paradiso, 1991). Not only is rodent masticatory apparatus highly distinct, but masticatory behaviour is also specialised in this unique group of mammals. Two mutually exclusive feeding modes are seen in rodents, chewing at the molar and gnawing at the incisors. Disparity between the length of the cranium and the length of the mandible means that it is not possible for both the molars (**Figure 1.2.1 a.**) and incisors (**Figure 1.2.1 b.**) to be simultaneously in occlusion. Thus, with respect to the cranium, the mandible is required to move anteriorly to meet incisal occlusion and posteriorly to attain molar occlusion (propaliny) (Cox et al., 2012, Hiimäe and Ardran, 1968, Becht, 1953).

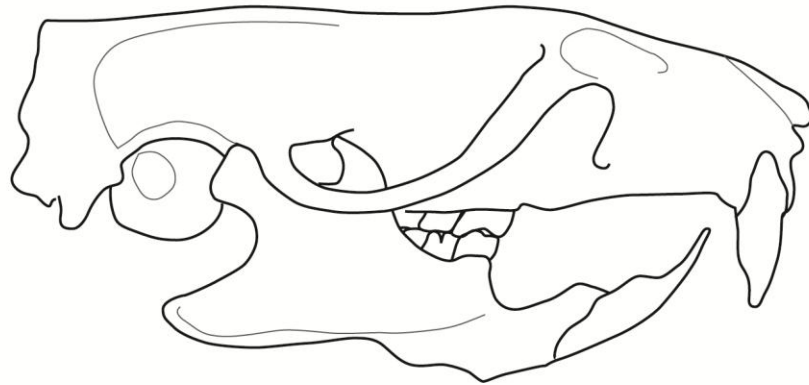
The combination of unique ever-growing incisors and the requirements of propaliny has resulted in characteristic specialisation of the rodent masticatory apparatus. The masticatory musculature of rodents is particularly specialised. The dominant jaw muscle in these species is the masseter muscle, accounting for between 60-80% of the total masticatory muscle mass (Turnbull, 1970). This however is not an undivided muscle, with authors distinguishing between several individual layers. While there is agreement that multiple layers of the masseter muscle are present in rodents, there is less concurrence on nomenclature. Throughout the literature exists a number of nomenclatures as regards both general mammalian and rodent craniofacial muscular anatomy (Druzinsky et al., 2011). In this thesis the system of Cox and Jeffery, 2011 (also that of Turnbull, 1970; Weijs, 1973, and Ball and Roth, 1995 among others) is followed, identifying three layers of the masseter muscle as the superficial masseter, deep masseter, and zygomaticomandibularis. The zygomaticomandibularis itself is divided into three portions: the anterior, posterior and infra-orbital. In addition the temporalis muscle is divided into two layers: lateral and medial, as reflects their anatomical relationships; and the pterygoid muscles are referred to in reference to their origin in and onto the pterygoid fossa (internal and

external). This system is elected due to its consistency with masticatory muscle nomenclature in many other mammalian groups (Storch, 1968, Druzinsky et al., 2011, Cox and Jeffery, 2011). A number of other authors opt to name the layers of the masseter muscle in rodents as the superficial, lateral and medial masseter (Hautier and Saksiri, 2009, Wood, 1965, Woods, 1972); while others (Offermans and De Vree, 1989, Satoh and Iwaku, 2006, Satoh and Iwaku, 2009, Satoh and Iwaku, 2004, Druzinsky, 2010a, Druzinsky, 2010b) use a combination of the two nomenclatures described above. In addition the rostral expansion of the zygomaticomandibularis, described here as the infra-orbital portion is referred to by some authors (Coldiron, 1977, Janis, 1983a) as the maxillomandibularis.

The rostral expansion of the zygomaticomandibularis portion of the masseter muscle is not present in all rodents, and the absence is believed to be the ancestral (protrogomorph) condition (**Figure 1.2.2 a.**) (Wood, 1965). In both the extant mountain beaver (*Aplodontia rufa*) (Druzinsky, 2010a) and many fossil rodents (Meng et al., 2003) this expansion is absent and masseteric origin is limited to the zygomatic arch (Cox et al., 2012). The masticatory musculature of all other extant rodent species includes an extension of the masseter onto the rostrum (Cox et al., 2012), yet within this diverse order a number of different forms of this extension exist. Traditionally the Rodentia order has been divided into three suborders: Sciuromorpha, Myomorpha, and Hystricomorpha (**Figure 1.2.2**), on the basis of the structure of the masticatory musculature and associated morphology of the cranium and mandible (Wood, 1965). While these morphotypes were originally classified as suborders of Rodentia (Brandt, 1855), it is now clear that these three divisions neither fit with accepted rodent phylogeny (**Figure 1.2.3**) nor represent monophyletic groups (Cox et al., 2012, Wood, 1965). Instead it may be useful to use the rostral expansion of the masseter muscle to define these three conditions. Sciuromorphs (including squirrels, beavers and pocket gophers) have an expansion of the deep masseter muscle, which originates beneath a widened anterior root of the zygomatic arch (**Figure 1.2.2 b.**). Hystricomorphs (including South American rodents and a number of Old World forms such as the springhare, porcupines and jerboas) possess an extension of the zygomaticomandibularis, which takes its origin on the rostrum and passes through an enlarged infra-orbital foramen and the orbit to

insert onto the mandible (**Figure 1.2.2 c.**). Finally, myomorphs (including mice, rats and the dormice) show a combination of both the sciurormorph and hystricomorph conditions, with both the zygomaticomandibularis and the deep masseter showing an expansion onto the rostrum. The deep masseter expansion passes under the zygomatic arch, while the zygomaticomandibularis passes lateral to the zygomatic arch and through the infraorbital foramen (**Figure 1.2.2 d.**) (Cox et al., 2012).

- a. **RAT CRANIUM AND MANDIBLE**
molar occlusion



- b. **MOUSE CRANIUM AND MANDIBLE**
incisal occlusion

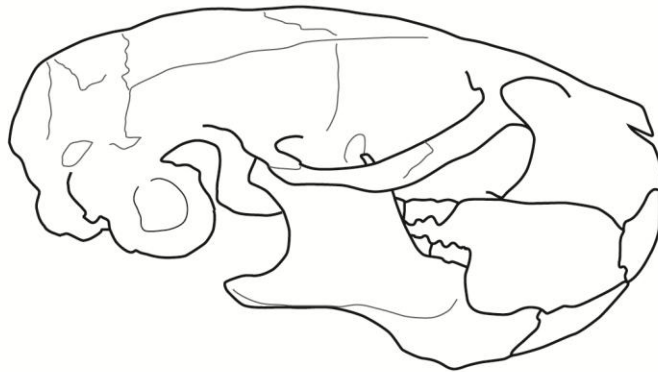
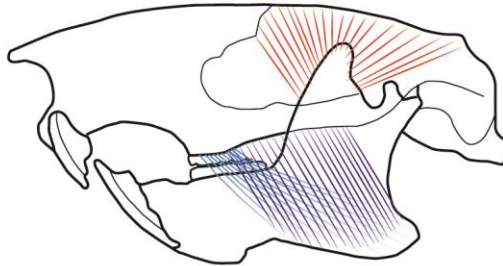
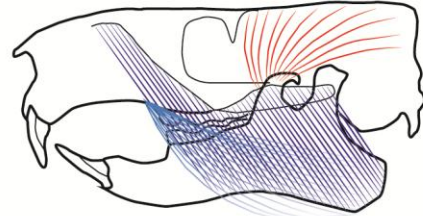


Figure 1.2.1: Depicting a. cranial and mandibular of the rat in molar occlusion; and b. cranial and mandibular anatomy of the mouse in incisal occlusion.

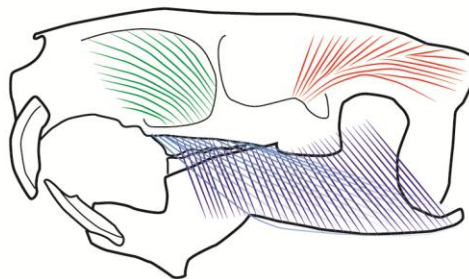
a. **PROTROGOMORPHOUS CONDITION**
Ischyrotomus (Eocene protrogomorph)



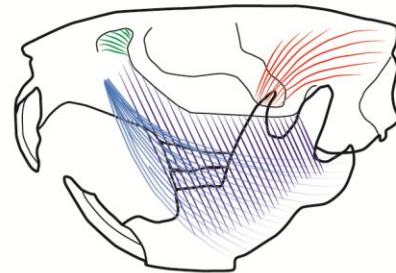
b. **SCIUROMORPHOUS CONDITION**
Marmota (sciurid)



c. **HYSTRICOMORPHOUS CONDITION**
Myocastor (caviomorph)



d. **MYOMORPHOUS CONDITION**
Ondatra (cricetid)



-  *Temporalis*
-  *Deep masseter*
-  *Superficial masseter*
-  *Rostral expansion of zygomaticomandibular (infra-orbital)*

Figure 1.2.2: Depicting rodent sub-orders/conditions on the basis of the structures of the masticatory musculature and associated cranial and mandibular morphology; adapted from Wood (1965). Showing *a.* the protrogomorphous condition; *b.* the sciurid condition; *c.* the hystricomorphous condition; and *d.* the myomorphous condition. Temporalis muscle fibres are depicted in red; deep masseter fibres in dark blue; superficial masseter fibres in pale blue; and zygomaticomandibularis fibres in green.

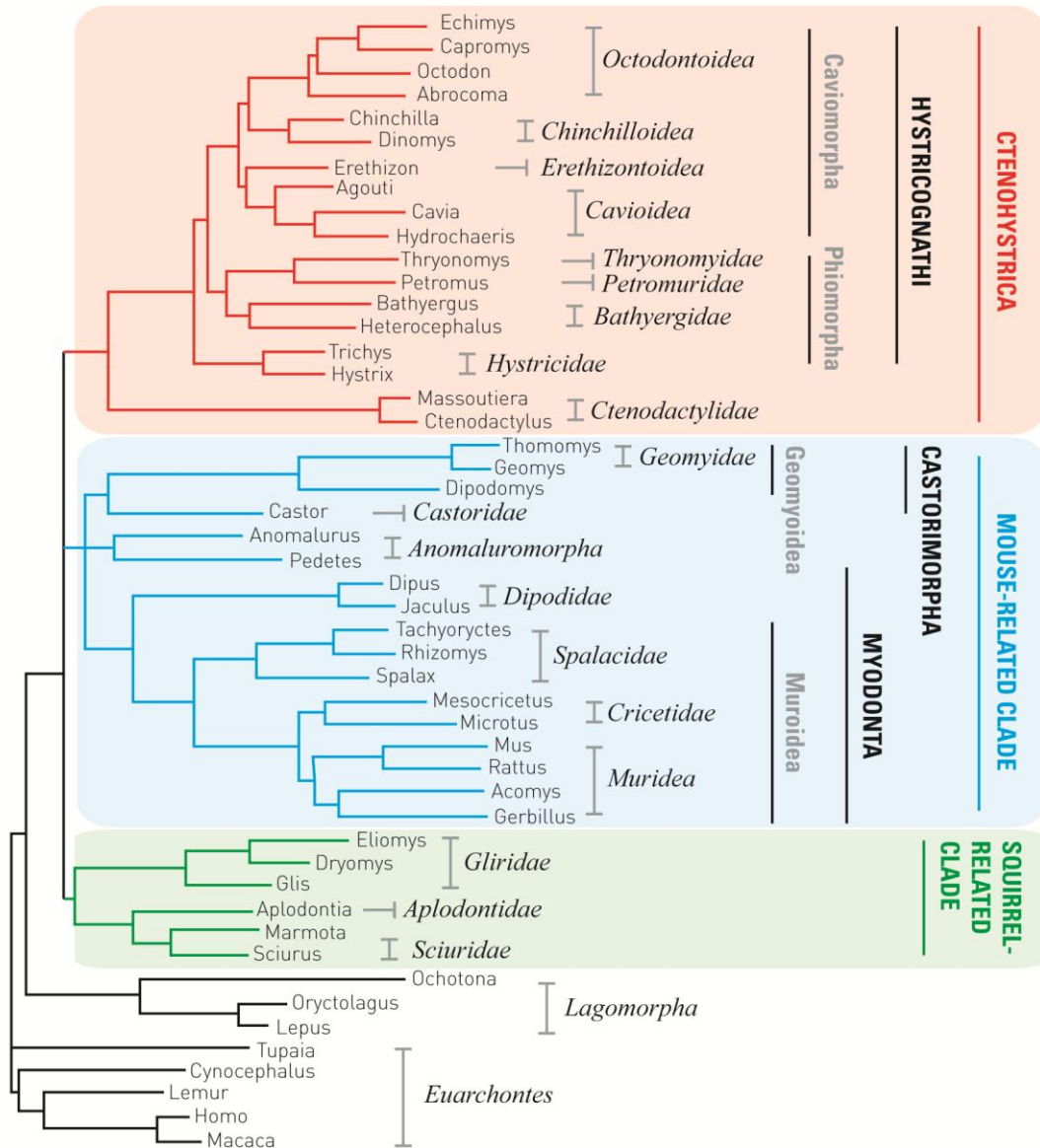


Figure 1.2.3: Rodent phylogeny adapted from Blanga-Kanfi et al. (2009) based upon analysis of six nuclear genes from all major rodent clades.

Craniofacial skeletal and muscular anatomy is well described in rodents in general: Ball and Roth, 1995 (*Sciurus, Microsciurus, Sciurillus, Tamiasciurus, Tamias, Glaucomys*); Byrd, 1981 (*Cavia*); Cox and Jeffery, 2011 (*Sciurus, Cavia, Rattus*); Druzinsky 2010a (*Aplodontia, Cynomys, Tamias, Marmota, Ratufa, Sciurus, Thomomys*); Gorniak, 1977 (*Mesocricetus*); Greene, 1935 (*Rattus*); Hautier and Saksiri, 2009, (*Laonastes*); Hautier, 2010 (*Ctenodactylus*); Offermans and De Vree, 1989 (*Pedetes*); Olivares et al., 2004 (*Aconaemys, Octomys, Tympanoctomys, Spalacopus, Octodon, Octodontomys*); Rinker, 1954 (*Sigmodon, Oryzomys, Neotoma, Peromyscus*); Rinker and Hooper, 1950 (*Reithrodontomys*); Satoh, 1997, 1998, 1999 (*Apodemus, Clethrionomys*); Satoh and Iwaku, 2004 (*Mesocricetus, Cricetulus, Tscherkia, Phodopus*); Satoh and Iwaku, 2006 (*Onychomys*); Satoh and Iwaku, 2009 (*Neotoma, Peromyscus*); Turnbull, 1970 (*Sciurus, Rattus, Hystrix*); Weijs, 1973 (*Rattus*); Wood, 1965 (*Marmota, Myocastor, Ondatra*); Woods, 1972 (*Proechimys, Echimys, Isothrix, Mesomys, Myocastor, Octodon, Ctenomys, Erethizon, Cavia, Chinchilla, Dasyprocta, Thryonomys, Petromus*); Woods and Howland, 1979 (*Capromys, Geocapromys, Plagiodontia, Myocastor*); Woods and Hermanson, 1985 (*Capromys, Geocapromys, Plagiodontia, Myocastor, Echimys, Octodon, Erethizon, Coendou, Dasyprocta, Atherurus, Thryonomys, Petromus*).

The mouse (*Mus musculus*) has been a dominant species in the investigation of the development, genetics and evolution of the mammalian skull. The house mouse has been widely utilised in studies of morphological variation and development (Boughner et al., 2008, Cray et al., 2011, Hallgrímsson and Lieberman, 2008, Lieberman et al., 2008, Vecchione et al., 2007, Willmore et al., 2006a, Byron et al., 2004, Klingenberg, 2002, Leamy, 1993, Morriss-Kay and Wilkie, 2005); integration and modularity (Hallgrímsson et al., 2006, Hallgrímsson et al., 2004b, Hallgrímsson et al., 2004a, Klingenberg et al., 2003, Mezey et al., 2000); and adaptive evolution and genetics (Renaud et al., 2010, Klingenberg and Leamy, 2001, Cheverud et al., 1991, Atchley et al., 1985a, Atchley et al., 1988, Atchley et al., 1985b, Ravosa et al., 2008b, Willmore et al., 2006b), and the role that this organism has to play in our understanding of craniofacial development, evolution form and function is ever increasing with the availability of knock-out strains (Hallgrímsson and Lieberman, 2008). It is thus surprising that little published data exists regarding the masticatory

musculature of this model organism. While description of skeletal morphology of the cranium and mandible of the mouse (Atchley et al., 1985b, Kawakami and Yamamura, 2008, Klingenberg et al., 2001, Leamy et al., 1999, Leamy et al., 2008, Macholán, 2008, Perlyn et al., 2006, Willmore et al., 2006a, Zelditch et al., 2004b, Zelditch et al., 2008) and embryology (Kaufman and Bard, 1999, Kaufman, 1992, Brune et al., 1999) is available; precise detail of the morphology of the masticatory musculature has been largely lacking from the literature. Prior to work outlined in this thesis (Baverstock et al., 2013), to the best of the author's knowledge only one publication existed describing the anatomy of the mouse masticatory musculature (Patel, 1978) and the latter work is lacking in the detail and precision granted by contemporary techniques. An initial aim of this thesis is to address this surprising gap in the literature, providing a comprehensive description of the masticatory musculature of *Mus musculus* as the preliminary basis for a series of prospective studies.

1.3 EVOLUTION OF COMPLEX MORPHOLOGIES, TRAITS AND SYSTEMS

Morphological integration, plasticity and the evolution of complex morphological structures are key concepts in evolutionary biology. Living organisms are highly complex and intricately organised systems. Within most organisms recognisable parts can be identified that appear to be separate entities, coherent in terms of their structure, function and developmental origins (Klingenberg 2008; Wagner, 1996; Schlosser and Wagner, 2004; Klingenberg, 2005a; Breuker et al., 2006b; Wagner et al., 2007). This independence however is by no means absolute. An organism required to act as a functioning whole demands coordination between and among parts, providing integration throughout the entire complex structure. This conflict between the relative autonomy of parts and the necessity of coordination has resulted in the concepts of morphological integration and modularity (Klingenberg 2008). Modularity describes the grades of connectivity within the whole, where individual units which are highly coherent, tightly integrated and relatively independent of other such units are referred to as modules. Integration refers to the cohesion between these modules that results from biological interaction and leads to a successfully functioning whole. Consequently integration describes the unity within and between parts, whilst modularity explains the level or strength of such integration within and between units; where integration within modules is strong relative to weaker integration between modules (Cheverud, 1996; Raff, 1996; Wagner, 1996; Wagner and Altenberg, 1996; Wagner et al., 2007; Klingenberg, 2008).

1.3.1 Modularity

Like plasticity, modularity is a universal property of all living things and plays an essential role in how they evolve. It would be false however to view organisms as a combination of separate units or modules, rather, it should be appreciated that organisms develop in a manner that creates modular behaviour or modularity. In this

regard the simultaneous individuality and connectedness of biological organisation is a key concept, where modularity describes both the discreteness of subunits, but also the strength of integration within and between parts (West-Eberhard, 2003).

The partially compartmented nature of organisms draws us to recognise modular traits. West-Eberhard, 2003 defines a modular trait as being recognisable by qualities such as: “a) recurrence in time or in space of the same set of elements together indicating that they are regulated as a set; b) temporal or spatial discreteness relative to other structures or behaviours; c) stereotypy of form; d) coordinated expression as a unit by a known mechanism or regulatory factor that, when experimentally manipulated, affects the trait as a unit; e) dissociability, or ability to be deleted or re-expressed as a unit; f) occurrence, with the same structure or location, in different individuals of the same species or higher taxon.”

Modularity and integration may be viewed from a number of different biological perspectives. These relationships may be considered in a developmental, genetic, functional or evolutionary context. (Klingenberg 2008; Cheverud 1996; Bastir & Rosas 2004).

1.3.1.1 Developmental modularity

Morphological forms are generated via developmental processes, and consequently modules may be defined by the developmental interactions that occur among the precursors that form the elements of the final structure. Developmental processes and interactions mutually influence each other to give rise to the coordinated development of the whole organism and modular parts within. As such interactions facilitate the transmission of genetic and environmental variation across different traits, developmental modularity influences the patterning of all components of morphological covariation within an organism (Klingenberg, 2008). By modulating the available morphological variation, developmental modularity effects both genetic and functional modularity (**Figure 1.3.1 a.**).

1.3.1.2 Genetic modularity

A single gene can have influence on multiple phenotypic traits. This results in genes having the capacity to produce joint effects on morphological traits and to form pleiotropic relations amongst these (Nadeau et al. 2003). As genetic variance in phenotypic traits is mediated by means of developmental processes, genetic and developmental modularity are closely related (**Figure 1.3.1 b.**). This relationship however is not necessarily a perfect congruence as the genetic variance is not exclusively controlled and manifested via developmental interactions. This is further complicated by the influence that genetic variance can have on the developmental pathways that give rise to the end morphology (Klingenberg, 2005; Klingenberg 2008).

1.3.1.3 Functional modularity

When considering the craniofacial skeleton it is possible to see that many functional interactions occur. The ability to perform mastication requires direct mechanical forces to be generated, yet mastication is not the solitary requirement of this region of morphology. Design trade-offs occur in the production of other functional capabilities such as respiration, vocalisation and prey capture and processing. The presence and interactions between these different functional requirements is encompassed in the term functional modularity (Klingenberg 2008). Again, functional modularity does not stand alone. As developmental processes produce the morphological forms that perform these vital functions, developmental modularity is believed to influence and interact with functional modularity (**Figure 1.3.1 c.**). The strength of this relationship however is yet to be determined (Breuker et al. 2006; Klingenberg 2008). Conversely functional modularity can influence developmental modularity. Mechanical loads, and therefore functions such as mastication, can

influence the rate and direction of tissue growth. Consequently processes such as bone remodelling provide a relationship between functional and developmental modularity (Enlow and Hans, 1996; Herring, 1993; West-Eberhard, 2003; Klingenberg 2008). Additionally, in theory, evolutionary processes should result in selection at a functional level and consequently a degree of convergence between functional and genetic modularity should occur (Cheverud, 1996; Wagner, 1996; Wagner & Altenberg, 1996; Klingenberg, 2008). Whilst there is some evidence to support this hypothesis (Ambruster et al. 2004; Cheverud et al. 1997; Klingenberg et al. 2004; Mezey et al. 2000) other studies suggest that as different morphological structures are able to perform corresponding functions a flexibility for neutral divergence could be present (Wainwright et al. 2005; Young et al. 2007).

1.3.1.4 Evolutionary modularity

Evolutionary modularity results from the association between different phenotypic traits and evolutionary divergence. As selection occurs in response to performance, and the modular structure of morphological units relates to function and hence performance, functional modularity is a key determinant of evolutionary modularity (**Figure 1.3.1 d.**). Equally, as evolutionary change occurs via selection and drift in reaction to genetic variance, genetic modularity contributes significantly to evolutionary modularity (Lande, 1979; Felsenstein, 1988; Klingenberg 2008).

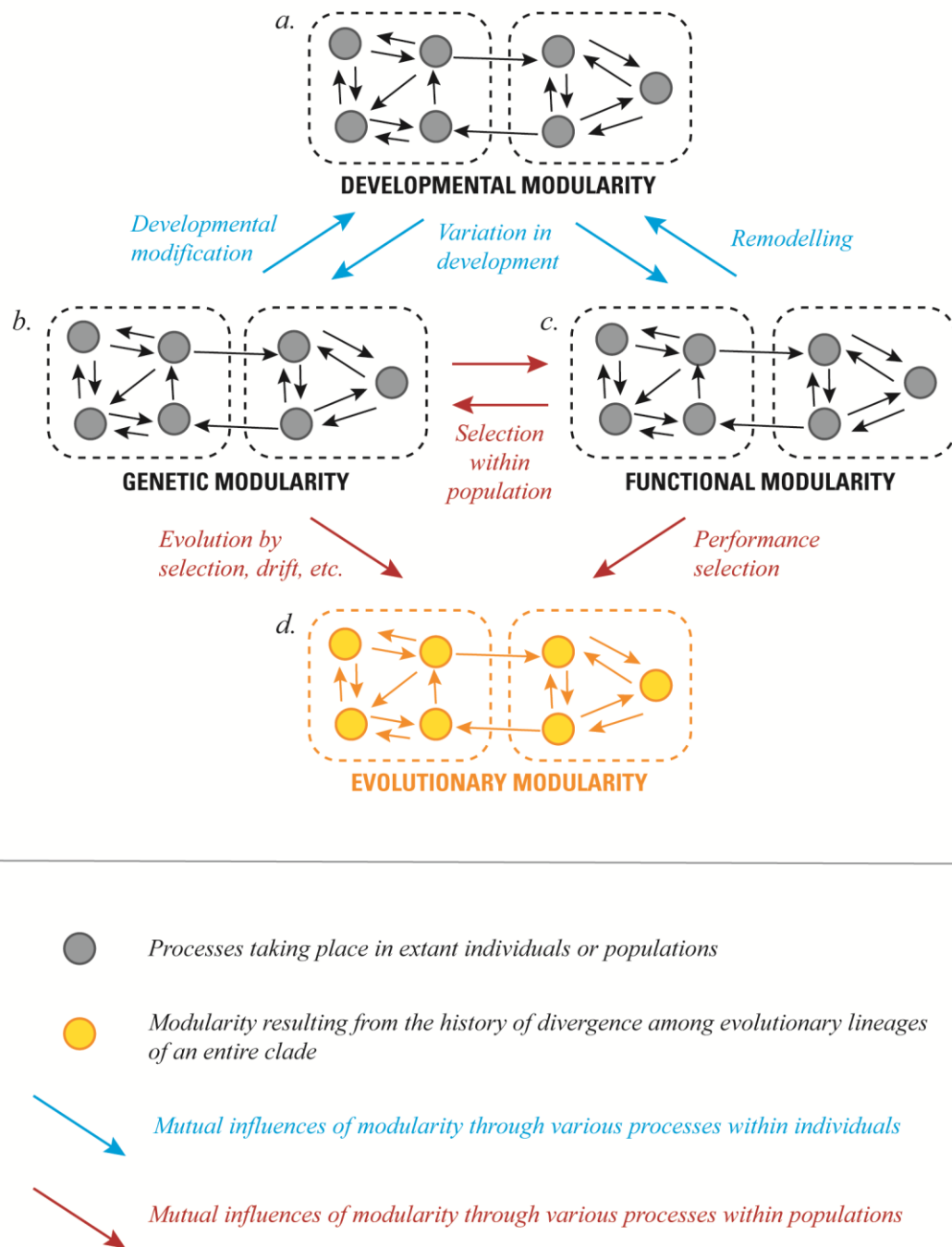


Figure 1.3.1: Adapted from Klingenberg (2008), showing the types of modularity that concern morphological variation and the connections between them, Types of modularity which are based upon processes that take place within extant individuals or populations are depicted in grey. Types of modularity resulting from the history of divergence among evolutionary lineages of an entire clade are depicted in orange, Influences that occur through various processes within individuals are depicted by blue arrows; and those influences that occur through various processes within populations are depicted in red.

1.3.2 Integration

Coordination between parts in terms of both development and function is a key factor in modularity. As an organism is required to act as a functioning whole, coordination between and among semi-independent parts is required to provide integration throughout the entire form. This cohesion between modular parts results in the necessity of viewing an organism as a 'modular' structure rather than being composed of entirely autonomous or independent modules. Modularity simultaneously describes the discreteness and boundaries between subunits, and the connectedness and integration between them. (West-Eberhard, 2003; Klingenberg, 2008). Whilst integration occurs within all divisions of an organism, grades of integration exist, with coordination and integration within modules being strong relative to weaker integration between modules. Whilst all parts are connected, some parts are more connected than others (Simon, 1973; West-Eberhard, 2003).

Morphological integration may be discerned and statistically analysed as covariation among morphological traits. Traits which are highly internally integrated yet show relative independence from other traits may be considered modular, whilst high degrees of covariance between all morphological traits of an overall structure may indicate strong integration of the whole (Klingenberg, 2005a). A number of authors have assessed morphological integration via patterns of covariance by means of correlations among distance measurements (Olson and Miller, 1958, Cheverud, 1982a, Leamy and Atchley, 1984, Zelditch, 1987, Cheverud, 1995), and by correlations amongst positions of landmark points (Klingenberg et al., 2003, Klingenberg and Zaklan, 2000, Bookstein et al., 2003, Bastir and Rosas, 2005, Bastir and Rosas, 2006, Bastir et al., 2005a, Ackermann, 2005, Burgio et al., 2009, Cobb and Baverstock, 2009b, Goswami, 2006, Goswami, 2007, Kulemeyer et al., 2009, Makedonska et al., 2012, Meloro et al., 2011). It is important to note however that both integration and modularity are dispositional concepts (Wagner et al., 1997) in that they describe potential rather than actual states. In the absence of variation, covariation cannot be present (Hallgrímsson et al., 2009). In an population with an integrated and modularised developmental system, covariation structure would not

emerge and thus be detectable via scientific analysis unless variation was first present. As such some authors define integration as *the tendency of a developmental system to produce covariation* (Hallgrímsson et al., 2009).

1.3.3 Plasticity

Plasticity is a common property of all organisms. Where *modularity* describes the grades of connectivity between semi-independent and dissociable parts of a whole, *plasticity* expresses the responsiveness of an organism or part of an organism to environmental inputs (West-Eberhard, 2003; Klingenberg, 2004; Klingenberg, 2008). The overarching modular nature of organisms may be seen as a secondary result of the universality of plasticity (West-Eberhard, 2003). The ability of an organism to react to, or modify its morphology, state, movement, or rate of activity in response to an environmental stimulus is known as phenotypic plasticity. This environmentally sensitive behaviour in effect produces intra-individual variation (Evans, 1953; Williams, 1992; West-Eberhard, 2003). It is the dual influence of environment and genetics during development that produces intra-individual variance, where within an individual environment may vary, but genes remain as a constant. Novel phenotypes arise within developmentally variable populations from pre-existing phenotypes, and plasticity enables such novel organisms or traits to possess functionality. The adaptive mutual adjustment among variable parts of an organism during development without genetic influences may be termed *phenotypic accommodation*. A functional phenotype can result despite significant variation and environmental change (West-Eberhard, 1998; Muller, 1989, Gerhart & Kirschner 1997; Walker, 1996; West-Eberhard, 1989, 1992, 2003). Such variation may be the results of numerous causes- genetic or environmental, normal or pathological. Regardless of cause, such adaptive phenotypic accommodation will occur enabling individuals to maintain function. This ability to amend a phenotype without genetic influences occurs in the presence, despite, and in response to unpredictable and sometimes significant degrees of genetic variation in many different aspects of morphology (West-Eberhard, 2003). The modification of morphology in response to

a change in one aspect of morphology can often show correlated changes within the overall system or organism that are so complex in their degree, and so highly integrated in terms of function that they could reasonably be assumed to have resulted from many generations of natural selection and genetic change at many loci. Such elaborate reconstruction of a phenotype without proportional restructuring of genome is what characterises adaptive phenotypic plasticity (West-Eberhard, 2003).

1.3.4 Modularity as plasticity

Whilst the universal modular nature of organisms may be seen as a secondary result of the universality of plasticity, modularity in turn contributes to phenotypic plasticity (West-Eberhard, 2003). The modular nature of morphology increases flexibility both in terms of the behaviour and morphology of an organism. By allowing the relative independent variation of parts, modularity enables variation to occur within a subspace without correspondingly large effects on neighbouring parts. This gives rise to a coherent larger trait such as the face whilst component structures such as noses, eyes and jaws can vary semi-independently; allowing hybrid phenotypes to accommodate an extensive array of features without serious functional detriment (West-Eberhard, 2003).

1.3.5 Hierarchical organisation

Hierarchical organisation is a central concept in both modularity (Larsen, 1997) and integration. Hierarchical organisation is another property common to all living organisms. All traits or modules within an organism may be viewed as a decomposable matrix of elements that are semi-independent in both their function and regulation (Atchely and Hall, 1991), but that possess different degrees of connectivity within and between each other. Integration within modules is by definition more substantial than that between modules, yet a reasonable strength of

integration between modules may be present. Thus levels of integration and connectivity between composite parts of a structure form a hierarchical network of interactions; where modules may exist within modules such that modules at one level may form the traits that make up modules at a higher level of organisation (Klingenberg, 2005a).

The notion of hierarchical organisation has substantial implications for the evolution of form. Such organisation results in an assortment of traits whose component units have the potential to vary somewhat independently of each other throughout both development and evolution, yet simultaneously may have levels of connectivity with other regions such that variation in one region may result in coordinated variation in other regions. This also has important implications in view of the key concept in evolution of homology. It may be extrapolated that homologous traits may vary in some respects whilst not in others rather than behaving as a fixed unit, and hence homology should be regarded not as an all or nothing phenomenon, but rather as a continuum of degrees of similarity attributable to common ancestry (West-Eberhard, 2003).

1.3.6 Evolvability

An integrated or modularised developmental system is likely to influence ability of that system to respond to selective change (the *evolvability* of the system). This is because the evolvability of a system depends upon the capacity to produce suitable variation for selection to act upon (Hansen, 2003, Griswold, 2006). Modular organisation and therefore semi-independence of parts is hypothesised to allow for adaptation of such discrete units without deleterious effects on other regions (Riedl, 1977, Raff, 1996, Wagner and Altenberg, 1996, Wagner and Mezey, 2004, Wagner et al., 2007a, Hansen, 2003, Hallgrímsson et al., 2009). Modularity has also however been posited to reduce mutational target size and thus hamper evolvability (Hansen, 2003, Wagner, 1996, Wagner and Altenberg, 1996). Integration and covariation of traits within a structure may limit and channel the evolutionary trajectory of that

structure (Pigliucci, 2003, Juenger et al., 2000), lowering the probability that a mutation will have beneficial effects on all traits within the structure (Klingenberg, 2005a, Orr, 2000, Griswold, 2006). Conversely however, in a highly coordinated system where an individual mutation effects a suite of traits throughout that system there may be increased probability that such a mutation will have a beneficial effect on at least one character. In such a scenario a net benefit could be achieved even if the acting mutation had deleterious effects on a number of trait (Griswold, 2006).

1.4 BONE BIOLOGY

1.4.1 Bone Architecture

The principal role of the bony skeleton may be seen as the provision of structural support for the body. Bones enable weight bearing and functional loading; opposition of muscle contraction which results in motion; protection of internal organs; as well as providing storage of calcium and harbouring of the hematopoietic stem cells from which blood and immune cells are derived (Nakashima et al., 2012, Sommerfeldt and Rubin, 2001). Bone however is not an inert and static material, but a dynamic organ (Takayanagi, 2007). It is now well established that an increase in bone loading results in an increase in bone mass, while a reduction in loading induces bone loss (Seeman and Delmas, 2006). Although to some extent the morphology and mass of the bony skeleton is determined by genetic factors, it is the ability of bone to remodel via local formation and resorption of mineralised tissue which results in its ability to balance competing activities and responsibilities (Nakashima et al., 2012, Sommerfeldt and Rubin, 2001).

Three distinct cell types are present in bone; osteoblasts, osteoclasts and osteocytes. Osteoblasts, located at the bone surface (along with their precursor), are responsible for the production and mineralisation regulation of the bone extracellular matrix. Highly anchorage dependent, osteoblasts rely on extensive cell-cell and matrix-cell contact by means of a variety of specific receptors and transmembranous proteins to maintain cellular function, and responsiveness to stimuli (both metabolic and mechanical) (Sommerfeldt and Rubin, 2001). A number of osteoblasts become ensnared by their own calcified matrix, altering their phenotype to become osteocytes. Trapped osteocytes within the matrix connect with cells at the bone surface and an extensive network of intercellular communication is built. This network of cellular connection may play a role in directing sites of new bone formation (Mosley, 2000, Donahue et al., 1995). Conversely, osteoclasts are highly specialised cells responsible for the resorption of fully mineralised bone. The apical membrane of osteoclasts forms a seal with the calcified bone matrix, and a resorption

bay is created beneath these cells into which lytic enzymes are secreted (Walker, 1972) (**Figure 1.4.1**). Osteocytes, the most abundant cells in bone, are derived from osteoblasts, yet are distinctly different to the latter in terms of both function and morphology (Sommerfeldt and Rubin, 2001). Smaller than osteoblasts, osteocytes have fewer organelles but an increased nucleus to cytoplasm ratio. Osteocytes also possess a higher number of cytoplasmic extensions (filopodia) which provide connections between one another and with bone-lining cells; generating a three-dimensional syncytium (Curtis et al., 1985). This osteocyte construct may coordinate the temporal and spatial recruitment of osteoblasts and osteoclasts (Burger and Klein-Nulend, 1999b), and thus is the sensing system of the latter two cells (Klein Nulend et al., 1995, Klein-Nulend et al., 2005, Burger and Klein-Nulend, 1999a, Mullender and Huiskes, 1997, Cowin, 2007, Gerhard et al., 2009).

Communication between osteoclasts and osteoblasts must exist to allow for coordination of bone formation and resorption. Osteoclasts and immune cells share several regulatory molecules, including transcription factors, signalling molecules, and cytokines, these which may mutually influence each other (Nakashima et al., 2012). Osteoprotegerin (OPG) and its ligand OPG-L (a transmembrane receptor expressed on osteoblasts and immune cells), bind to a transmembranous receptor expressed on osteoclast precursor cells (RANK - receptor activator of NF- κ B). OPG-L and RANK interact to initiate a gene expression and signalling cascade that results in the promotion of osteoclast formation (Sommerfeldt and Rubin, 2001). Osteoclasts secrete OPG which acts as a soluble competitive binding partner for RANKL (receptor activator of nuclear factor κ B ligand), resulting in the inhibition of osteoclast formation, and thus bone resorption (Hofbauer et al., 2000) (**Figure 1.4.1**). RANKL is also essential for immune regulation. Sufferers of rheumatoid arthritis have excessive activation of the immune system and are at an increased risk of osteoporosis (Takayanagi, 2007, Lorenzo et al., 2008); and mice deficient in immunomodulatory molecules have been shown to develop abnormal osteoclast phenotypes (Takayanagi, 2007).

Cells make up only 2-5% of the extracellular matrix of bone, with the remaining matrix composed of additional organic material (20%), water (5%) and inorganic mineral hydroxylapatite (70%). In contrast, freshly synthesised bone matrix prior to

mineralisation consists primarily of collagen. Additional proteins are embedded in the extracellular matrix. While some of these proteins may be involved in signalling, others may be functional during the mineralisation process (Sommerfeldt and Rubin, 2001). Mice lacking osteonectin have been shown to have reduced bone remodelling (Delany et al., 2000), while osteocalcin-deficient mice have been demonstrated to show increased bone formation (Ducy et al., 1996). The majority of non-collagenous proteins in bone consist of proteoglycans, some of which have a role in defining the spatial organisation of the extracellular matrix, and may play a role in facilitating cellular interactions and/or signalling with growth factors during development (Sommerfeldt and Rubin, 2001, Aszódi et al., 2000).

1.4.2 Bone Modelling and Remodelling

The microstructural mechanisms of bone adaption are encompassed by the terms bone modelling and bone remodelling. In modelling, bone formation and resorption are uncoupled, such that bone is either added or removed to separate surfaces (the periosteal or endosteal bone surfaces) and thus modelling may lead to an alteration of the gross morphology of a bone (Currey, 2002, Gerhard et al., 2009, Frost, 1987, Frost, 1990). In remodelling, bone formation and resorption are coupled, taking place at the same site. All surfaces may be affected, including the cortical shell, trabecular compartment, and vascular cavities, yet remodelling has been shown to be more sensitive in the trabecular compartment (Gerhard et al., 2009).

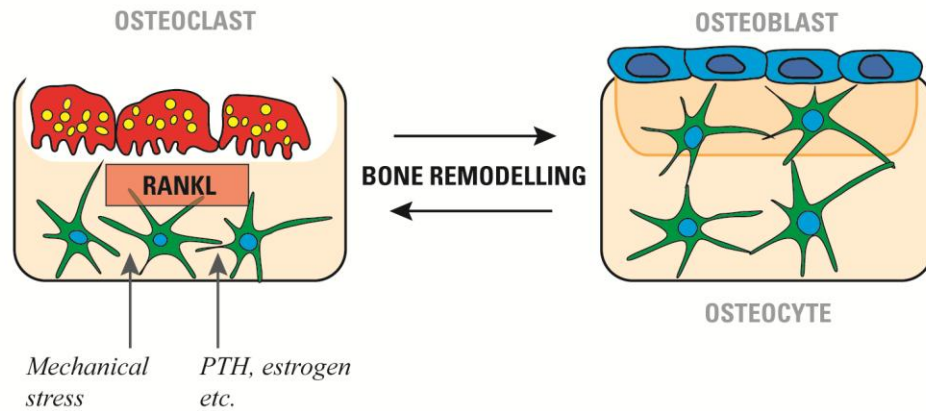
BONE RESORPTION*Initiation of bone remodelling*

Figure 1.4.1: Adapted from Nakashima et al. (2012). Osteocytes are the command cell at the time of the initiation of bone remodelling through RANKL expression. Osteocytes are embedded within the lacuno-canalicular network. Based upon the site of localisation, osteocytes are thought to orchestrate bone homeostasis by regulating both osteoblasts and osteoclasts.

1.4.3 Formation of the Bones of the Cranium and Mandible

The vertebrate skeleton is produced via complex, coordinated and synergistic interactions between three distinct cell lines, those derived from the neural crest; sclerotome cells; and cells of the lateral plate mesoderm. The vertebrate skull is formed from cranial skeletogenic mesenchyme derived from two distinct embryonic sources: the development of the face, anterior cranial base, and anterior cranial vault (frontal bone) begin with a cell line derived from neural crest cells, while the posterior cranial vault and posterior cranial base are derived from mesoderm (Jiang et al., 2002, Noden and Trainor, 2005).

The first phase in the development of skeletal structures is the formation of mesenchymal condensations (Hallgrímsson et al., 2007, Hall, 2005). Increased local proliferation of mesenchymal cells results in such condensations which migrate towards a central area and form filopodial connections between cells (Hall, 2005). Differentiation into either osteoblasts or chondrocytes then occurs, depending on the type of ossification, intramembranous or endochondral respectively (Hallgrímsson et al., 2007). The individual bones of the skull are derived from these condensations (**Figure 1.4.2**).

During intramembranous ossification, mesenchyme that has formed a membranous sheath condenses and becomes highly vascular. Some mesenchymal cells may then differentiate directly into osteoblasts, depositing osteoid tissue. Calcium phosphate is then deposited into the osteoid tissue, forming bone. This type of osteogenesis is found during development of the flat bones of the skull (the frontal and parietal bones), the maxilla and the mandible. Growth of these bones occurs through the proliferation and differentiation of osteoblasts at the sutures or margins (Govindarajan and Overbeek, 2006, Sommerfeldt and Rubin, 2001).

Endochondral bone formation occurs if differentiation of mesenchymal cells differentiate into chondrocytes, laying down a cartilaginous template that is later replaced by bone. During endochondral ossification, transcription factors induce chondrocytes in the growth plate to mature into hypertrophic chondrocytes, which lay down a matrix rich in Collagen X, and secrete vascular endothelial growth factor

(VEGF) (Govindarajan and Overbeek, 2006, de Crombrughe et al., 2001, Gerber et al., 1999). VEGF draws in both osteoclasts and osteoblasts, as well as promoting the invasion of blood vessels from the perichondrium (Govindarajan and Overbeek, 2006).

Figure 1.4.2

DEVELOPMENT OF THE CRANIOFACIAL SKELETON

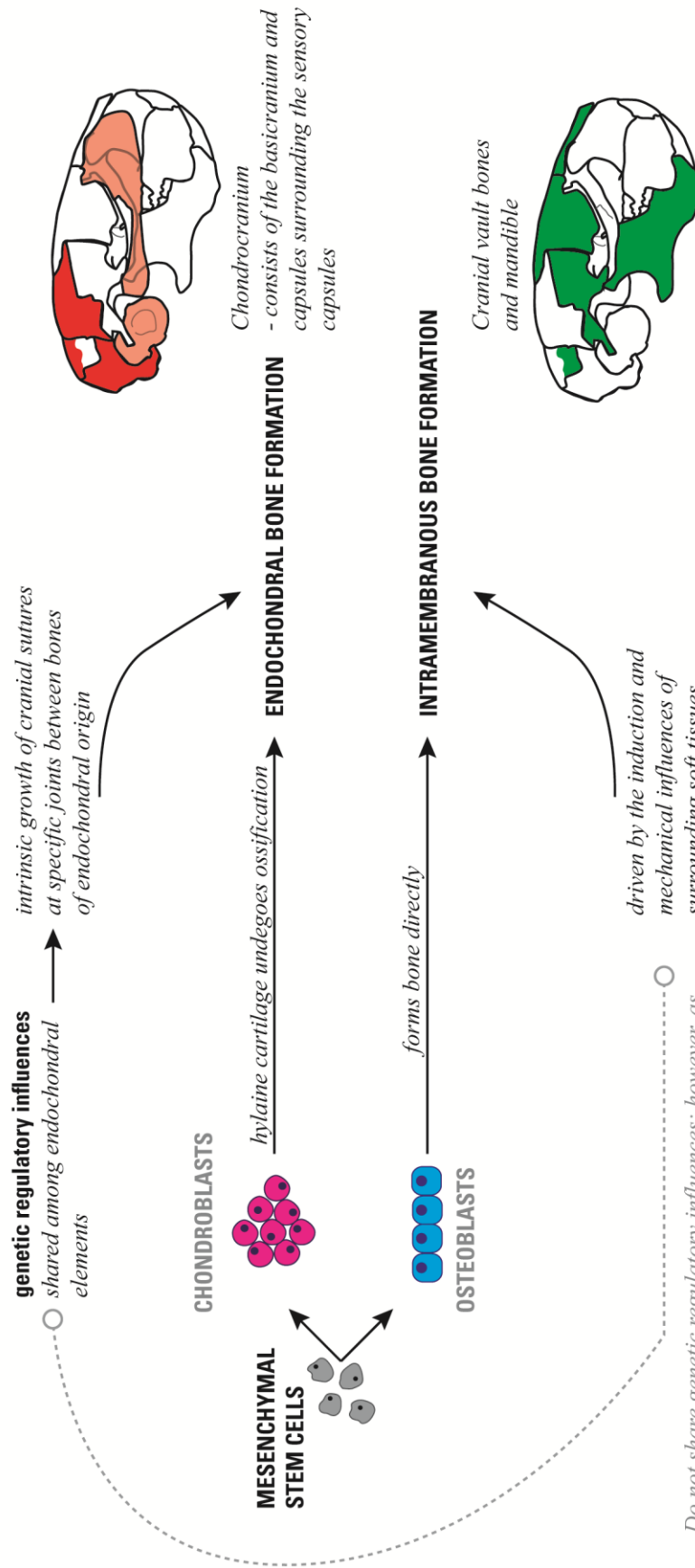


Figure 1.4.2: Depicting endochondral and intramembranous bone formation in the cranium and mandible, and regulatory influences.

The sample utilised in this thesis consists of three strains of mice, a common wild-type strain (C57BL/6J) and two mutant strains: brachymorph and pten. Brachymorph and pten mouse strains display extremes of cranial length, generated via specific mutations that effect chondrocranial growth. The brachymorph mutation (ul Haque et al., 1998, Kurima et al., 1998) results in reduction of cranial length via an autosomal recessive mutation in the phosphoadensine phosphosulfate synthetase 2 gene (*Paps2*). The cartilage extracellular matrix of brachymorph mice is affected, dramatically reducing all skeletal elements that rely on cartilage growth (Hallgrimsson et al., 2007). The pten mutation Cre-Lox driven tissue-specific knockout of the *Pten* (tumour-suppressor with tensin homology) gene. *Pten* negatively regulates the pathway responsible for controlling proliferation, differentiation, size and survival of chondrocytes. Thus in *Pten*^{flox/flox} mice cartilage growth is increased, and therefore endochondral bone growth is increased (Hallgrimsson and Lieberman, 2008, Ford-Hutchinson et al., 2005).

During development genetic regulatory influences are shared amongst endochondral elements, but not between endochondral and intramembranous elements. However, as intramembranous bone formation is largely driven by the induction and mechanical influences of the surrounding soft tissues (Opperman, 2000, Spector et al., 2002, Wilkie and Morriss-Kay, 2001, Yu et al., 2001); and as the bones of the skull are physically adjacent endochondral bone growth may have secondary or epigenetic influence on intramembranous bone growth (Hallgrimsson et al., 2007).

As both pten and brachymorph mutations target cartilage growth alone, and the early mandible is formed via intramembranous ossification (Ramaesh and Bard, 2003), neither mutation is expected to have a direct genetic influence on mandibular morphology. Thus any morphological adaptation seen in the mandible of these two mutant strains when compared to the control wild-type strain (C57BL/6J) may be reasonable assumed to be secondary epigenetic effect in response to changes in morphology of endochondral elements (**Figure 1.4.3**).

DEVELOPMENT OF THE CRANIOFACIAL SKELETON IN CONTEXT OF MUTANT STRAIN

Figure 1.4.3

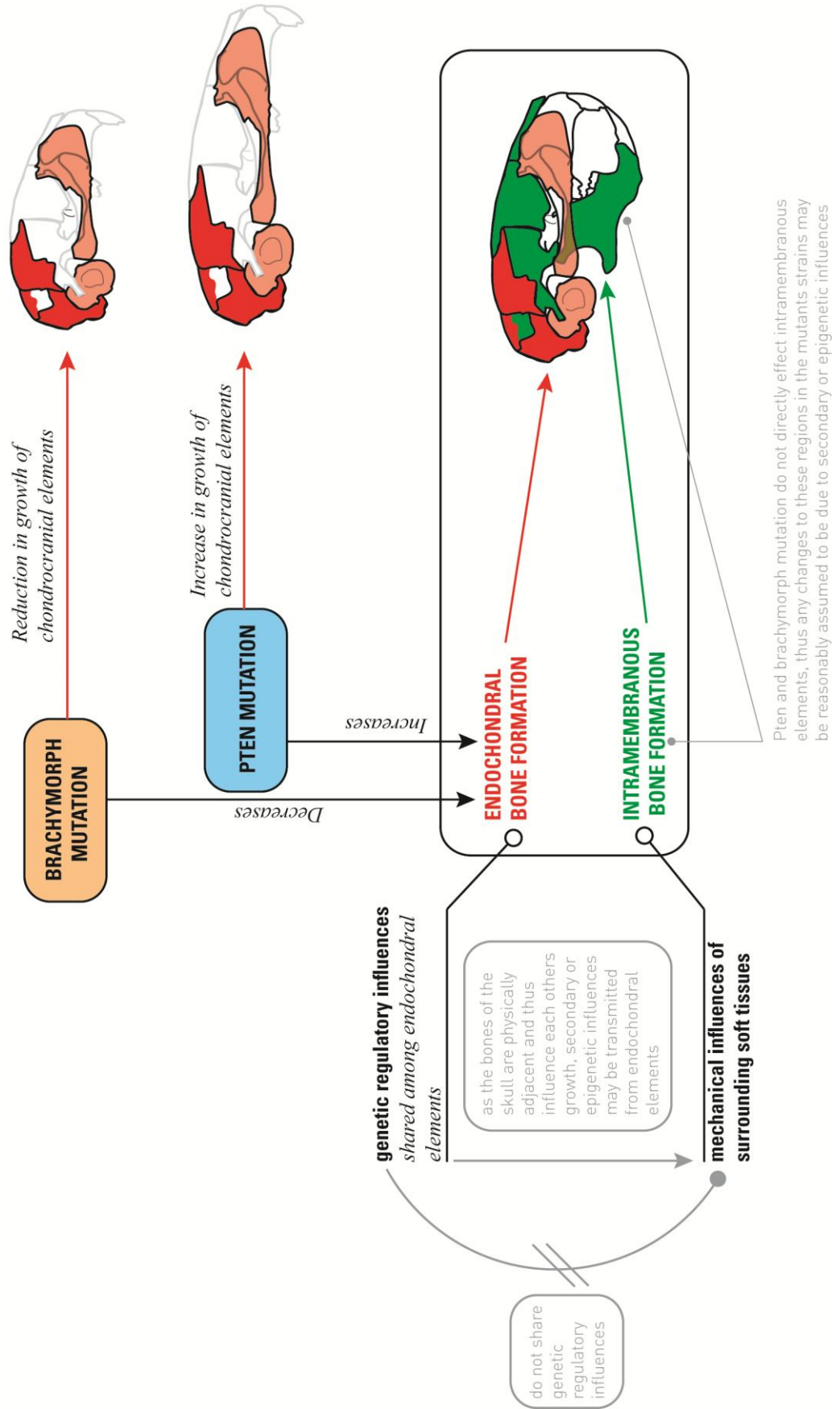


Figure 1.4.3: Depicting the influence of the pten and brachymorph mutations on bone formation in the cranium and mandible.

Meckel's cartilage may however have some contribution to the morphogenesis of the mandible. (Bhaskar et al., 1953, Glasstone, 1971, Ramaesh and Bard, 2003). This mandibular cartilage forms at approximately day 12.5 of pre-natal growth (E12.5) as a rostral process and two lateral rods that fuse together and grow (Chai et al., 1994, Miettinen et al., 1999), with some influence on jaw lengthening prior to disintegration at approximately E16 (Ramaesh and Bard, 2003). There appears however to be no direct evidence that Meckel's cartilage regulates mandibular morphogenesis (Ramaesh and Bard, 2003), and any contribution this cartilage does have is thought to be transient and not of significance to growth, or influential in the length or width of the mandible (Frommer and Margolies, 1971). The mandibular condyle does however develop through a method of endochondral ossification, although this particular type of ossification may not be that of classical endochondral ossification (Silbermann and Frommer, 1972). It may therefore be reasonably assumed in both the brachymorph and pten mutant mouse strains the vast majority, if not all, potential variation in mandibular form when compared to the control is likely a secondary and epigenetic effect of variation in cranial length.

1.4.4 Mechanical Stimuli and Bone Plasticity

The formation of bone is a dynamic process that involves the activity of multiple genes which regulate transitions between the maturation and growth of cells (Smith and Hall, 1990, Atchley and Hall, 1991, Atchley, 1993, Hogan, 1996, Skerry et al., 2000, Chen et al., 2004, Yoon and Lyons, 2004, Tsumaki and Yoshikawa, 2005, Wutzl et al., 2006). These complex genetic pathways which regulate the growth and maturation of cells, as well as the remodelling of cartilage and bone ultimately form skeletal morphology and produce phenotypic diversity. While genes obviously carry hereditary material which in part determine the phenotype of an organism or morphology of skeletal structure (Niven, 1933, Murray and Huxley, 1925, Murray, 1936), mechanical stimuli up-regulate or down-regulate genes prior to their translation into macroscopic growth (Mao and Nah, 2004). Thus the regulation of the complex genetic pathways themselves however comes from external stress (Herring,

1993, Huiskes, 2000, Skerry et al., 2000, Rauch and Schoenau, 2001, Moore, 2003, Müller, 2003, Lobe et al., 2006). Both internal and external stresses induce differentiation and growth, and thus determine much of the phenotypic variation found in skeletal structures (Frost, 1987, Huiskes, 2000, Rauch and Schoenau, 2001, Mao and Nah, 2004, Badyaev and Foresman, 2004, Young and Badyaev, 2007, Badyaev et al., 2005).

While our understanding of the mechanical activation of cartilage and bone cells is incomplete (Mao and Nah, 2004), it is known that mechanical forces play a vital role in the regulation of osteogenesis and chondrogenesis in addition to bone repair and remodelling (Herring and Lakars, 1981, Lanyon, 1984, Frost, 1987, Atchley et al., 1991, Thorogood, 1993, Huiskes, 2000, Skerry et al., 2000, Rauch and Schoenau, 2001, Mao and Nah, 2004, Carter et al., 1998, Mao, 2002, van der Meulen and Huiskes, 2002). Forces induced on skeletal tissues from muscular contraction (or exogenous sources) may be either static or cyclical (Mao and Nah, 2004). Repeated cycles of change in force magnitude are particularly important in the induction of strain in bone and cartilage cells, as the latter respond more rapidly to rapid oscillations in force magnitude rather than to constant force (Grodzinsky et al., 2000, Elder et al., 2001, Sommerfeldt and Rubin, 2001, Mao and Nah, 2004, Mao, 2002, Srinivasan et al., 2002, Turner et al., 2002, Wang and Mao, 2002b, Wang and Mao, 2002a). *In vivo* mechanical loads result in the deformation of bone, causing stretching of the bone cells both lining and within the bone matrix. This deformation of bone and thus bone cells leads to fluid movement within the canaliculae of the bone (Duncan and Turner, 1995, McLeod et al., 1998). The anabolic effects of such fluid flow appear to evoke deformation of transmembrane channels, extracellular matrix molecules, intranuclear structures and cell cytoskeletons (Mao, 2002, Gillespie and Walker, 2001, Guilak and Mow, 2000, Guilak, 1995). Thus mechanical forces lead to tissue strain and cell membrane and cytoskeleton deformation, this eliciting a series of mechanotransduction events (**Figure 1.4.4**) (Mao and Nah, 2004). These events lead to the proliferation and differentiation of bone and cartilage cells, that is, growth and development, visible as the macroscopic changes of the morphology of the mandible from newborn to adult (Mao and Nah, 2004).

As muscle stimulation influences bone development, growth and remodelling (Enlow, 1963, Lanyon and Rubin, 1984, Lanyon, 1993, Frost, 1987), modification to either muscle activity or muscle morphology may induce phenotypic variation through skeletal plasticity (Young et al., 2007). Populations may however differ in their sensitivity to muscle stimulation (Levins, 1968, Padilla and Adolph, 1996, Young and Badyaev, 2007). The intensity, frequency and duration of muscle activity needed to induce a plastic response in a skeletal component, such as a change in growth or the induction of remodelling, often differs between and across populations (Duncan and Turner, 1995, Heaney, 1995, Parfitt, 1997). Therefore, across species and populations, an evolved difference in reaction norms may result from selection over time on trait function (Scheiner, 1993, Schlichting and Pigliucci, 1998, West-Eberhard, 2003, Badyaev, 2005), leading to the development of distinct morphological adaptations (Young et al., 2007).

Bone biology, development and plasticity underpin the concepts and questions addressed in this thesis. The model mouse sample employed in this work was selected due to the different types of bone formation responsible for the development of the cranium and mandible. Both mutations selectively affect cartilage growth, and thus, in the two mutant strains, each mutation has significant impact on the development and phenotype of crania, yet limited or no direct influence on development of the mandibles. If the craniomandibular complex is a highly integrated structure (see **Section 1.3**) however, the close physical and functional proximity of these two semi-independent structures may result in epigenetic plastic adaptation in the mandible such that correlation is maintained with crania. Adjacency of the mandible to the cranium may lead to epigenetic influence on mandibular intramembranous bone growth from cranial endochondrial bone growth. In addition, as the cranium and mandible form one functional unit, mechanical stimuli from external stresses as a result of mastication may regulate mandibular bone growth, such that epigenetic macroscopic growth occurs in pertinent regions resulting in mandibular morphology that is correlated with cranial morphology.

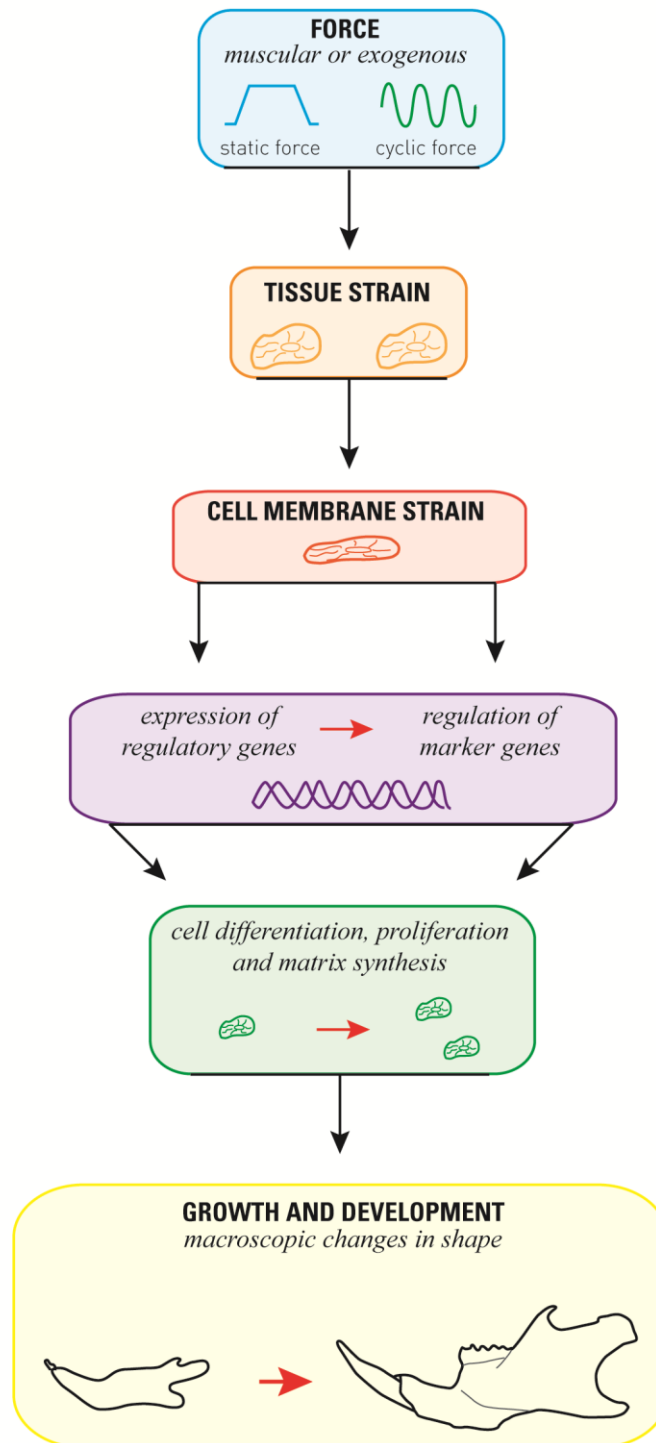


Figure 1.4.4: Adapted from Mao and Nah (2004) depicting mechanotransduction pathways describing how exogenous forces induce ultimate changes in the macroscopic shape of skeletal structures such as the mandible. Supporting evidence can be found in (Mao, 2002, Duncan and Turner, 1995, Guilak, 1995, Gillespie and Walker, 2001).

1.5 MUSCLE BIOLOGY

1.5.1 Fibre Architecture

In order to understand skeletal muscles, the internal arrangement of muscle fibres, referred to as fibre architecture (Lieber, 2002) must be examined. Skeletal muscles consist of collections of multinucleated cells called fibres, lying side by side and running approximately parallel to the muscles line of action (**Figure 1.5.1 b.**). The majority of the intracellular space within each muscle fibre is occupied by protein filaments called myofibrils (**Figure 1.5.1 c.**). Each myofibril is made up of a continuous chain of sarcomeres (**Figure 1.5.1 d.**). Sarcomeres are the basic contractile elements of the muscle, each able to generate a vectoral force when active. Directionally aligned, sarcomeres work cooperatively such that when activated tension arises along the axis of the myofibrils and thus along the axis of the muscle fibres and muscle itself (Sciote and Morris, 2000, Kardong, 2002, Hall, 2010).

From a dense region within each sarcomere, referred to as the Z line, extends a lighter region made up of ‘*thin filaments*’ of the protein *actin* (**Figure 1.5.1 e.**). The thin actin filaments interlock with ‘*thick filaments*’ of the protein myosin, creating a darker area known as the *A band*, with the central section of the *A band* forming a lighter area called the *H zone* (**Figure 1.5.1 e.**). Muscle contraction is a result of interaction within sarcomeres between the actin filaments and *cross bridges* extending from the myosin filaments (Sciote and Morris, 2000).

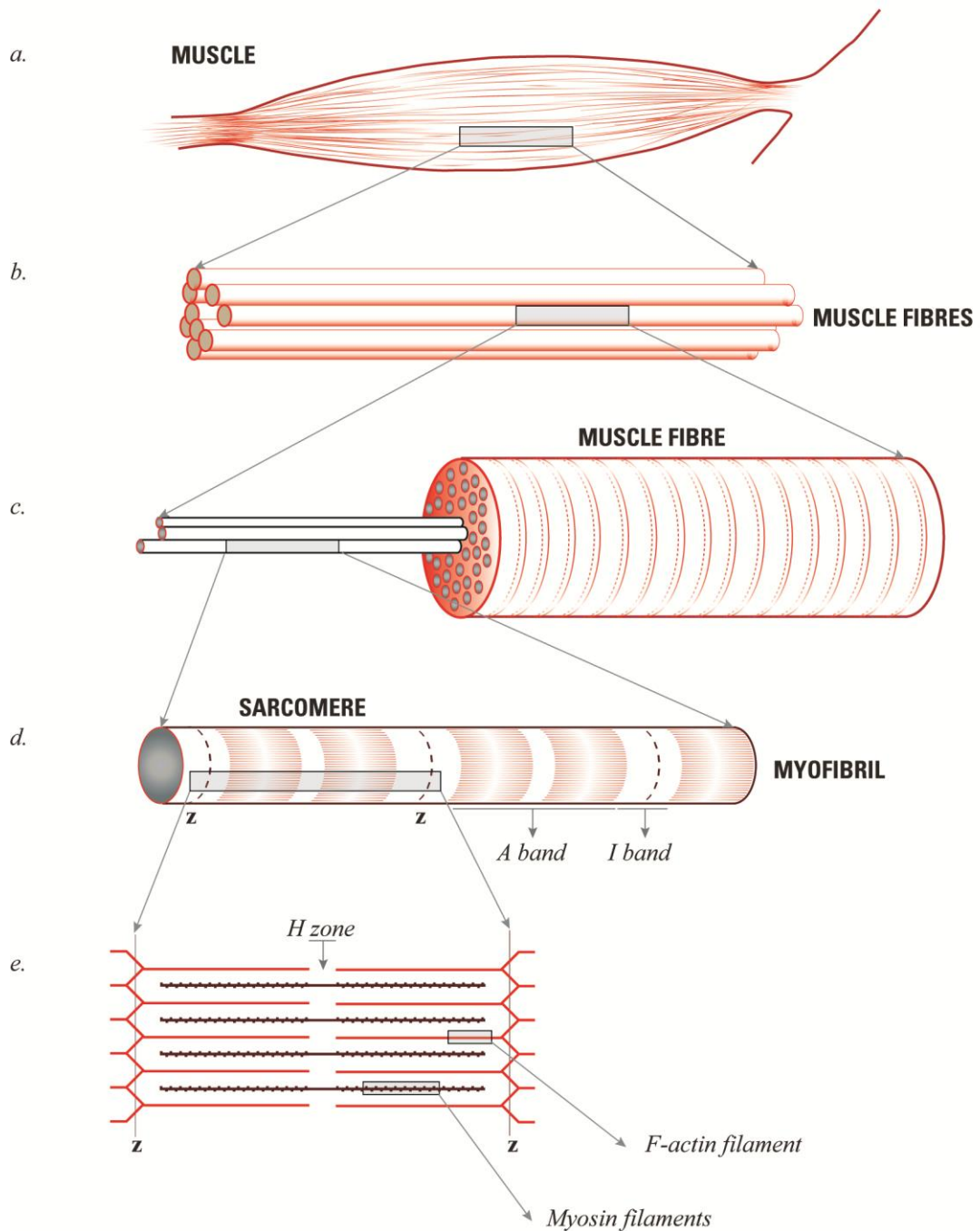


Figure 1.5.1: Adapted from Guyton and Hall (2006); showing the organisation of skeletal muscle from the gross to molecular level. *a.* depicts the whole muscle; *b.* a bundle of muscle fibres; *c.* a cross-section of single muscle fibre; *d.* a single myofibril and *e.* the arrangement of actin and myosin filaments within a sarcomere.

1.5.2 Length Tension Relationships

Chemical cross-bridges between the thick myosin filaments and thin actin filaments form and reform causing these filaments to ratchet or slide past each other and thereby contraction of the sarcomere (Kardong, 2002). Sarcomeres thus undergo relative changes in length during muscle contraction (Sciote and Morris, 2000, Huxley and Niedergerke, 1954, Huxley, 1957, Huxley and Hanson, 1954). **Figure 1.5.2** shows the relaxed and contracted states of a sarcomere and therefore a myofibril. In the relaxed state there is little overlap between the two successive ends of the actin filaments. In the contracted state these filaments have been pulled towards and past each other such that their ends overlap and they lie among the myosin filaments. The *Z disks* are pulled inwards by the actin filaments so as to meet ends of the myosin filaments, reducing the length of the *I bands* (Kardong, 2002).

RELAXED AND CONTRACTED STATE OF A MYOFIBRIL

Figure 1.5.2

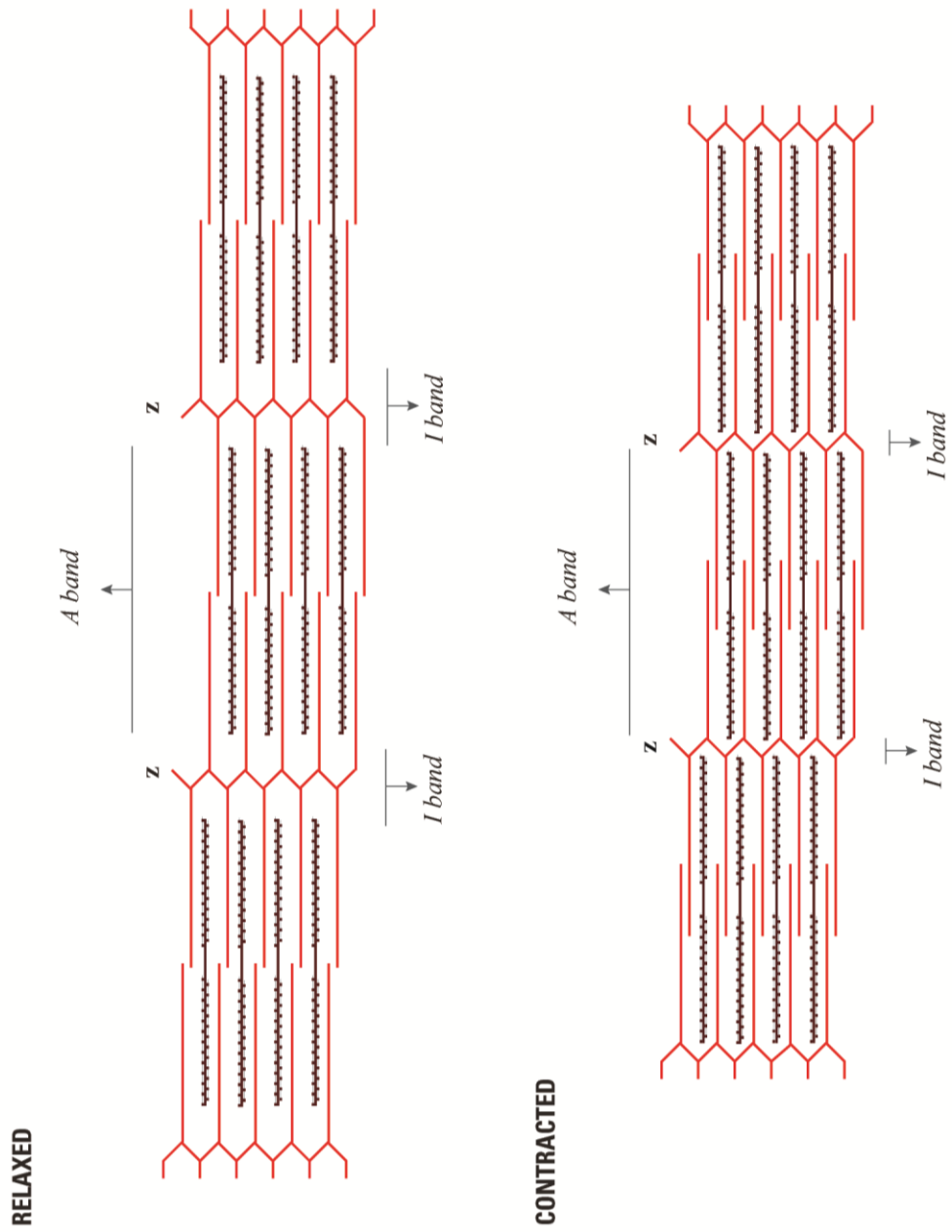


Figure 1.5.2: Adapted from Guyton and Hall (2006); showing relaxed and contracted states of a myofibril. Actin filaments are shown in red and myosin filaments in black.

Sarcomeres undergo relative changes in length during muscle contraction (Sciote and Morris, 2000, Huxley and Niedergerke, 1954, Huxley, 1957, Huxley and Hanson, 1954). The mechanical arrangement of overlapping thin actin filaments and thick myosin filaments within the sarcomere during muscle contraction results in changes to levels of active tension within the muscle. **Figure 1.5.3, inset 1** depicts the relationship between sarcomere length and the amount of tension developed by a muscle fibre during contraction. When there is no overlap between actin and myosin filaments (point D) no tension is developed. As the sarcomere shortens and overlap develops between the actin and myosin filaments, tension progressively increases (points D – C). As the sarcomere length decreases to approximately $2.2\mu\text{m}$, the actin filaments have overlapped with all of the myosin cross-bridges yielding maximum tension, with actin filaments having not yet made contact with the centre of the myosin filament (points C – B). As the sarcomere further shortens it maintains full tension until a length of approximately $2\mu\text{m}$, when the ends of the actin filaments start to overlap each other as well as the myosin filaments (point B). When sarcomere length has fallen to approximately $1.65\mu\text{m}$, the two Z disks border then ends of myosin filament and the strength of contraction rapidly decreases (point A). As the contraction proceeds further and the sarcomere reaches its shortest length, the ends of the myosin filaments begin to crumple and tension approaches zero (Guyton and Hall, 2006).

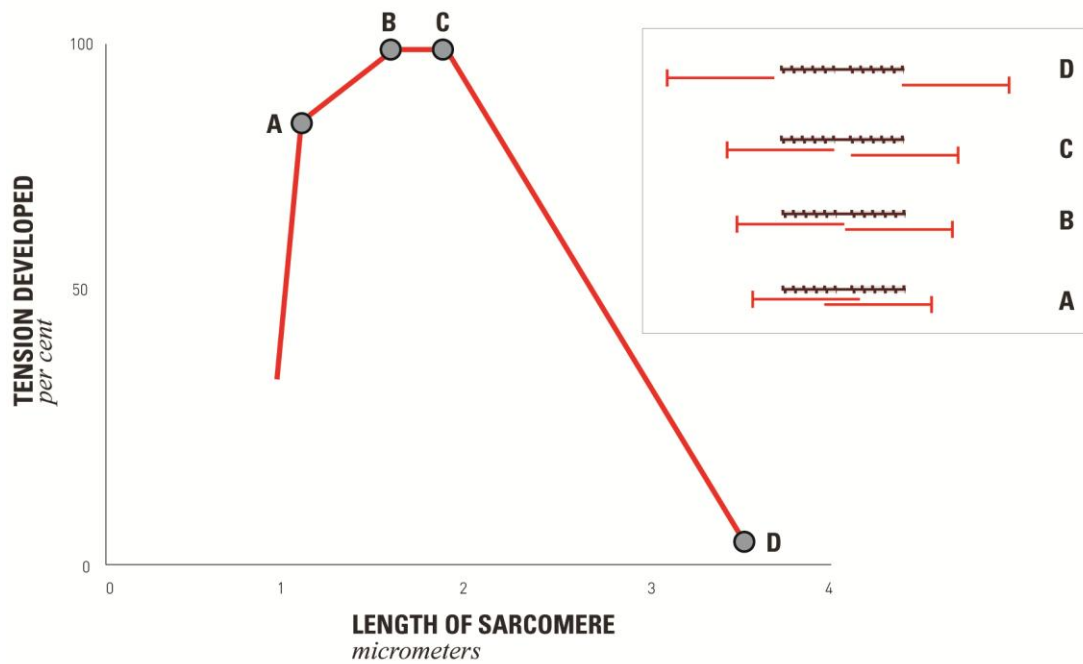
As sarcomeres within a muscle do not always contract to the same degree, and as a whole muscle contains substantial amounts of connective tissue, the length-tension curve for a whole muscle has different properties to that of an isolated sarcomere or muscle fibre (Kardong, 2002, Guyton and Hall, 2006). The same general slope and normal range of contraction is present when considering a muscle as a whole, with the active tension of a muscle decreasing as sarcomere length increases about normal lengths ($2.2\mu\text{m}$) (**Figure 1.5.3 inset 2**) (Guyton and Hall, 2006).

As the length-tension relationship of a muscle is a result of the arrangement of overlapping thick and thin filaments, tension produced by a muscle is not constant but instead varies according to the muscles fixed length when activated (Kardong, 2002, Hildebrand and Goslow, 2001). When the whole muscle has a length of approximately $2\mu\text{m}$ (normal resting length) appropriate maximum contraction is

achieved, yet the increase in active tension during contraction is reduced when the muscle has a length above the norm (sarcomere length greater than $2.2\mu\text{m}$) (**Figure 1.5.3 inset 2**) (Hall, 2010). In a muscle fixed in a lengthened position there is little overlap between filaments, decreased cross-bridge formation and thus relatively decreased tension. Only at a normal or intermediate length is cross-bridge formation and tension produced optimised (Kardong, 2002, Hildebrand and Goslow, 2001).

The length-tension relationship of a muscle is important when considering the morphology of a bone-muscle system. As active tension is only maximised at specific intermediate fibre lengths, a muscle that acts over a relatively long distance may not achieve maximum force across its full range of motion. Thus in some skeletal systems multiple muscles may act in concert to produce the same bony motion. During such a motion each contributing muscle may reach its optimal tension at a different point, such that as the bone moves or rotates at each stage a different muscle may be responsible for providing maximum force. In other scenarios increased joint force may be achieved at a particular instant when the length-tension curves of more than one muscle acting to move the same bone are roughly speaking the same. In the case of the human jaw, major jaw-closing muscle concurrently reach their optimal force, and thus maximum bite force is produced at the half-open position of the jaw (Kardong, 2002).

1.



2.

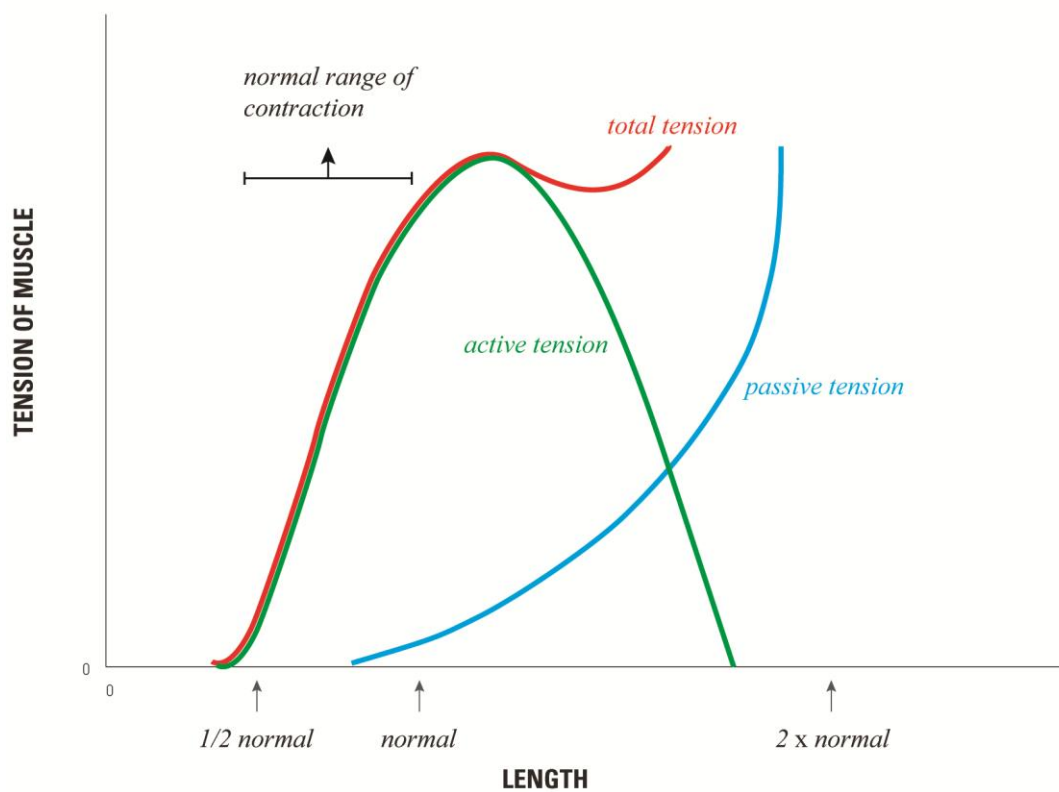


Figure 1.5.3: Adapted from Guyton and Hall (2006); showing 1. the length-tension relationship for a single fully contracted sarcomere; and 2. the muscle length to tensions relationship in a muscle both before and during muscle contraction.

1.5.3 Cross Sectional Area

While the length of individual muscle fibres is an important determinant of muscle function, cross sectional area is another critical architectural factor influencing the amount of force a muscle can produce (Taylor et al., 2009). The morphological cross sectional area of a muscle may be defined as the cross-sectional area of the muscle perpendicular to its longitudinal axis its thickest part. The physiological cross sectional area of a muscle may be defined as the cross-sectional area of all muscle fibres perpendicular to their longitudinal axis. Thus in muscles in which all fibres run parallel to the longitudinal axis of the muscle, physiological and morphological cross-sectional areas are equivalent. However, when the architecture of a muscle is such that fibres run obliquely to the long axis, physiological cross-sectional area becomes a more accurate measure of a muscles ability to produce tension (Kardong, 2002).

Physiological cross-sectional area theoretically corresponds to the aggregate of cross-sectional areas of all muscles fibres within a particular muscle, and has been experimentally shown to be proportional to the maximum force generation of a muscle (Taylor et al., 2009, Gans and Bock, 1965, Powell et al., 1984). The greater the number of fibres present, the greater the maximum force produced; thus muscles of equal physiological cross sectional area, regardless of length, generate equivalent force (**Figure 1.5.4**) (Kardong, 2002).

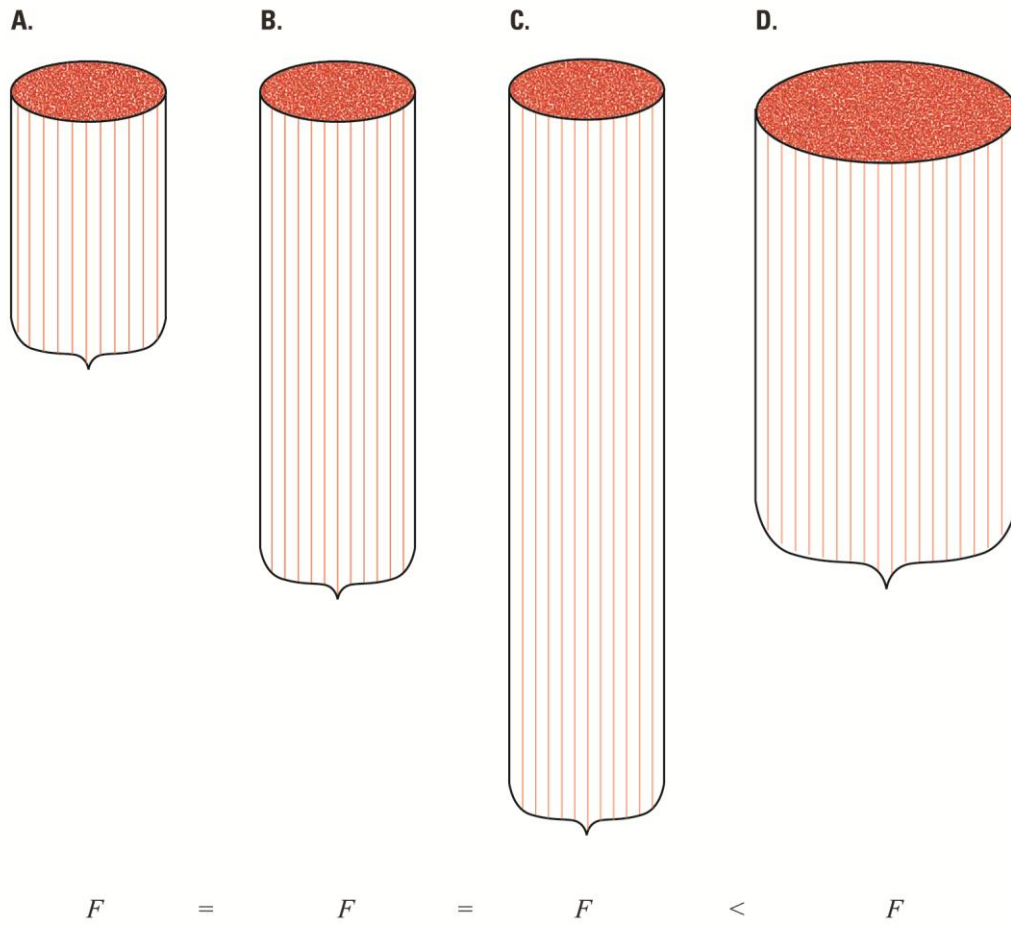


Figure 1.5.4: Adapted from (2002); depicting how muscle force is proportional to cross-sectional area. Insets A-C depict muscles that are of different length but have equal cross-sectional area and therefore produce the same force. Inset D. depicts a muscle with a greater cross-sectional area and thus more muscle fibres and greater tension generating capacity when all other things are equal.

1.5.4 Fibre Orientation

While the amount of force produced by a muscle is proportional to its cross-sectional area, this area is usually related to fibre type and orientation (Edgerton et al., 1995, McCall et al., 1996). The potential tension and force that a muscle is capable of generating, all other factors being equal, is also dependent on the orientation of its constituent fibres. Two general muscle fibre arrangements may be distinguished. Muscles in which fibres lie in parallel along the line of action or tension are referred to as parallel muscles. Muscles in which fibres lie obliquely to the line of action or force, inserting onto a common tendon are known as pinnate muscles (**Figure 1.5.5**). Mechanical advantages and disadvantages are features of each type of muscle (Kardong, 2002).

Generation of tension and force in both parallel and pinnate muscles is based upon the contraction of sliding actin and myosin filaments, with different mechanical properties arising due to differences in fibre arrangement. Pinnation allows the greater packing of fibres within the same overall muscle volume, yet fibre length is often reduced. Decrease in fibre length in combination with an inclined in the angle at which fibres lie relative to the line of action results in a muscle that has relatively reduced shortening and thus moves over a shorter distance. The increased fibre packing present in pinnate muscles however increases the amount of usable force generated along the line of muscle action. In comparison, parallel muscles are proficient at moving light loads through long distances (Kardong, 2002).

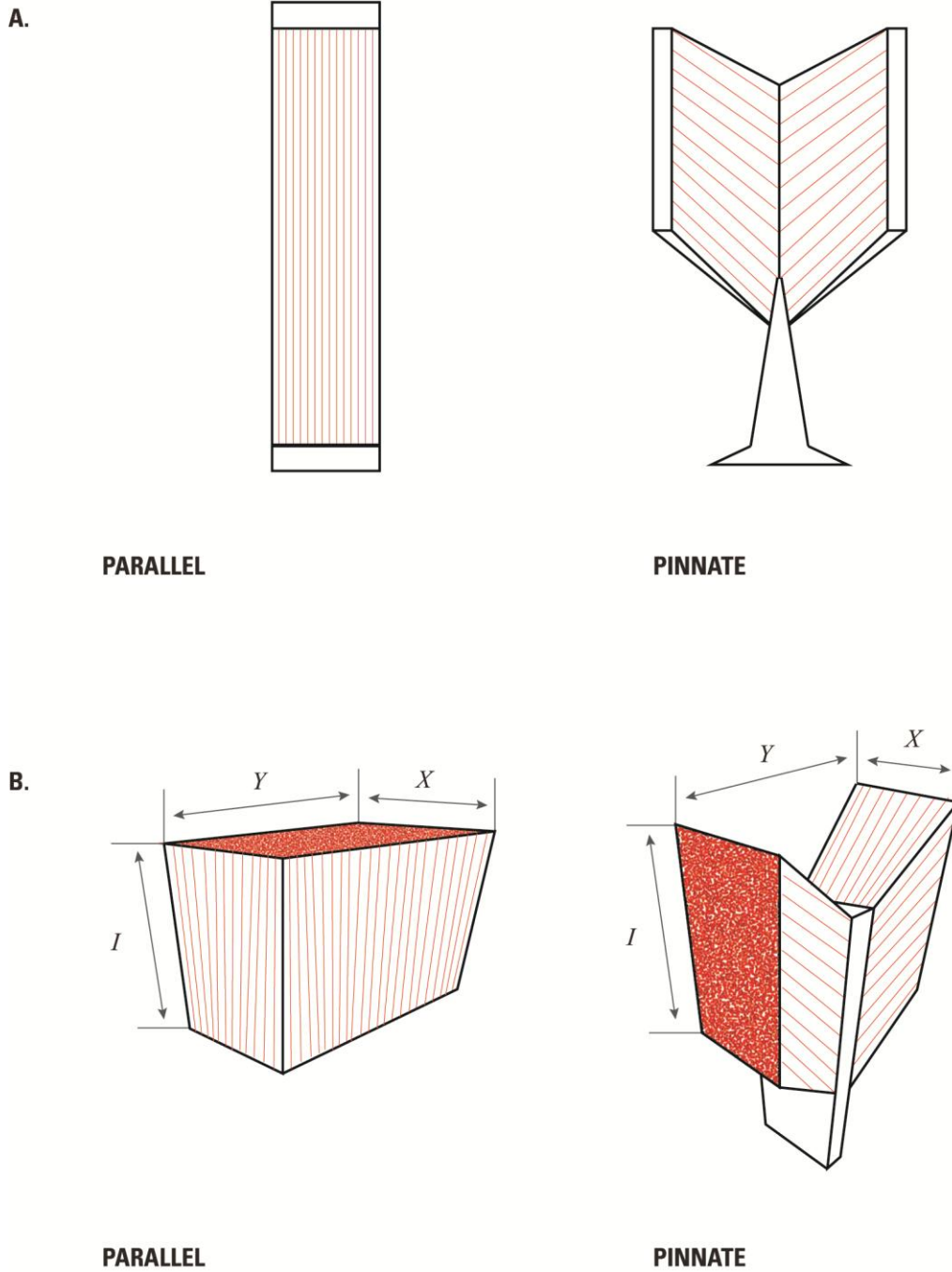


Figure 1.5.5: Adapted from Kardong (2002) showing *a.* parallel arrangement with muscle fibres aligned along the line of action, and pinnate arrangement with fibres oblique to the line of action; and *b.* the pinnate arrangement permitting the packing of more fibres within the same volume than the parallel arrangement does.

1.5.5 Myofibril Composition

While the organisation of fibres within a muscle and anatomical and geometric arrangements of muscle attachment sites on skeletal elements are important aspects of muscle function, the principal determinant of performance and movement of a muscle is directed by actin-myosin interactions with sarcomeres (Sciote and Morris, 2000). The relationship between the composition and performance of muscle fibres is now well investigated (Buonanno et al., 1998, Buonanno and Rosenthal, 1996, Abe et al., 2002, Usami et al., 2003), and as such evaluation of muscle fibre types and contractile protein isoforms allows further understanding of muscle function (Usami et al., 2003).

Myosin, composed of two heavy chains and four light chains, accounts for approximately half the total protein composition of myofibrils and is a vital protein required for muscle contraction (Pette and Staron, 1990, Shida et al., 2005, Usami et al., 2003). Myosin heavy chain (MHC) molecules, which form a major share of myosin molecules present in myofibrils, and are known to appropriately reflect muscle function (Shida et al., 2005). Nine isoforms of MHC in mammalian skeletal muscle have been identified: MHC-1; MHC-2a; MHC-2b; MHC-2d; MHC-eo; MHC-m; MHC- α ; MHC-emb and MHC-p (Brueckner et al., 1996, Gojo et al., 2002, Usami et al., 2003, Schiaffino and Reggiani, 2011, Schiaffino and Reggiani, 1996, Shida et al., 2005, Hori et al., 1998, Pette and Staron, 1990). These isoforms may be broadly classified into two type based upon contraction speed: fast muscle isoforms (MHC-2a; MHC-2b; MHC-2d) and slow muscle isoforms of which there is only one (MHC-1) (Brueckner et al., 1996, Schiaffino and Reggiani, 1996, Shida et al., 2005). Three isoforms (MHC-eo; MHC-m; MHC- α) are expressed in only specific muscles such as the extraocular muscles, heart muscle, and jaw closing muscles of primates. Two further isoforms (MHC-emb and MHC-p) are exclusive to certain embryonic stages (Usami et al., 2003, Schiaffino and Reggiani, 2011, Hoh and Hughes, 1988, Lyons et al., 1990, Pette and Staron, 1990).

Recent studies have investigated the muscle fibre composition of masticatory muscles, identifying the types of MHC isoforms present (Gojo et al., 2002, Usami et

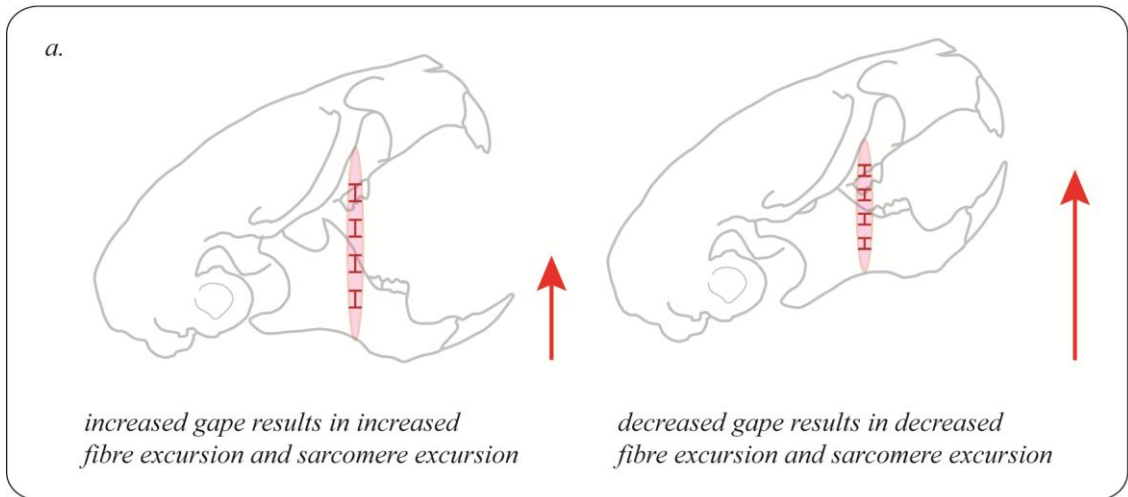
al., 2003, Shida et al., 2005). The presence of only fast-type MHC isoforms is reported in adult mice (Tuxen and Kirkeby, 1990, Eason et al., 2000, Shida et al., 2005), yet the potential for and manner of changes in fibre composition during ontogeny is yet to be fully elicited (Shida et al., 2005). Changes in the protein properties of mouse masseter muscle fibres during weaning suggests a potential functional adaptation in MHC isoforms in response to the post-weaning motion of chewing (Gojo et al., 2002). The presence of MHC-2b, which is believed to have a relatively fast contraction speed, was found to be predominantly coincident with the weaning period in the superficial masseter of the mouse (Gojo et al., 2002, Shida et al., 2005).

1.5.6 Trade-off Between Gape and Muscle Force Capacity

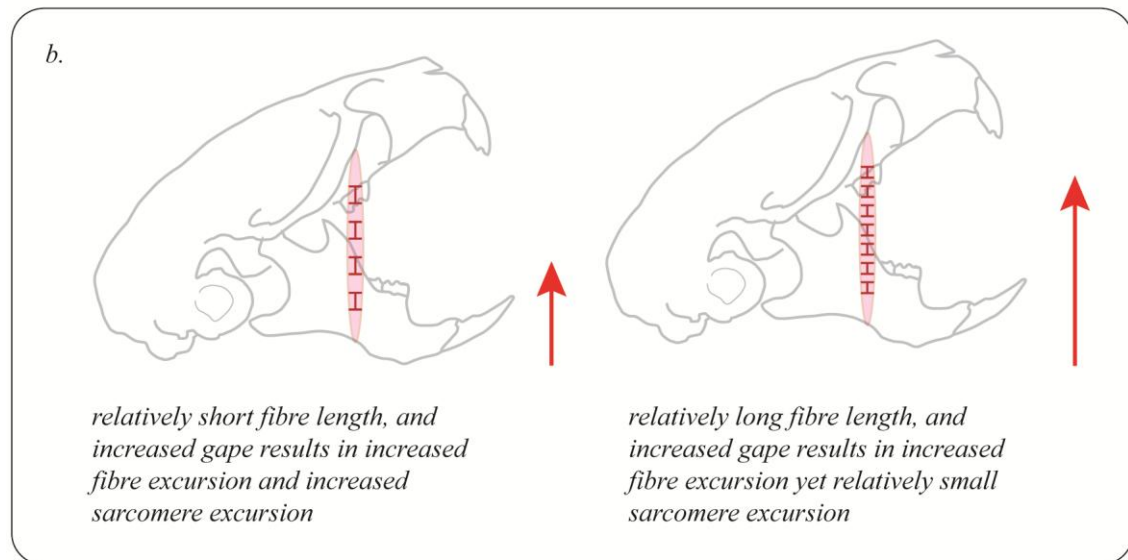
As described above, the length tension curve describes the amount of isometric force that a muscle can produce at a given sarcomere length (Eng et al., 2009, Gordon et al., 1966, Lieber and Boakes, 1988). Less advantageous positions on this curve are likely to have negative consequences for maintenance of active muscle force. A muscle fixed in a lengthened position will have limited overlap between filaments, decreased cross-bridge formation and thus relatively decreased tension. Cross-bridge formation and tension are only optimised when sarcomeres at a normal or intermediate length (Kardong, 2002, Hildebrand and Goslow, 2001). Thus in the mammalian jaw, gape angle may influence the amount of active force produced by the masticatory muscles. This theory is supported by analyses of gape angle and muscle function suggest that there is a trade off between gape angle and the mechanical advantage of the masticatory muscles (Dumont and Herrel, 2003, Herring and Herring, 1974, Turkawski and Van Eijden, 2001, Paphangkorakit and Osborn, 1997, Lindauer et al., 1993). Generally speaking, in mammals, a large gape angle results in stretching of the masticatory muscles, and thus excursion of muscle fibres and sarcomeres (Dumont and Herrel, 2003). As fibre length is a measure of the number of sarcomeres in series, the absolute stretch or excursion of a muscle fibres is equivalent to the excursion of each individual sarcomere in the series (Eng

et al., 2009, Gans, 1982, Williams and Goldspink, 1971, Williams and Goldspink, 1978). Thus, for a given sarcomere length, progressively increasing gape angles will result in progressively increasing fibre excursion and sarcomere excursion (**Figure 1.5.6 a.**). When a muscle acts from a gape angle that is great enough that sarcomere excursion has reached the point where that muscle is acting on the descending limb of the L-T curve, the ability to maintain muscle force will be decreased (Koolstra and van Eijden, 2004, Peck et al., 2000, Eng et al., 2009). Conversely, when a muscle is acting on the ascending limb of the L-T curve, increasing muscle length will lead to increasing muscle force until the point at which muscle length reaches the plateau of the curve (Eng et al., 2009). Thus, as a consequence of the length-tension relation of muscles, there appears to be an optimum gape angle at which maximum muscle force may be produced (Dumont et al., 2009, Manns et al., 1979, Mackenna, 1983, Fields et al., 1986, Kardong, 2002, Christiansen and Adolfssen, 2005). Decreasing bite force in relationship to increasing gape angles have been experimentally demonstrated in humans (Mackenna, 1983, Fields et al., 1986, Paphangkorakit and Osborn, 1997, Lindauer et al., 1993), primates (Vinyard et al., 2004), bats (Dumont and Herrel, 2003) and rodents (Nordstrom and Yemm, 1974, Williams et al., 2009), and theoretically in dingos (Bourke et al., 2008); while increased jaw muscle force production with increased muscle stretch has been demonstrated in a number of species (Nordstrom et al., 1974, Thexton and Hiiemae, 1975, Mackenna and Türker, 1978).

CONSTANT FIBRE LENGTH; VARIED GAPE



CONSTANT GAPE; VARIED FIBRE LENGTH



↑
muscle force performance

Figure 1.5.6: Showing the trade-off between gape and muscle force capacity. Inset *a.* depicts a muscle fibre of constant length at two different gapes. With increased gape there is increased sarcomere excursion, reducing force producing capacity of that fibre. Inset *b.* depicts two muscle fibre lengths at the same wide angled gape. With an increase in muscle fibre length and thus the number of sarcomeres, there is a reduction in individual sarcomere excursion and therefore an increase in force producing capacity of the muscle fibre.

Specialised mammalian taxa however show adaptation in both muscle attachment positions and internal muscular architecture that have resulted in species, such as those of the order carnivora, that are able to produce high muscle and thus bite forces at large gape angles (Sharon and Radinsky, 1980). Conversely others such as herbivores are adapted to producing high bite forces at low gape angles (Dumont et al., 2009). An increase in muscle fibre length and thus the number of sarcomeres in series, would result in a reduction in individual sarcomere excursion at high gapes when compared to the sarcomere excursion of a shorter muscle fibre at the same gape (**Fig 1.5.6 b.**). Indeed, Eng et al. (2009), in support of hypotheses of Taylor and Vinyard (2004), found that the relatively long jaw-closing muscle fibres of marmosets reduced muscle stretch at wider gapes, resulting in comparatively large bite forces at the extremes of jaw opening (see also Vinyard et al., 2003). Thus, in marmosets, the trade-off gape and force production is limited by relatively long jaw muscle fibres which facilitate wide gapes without negatively impacting muscle force production (Eng et al., 2009). A number of studies, both theoretical and experimental find adaptations in a wide range of species that compensate for the length-tension gape trade-off. Such adaptations include not only modification of fibre architecture (Eng et al., 2009, Williams et al., 2009, Langenbach and Hannam, 1999, Janis, 1983a), but also craniofacial architectural adaptations such as reduced condyle height (reducing muscle stretch at wide gapes) (Sharon and Radinsky, 1980, Vinyard et al., 2003) and reduced distance between the TMJ and muscle origin and insertions and the reduction in the angle between these two lines (stretch factor) (Weijs and Dantuma, 1975b, Satoh and Iwaku, 2006, Herring and Herring, 1974, Ravosa, 1990).

1.5.7 Muscle plasticity

Not only have adaptations of muscular morphology and architecture occurred over evolutionary time in order to meet species performance needs, but plastic adaptation over an individual's life-time also occur in these soft tissues. During ontogeny, masticatory musculature is modified in terms of its architecture (Herring and Wineski, 1986, Herring et al., 1991, Korfage et al., 2006); fibre composition (Maxwell et al., 1979, Shelton et al., 1988, Bredman et al., 1992, Anapol and Herring, 2000, Korfage et al., 2006, Abe et al., 2007, Langenbach et al., 2007), and in terms of mechanical advantage (Ravosa, 1991, Ravosa et al., 2010). Muscle plasticity may also occur in response to dietary modification (Taylor et al., 2006, Bernays, 1986, Ravosa et al., 2010). The transition from an infant to adult diet generally requires a greater force production capacity, and this may be achieved in some species via an increase in the number of type II muscle fibres (Sciote and Morris, 2000). Postnatal increases in type II muscle fibre cross sectional area have been found in a number of species, including mice, rabbits, monkeys and dogs (Maxwell et al., 1979, Shelton et al., 1988, Bredman et al., 1992, Anapol and Herring, 2000, Korfage et al., 2006, Abe et al., 2007, Langenbach et al., 2007). Experimental analyses have also shown alteration to abundance, type and cross-sectional area of masticatory muscle fibre types in response to the introduction of a high-fracture resistant diet (Ravosa et al., 2010). Attachment sites for jaw closing muscles may also exhibit postnatal plasticity in association with muscle hyperplasia, although this response is yet to be directly linked to altered loading and thus dietary changes (Byron et al., 2006, Byron et al., 2004, Nicholson et al., 2006, Ravosa et al., 2010). Such masticatory muscle attachment site plasticity may result in relatively long muscle in-levers, and thus an increase in the mechanical advantage of the masticatory system, conferring larger force production capacity at the dentition (Ravosa and Hylander, 1994, Ravosa, 1996, Ravosa, 1991, Ravosa and Daniel, 2010).

1.6 MASTICATORY BIOMECHANICS

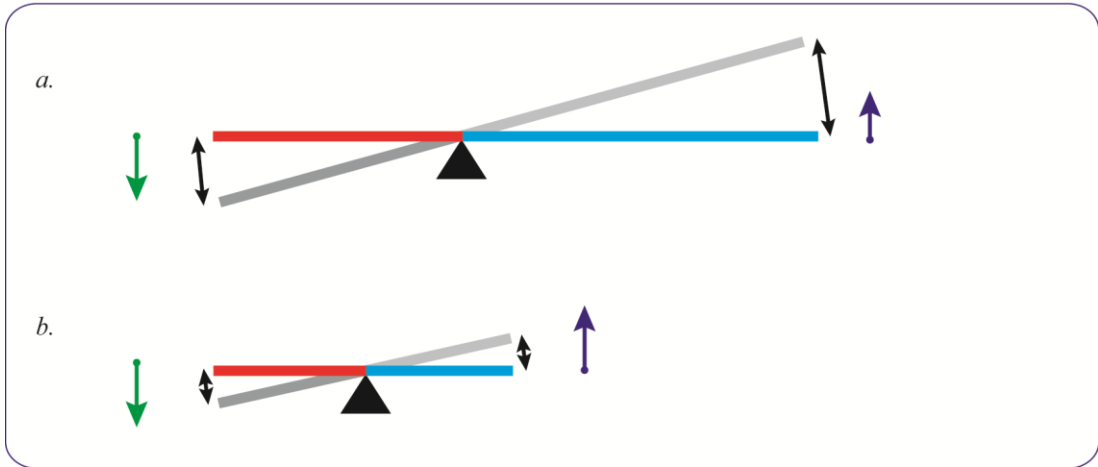
Mammalian jaws essentially function as lever systems, and thus biomechanical design principles may be used to explain the performance and often ecological differences associated with variation in mandibular and cranial morphology (Herrel et al., 2003).

Jaws operate as third class levers, that is, with the input force intersecting the out-lever between the pivot (fulcrum) and the point at which an output force is produced. The jaw-closing masticatory muscles supply the input force, the temporomandibular joint acts as the pivot or fulcrum, and the output force is produced at the dentition (Smith and Savage, 1956, Crompton and Hiiemae, 1969, Greaves, 1974, Hildebrand, 1988, Herrel et al., 2003).

In simple lever systems, the force exerted is determined by: the input force, the distance between the in-lever and the fulcrum, and the distance between the out-lever and the fulcrum (**Figure 1.6.1**). The shorter the out-lever becomes, the larger the output force of the system (**Figure 1.6.1 b**). However, within a given time increment, for a given input force, the displacement of the lever will also be determined by the length of the two lever arms. An increase in out-lever length will result in an increase in displacement within the same time period, and thus also a higher velocity of movement (**Figure 1.6.1 a**).

While the jaw closing system of mammals operates as a third order lever system, the biomechanical principals are the same. An increase in the out-lever length of the jaw (a long mandible) will result in increased speed (rapid opening closing of the jaw) but with reduced force at the dentition (**Figure 1.6.1 c**); while a decrease in the out-lever length (a short mandible) will result in decreased speed yet a powerful bite (**Figure 1.6.1 d**). Thus force transmission trades off directly with speed (Wainwright and Richard, 1995, Westneat, 1994).

SIMPLE LEVER SYSTEM



THIRD ORDER LEVER SYSTEM

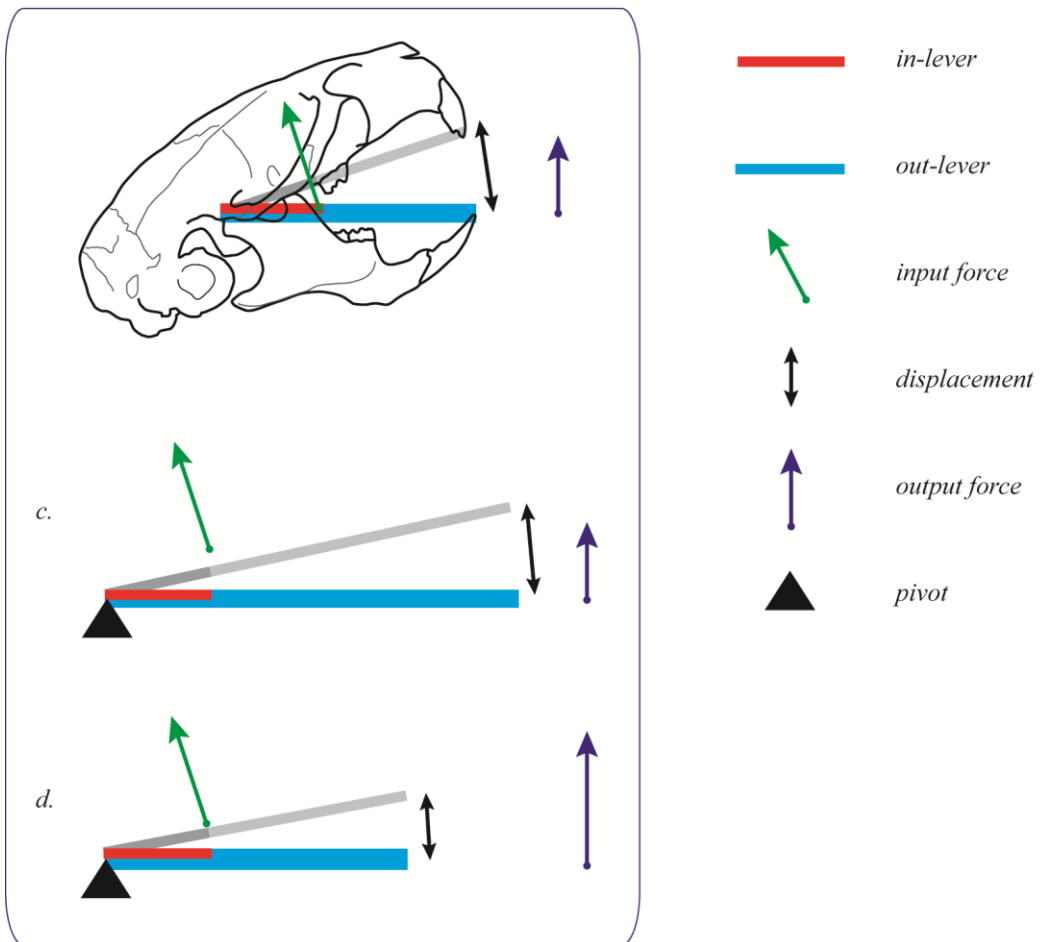


Figure 1.6.1: Adapted from Herrel et al. (2003); depicting the biomechanical trade-offs between speed and force generation in lever arm systems.

By modelling the jaw as a static third-class lever, mechanical advantage, a measure of the efficacy of lever system and thus how much force is transferred through it, may be calculated (Anderson, 2008, Vinyard, 2008). Each muscle in-lever is calculated as the distance from the fulcrum to the point at which the input (muscle) force is applied to the lever. The jaw out-lever is calculated at the distance from the point at which the output force (force applied by the dentition) is applied by the lever. Mechanical advantage is proportional to the ratio of the in- and out- levers. Thus variation in skull morphology leading to changes to either or both the in- and out- lengths may alter the mechanical advantage of the system and thus the production of force at the dentition. When the in-lever length and input force remain static, a reduction in the distance between the temporomandibular joint (the fulcrum) and the dentition (reduced out-lever length) will reduce the speed of jaw closure but increase the mechanical advantage of the system and therefore the force production at the dentition (**Figure 1.6.2 a.**). Conversely and increase in jaw length (out-lever length) will increase the speed of jaw closure yet reduce mechanical advantage and force production. Alterations to muscle in-lever lengths however also impact on the mechanical advantage of the system (Smith and Savage, 1956, Reduker, 1983). When out-lever length and input force are constant, a reduction in in-lever length will decrease mechanical advantage, and on the other hand an increase in in-lever length will increase mechanical advantage (**Figure 1.6.2 b.**). The trade-off between speed and force of the lever arm system when jaw out-lever length is varied may therefore, theoretically, be compensated for via alteration to muscle in-lever lengths. While an increase in out-lever length will increase speed at the cost of force, an increase in muscle in-lever length alongside an increase out-lever length has the potential to compensate for force trade-off. Herbivores may be predicted to show an increase in jaw closing muscle in-levers alongside a decrease in jaw out-lever length, leading to high bite forces at the cost of speed. Carnivores may be predicted to show an increase in jaw opening muscle in-levers in association with increased jaw out-levers, conferring rapid jaw movements (Metzger and Herrel, 2005). Variation in both the in-lever length alongside the out- lever length however also has the potential to maintain mechanical advantage of the system (**Figure 1.6.2 c.**). Thus markedly different jaw shapes may possess the same mechanical advantage (**Figure 1.6.3**). An elongation of the mandibular ramus while corpus length is held constant will alter

both the in- and out-lever of the jaw (**Figure 1.6.3 b.**), while a shortening of the corpus while the ramus is held constant (**Figure 1.6.3 c.**) could achieve the same lever ratio and thus mechanical advantage (Vinyard, 2008).

Mechanical advantage of the jaw is a widely used measure of performance potential amongst species (Adams and Rohlf, 2000, Westneat, 2003, Wainwright et al., 2004, Metzger and Herrel, 2005, Stayton, 2006, Vincent et al., 2007). In this thesis mechanical advantage is measured as a ratio of the jaw out-lever and muscle in-lever in a model sample of mice representing variation in cranial length. Variation in cranial length is present both within and between many species, and also is seen to occur both during development and evolution. Any variation in cranial length is likely to modify the jaw out-lever and thus the mechanical advantage of an individual. Modification to the mechanical advantage, and thus efficiency of the masticatory lever arm system to transmit force, has the potential to introduce performance differences between individuals. As cranial length variation is commonly seen between individuals and species, and during development and evolution, this thesis aims to explore the capacity of the craniomandibular complex to plastically adapt to compensate for changes in the jaw out-lever such that mechanical advantage is maintained. In a highly integrated complex (**Section 1.3**), it is proposed that variation in cranial length and therefore out-lever length could lead to compensatory plastic adaption (**Section 1.3.3**) in regions such as those influencing masticatory muscle attachment sites, such that muscle in-lever lengths were epigenetically adapted in concert with out-lever lengths and mechanical advantage maintained. While functionally driven adaptive plasticity within the craniomandibular complex in response to varied cranial length is little explored in the literature, a number of authors have investigated the mechanical advantage of the masticatory system both during ontogeny and between species.

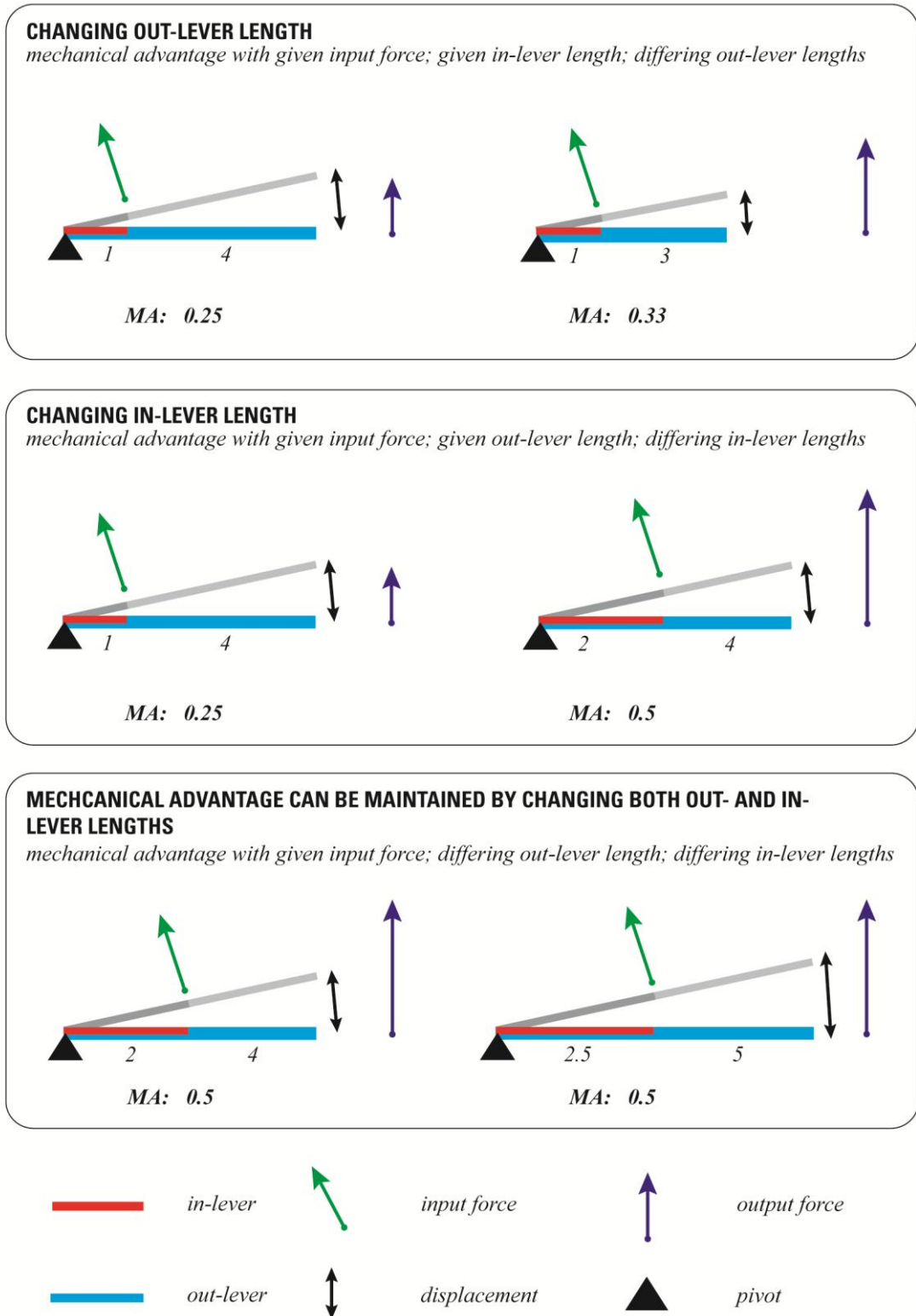


Figure 1.6.2: The influence of in- and out-lever lengths on mechanical advantage (force generation) in lever arm systems. When all other things remain equal, reducing out-lever length increases mechanical advantage (MA) and increasing in-lever length increases MA. Alteration to both in- and out-lever lengths can yield the same ratio (MA) despite absolute differences in lengths.

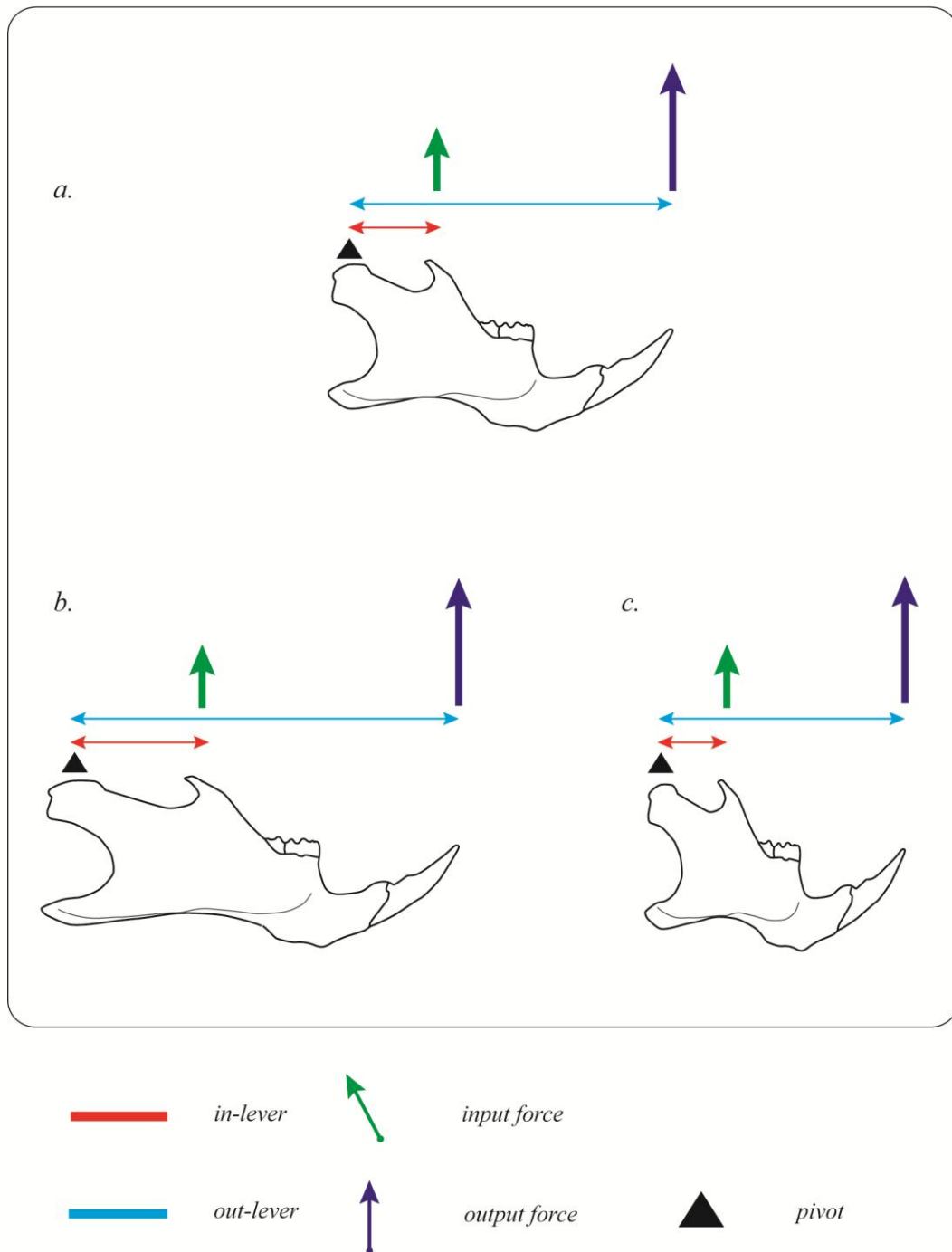


Figure 1.6.3: Adapted from Vinyard (2008); depicting theoretical changing jaw shapes with equivalent functional consequences. Inset *a.* depicts a theoretical jaw morphology with a given in-lever (red), out-lever (light blue) and input force (green), conferring a particular output force (dark blue). Inset *b.* depicts an alternative theoretical jaw shape, where the mandibular ramus is elongated and the mandibular corpus held constant when compared to inset *a.* This results in an increase in both the in- and out-lever length, maintaining the same ratio as in inset *a.* such that with the given input force the same out-put force is achieved. Inset *c.* depicts a jaw morphology with a shortened mandibular corpus yet constant ramus length when compared to inset *a.* In this theoretical example both the in-lever and out-lever are proportionally reduced, resulting in the same out-put force for a given input force as in insets *a.* and *b.*

While in baboons the efficiency of the masticatory system is reported to reduce throughout growth due to a progressive elongation of the muzzle (Oyen et al., 1979), the mechanical advantage of the masticatory muscles in macaques is suggested to increase with growth due to these muscles becoming more closely positioned to the distal molars (Dechow and Carlson, 1990). The latter authors also find a size related trend, with smaller adults showing greater mechanical efficiency than their larger counterparts. This result was found to be due to comparable muscle in-lever arms in different sized specimens but increased out-lever lengths in those with longer faces, thus reducing mechanical advantage in these individuals (Dechow and Carlson, 1990). Other authors however have found a relative maintenance of the mechanical advantage of the masticatory system despite the dramatic size and shape changes associated with ontogeny. La Croix et al. (2011b) found early achievement of adult mechanical advantage measures in an ontogenetic sample of coyotes, proposing that this early attainment of mechanical efficiency may assist the feeding performance of juveniles who have a reduced bite force when compared to adults. Similar results are reported in the spotted hyena, where mechanical advantage of the masseter muscle was found to be maintained throughout ontogeny (Tanner et al., 2010). Mechanical advantage of the temporalis muscle in the spotted hyena was found to be greater in adults than in juveniles (Binder and Van Valkenburgh, 2000). As mechanical advantage of the jaw closing muscles is greater when bites are placed closer to the jaw joint (Turnbull, 1970, Hildebrand, 1988), the authors attribute this increase in mechanical advantage to be due to a more posterior positioning of the dentition relative to the jaw joint (Binder and Van Valkenburgh, 2000, Biknevicius, 1996). Other authors however have also found a maintenance of mechanical advantage despite specimen size differences. The mechanical advantage of jaw-adductor muscles in banded watersnakes were found not to alter alongside either head or body size, and thus both large and small snakes retain the same jaw-closing efficiency (Vincent et al., 2007). Comparable results showing a maintenance of mechanical advantage with increasing body size are also reported in lizards (Meyers et al., 2002), frogs (Birch, 1999), and fish (Richard and Wainwright, 1995).

Mechanical advantage is however not the only biomechanical measure indicating the force production capacity of the cranium and mandible. One of the key functional

performance measure of the craniofacial complex when considering masticatory ability is bite force (Herrel et al., 2002, Herrel et al., 2001, Aguirre et al., 2003, Freeman and Lemen, 2007). Both *in vivo* bite force measurement (Hylander et al., 1992, Aguirre et al., 2002, Dumont et al., 2009, Santana and Dumont, 2009, Williams et al., 2009, Santana et al., 2010, Measey et al., 2011, Vanhooydonck et al., 2011, Schaerlaeken et al., 2012, Chazeau et al., 2013), and estimates of bite force capacity (Thomason et al., 1990, Thomason, 1991a, Christiansen and Wroe, 2007, Ellis et al., 2008, Curtis et al., 2010b, Davis et al., 2010, Wroe et al., 2005) are commonly used to investigate the relationship between the form and function of the cranium and mandible. Bite force estimates are based upon measures of cranial and mandibular morphology, muscle morphology and muscle physiology. By modelling the jaw as a third-class lever (Crompton, 1963, Greaves, 1978) and providing a measure of masticatory muscle force magnitudes, an approximation of the bite force of a particular phenotype may be calculated. Muscle force magnitude itself may be estimated from masticatory muscle data including attachment areas, directions and locations relative to the temporomandibular joint, pinnation and mass (Weijjs and Dantuma, 1975b, Antón, 1999, Ross et al., 2005, Curtis et al., 2010b). Physiological cross-sectional area (PCSA) is the standard measure of muscle area (Antón, 1999, Perry, 2008, Taylor et al., 2009, Curtis et al., 2010b, Davis et al., 2010, Santana et al., 2010, Herrel et al., 2008), while estimates of PCSA are also possible (Kiltie, 1982, Kiltie, 1984, Thomason, 1991a, Davis et al., 2010). Multiplication of PCSA values with muscle stress measures provides an estimate of muscle force magnitude (Mendez and Keys, 1960, Van Ruijven and Weijjs, 1990).

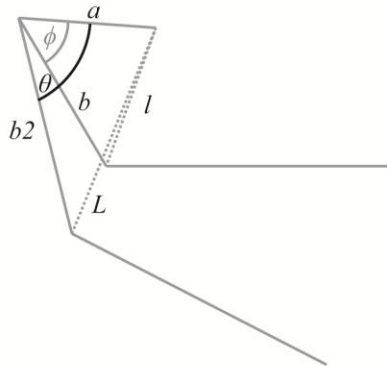
Bite force is influenced by multiple parameters, including both cranial and mandibular morphology as well as jaw muscle anatomy, architecture, orientation and position. An increase in muscle fibre pinnation (increasing the packing of muscle fibres), an increase in masticatory muscle PCSA and an increase in the mechanical advantage of the masticatory system will all have the result of increasing bite force (Smith and Savage, 1956, Turnbull, 1970, Taylor and Vinyard, 2004, Perry and Wall, 2008). Many of these aspects which increase bite force capacity may however simultaneously decrease gape capacity, and thus there is often a trade-off between bite force and gape (Williams et al., 2009). An increase in muscle fibre length, a

reduction in the height of the mandibular condyle, an increase in the anteroposterior length of the mandibular condyle, an increase in the ratio of the distance from the condyle to the origin and insertion of the masseter, and an increase in jaw length all have the effect of increasing gape capacity (Herring and Herring, 1974, Herring, 1975, Smith, 1984, Gans and De Vree, 1987, Vinyard et al., 2003, Taylor and Vinyard, 2004, Perry and Wall, 2008). A decrease in bite force capacity in association with increased gape has been reported in a range of species (Mackenna, 1983, Fields et al., 1986, Lindauer et al., 1993, Paphangkorakit and Osborn, 1997, Nordstrom and Yemm, 1974, Dumont and Herrel, 2003, Vinyard et al., 2004, Bourke et al., 2008).

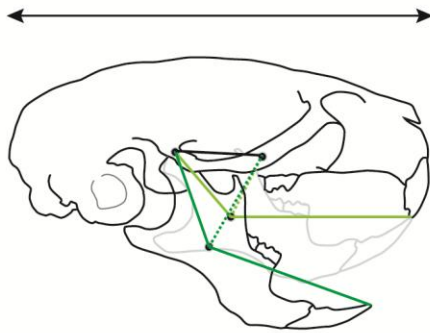
As discussed in **Section 1.5** (Muscle Biology) an increase in muscle fibre length may allow some specialists to produce high bite forces at wide gapes (Eng et al., 2009, Taylor and Vinyard, 2004, Vinyard et al., 2003). Adaptation to muscular attachments and the bony morphology of both the cranium and mandible may also allow high forces to be produced at the dentition at wide angled gapes. Stretch factor is a measure which relates the effect of muscle stretch and gape angle to the force producing capacity of the masticatory apparatus (Williams et al., 2009, Herring and Herring, 1974). **Figure 1.6.4 a.** illustrates calculation of the stretch factor for the deep masseter in hypothetical mouse skulls. Lengths a and b represent distances from the origin and insertion of the deep masseter muscle, respectively, to the temporomandibular joint, and ϕ is the angle between these two lengths. Length l represents the length of the muscle when the dentition are in occlusion. Length b_2 represents the distance from the muscle insertion to the TMJ and, L the length of the muscle when the jaw is rotated through the angle θ (Herring and Herring, 1974). Stretch factor (L/l) may be decreased by increasing the difference between the distance from the TMJ to the muscles origin and the distance from the TMJ to the muscles insertion (the ratio of lines a and b). Stretch factor is also decreased when the angle formed by lines a and b increases (Herring and Herring, 1974, Williams et al., 2009). Any such decrease in stretch factor is favourable for producing force at a large gape, and any changes in lengths a and b , and angle ϕ will alter the muscles line of action, and thus the spectrum of jaw movements that can be produced (Herring and Herring, 1974).

This thesis examines both the form and function of the cranium and mandible in a model sample of mice showing extremes of cranial length, the latter being a key morphological variant seen both within and between species and in development and evolution. Mutations specifically targeting cartilage growth are present in two strains of mice, and as such direct effects are limited to crania. The ability of the complex to plastically adapt in order to maintain both correlation between cranial and mandibular form, and function is assessed. The measure of function assessed is mechanical advantage, taken as the ratio of the muscle in-lever length and jaw out-lever length. As the morphological variance of the sample is dominated by cranial length differences, key differences are expected to be present between strains in terms of jaw out-lever length. As mastication is a critical function, it is predicted that a mechanism may exist by which the impact of individual, or developmental stage differences in key functional parameters such as cranial and thus out-lever length are minimised. An isolated change in cranial length would result in a change in mechanical advantage and thus the functional performance of the complex in terms of mastication. Plastic adaptation (see **Section 1.3**) in other regions of the complex could result in the coordinated epigenetic adaptation of muscle in-levers such that performance in terms of mechanical advantage was maintained despite differences in cranial length.

A. CALCULATION OF STRETCH FACTOR

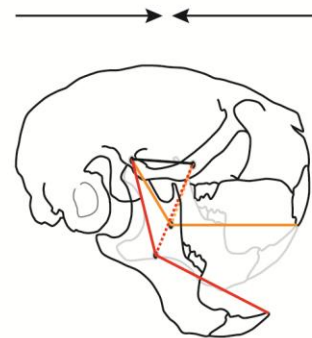


B.



relative increase in stretch factor
relative decrease in the ability to produce force at large gapes

C.



relative decrease in stretch factor
relative increase in the ability to produce force at large gapes

D. COMPARISON OF STRETCH FACTOR FOR SKULLS B. AND C.

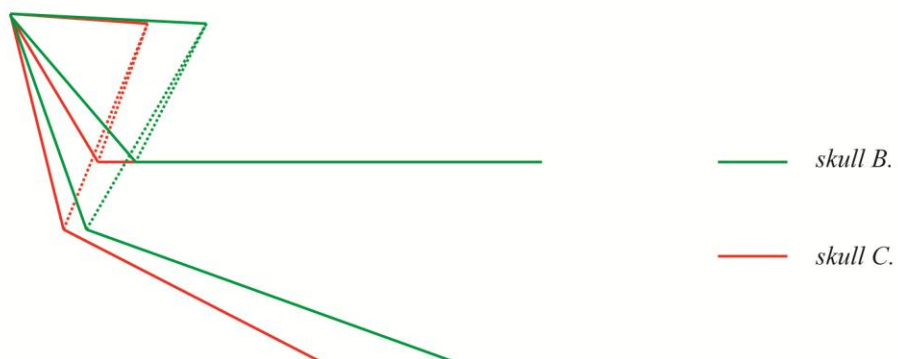


Figure 1.6.4: Calculation of stretch factor, theoretical depiction of changing cranium and mandibular shapes with different abilities to produce force at wide gapes; adapted from Herring and Herring (1974).

1.7 CONCLUSION TO INTRODUCTION

This thesis aims to explore the potential of the cranium and mandible to plastically adapt in a coordinated manner in response to alteration to once component of form early on in development. This plastic potential is investigated in terms of both form and function. An overview of concepts behind both these broad aims and more specific questions to be addressed, as well as the model sample utilised in this thesis, have been explored through this introduction.

A cranial length mouse model is employed, reflecting both morphological change occurring in development, and common patterns of morphological variance observed intra- and inter-specifically. Three strains of mice, two mutant strain and one common wild-type strain make up the model sample. The brachymorph mutant strain has a cranial phenotype dominated by a reduction in length, and the pten mutant strain has a cranial phenotype dominated by an increase in length. As both mutant strains have the same genetic background strain as the wild-type sample, the C57 wild-type strain has an intermediate length when compared to the mutant strains which display the extremes of cranial length. Both the brachymorph and pten mutations specifically target cartilage growth (**Section 1.4**), and thus the overwhelming influence of both mutations is limited to the cranium. Mandibular morphology observed in the two mutant strains which diverges from that of the wild-type strain may therefore reasonably be held to stem from epigenetic plastic adaptation (**Section 1.3**). This model sample is thus ideal to explore questions regarding the plastic potential of the craniomandibular complex. Firstly this thesis aims to address whether a mutationally induced change in cranial length leads to epigenetic plastic adaptation in the mandible such that cranial and mandibular morphology remain coordinated. Secondly this thesis aims to address whether plastic adaptation in regions of the overall complex may maintain parameters of functional performance when such an isolated regional change (in cranial length) is introduced.

Further details and exploration of the sample utilised, and methods applied in this thesis are given in **Chapter 2**.

In order to address these two broad aims, firstly a comprehensive understanding of the anatomy of the *Mus musculus* cranium and mandible must be present, both in terms of bony (**Section 1.4**), and muscular (**Section 1.5**) morphology. While the cranial skeletal anatomy of both rodents in general, and more specifically the mouse is well documented (**Section 1.2**), surprisingly the masticatory musculature of *Mus musculus* is poorly described in the current literature. **Chapter 3** of this thesis therefore focuses attention on providing a clear and detailed description of the masticatory musculature of *Mus musculus*, using modern day scanning and imaging techniques. Details and data elucidated in this study are then able to be utilised to develop appropriate methods to address the key aims of this thesis.

When a specific mutation primarily influencing cranial length is introduced to a common mouse strain, the potential of the mandible to plastically adapt to have a form correlated with that of its crania is explored in **Chapter 4**. It is predicted that strong integration (**Section 1.3**) between the cranium and mandible will result in strong patterns of covariance between crania and mandibles in all three strains, despite the presence of mutations in two strains which influence chondrocranial growth alone. Such finding of strong covariance between cranial and mandibular morphology would therefore indicate mandibular morphology in the two mutant strains to be largely influenced by epigenetic plastic adaptation. Furthermore it is predicted that as patterns of integration and modularity are likely developmental and/or functional in nature (**Section 1.3**), patterns of covariance between crania and mandibles in all three strains are likely to show common elements.

The potential of the craniomandibular complex to plastically adapt to maintain function is addressed in **Chapter 5**. Taking the mechanical advantage of the lever arm system of the jaw (**Section 1.6**) as a measure of masticatory functional performance, the capacity of the cranium and mandible to plastically adapt to maintain function is explored. It is predicted that in a highly integrated craniomandibular complex, a change in jaw out-lever length could result from a plastic change in mandibular length in coordination with a mutationally induced change in cranial length. An isolated change in jaw-out lever length would result in a reduction of mechanical advantage of the lever-arm system of the jaw (**Section 1.6**). In a highly integrated complex where a change in cranial length resulted in a

compensatory plastic change in mandibular length, it might also be predicted that a change in mandibular and therefore jaw out-lever length could lead to correlated plastic adaptation in other regions of the complex, such that muscle in-lever length too saw adaptation. A reduction in muscle in-lever length alongside a reduction in jaw out-lever length, and an increase in muscle in-lever length alongside an increase in jaw out-lever length could both serve to maintain mechanical advantage and thus one parameter of masticatory performance potential. **Chapter 5** thus explores the capacity of the cranium and mandible to plastically adapt in order to maintain one element of masticatory functional performance when variation in one critical parameter of form is introduced early on in development.

2.1 MATERIALS

2.1.1 Sample details

The sample utilised in this thesis consists of three strains of mice, two mutant mice strains and a wild-type control strain. Mutations present in both the brachymorph and pten strains influence chondrocranial growth early on in development, resulting in a reduction in cranial length in the brachymorph strain, and an increase in cranial length in the pten strain. Both brachymorph and pten mutations are expressed on the same genetic background strain (C57BL/6J) as the control wild-type mouse. Thus a model sample of three mouse strains of varying cranial length is constructed (**Figure 2.1.1.**).

Micro-CT scans of whole heads including soft tissue, for all three strains, were provided by Benedict Hallgrímsson, University of Calgary. To control for age and strain within the sample, both mutant strains as well as the wild-type strain were adult mice (490 days) from similar genetic backgrounds (C57BL/6J). Brachymorph mutants were sourced from the Jackson Laboratory (C57BL/6J background, the Jackson Laboratory, Bar Harbor, ME, USA). To generate the Pten mutant sample, mice with floxed Pten (tumour-suppressor phosphatase with tensin homology) alleles (90% C57BL/6J background) were provided by T. W. Mak (Ontario Cancer Institute, ON, Canada). These floxed Pten mice were then crossed with transgenic mice (on a C57BL/6J background), sourced from the Jackson Laboratory (The Jackson Laboratory, Bar Harbor, ME, USA), expressing Cre recombinase under control of the relatively cartilage-specific Col2a1 gene promoter (Ovchinnikov et al., 2000, Hallgrímsson et al., 2007). All heterozygous pten individuals were removed from the sample.

Mice of all three strains were micro CT-scanned (Scanco Viva-CT40, Scanco Medical AG, Basserdorf, Switzerland) at 35- μ m resolution (70 kV, 160 mA, 500 projections) (Hallgrímsson et al., 2007).

A total of 76 individuals make up the sample used in this thesis (28 wild-type; 25 brachymorph; 23 pten). For **Chapter 5** five individuals were removed from the sample due to an inability to clearly define the masticatory muscle attachment areas required to calculate mechanical advantage, leaving a sample of 71 individuals (25 wild-type; 24 brachymorph; 22 pten).

BRACHYMORPH

a. cranium



b. mandible



C57

d. cranium



e. mandible



PTEN

f. cranium



g. mandible



Figure 2.1.1: Depicts representative average cranial and mandibular phenotypes for brachymorph (insets *a* and *b*); C57 (insets *d* and *e*) and pten (insets *f* and *g*) strains.

2.1.1.1 *C57 (wild-type) strain*

The C57BL/6J (C57) mouse strain (**Figure 2.1.1; insets d and e.**) is one of the most common backgrounds for transgenic mice (Hallgrímsson et al., 2004b, Hallgrímsson et al., 2004a). This inbred mouse strain is also the most commonly used strain in biomedical research, utilised in a wide range of studies (Black et al., 1998, Champy et al., 2008, Drake et al., 2001, Toye et al., 2005, Chinwalla et al., 2002). Maintained by brother and sister mating for hundreds of generations (www.Jax.org), the C57BL/6J strain has minimal genetic variance (Hallgrímsson et al., 2006), and is a permissive for the maximal expression of most mutations (Jackson-Laboratory, 2013). This strain forms the background strain upon which both the *pten* and *brachymorph* mutations are expressed, and thus is the appropriate control strain against which to compare the *brachymorph* and *pten* mutant strains. This strain has also been the standard control in a number of other morphological investigations utilising mutant mouse strains including the *pten* and *brachymorph* strains (Jamniczky and Hallgrímsson, 2009, Hallgrímsson et al., 2004b, Hallgrímsson et al., 2004a, Hallgrímsson et al., 2006).

2.1.1.2 *Pten strain*

Pten mutants (**Figure 2.1.1; insets f and g.**) have a relatively long-faced morphology that results from crossing mice with floxed *Pten* alleles with transgenic mice on a C57BL/6J background, a technique referred to as conditional gene deletion.

Conditional gene deletion is often approached via the Cre/LoxP system, this being a technique which allows the creation of tissue-specific knockout mice. Cre- and loxP-containing strains are developed independently and then crossed to generate offspring that carry both additions. The first strain contains a targeted gene flanked by two loxP sites, this commonly being termed a ‘floxed’ gene. The second strain is

a conventional transgenic mouse line (one in which cloned genetic material has been transferred) expressing Cre recombinase under the control of a tissue- or cell-specific promoter. Cre recombinase of the P1 bacteriophage efficiently catalyses two of its consensus DNA recognition sites (*loxP* sites). Offspring generated via the crossing of the floxed strain and the Cre-expressing strain may inherit both the floxed gene and the Cre- transgene. In such individuals, tissues in which the Cre recombinase is expressed the floxed DNA segment will be excised and hence rendered inactive, whilst cells and tissues in which the Cre recombinase is not expressed the floxed gene will remain active (Kos, 2004, Rajewsky et al., 1996, Gassmann and Hennet, 1998, Rossant and McMahon, 1999, Orban et al., 1992, Nagy, 2000, Hamilton and Abremski, 1984).

PTEN (phosphatase and tensin homolog deleted on chromosome 10) is a tumour suppressor gene (Sansal and Sellers, 2004) that negatively regulates the phosphatidylinositol 3' kinase signalling pathway. Phosphatidylinositol 3' kinase enzymes are involved in cellular functions such as growth, proliferation, differentiation and survival (Sansal and Sellers, 2004, Hallgrímsson et al., 2007). The transgenic mice used in combination with mice with floxed Pten alleles express Cre recombinase under control of the relatively cartilage-specific *Col2al* gene promoter (Hallgrímsson et al., 2007). *Col2al* refers to the pro α 1(II) collagen gene which encodes Type II collagen, the latter being a principal marker of chondrocyte differentiation (Ovchinnikov et al., 2000, Mayne, 1990).

Through the breeding of floxed pten mice with *Col2al-Cre* mice individuals are developed that carry both the floxed gene and the Cre- transgene. In these individuals the negative regulation of the phosphatidylinositol 3' kinase signalling pathway is blocked and thus cellular functions such as the growth and proliferation is increased, and this increase is specific to type II collagen. Only homozygous (Cre fl/fl) individuals were included in the sample.

2.1.1.3 *Brachymorph strain*

Brachymorph (bm) mutants (C57/BL/6J background, the Jackson Laboratory, Bar Harbor, ME, USA) have a relatively short-faced morphology that results from an autosomal recessive mutation in the phosphoadenosine-phosphosulfate synthetase 2 gene (*Papss2*) (Kurima et al., 1998). The *Papss2* gene mutation in the brachymorph mouse results in an extracellular matrix alteration that leads to a dramatically reduced growth of cartilage, thus all skeletal elements that rely upon cartilage are abnormally small (Hallgrímsson et al., 2006, Kurima et al., 1998, Orkin et al., 1976, Lane and Dickie, 1968, Ford-Hutchinson et al., 2005). As the growth of dermatocranial elements does not directly depend upon cartilage growth in the skull the direct effects of this mutation should be confined to the chondrocranium (Kaufman and Bard, 1999, Hallgrímsson et al., 2006). The brachymorph mutant phenotype (**Figure 2.1.1; insets a and b.**) is characterised by a shortened yet complex craniofacial morphology with a distinctive dome-shaped cranium (Ford-Hutchinson et al., 2005). Further details of the *Papss2* gene mutation in the brachymorph mouse are given in Hallgrímsson et al. (2006) and Ford-Hutchinson et al. (2005).

2.1.2 Sample exploration

Both mutant strains (*pten* and *brachymorph*) have a known specific mutation which selectively affects chondrocranial growth, with no known effect on either mandibular or muscular development or morphology. These mutations result in a relatively long-faced morphology in the *pten* mutant and a relatively short-faced morphology in the *brachymorph* mutant. However, while the *brachymorph* morphology results from an autosomal recessive mutation in the phosphoadenosine-phosphosulfate synthetase 2 gene (*Papss2*) (Kurima et al., 1998, ul Haque et al., 1998), the *pten* morphology is the result of the crossing of mice with floxed *Pten* alleles with transgenic mice (C57BL/6J background) expressing Cre recombinase under control of the relatively cartilage-specific *Col2a1* gene (Ovchinnikov et al., 2000; Hallgrímsson et al., 2007).

We might therefore expect that despite the two mutations having analogous yet opposite effects on cranial morphology, as the methods involved in the development of these two forms differ there may too be differences in ways in which these two extremes of cranial length are achieved by the mutant strains. For example, it is possible that the pten mutation predominantly increases chondrocranial growth in a more anterior region of the cranium, whilst the brachymorph mutant shows decreased chondrocranial growth in the posterior regions of the cranium.

In this section the morphology of the sample is explored. Firstly differences in craniomandibular length between the three strains are examined by means of three dimensional linear measurements taken on both the cranial base and the mandible. Secondly, principal component analysis is employed to describe key differences in form between the three strains in both the crania and mandibles. Thirdly principal component analysis is applied to each individual strain to establish key patterns of morphological variance within each strain.

2.1.2.1 Exploration of sample cranial and mandibular lengths

The pten mutant has a relatively long-faced morphology (Hallgrímsson et al., 2007), the brachymorph mutant a relatively short-faced morphology (Hallgrímsson et al., 2006, Ford-Hutchinson et al., 2005), and the C57 ‘wild-type’ morphology reflects a point midway between the two extremes of the mutant forms.

In order to ascertain whether there is a true statistical difference in craniomandibular length between the three strains of mice in our sample, three dimensional linear measurements were taken on both the cranial base and the mandible of all individuals.

A threshold was applied to Micro-CT scans of all individuals in Amira5 visualisation software (VisageImaging, 2008) in order to generate a three dimensional surface of both the crania and mandibles (details of methodology and validation given in **Section 2.2.2.1**). Three dimensional linear measurements were computed on both the

cranial base, and the mandible. To evaluate cranial length in the three strains, three measurements were taken on the cranial base: length ab_c ; length bc_c and length ac_c (**Table 2.1.1, Figure 2.1.2**). To assess mandibular length in the three strains, three measurements were taken on the cranial base: length ab_m ; length bc_m and length ac_m (**Table 2.1.1, Figure 2.1.3**). These lengths were selected in order to represent differing portions of the structures. Lengths ab_c and ab_m represent an anterior region of the cranium and mandible respectively, lengths bc_c and bc_m represent a posterior portion of the cranium and mandible respectively, and lengths ac_c and ac_m give an approximation of the overall length of each structure.

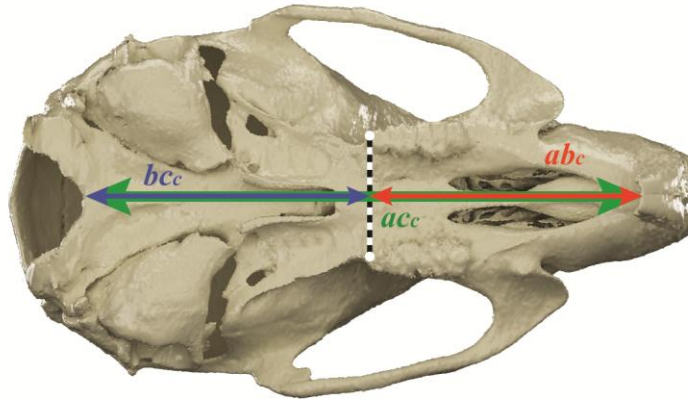


Figure 2.1.2: Linear measurement taken on crania. Length ab_c represents the anterior region of the cranium; length bc_c the posterior region; and length ac_c the full length of the cranium. See **Table 2.1.1** for definitions of lengths.

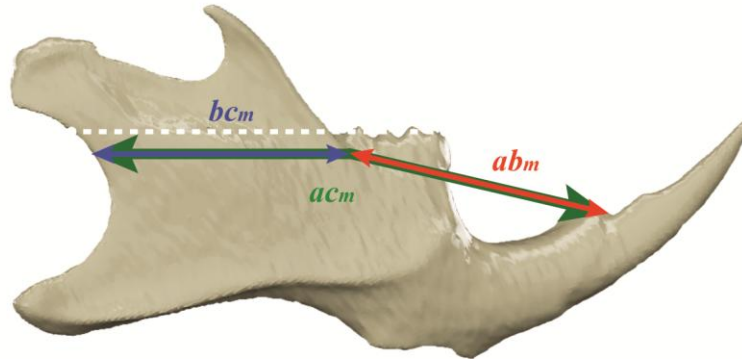


Figure 2.1.3: Linear measurement taken on mandibles. Length ab_m represents the anterior region of the mandible; length bc_m the posterior region; and length ac_m the full length of the mandible. See **Table 2.1.1** for definitions of lengths.

Table 2.1.1

DEFINITIONS OF LENGTHS COMPARED BETWEEN STRAINS

	Length	Description of length
<i>Cranial linear measurements</i>	ab _c	The mid-line point of the most anterior part of the ventral alveolar bone (between the maxillary incisors) - to - the mid-line point perpendicular to the posterior margin of the maxillary third molars
	bc _c	The mid-line point perpendicular to the posterior margin of the maxillary third molars - to - the midline point at the antero-inferior margin of the foramen magnum
	ac _c	The mid-line point of the most anterior part of the ventral alveolar bone (between the maxillary incisors) - to - the midline point at the antero-inferior margin of the foramen magnum
<i>Mandibular linear measurements</i>	ab _m	The mid-line point of the most anterior part of the dorsal alveolar bone (between the mandibular incisors) - to - the intersection of the molar alveolar rim and the base of the coronoid process
	bc _m	The intersection of the molar alveolar rim and the base of the coronoid process - to - the most posterior edge of the mandibular ramus in the occlusal plane
	ac _m	Length ab _m + length bc _m

Following collection of linear measurements, data was analysed via the production of box-plot graphs for each length, and ANOVA analyses to determine significant differences between strains for each length.

A significant difference in overall length of the cranium (ac_c) between all three strains was found (**Figure 2.1.4**). A significant difference in overall length of the mandible (ac_m) between all three strains was also found (**Figure 2.1.5**). However, the two mutant strains differed in the way in which they achieved an overall difference in length from the C57 (wild-type) strain.

For cranial measurements the pten strain showed no statistical difference from the C57 strain in the posterior length (bc_c), but a statistical difference from the C57 strain in the anterior length (ab_c) (**Figure 2.1.4**). Conversely, for cranial measurement, the brachymorph strain showed no statistical difference from the C57 strain in the anterior length (ab_c), but a statistical difference from the C57 strain in the posterior length (bc_c) (**Fig 2.1.4**). This suggests that the pten strain achieves an overall increase in cranial length when compared to the wild-type by predominantly increasing length in the anterior region of the cranium (**Figure 2.1.6; inset f**), whilst the brachymorph strain attains an overall decrease in cranial length when compared to the wild-type by predominantly reducing length in the posterior region of the cranium (**Fig 2.1.6; inset a.**).

CRANIAL LENGTH COMPARISON

Figure 2.1.4

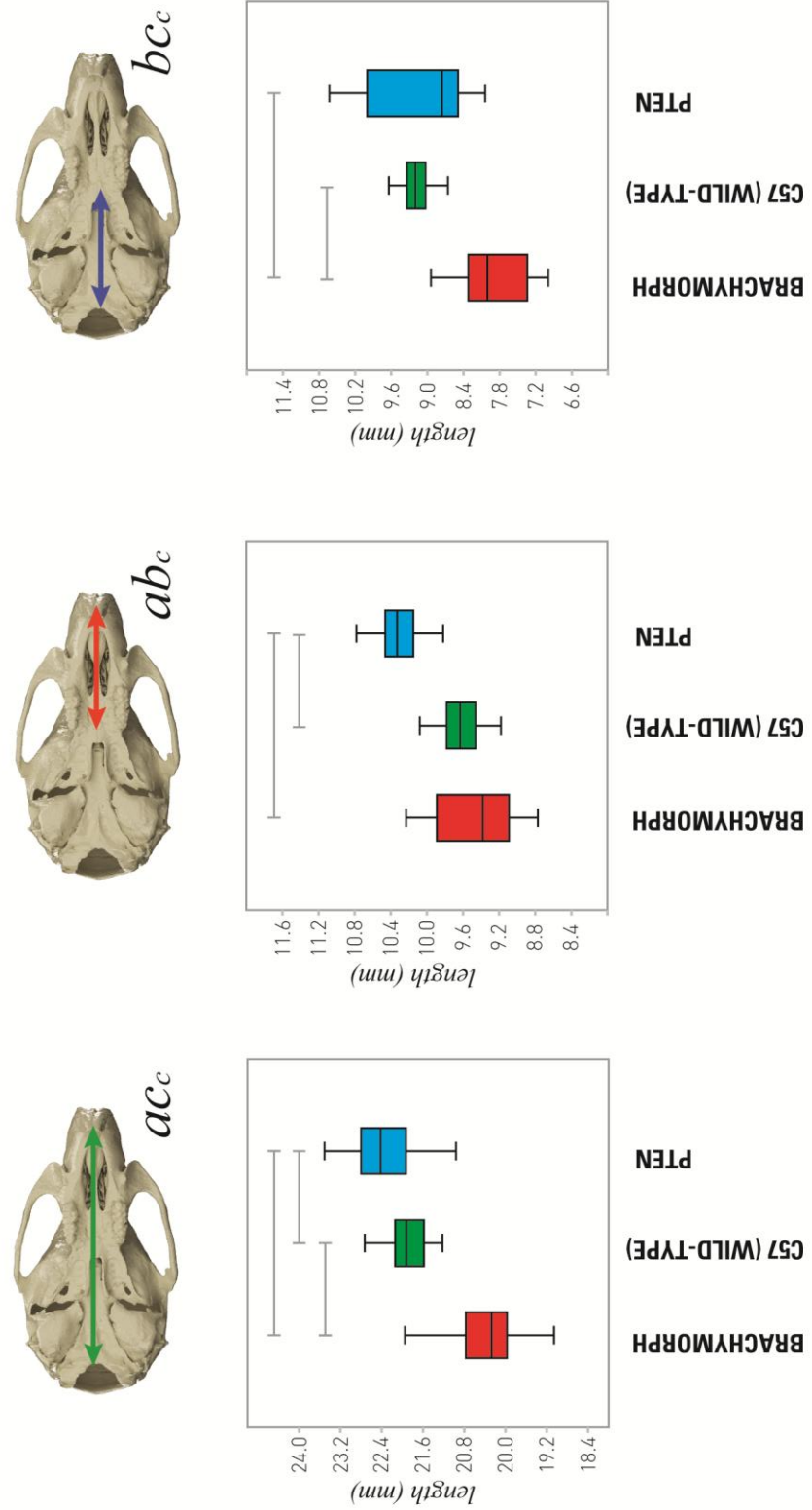


Figure 2.1.4: Box plots showing differences in cranial lengths between the three strains, brachymorph (red), C57 (green) and pten (blue). Grey lines indicated significant differences between two strains in terms of the relevant measure.

depicts significant difference between strains ($p < 0.05$)

Figure 2.1.5

MANDIBULAR LENGTH COMPARISON

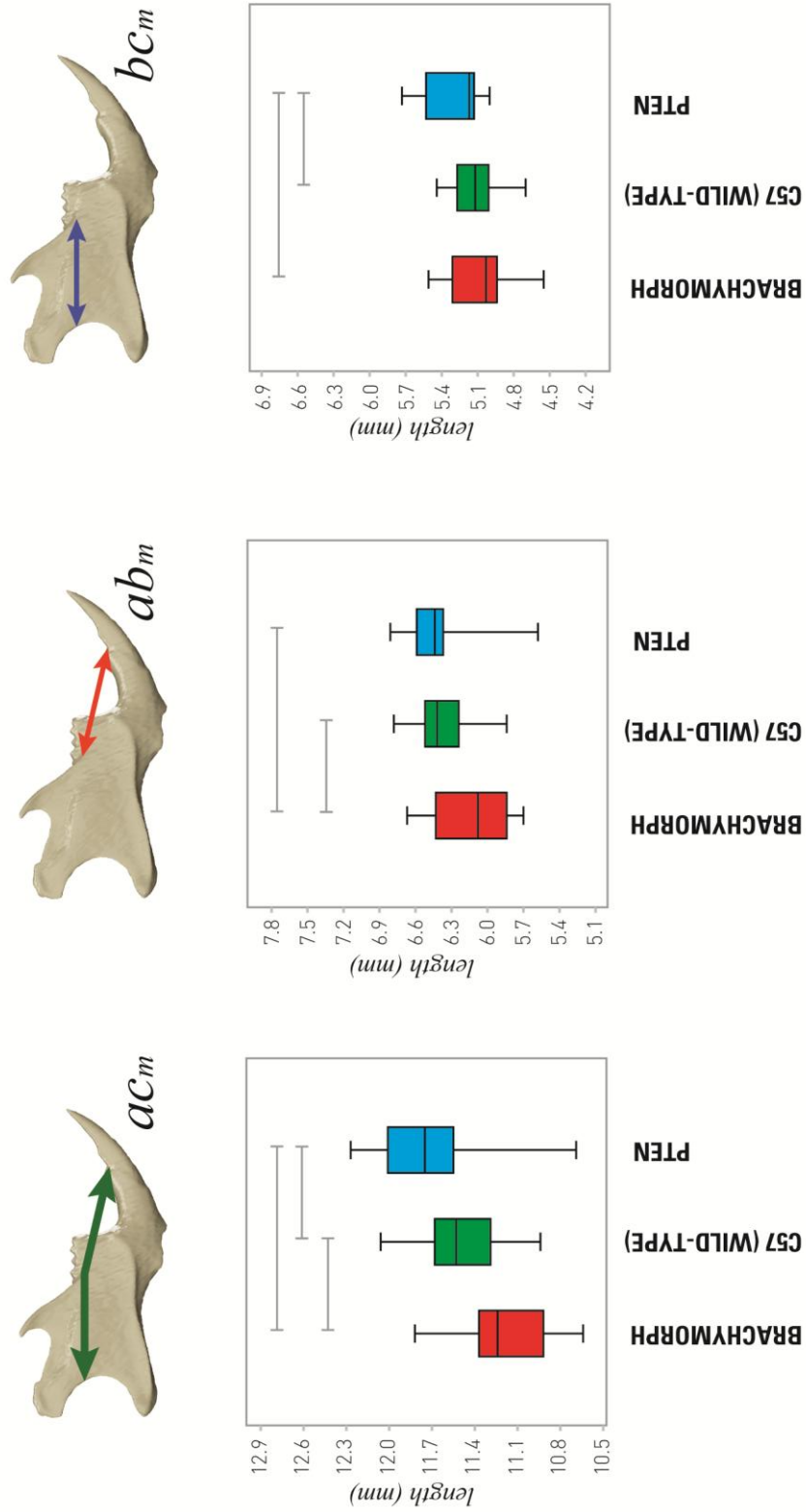


Figure 2.1.5: Box plots showing differences in mandibular lengths between the three strains, brachymorph (red), C57 (green) and pten (blue). Grey lines indicated significant differences between two strains in terms of the relevant measure.

depicts significant difference between strains ($p < 0.05$)

For mandibular measurements the brachymorph strain showed no statistical difference from the C57 strain in the posterior length (bc_m), but a statistical difference from the C57 strain in the anterior length (ab_m) (**Figure 2.1.5**). On the other hand, for cranial measurement, the pten strain showed no statistical difference from the C57 strain in the anterior length (ab_m), but a statistical difference from the C57 strain in the posterior length (bc_m) (**Figure 2.1.5**). This suggests that in opposition to results found in the cranium, the pten strain achieves an overall increase in mandibular length when compared to the wild-type by predominantly increasing length in the posterior region of the mandible (**Figure 2.1.6; inset g**), whilst the brachymorph strain attains an overall decrease in mandibular length when compared to the wild-type by predominantly reducing length in the anterior region of the mandible (**Figure 2.1.6; inset b**).

These results also demonstrate that the mandibles of the two mutant strains have adapted to fit their respective crania. The mutations present in the brachymorph and pten strains are confined to the chondrocranium (Hallgrímsson et al., 2006, Hallgrímsson et al., 2007) and thus have no direct influence on the development of the mandible. Results here show a significant difference in overall length of the mandible (ac_m) between all three strains, with the pten mandible significantly longer, and the brachymorph mandible significantly shorter than the wild-type mandible. This provisionally indicates plastic adaptation in the mandibles of the two mutant strains in order to maintain appropriate occlusion with their crania.

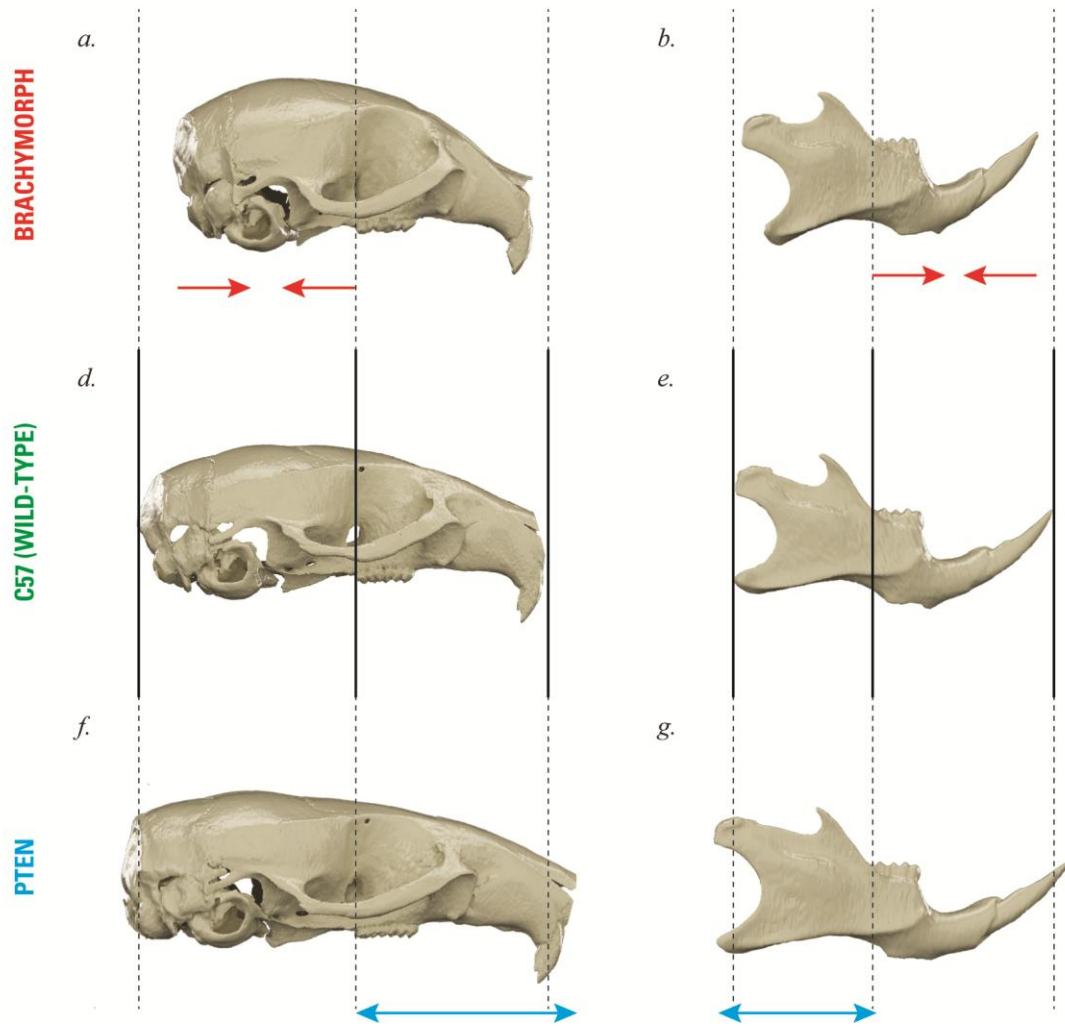


Figure 2.1.6: Depiction of regions of mutant strains showing significant differences in length when compared to the wild-type (C57) strain.

2.1.2.2 *Exploration of inter-strain variance*

To further explore the cranial and mandibular form of the three strains of *Mus musculus* that compose the sample of this research project, geometric morphometric analyses were applied.

A general threshold was applied to micro-CT scans of all individuals in Amira5 (VisageImaging, 2008) in order to generate a three dimensional surface of both the crania and mandibles (details of methodology and validation given in **Section 2.2.2.1**). A set of 65 three-dimensional (3D) landmarks describing cranial form (**Figure 2.1.7; Table 2.1.2**), and a set of 39 3D landmarks describing mandibular form (**Figure 2.1.8; Table 2.1.3**), were developed and digitised for all individuals in the sample in Amira5 (VisageImaging, 2008).

Both cranial and mandibular landmark sets were symmetrised (see **Section 2.2.2.2**) Procrustes superimposition of landmark coordinates (see **Section 2.2.1.1**) was performed, followed by principal component analysis.

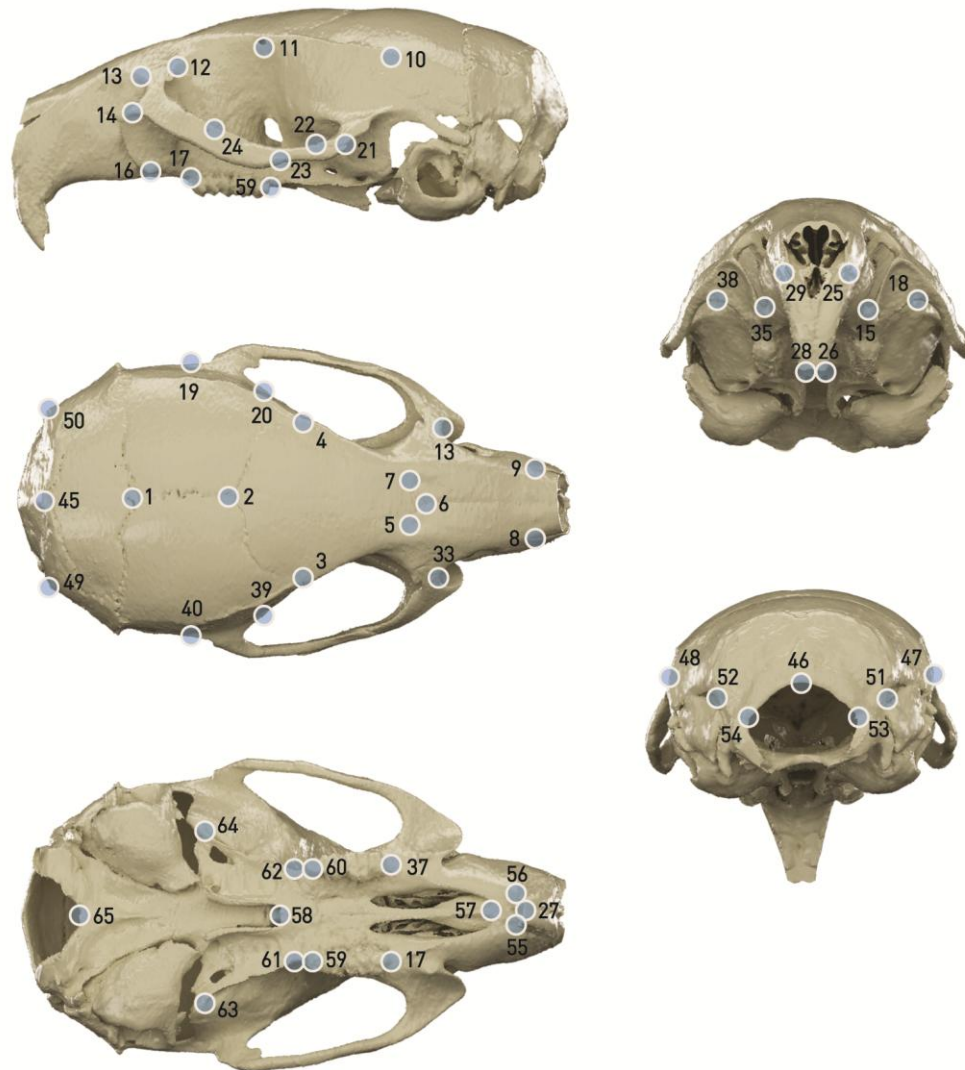


Figure 2.1.7: Depiction of three-dimensional landmarks applied to crania. Corresponding landmark definitions are given in **Table 2.1.2**.

Table 2.1.2

CRANIAL LANDMARK DEFINITIONS

Landmark number			Landmark description
left	right	midline	
			1 Lambda - the midline intersection of the sagittal and lambdoidal sutures
			2 Midline point of the fronto-parietal suture
4	3		Fronto-temporal-parietal junction (anterior projection of parietal in superior view)
7	5		Posterior most point of the premaxilla-nasal suture
			6 Posterior most midline point of the nasal suture, at the junction of the naso-frontal suture
9	8		Anterior most point at the intersection of the premaxillae and nasal bones
10	30		Central point of the squamoso-parietal suture
11	31		Superior most point of the anterior ethmoidal foramen
12	32		Intersection of fronto maxillary suture with orbital rim
13	33		Superior most border of infraorbital foramen
14	34		Anterior most point along inferior zygomatic rim of the maxilla
15	35		Inferior most point of the infraorbital foramen
16	36		Attachment point of the superficial masseter muscle tendon
17	37		Anterior edge of the alveolus of the first maxillary molar
18	38		Point of greatest curvature on the ventral surface of the maxilla
19	39		Point of greatest curvature along posterior edge of zygomatic process of temporal bone
20	40		Point of greatest curvature along anterior edge of zygomatic process of temporal bone
21	41		Postero-ventral temporal-zygomatic junction on zygomatic arch
22	42		Postero-dorsal temporal-zygomatic junction on zygomatic arch
23	43		Antero-ventral temporal-zygomatic junction on zygomatic arch
24	44		Antero-dorsal temporal-zygomatic junction on zygomatic arch
25	29		Superior most midline point at the alveolar margin of the maxillary incisor
26	28		Central point on tip of maxillary incisor
			27 Midline most inferior point between the two maxillary incisors
			45 Intersection of interparietal and occipital bones at the midline
			46 Dorsal midline border of foramen magnum
48	47		Point of greatest breadth of the cranium
50	49		Most lateral inferior point on the occipital bone
52	51		Posterior most point at the juncture between the petriotic capsule and occipital bone
54	53		Lateral most point of the foramen magnum
55	56		Posterior edge of the alveolus of the maxillary incisor
			57 Anterior midline margin of incisive foramen
			58 Midline junction between palate and presphenoid
59	60		Posterior edge of the alveolus of the third maxillary molar
61	62		Point of least breadth of the cranial base, and the juncture between the palatine and external pterygoid process
63	64		Posterior most point of the external pterygoid process
			65 Ventral midline border of foramen magnum

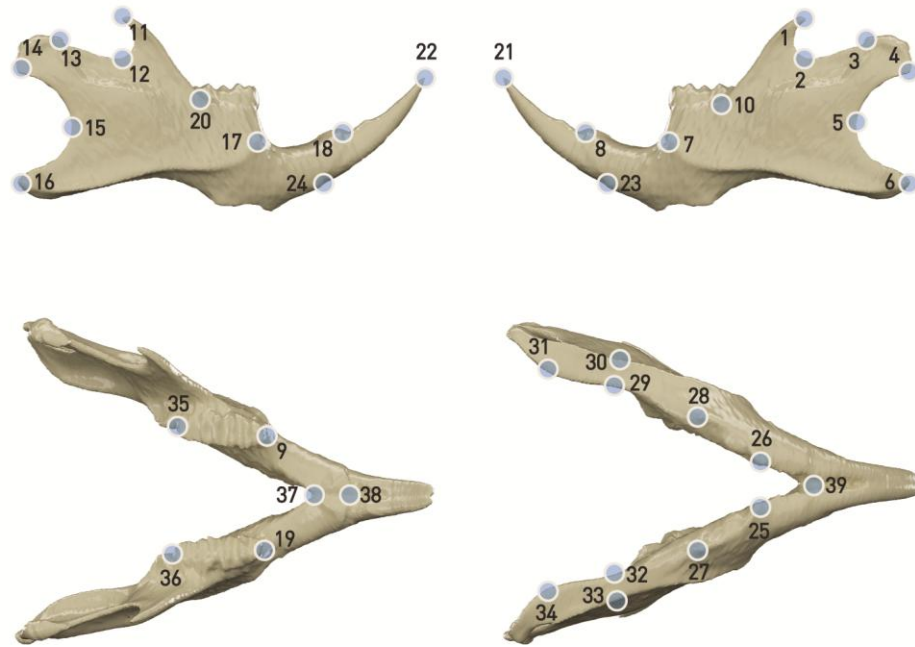


Figure 2.1.8: Depiction of three-dimensional landmarks applied to mandibles. Corresponding landmark definitions are given in **Table 2.1.3**.

Table 2.1.3

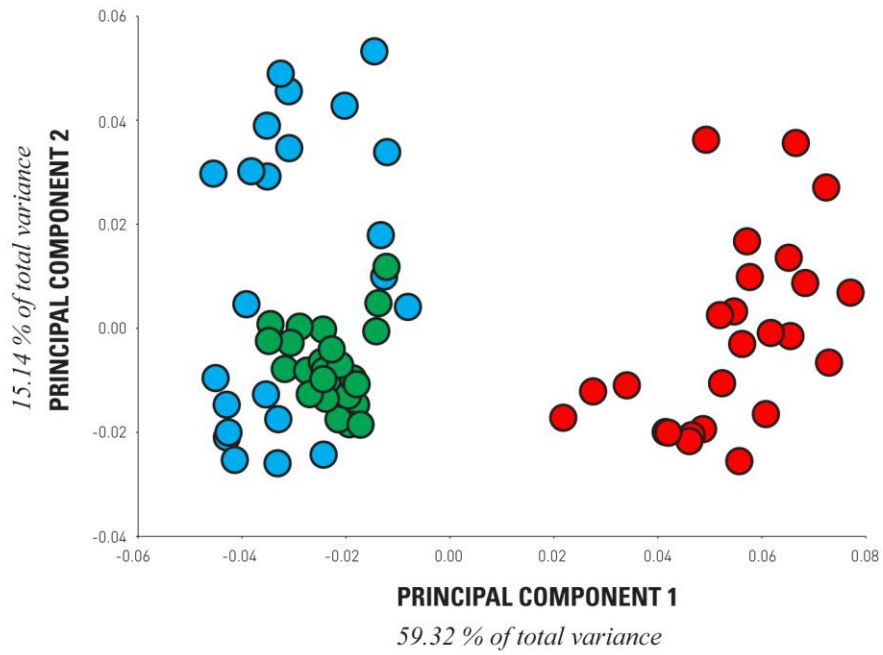
MANDIBULAR LANDMARK DEFINITIONS

Landmark number			Landmark description
left	right	midline	
1	11		tip of coronoid process
3	12		most inferior point on mandibular notch
3	13		anterior most point on condyloid process
4	14		posterior inferior most point on condyloid process
5	15		point of greatest curvature
6	16		posterior most point on angular process
7	17		anterior most point on the masseteric ridge
8	18		superior most point on incisor alveolar rim in the midline
9	19		anterior edge of the alveolus of the mandibular third molar
10	20		intersection of molar alveolar rim and base of the coronoid process
21	22		tip of mandibular incisor
23	24		ventro-posterior edge of the alveolus of the mandibular incisor
25	26		anterior most point on the tuberosity of the insertion site of mandibular transverse muscle
27	28		posterior most point on the tuberosity of the insertion site of mandibular transverse muscle
32	29		narrowest point on ventral surface of mandible, buccal surface
33	30		narrowest point on ventral surface of mandible, lingual surface
34	31		point of greatest curvature on the ventral surface of the angle of the mandible, buccal surface
35	36		posterior edge of the alveolus of the mandibular third molar
		37	posterior most border of symphysis on dorsal surface of mandible
		38	anterior most border of symphysis on dorsal surface of mandible
		39	anterior inferior most point of symphysis, ventral surface of mandible

Figure 2.1.9 shows the first and second principal components of inter-strain shape variance in the cranium. The first axis of variance (accounting for 59.32% of total shape variance) describes the extremes of cranial length. Alongside a decrease in cranial length at the more brachymorphic extreme, an increase in cranial height is seen. Conversely alongside a increase in cranial length at the opposite extreme of the first principal component, a decrease in cranial height is seen. On this axis differences between the pten strain and the wild-type strain are less marked than those between either of the latter and the brachymorph strain.

The second principal component of shape variance in the cranium (15.14% of total shape variance) shows little alteration in overall cranial length, but instead the extremes of curvature of the cranium. At the positive extreme of the axis an increase in curvature of the cranium is seen, alongside a relative increase in the anterior region in comparison to the posterior region of the cranium, combined with a ventral rotation of the rostrum. At the negative extreme of this axis a flattening of the cranium is seen, alongside a relatively short anterior region in comparison to the posterior region of the cranium together with a relatively dorsally rotated and thus flattened rostrum.

Both the pten and brachymorph mutant strains show a greater degree of intra-strain cranial variance for both the first and second principal components than the wild type strain, yet this is particularly marked for the pten strain on the second principal component axis. It has previously been noted that mutant strains show greater variance. Indeed phenotypic variance in terms of both size and shape has been found to be dramatically increased in brachymorph mice (Hallgrímsson et al., 2006).



PRINCIPAL COMPONENT 1

negative warp -0.1

positive warp 0.1



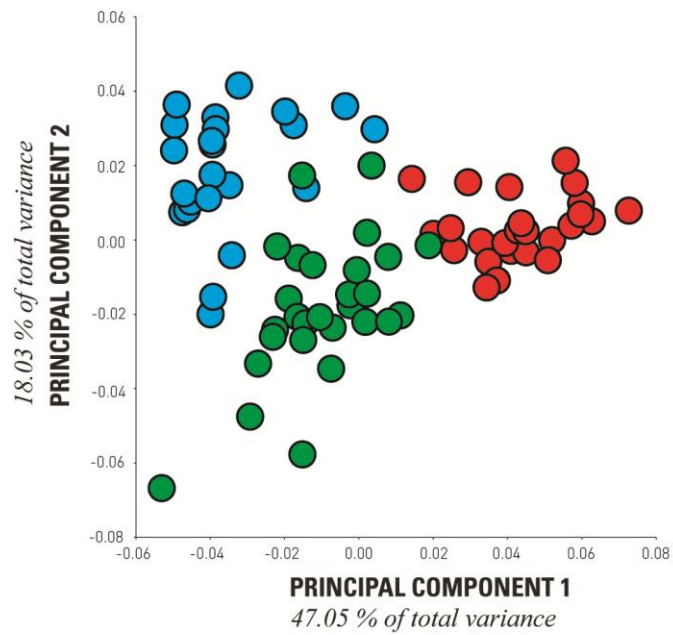
PRINCIPAL COMPONENT 2

negative warp -0.1

positive warp 0.1



Figure 2.1.9: Principal component analysis of brachymorph (red markers); C57 (green markers) and ptn (blue markers) crania. Insets show warps along PC1 (59.32% of total variance); and PC2 (15.14% of total variance) to 0.1 and -0.1 on each axis.



PRINCIPAL COMPONENT 1

negative warp -0.1



positive warp 0.1



PRINCIPAL COMPONENT 2

negative warp -0.1



positive warp 0.1



Figure 2.1.10: Principal component analysis of brachymorph (red markers); C57 (green markers) and ptn (blue markers) mandibles. Insets show warps along PC1 (47.05% of total variance); and PC2 (18.03% of total variance) to 0.1 and -0.1 on each axis.

Figure 2.1.10 shows the first and second principal components of inter-strain shape variance in the mandible. The first axis of variance (accounting for 47.05% of total shape variance) describes the extremes of mandibular length. Alongside a decrease in mandibular length at the more brachymorphic extreme, an increase is seen in mandibular width, and an overall impression of greater robusticity. Conversely, a relative increase in mandibular length is seen alongside a relative decrease in width and a more gracile mandibular appearance.

The second axis of variance (accounting for 18.03% of the total shape variance in the mandible) describes the extremes of mandibular height. At the positive extreme of the axis a relative increase in mandibular height is seen. This occurs alongside a relative inwards rotation at the condyle and a ventral-lateral lengthening and rotation of the angle of the mandible. At the negative extreme of the second principal component a relative decrease in mandibular height is seen. This occurs alongside a relative outwards rotation at the condyle and a relatively shortened, dorso-medially rotated of the angle of the mandible.

For both the first and second principal components of variance in the mandible, little difference is seen in the degree of intra-strain variance in the three strains.

Results of inter-strain principal component analyses of the cranium and mandible confirm that the main shape variance and difference between the brachymorph, pten and C57 strains in both the mandible and cranium is length. The brachymorph mutant shows a relatively decreased cranial and mandibular length, the pten mutant a relatively increased cranial length, and the C57 wild-type strain falls in a length range between the mutant strains.

2.1.2.3 *Exploration of intra-strain variance*

Principal component analyses (PCA) were also carried out to assess variation in both the cranium and mandible within each strain. These analyses were performed to not only assess key pattern of shape variance within each strain, but also to determine whether common patterns of morphological variance were present in all three strains despite differing relative cranial lengths and methods of achieving the latter length differences. Cranial and mandibular landmarks analysed are those detailed in **Section 2.1.2.2**; with both data sets symmetrised prior to carrying out PCA (for details of geometric morphometric methods see **Chapter 3**).

Results of intra-strain PCA reveal comparable patterns of variance in the brachymorph (**Figure 2.1.11**), C57 (**Figure 2.1.12**), and pten crania (**Figure 2.1.13**). In all three strains cranial variance across the first two principal components shows a general pattern of phenotypes of varying cranial length. Longer crania are associated with a decrease in cranial height and width. A common pattern of variance is also seen within all three strains in terms of relative curvature of crania, with one extreme displaying relative flat crania (relative dorsal rotation at both the occipital and rostral regions) with the other extreme displaying relatively curved crania (relative ventral rotation at both the occipital and rostral regions).

Common patterns of mandibular variance are also found within all three strains. The first two principal components of variance within the brachymorph (**Figure 2.1.14**), C57 (**Figure 2.1.15**), and pten mandibles (**Figure 2.1.16**), identify relative extremes of mandibular length within each group. Common patterns of intra-strain variance are also found in terms of the relative length of the mandibular condyle, and the relative length of the angle of the mandible. Patterns of variance regarding the relative width of the mandible (relative position of the two hemi-mandibles) are less clear.

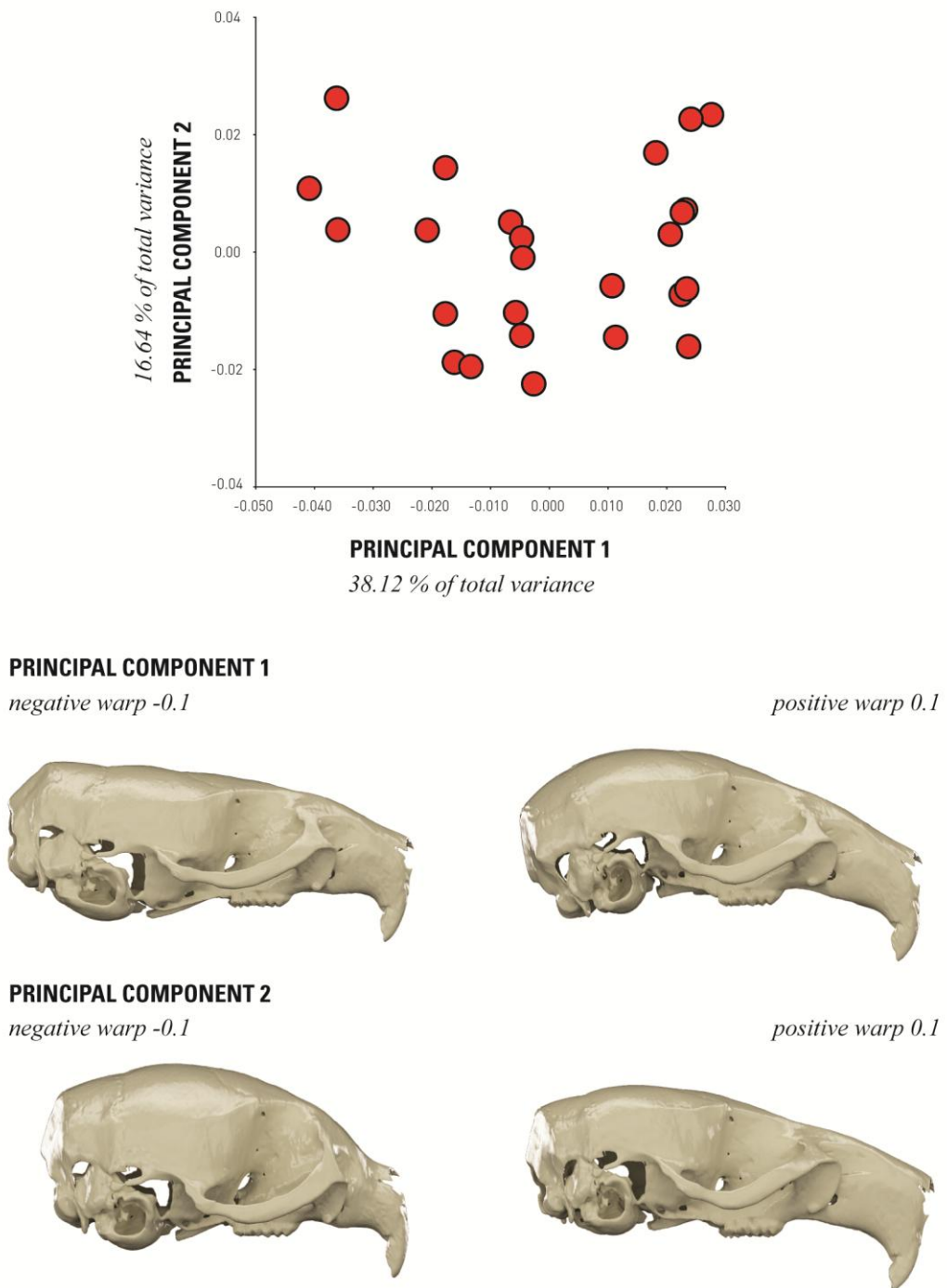
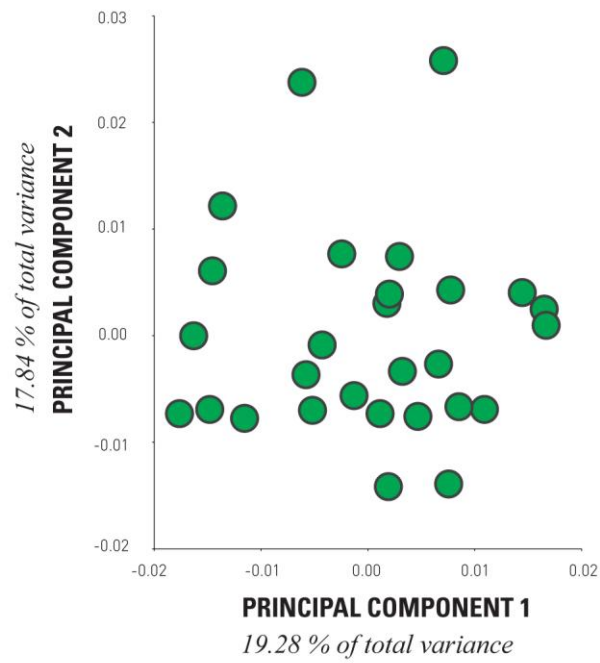


Figure 2.1.11: Principal component analysis of brachymorph crania. Insets show warps along PC1 (38.12% of total variance); and PC2 (16.64% of total variance) to 0.1 and -0.1 on each axis.



PRINCIPAL COMPONENT 1

negative warp -0.1

positive warp 0.1



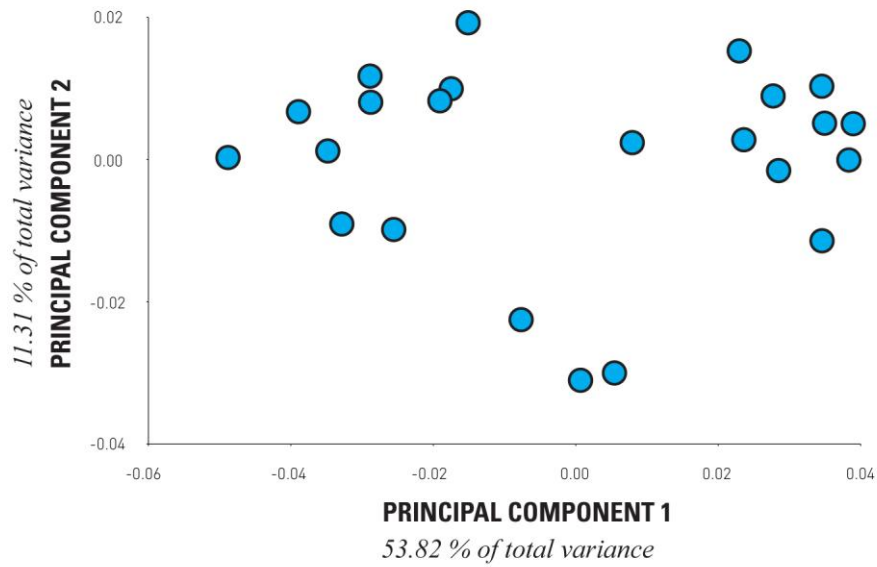
PRINCIPAL COMPONENT 2

negative warp -0.1

positive warp 0.1



Figure 2.1.12: Principal component analysis of C57 crania. Insets show warps along PC1 (19.28% of total variance); and PC2 (17.84% of total variance) to 0.1 and -0.1 on each axis.



PRINCIPAL COMPONENT 1

negative warp -0.1

positive warp 0.1



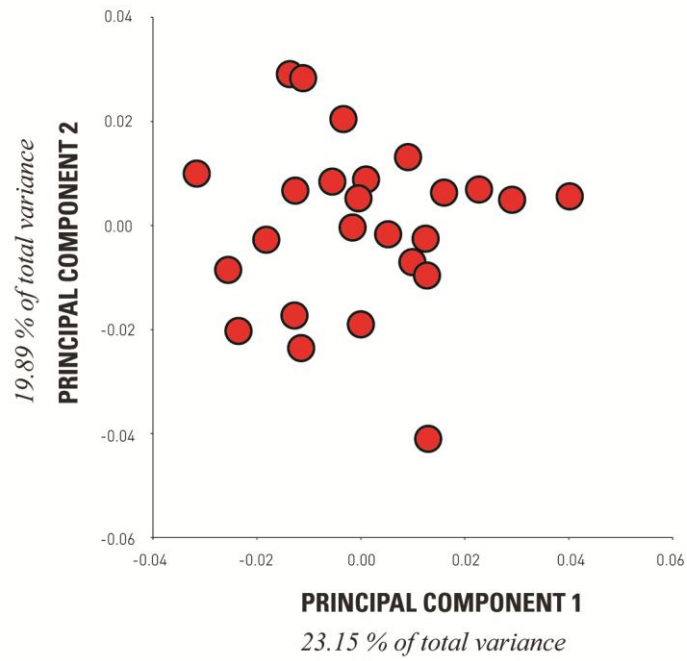
PRINCIPAL COMPONENT 2

negative warp -0.1

positive warp 0.1



Figure 2.1.13: Principal component analysis of pten crania. Insets show warps along PC1 (53.82% of total variance); and PC2 (11.31% of total variance) to 0.1 and -0.1 on each axis.



PRINCIPAL COMPONENT 1

negative warp -0.1



positive warp 0.1



PRINCIPAL COMPONENT 2

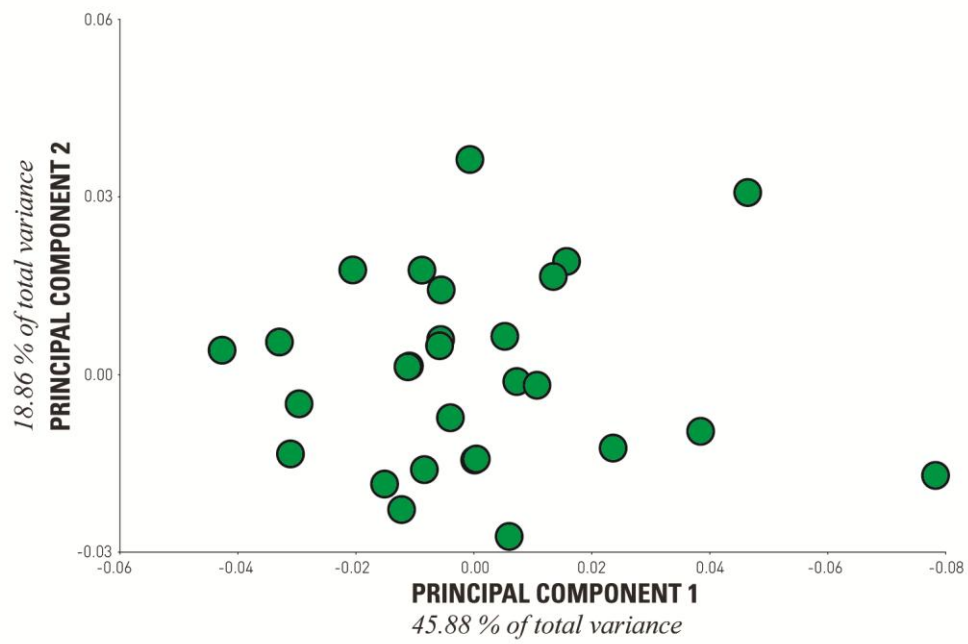
negative warp -0.1



positive warp 0.1



Figure 2.1.14: Principal component analysis of brachymorph mandibles. Insets show warps along PC1 (23.15% of total variance); and PC2 (19.89% of total variance) to 0.1 and -0.1 on each axis.



PRINCIPAL COMPONENT 1

negative warp -0.1



positive warp 0.1



PRINCIPAL COMPONENT 2

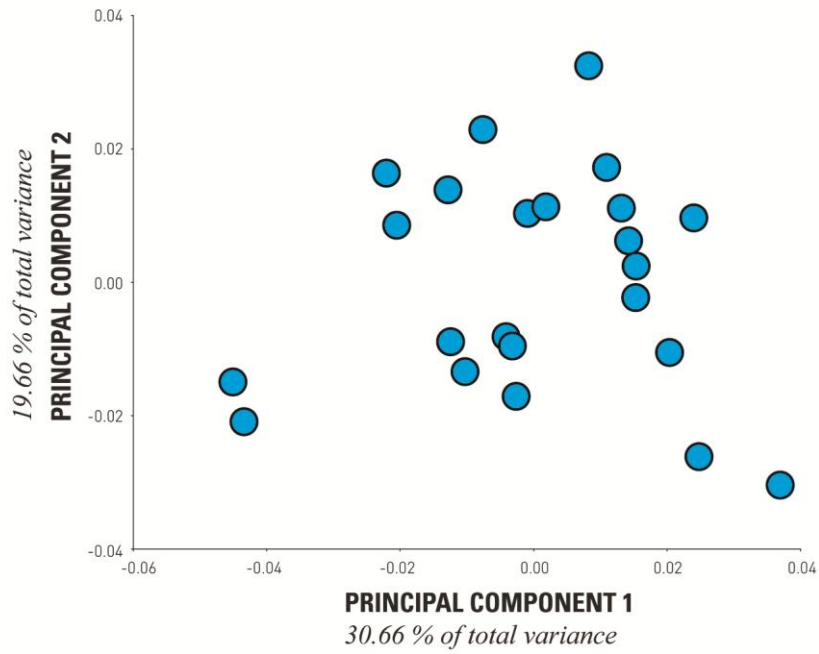
negative warp -0.1



positive warp 0.1



Figure 2.1.15: Principal component analysis of C57 mandibles. Insets show warps along PC1 (45.88% of total variance); and PC2 (18.86% of total variance) to 0.1 and -0.1 on each axis.



PRINCIPAL COMPONENT 1

negative warp -0.1



positive warp 0.1



PRINCIPAL COMPONENT 2

negative warp -0.1



positive warp 0.1



Figure 2.1.16: Principal component analysis of pten mandibles. Insets show warps along PC1 (30.66% of total variance); and PC2 (19.66% of total variance) to 0.1 and -0.1 on each axis.

2.2 METHODS

2.2.1 Geometric Morphometric and Statistical Methods

Geometric morphometric methods allow the quantitative analysis of biological shape, permitting sophisticated questions regarding the shape of phenotypes to be addressed (Bookstein et al., 1985, Bookstein, 1991, Marcus et al., 1996, Dryden and Mardia, 1998, MacLeod and Forey, 2004, Zelditch et al., 2004a, Mitteroecker and Gunz, 2009). Led by the biological question posed, an *a priori* set of landmarks providing adequate coverage of the morphology of interest and which are anatomically homologous, repeatable and reliable, are defined and collected (O'Higgins and Jones, 1998, Zelditch et al., 2004a, Slice, 2007). By removing the effects of location, orientation, and scale of the landmark configuration (Procrustes superimposition), shape is the geometric information retained. Procrustes shape coordinates (Kendall, 1977) may then be used for statistical analysis. Shape data derived from Procrustes superimposition lies in a non-linear, hyper-hemispherical shape space, where each landmark configuration is represented by a single point. First described by Kendall (Kendall, 1984, Kendall, 1977) this multidimensional shape space (of dimensionality $(k-1)m$ for 2D data and $(k-1)m$ for 3D data, where k represents the number of landmarks, and m represents the number of dimensions), is a metric space which may be approximated locally by a Euclidean tangent space (Mitteroecker and Gunz, 2009, O'Higgins and Jones, 1998, Slice, 2001). As such common statistical methods based upon linearity may be performed.

2.2.1.1 *Principal component analysis*

Principal component analysis (PCA) is a commonly employed method of reducing a large set of variables to a limited number of dimensions, these which represent the principal components of shape variation in the data. Computed via an eigen-decomposition of a covariance matrix, Procrustes distances among specimens are

preserved. By plotting principal component axes, shape or form variables may be assessed for trend, group differences, outliers etc. Weighting for linear combinations of the original variables are contained within principal components (PC), and as such may be visualised as shape deformations/relative warps (Bookstein, 1991). While each PC represents a statistically independent mode of variation, these should not be interpreted as biological meaningful factors with the exception of the first PC of an analysis of a *single* species or population, which in some cases (where allometric variation is dominant, such as in an ontogenetic sample) represents allometry (Klingenberg, 1998, Mitteroecker and Gunz, 2009, Mitteroecker and Bookstein, 2007, Adams et al., 2011).

2.2.1.2 *Partial least squares analysis*

Partial least squares analysis (also known as singular warp analysis) is a method used to explore patterns of covariation, that is, the relationship between two or more blocks of variables measured on the same object or specimen (Rohlf and Corti, 2000, Bookstein et al., 2003, Wold, 1966). Where variation is present such analysis permits the investigation of patterns of morphological integration (Zelditch et al., 2004a, Bastir and Rosas, 2006, Gunz and Harvati, 2007).

By modelling covariation between two set of variables present in the same entity, linear combinations (singular axes) are identified between the two sets, providing a low-dimensional basis upon which to compare these blocks of variables. Like regression analysis, Partial Least Squares (PLS) analysis explores the relationship between two sets of variables, yet in the latter analysis no one set of variables is assumed to be dependent upon the other and instead both sets are treated equally and viewed as jointly related to an underlying cause. Singular axes of such variables which are assumed to reflect responses to underlying variables are known as latent variables. Latent variables identified in one block which show the greatest correlation with latent variables in the second block are paired (Rohlf and Corti,

2000, Bookstein et al., 2003, Klingenberg, 2009, Bastir et al., 2005a, Bastir and Rosas, 2006, Zelditch et al., 2004a).

PLS analysis bears resemblance to PCA in the definition of axes. A between-block variance-covariance matrix is decomposed into mutually orthogonal axes, with the percentage of covariance between the two blocks for each axes determining the order of the axes. While in PCA total sample variance is reduced to a limited number of dimensions, singular value decomposition in PCA represents between-block covariance in low dimensionality (Bastir et al., 2005a, Bastir and Rosas, 2004, Bastir and Rosas, 2006).

A value for statistical significance of the covariance between the two blocks of data may be determined by means of a permutation test in which the null hypothesis of complete independence between the two blocks is simulated (Manly, 2007). An RV coefficient which quantifies the strength of covariance between the two blocks may also be calculated. This scalar measure identifies the total amount of covariance between the two blocks, indicating the overall strength of association between the blocks (Escoufier, 1973). An RV coefficient of zero indicates no association at all between the two blocks, while an RV coefficient of one reveals no difference between the two blocks except potentially in terms of rotation, scaling or translation (Klingenberg, 2009).

When assessing patterns of covariation between groups, the presence of multiple populations or strains may be adjusted for by the use of a *pooled within-group* covariation matrix. In such an analysis deviations of observation from group averages rather than deviations from the grand mean are assessed (Klingenberg et al., 2003, Klingenberg, 2009, Mitteroecker and Bookstein, 2008). In this case an assumption is made that the pattern of covariation observed between the two blocks of variables is the same in the different groups (Klingenberg, 2009).

2.2.1.3 *Vector direction comparison*

As PLS axes correspond to directions in shape tangent space, it is possible to objectively compare whether two or more PLS analyses show corresponding patterns of covariance by computing the angle between the PLS vectors. Such vector comparisons have been utilised in both traditional and geometric morphometrics, and may be applied not only to PLS analyses, but also principal component and regression analyses (Klingenberg and Zaklan, 2000, Klingenberg and McIntyre, 1998, Klingenberg and Zimmermann, 1992, Cheverud, 1982b). After scaling the two column vectors of interest to unit length, the angle between the two may be calculated as the arc-cosine of the inner product of the vectors (Hunt, 2007, Gómez-Robles and Polly, 2012). The statistical significance of such an angle may be established by means of either simulation of angles between pairs of random vectors within the multivariate space in question, or via a closed-form formula (Li, 2011).

Angles between vectors of a multivariate space fall within a range of 0° to 90° . The direction of two vectors are indistinguishable when an angle of 0° is present; while the directions of the two are highly dissimilar when an angle of 90° is found. When the angle between two vectors ranges between 20° and 60° (alongside a significant *p-value*) a similarity of vector direction is revealed, indicating similarity of patterns of covariance along the two relevant axes (Gómez-Robles and Polly, 2012, Renaud et al., 2009).

To perform such a vector comparison, the PLS axes in question must lie within the same multivariate space. All data to be compared is thus subjected to a global generalised Procrustes superimposition. Following this global registration data is divided into subgroups of interest, such as the separate strains or species to be compared. An individual PLS analysis is carried out for each sub-group after which angles between PLS vectors for each subgroup may be calculated and compared.

2.2.1.4 *Percentage variance calculation*

As discussed above (section 2.2.2.2) PLS analysis provides both quantification of the percentage of covariance explained by each singular warp between two defined blocks of variables, and a measure of the overall association between the two blocks in the form of an RV coefficient. No quantification is however provided by software performing PLS analyses as to the percentage of total shape variance in the sample accounted for by patterns of covariance described by PLS. By initially performing PCA of each block assessed by the PLS analysis, this percentage of variance accounted for by the identified covariance may be calculated for each block for each singular warp. The latter measure is computed as the variance of scores for one PLS axis for one block of variables, divided by the sum of eigenvalues for the same block.

2.2.1.5 *Modularity hypothesis*

While PLS analysis provides information regarding patterns of covariation between two blocks of data and as such may provide insight into patterns of integration between two regions; modularity within a morphological structure may be assessed via a modularity hypothesis. Morphological shape analysis software *MorphoJ* (Klingenberg, 2012) allows hypotheses of modularity to be addressed. This analysis examines whether hypothetical pre-defined partitions within a whole structure show a low degree of covariation when compared to numerous alternative partitions of that whole. A low degree of covariation between the defined sub-regions when compared to randomly generated alternative partitions does not itself imply modularity, but rather indicates covariation between the defined regions is weaker than the majority of alternative partitions and thus a hypothesis of modularity cannot be rejected (Drake and Klingenberg, 2010, Klingenberg, 2009, Jamniczky and Hallgrímsson, 2011, Sanger et al., 2012).

2.2.1.6 *Regression*

In order to assess the influence of a single variable, such as age or an environmental or functional factor, a multivariate regression of shape variables on the external variable in question may be performed (Bookstein, 1991, Monteiro, 1999). Allometry is assessed via the regression of shape on the logarithm of Centroid Size (Mitteroecker et al., 2004). The resulting regression coefficient vector, which quantifies the average effect of the chosen variable on shape, may be visualised as shape deformation (Mitteroecker and Gunz, 2009).

2.2.2 Pre-processing for Geometric Morphometric Methods

2.2.2.1 *Surface generation by thresholding*

The sample employed in this thesis was provided by Benedikt Hallgrímsson in the form of micro-Computerised Tomography (micro-CT) scans of each individual.

Computed tomography is a technique that is able to produce a complete image volume of an object from a large series of two-dimensional X-ray images taken around a single axis of rotation. Micro-CT is like computed tomography (CT), but provides much greater detail as resolutions are in the micrometer (μm) range in comparison to CT where customary resolutions are in the millimetre range. While both CT and microCT data are usually stored, and can be imaged as a stack of thin slices through the original object, such imaging techniques do not automatically provide a three dimensional solid surface image. Although individual slices contain all the structural information existing within the particular single frame, in morphometric studies usually a virtual representation of the geometry in question must be rendered or reconstructed from the raw microCT data (Weber and Bookstein, 2011).

MicroCT scans of the sample were viewed and processed in three dimensional visualisation software Amira 5.2 (VisageImaging, 2008). Data for each individual was provided by Benedikt Hallgrímsson as an amira script file (*.hx) and as such was recognised by the software as a volume stack of image slices. Scans of all individuals have a resolution of 0.035 x 0.035 x 0.035mm, and have approximately 600 slices.

A three-dimensional description of an individual was produced and viewed by rendering the volume of each micro-CT scan as an isosurface. An isosurface is a surface rendered as a volume representing points that have equal values of some characteristics. In the case of a microCT scan this means that voxels have a grey value between a chosen threshold. For example, if a threshold limit is defined as between 0 and 6000, then all voxels within this range are treated as having a value of 1, and all other values are treated as having a value of 0. Those voxels treated as having a value of zero are then dismissed in regard to display, while those with a value of 1 are used to calculate the image (Weber and Bookstein, 2011). Surface creation is based on a mathematical algorithm, such as the marching cubes algorithm of Lorensen and Cline (1987). A polygonal surface is produced by the construction of polygons on the edge-points of cubes formed from eight neighbouring voxels. Polygons are then weaved together to create a geometric surface.

In order to assess the morphology of the sample via the placement of landmarks on the crania and mandible of specimens, an isosurface of each individual was rendered. Prior to rendering isosurfaces a comparative study was carried out to assess the sensitivity of applying different threshold values.

One individual from both the pten and C57 mouse strains and two individuals from the brachymorph strain were selected at random. Five different threshold limits were applied (5000; 5500; 6000; 6500; 7000) to each specimen, creating five isosurfaces for each (**Figure 2.2.1**). Three dimensional landmarks were then digitised on both the cranium (67 landmarks) and mandible (39 landmarks) of all surfaces (see **Section 2.1.2.2** for details of both cranial and mandibular landmarks). Landmark collection was repeated for all five isosurfaces for the pten individual.

Raw landmark coordinates were subjected to generalised Procrustes superimposition followed by principal component analysis. Results of both cranial (**Figure 2.2.2**) and mandibular (**Figure 2.2.3**) analyses show differences between the five thresholds for each individual to be dramatically smaller than both inter- and intra- strain differences. Differences between the five thresholds for each individual were also comparable to landmarking error (difference between pten individual repeat).

As differences between thresholds gave no greater error than the human error involved in the digitising of landmarks, a threshold of 6500 was selected to apply to the entire sample in order to generate surfaces from which to collect landmark data. This threshold value was selected due to its preservation of all cranial and mandibular morphological detail across the entire sample without the introduction of skeletal artefacts (**Figure 2.2.1**).

5000



5500



6000



6500



7000



Figure 2.2.1: Images of isosurfaces generated from five different threshold values: 5000; 5500; 6000; 6500 and 7000.

PCA OF CRANIAL LANDMARKS - THRESHOLDING COMPARISON

Figure 2.2.2

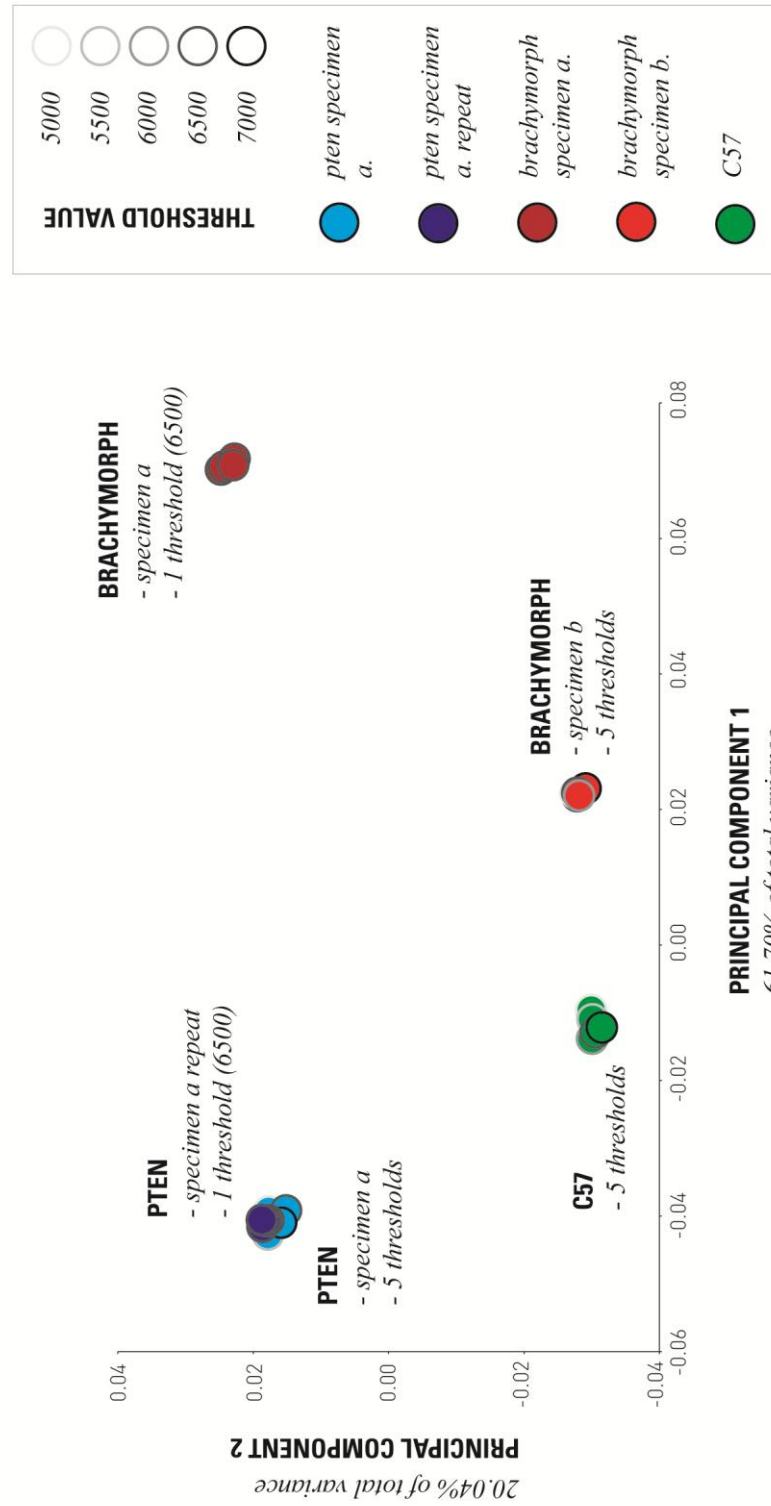


Figure 2.2.2: Principal component analysis of cranial landmarks following cranial surface generation at five different threshold values. PC1 (61.70% of total variance) and PC2 (20.02% of total variance) show variance of four different specimens: *pten specimen a* (pale blue); *brachymorph specimen a* (dark red); *brachymorph specimen b* (red); *C57* (green), and one repeat: *pten specimen a. repeat* (dark blue) following landmark digitisation at five different threshold values.

PCA OF MANDIBULAR LANDMARKS - THRESHOLDING COMPARISON

Figure 2.2.3

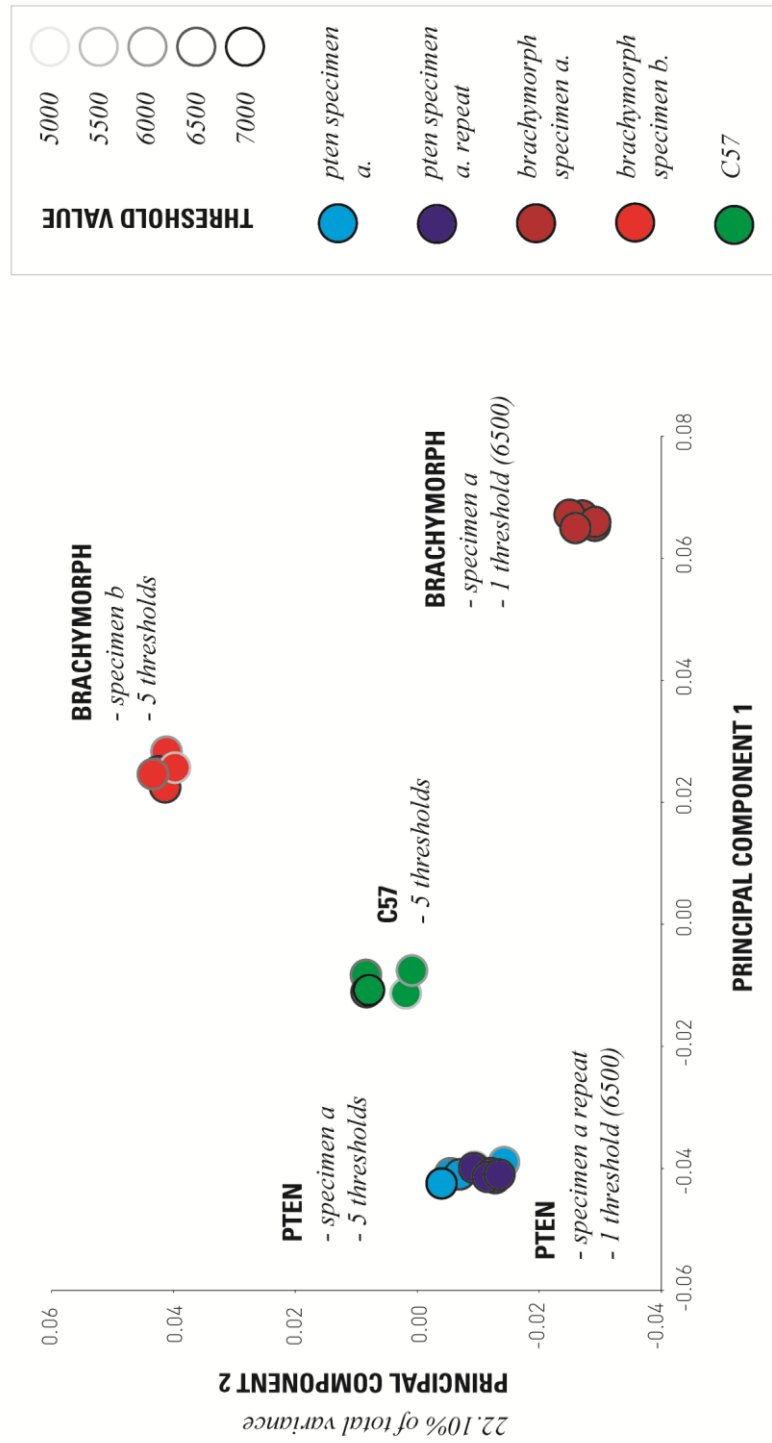


Figure 2.2.3: Principal component analysis of mandibular landmarks following cranial surface generation at five different threshold values. PC1 (68.60% of total variance) and PC2 (22.10% of total variance) show variance of four different specimens: *pten specimen a* (pale blue); *brachymorph specimen a* (dark red); *brachymorph specimen b* (red); C57 (green), and one repeat: *pten specimen a. repeat* (dark blue) following landmark digitisation at five different threshold values.

2.2.2.2 *Landmark selection*

Cranial and mandibular landmarks were selected which provided adequate coverage of these structures, and which were anatomically homologous, repeatable and reliable (O'Higgins and Jones, 1998, Zelditch et al., 2004a, Slice, 2007). Landmark sets were developed with the consideration of the potential future application to wider samples including those containing other species of the rodent order. Details of full landmark sets for both the cranium and mandible are given in **section 2.2.1**. The number of landmarks within both the cranial and mandibular sets were reduced for later analyses in order to maximise the relevance and statistical power of each analysis. Details of alternative landmark sets adapted from these original landmark sets are given in each section in connection with the analyses performed.

2.2.2.2 *Object symmetry*

Prior to application of geometric morphometric techniques cranial landmarks (which are bilaterally symmetric) were given object symmetry (symmetrised). A technique of inducing symmetry within a landmark data set was carried out due to the results of a pilot study which revealed a degree of asymmetry within the crania of the sample resulting in the partial veiling of both patterns of variation and covariation. This object symmetry procedure entails generating a reflected copy of the landmark configurations, such that the original landmark set is retained and an additional copy of this set is produced but in which the X coordinate for each landmark coordinate is rendered negative. In this new data set, landmarks on the left and right sides of the median axis of the configuration are relabelled. A mean is the generated of the original and the new reflected relabelled sets, providing a new symmetric data set (Klingenberg et al., 2002, Mardia et al., 2000, Burgio et al., 2009).

2.2.2.3 *Mandibular division*

The mouse mandible has a weak ligamentous symphysis attaching the left hemi-mandible to the right hemi-mandible, and may, as in the rat, allow the two hemi-mandibles to be pulled towards the mid-sagittal line during grinding (Weijs, 1975, Weijs and Dantuma, 1975a, Hiimäe and Ardran, 1968). This fibrocartilage joint has been suggested to act as a hinge for the horizontal rotation of the hemi-mandibles, and as such provide a flexible mandibular symphysis which permits bilateral chewing by reducing the potential for food particles to be dropped onto the buccal side (Sato, 1999). This weak symphysis and movement of the two hemi-mandibles relative to each other however poses a problem during the shape analysis of a whole mouse mandible. If the mandible is analysed as a whole, shape variation revealed by PCA is dominated by shifting of the position of one hemi-mandible relative to the other, obscuring patterns of skeletal variance. To remove this effect, in **Chapter 4**, the mandibular landmark set is divided into left and right hemi mandibles (see **Chapter 4.2**).

2.2.3 Biomechanical Methods

2.2.3.1 *Surface generation*

Automatic thresholding was used to capture the full geometry of both the cranium and mandible (see **Section 2.2.2.1**). Manual segmentation was then carried out in Amira 5.2 (VisageImaging, 2008) in order to divide the automatically generated surface into individual cranial and mandibular surfaces for each individual. A separate cranial and mandibular surface file was subsequently saved for each specimen.

2.2.3.2 *Realignment of cranial and mandibular surfaces*

Micro-CT scans of individuals revealed a wide variety of occlusions throughout the sample. In order to carry out biomechanical analyses on the sample it was necessary to correct for such differences in the relative positions of the upper and lower jaws between individuals. Individual cranial and mandibular surface files (see **Section 2.2.3.1**) were re-orientated and aligned relative to each other such that incisal occlusion was met in all specimens. Realignment of cranial and mandibular surfaces was carried out in Amira 5.2 (VisageImaging, 2008). A *landmarks (2 set)* module was utilised, with corresponding landmarks being placed on both the cranium and mandible. Six landmarks were placed on the cranium (left and right maxillary incisor tips; centre of the left and right third maxillary molars; and the centre of the left and right glenoid fossa), and six landmarks on the mandible (left and right mandibular incisor tip; centre of the left and right third mandibular molars; and the centre of the left and right mandibular condyles). A *landmark surface warp* was then performed in order to align the two landmark sets, and thus the cranial and mandibular surfaces. Fine manual re-orientation and alignment was conducted following the *landmark surface warp*, to ensure that in all specimens maxillary and mandibular incisor tips

were in direct occlusion, and that the mandibular condyle was in contact with the articular surface of the glenoid fossa.

2.2.3.3 *Mechanical advantage calculation*

Mechanical advantage, a measurement of the efficiency of the masticatory lever arm system may be assessed by modelling the jaw as a static third-class lever (Adams and Rohlf, 2000, Westneat, 2003, Wainwright et al., 2004, Metzger and Herrel, 2005, Stayton, 2006, Vincent et al., 2007, Smith and Savage, 1956, Throckmorton et al., 1980). A muscle in-lever length (moment arm), and a jaw out-lever length are first calculated, and mechanical advantage is the ratio of these two lengths.

In this thesis mechanical advantage is calculated for three key-masticatory muscles: the superficial masseter; the deep masseter; and the temporalis muscles. Mechanical advantage was calculated for the right hand side of the cranium and mandible alone.

2.2.3.4 *Jaw out-lever*

Following realignment of cranial and mandibular surfaces such that incisal occlusion was met (see **Section 2.2.3.2**) the bite point of interest was at the tip of the incisors. A bite force vector (**BFV**) was defined as the line perpendicular to the occlusal plane, passing through the tip of the incisors (**Figure 2.2.4**).

The jaw out-lever (**JoL**) was calculated as the perpendicular distance from the fulcrum (centre of the mandibular condyle) to the BFV.

Figure 2.2.4 depicts the calculation of the JoL in two dimensions. Both the distance from the fulcrum to the bite point, and the angle between this length and the occlusal plane (*angle i.*) may be measured. As both the JoL and occlusal plane (OP) are perpendicular to the BFV *angle ii.* is equivalent to *angle i.* As both the distance from

the fulcrum to the bite point, and *angle ii* are known, the JoL may be calculated via trigonometry in this two-dimensional scenario. This methodology however does not account for any potential mediolateral difference between the OP and the distance from the fulcrum to the bite point.

In order to calculate the JoL incorporating the third-dimension present in the sample, the dot product was used.

Four three-dimensional landmarks were placed on the mandible of each individual (**Figure 2.2.5**). The four landmarks give the three-dimensional coordinates needed for the calculation of three three-dimensional lengths (*length ac; length bc; length db*). Angles between planes were established via the dot product:

$$\Theta = \arccos(\mathbf{n} \cdot \mathbf{m} / |\mathbf{n}| |\mathbf{m}|)$$

where **n** and **m** are the normal vectors between the two planes and Θ is the angle between them.

Thus a three-dimensional measure of the JoL was established for each individual as the perpendicular distance from the fulcrum (centre of the mandibular condyle) to the BFV.

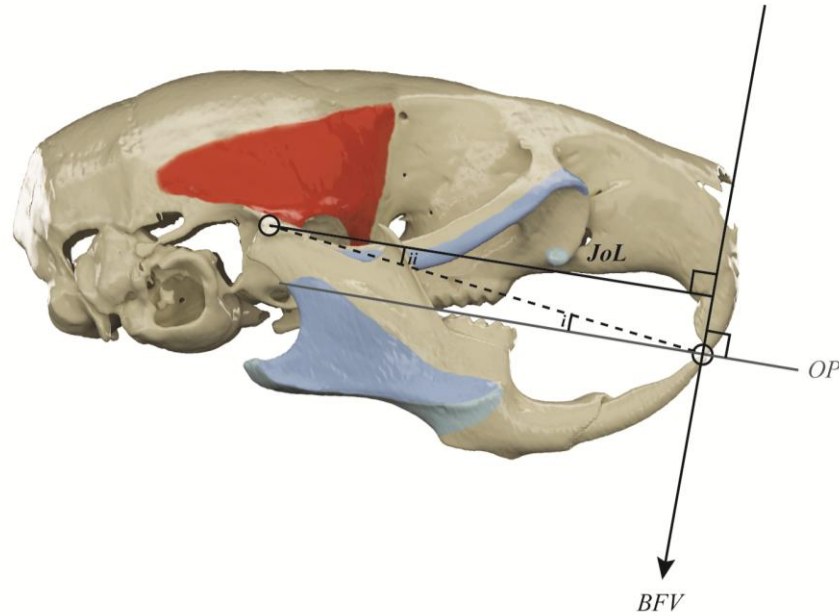


Figure 2.2.4: Calculation of jaw out-lever. Spherical points identify the fulcrum (centre of mandibular condyle), and the tip of the mandibular incisor. The bite force vector (*BFV*) is taken as perpendicular to the occlusal plane, passing through the tip of the mandibular incisor. Jaw out-lever (*JoL*) is the perpendicular distance from the fulcrum to the *BFV*. In a two dimensional analysis *JoL* could be calculated via trigonometry by establishing the distance from the fulcrum to the incisor tip and measuring angle *i* (angle between the latter line and the *OP*), thus also finding angle *ii*.

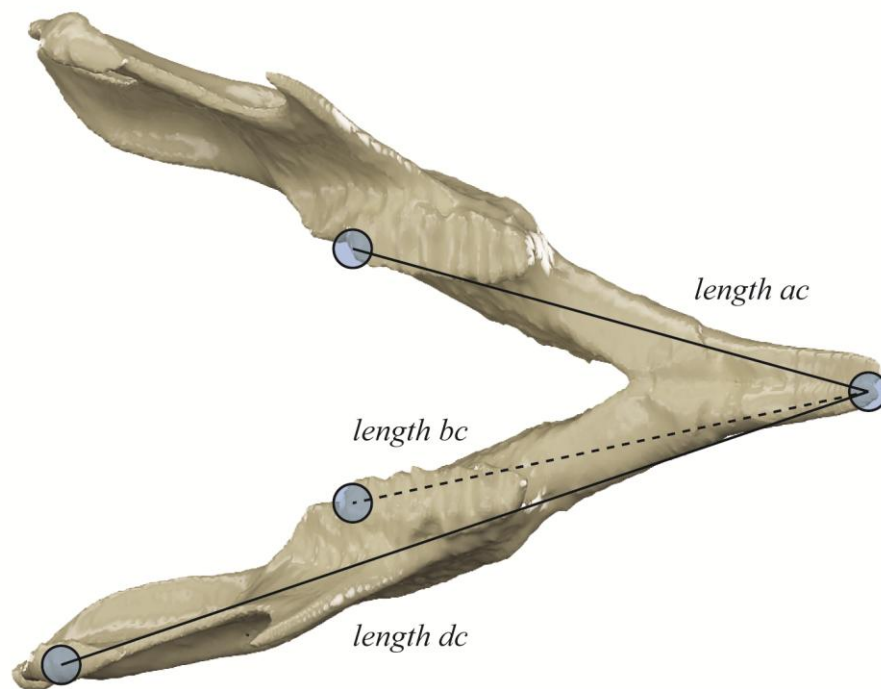


Figure 2.2.5: Pale blue markers indicate position of three dimensional coordinates used to determine lengths ac ; bc and dc . These coordinates and lengths are used to calculate angles between planes using the dot product, accounting for the mediolateral third dimension in calculation of jaw out-lever length.

2.2.3.5 *Muscle in-lever / Muscle Force Vectors*

Muscle in-lever is taken as the perpendicular distance from the fulcrum (centre of the mandibular condyle) to the muscle force vector (MFV). This length may also be termed the muscle moment arm (perpendicular distance from the pivot to the line of action of the force) although throughout this work these distances will be referred to as the muscle in-lever as per the above definition.

Biomechanical analyses were focussed on three key jaw-closing muscles: the superficial masseter, the deep masseter and the temporalis muscle. As masticatory muscle morphology and attachment areas in the mouse are both complex in terms of geometry and in some cases cover expansive areas of both the cranium and mandible; in order to fully capture the directionality of each muscle group three lines of action were established for each muscle. A centre line of action, and a line of action at both the anterior and posterior extremes of each muscle origin and insertion were considered. In order to establish these three lines of action two different methodologies were explored (see **Sections 2.2.3.6** and **2.2.3.7**).

2.2.3.6 *Curve generation*

The first method by which to establish three lines of action for each masticatory muscles was to generated a three dimensional curve on the dorsal border of each muscle origin and on the ventral border of each muscle insertion. These curves were placed on the cranial and mandibular surfaces in Amira 5.2 (VisageImaging, 2008) using the *B-spline* module. As this module divides each curve placed into 100 equidistant segments, the centre point of each curve and thus attachment border can be established. Thus by finding the centre point of each muscle origin and insertion, a line passing through both of these central points for each muscle could be established as the central MFV (**Figure 2.2.6**). The anterior MFV was taken as a line passing through the anterior border of the muscle origin and the anterior border of

the muscle insertion. The posterior MFV was taken as a line passing through the posterior border of the muscle origin and the posterior border of the muscle insertion.

Muscle in-lever length could then be calculated via trigonometry for each line of action and for each muscle, as the perpendicular distance from the fulcrum (centre of the mandibular condyle) to the muscle force vector (MFV) (**Figure 2.2.6**).

This methodology was carried out for one individual of each strain in order to compare with an alternative methodology described in **section 2.2.3.7**. Muscle in-lever length was calculated for the central line of action. Measurements for each individual were repeated such that three muscle in-lever lengths were calculated for each.

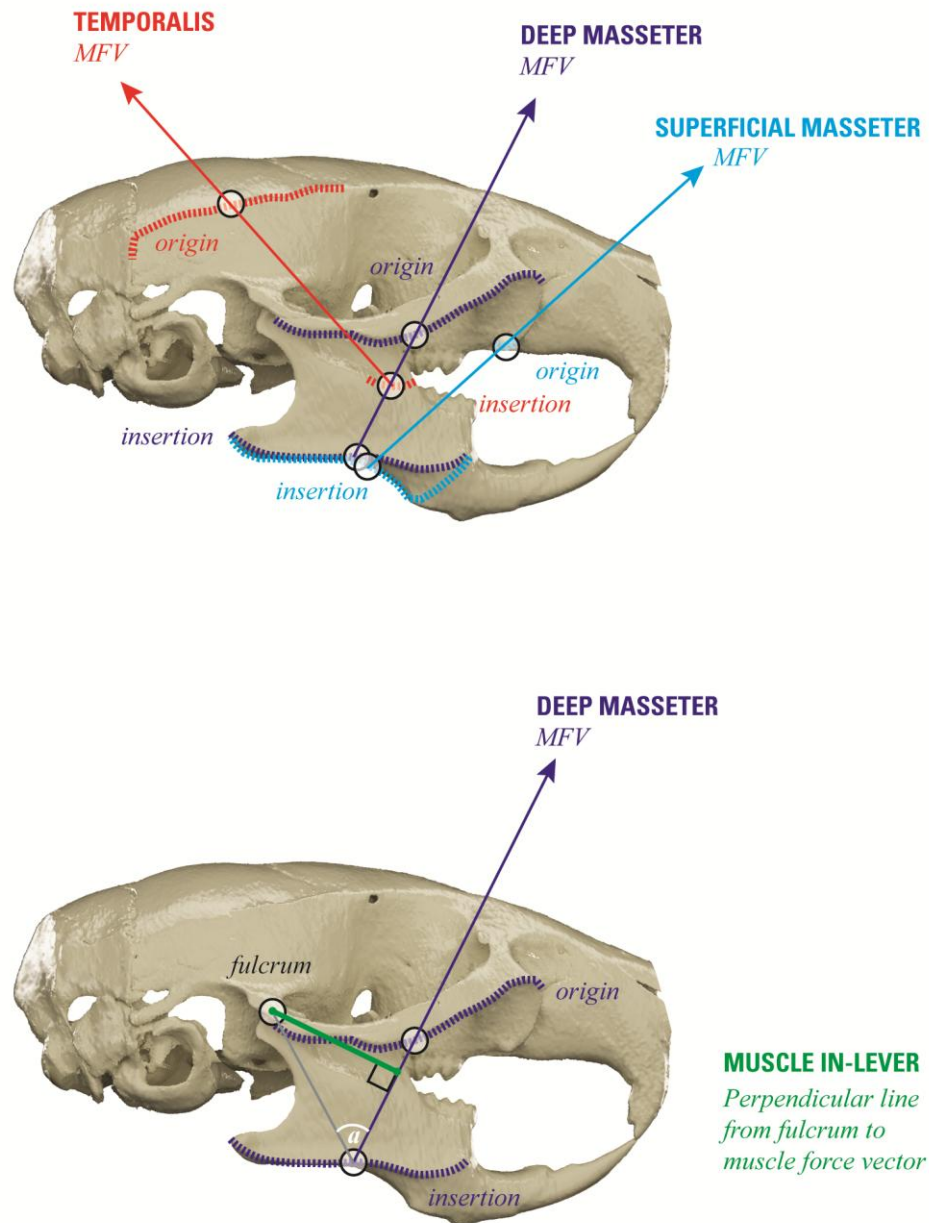


Figure 2.2.6: Inset A. depicts the method of applying a curve to the dorsal border of each muscle origin and to the ventral border of each muscle insertion. The mid-line point of each curve was determined (circular markers). Central muscle force vectors (MFV) for each muscle (superficial masster (pale blue); deep masseter (dark blue) and temporalis (red)) were determined as the line passing through the midpoint of the origin and insertion curve. Inset B. demonstrates calculation of the muscle in-lever (via trigonometry) for each muscle as the perpendicular distance from the fulcrum (centre of mandibular condyle) to the relevant MFV.

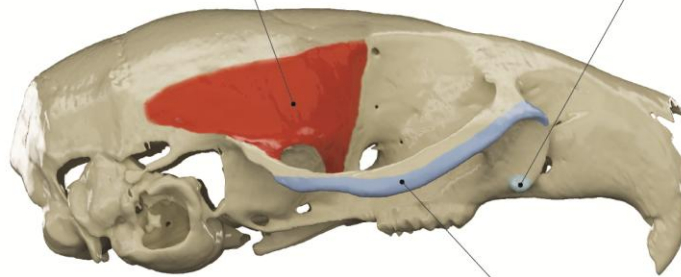
2.2.3.7 Attachment area surface generation

A second method of establishing three muscles force vectors, and thus three muscle in-levers for each muscle was explored. This alternative method was developed, based upon work of Davis et al. (2010), in order to encompass comprehensive detail regarding both muscle origin and insertion attachment areas into the resolution of MFV directions. As the geometry of masticatory muscle attachment areas in the mouse is somewhat complex, simply establishing the mid-line of one border of an attachment area may be misleading in terms of where the bulk of a muscle, and thus a muscle force vector lies. Thus in order to account for the full geometry of each attachment area, a method was developed by which to calculate the centroid of each muscle origin and insertion, from which to establish a centroid line of action for each muscle.

Cranial and mandibular surface files were imported into Autodesk 3D studio max (Autodesk, 2013). Attachment areas for the three muscles in questions were defined based upon both visible bony markings on these surface files and anatomical knowledge of the masticatory musculature of *Mus musculus* (see **Chapter 3**). Surface polygons pertaining to muscle origins and insertion for each muscle were selected and individually isolated. An individual surface was thus created for six attachment areas (superficial masseter origin; superficial masseter insertion; deep masseter origin; deep masseter insertion; temporalis origin; temporalis insertion) for each specimen (**Figure 2.2.7**). These attachment surface files were then imported into AreaCentroid (Matlab program (Mathworks); Area_Centroids_From_STL, available upon request), a program which allows the calculation of the centroid of a surface file. Three dimensional coordinates for the centroid of each attachment area were exported from AreaCentroid, and manually re-formatted into a landmark file to be read in Amira 5.2 (VisageImaging, 2008). Surface files for each attachment area, alongside landmark coordinates for the centroid of each area were then imported into Amira 5.2.

cranium - lateral view

TEMPORALIS
origin

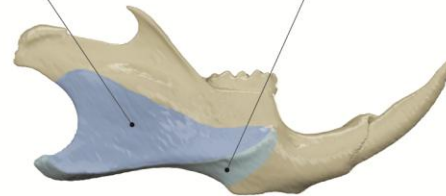


SUPERFICIAL MASSETER
origin

DEEP MASSETER
origin

mandible - lateral view

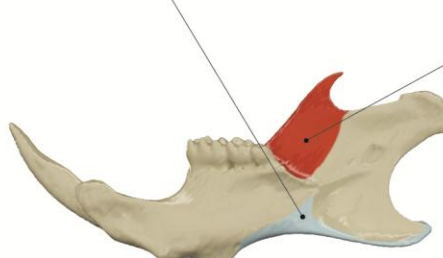
DEEP MASSETER
insertion



SUPERFICIAL MASSETER
insertion

mandible - medial view

SUPERFICIAL MASSETER
insertion



TEMPORALIS
insertion

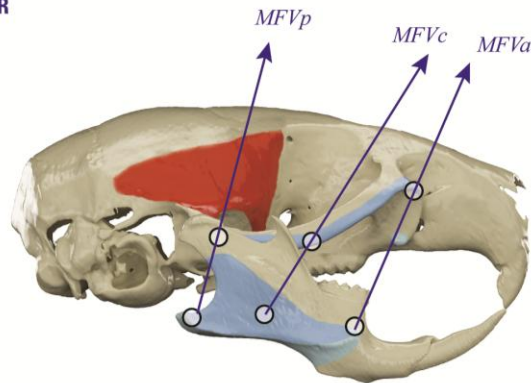
Figure 2.2.7: Depiction of muscle origin and insertion areas for the superficial masseter (pale blue); deep masseter (dark blue) and temporalis (red) muscles. Each individual attachment area was generated as a separate surface files from which to calculate the area centroid.

Landmarks coordinates for the anterior and posterior extremes of each attachment areas were added to those for the centroid of each area imported into the software.

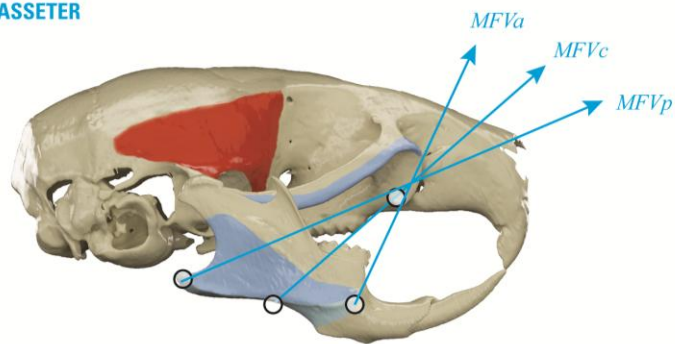
The centroid MFV was taken as a line passing through the centroid point of the muscle origin and the centroid point of the muscle insertion. The anterior MFV was taken as a line passing through the most anterior point of the muscle origin and the most anterior point of the muscle insertion. Finally, the posterior MFV was taken as a line passing through the most posterior point of the muscle origin and the most posterior point of the muscle insertion (**Figure 2.2.8**). Establishing these three MFVs allowed calculation of the MiL for each MFV via trigonometry.

Initially, this methodology was carried out for one individual of each strain in order to compare with the methodology described in **Section 2.2.3.6**. Creation of individual surface files for each muscle attachment area and centroid MFV determination were repeated three times for each individual such that three muscle in-lever lengths were calculated for each.

DEEP MASSETER



SUPERFICIAL MASSETER



TEMPORALIS

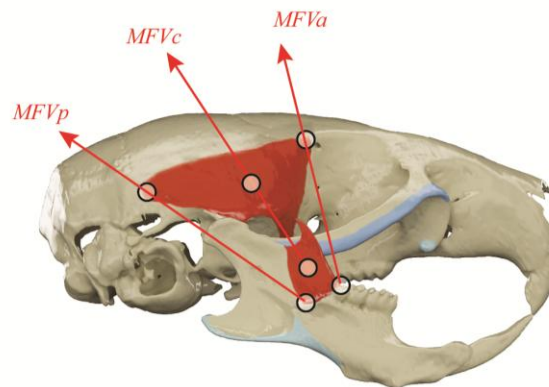


Figure 2.2.8: Depiction of muscle force vectors determined from attachment sites for three key masticatory muscles. An anterior (MFV_a), centroid (MFV_c) and posterior (MFV_p) muscle force vector is established from origin and insertion sites for the deep masseter (dark blue); superficial masseter (pale blue) and temporalis (red).

2.2.3.8 *Comparison of in-lever calculation methods*

Two methods (described in detail in **Sections 2.2.3.6** and **2.2.3.7**) of establishing MFVs and MiLs for three muscles were compared.

Figure 2.2.9 shows box plots comparing MiL for three repeats of one individual of each strain, for the two methodologies. Little difference in results generated from the two methodologies is seen for either the superficial or deep masseter, although some differences are apparent in MiL between the two methods for the temporalis muscle. **Table 2.2.1** however gives results of an analysis of variance between the groups (ANOVA), showing that there is no significant difference between central/centroid muscle in-lever lengths calculated from a 'curves' and a 'attachment area' methodology for any muscles for any strains. Full data is given in **Table 2.2.2**.

As no significant difference was found between the two methodologies, the 'attachment areas' method was selected in order to measure MiL for the entire sample. This was due to the latter method taking into account the whole muscle attachment area for each muscle, and thus perhaps providing a more biologically accurate manner of determining MFV, and thus MiL.

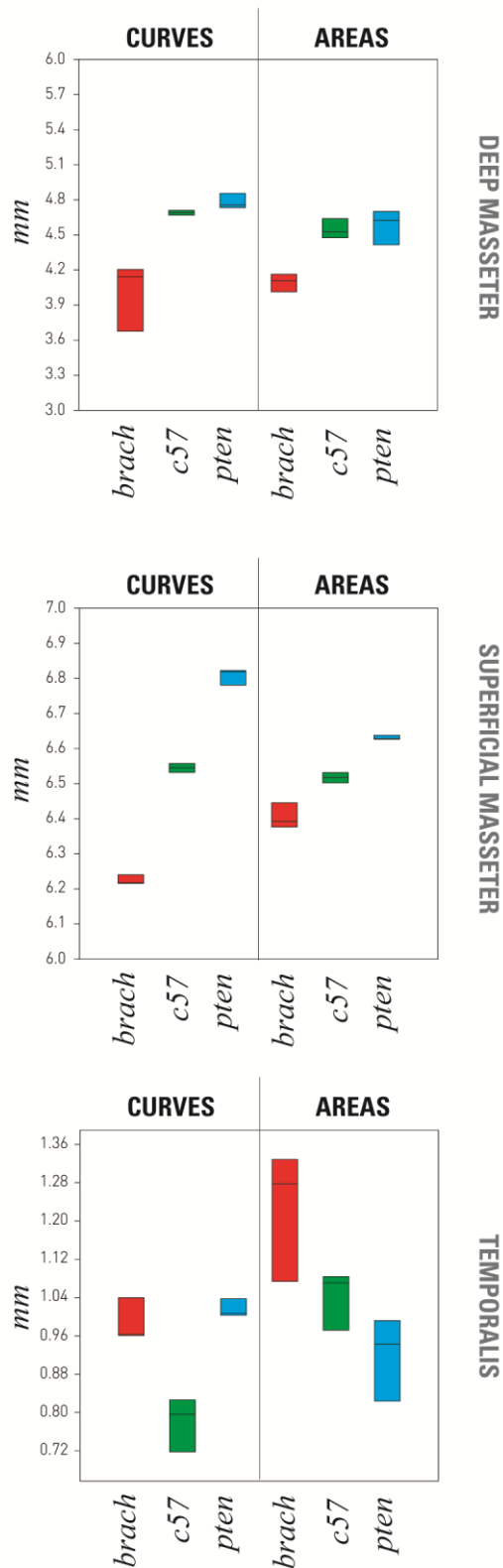


Figure 2.2.9: Box plots depicting differences in muscle in-lever length calculated via two different methodologies (*curves* - central point of muscle attachments determined via placement on curves on crania and mandibles; and *areas* - centroid point of muscle attachments determined via generation of individual surfaces for each attachment area). Three different muscles were assessed (deep masseter; superficial masseter and temporalis) for one individual of each strains[43 (brachymorph (red) C57 (green) pten (blue)), with three repeats performed for each individual.

Table 2.2.1

COMPARISON OF IN-LEVER VARIANCE BETWEEN METHODOLOGIES

		Tukey's pairwise comparisons: p(same)
Deep Masseter	<i>Brachymorph</i>	0.9992
	<i>C57</i>	0.9094
	<i>Pten</i>	0.463
Superficial Masseter	<i>Brachymorph</i>	0.6493
	<i>C57</i>	1
	<i>Pten</i>	0.6811
Temporalis	<i>Brachymorph</i>	0.2085
	<i>C57</i>	0.1116
	<i>Pten</i>	0.9977

Table 2.2.2. COMPARISON OF IN-LEVER MEASUREMENTS BETWEEN METHODOLOGIES

	Deep Masseter			Superficial Masseter			Temporalis		
	condyle to muscle insertion	angle a	calculated muscle lever length	condyle to muscle insertion	angle a	calculated muscle lever length	condyle to muscle insertion	angle a	calculated muscle lever length
<i>Brachymorph repeat 1</i>	6.04	37.5	3.6769	6.59	70.6	6.2158	4.79	11.6	0.9631
<i>Brachymorph repeat 1</i>	6.02	43.5	4.1438	6.62	70.5	6.2402	4.96	12.1	1.0397
<i>Brachymorph repeat 1</i>	6.03	44.2	4.2039	6.6	70.4	6.2175	4.82	11.5	0.9609
<i>C57 repeat 1</i>	6.34	48	4.71	6.75	75.4	6.5320	4.54	10.1	0.7961
<i>C57 repeat 1</i>	6.36	47.4	4.69	6.77	75.6	6.5573	4.76	10	0.8265
<i>C57 repeat 1</i>	6.36	47.3	4.67	6.77	75.2	6.5453	4.64	8.9	0.7178
<i>Pten repeat 1</i>	6.35	48.5	4.7558	6.94	79.3	6.8193	5.25	11.4	1.0377
<i>Pten repeat 1</i>	6.34	50	4.8567	6.86	81.3	6.7810	5.14	11.3	1.0071
<i>Pten repeat 1</i>	6.34	48.3	4.7336	6.93	79.9	6.8226	5.21	11.1	1.0030
<i>Brachymorph repeat 1</i>	5.09	54.9	4.1643	6.69	72.4	6.3768	4.43	15.3	1.0738
<i>Brachymorph repeat 1</i>	5.06	52.5	4.0144	6.66	73.7	6.3923	4.37	17	1.2776
<i>Brachymorph repeat 1</i>	5.1	53.7	4.1102	6.67	75.1	6.4457	4.37	17.7	1.3286
<i>C57 repeat 1</i>	5.33	60.5	4.6389	6.71	75.7	6.5020	4.49	12.5	0.9718
<i>C57 repeat 1</i>	5.36	57.6	4.5255	6.72	76.4	6.5316	4.49	13.8	1.0710
<i>C57 repeat 1</i>	5.35	56.8	4.4767	6.7	76.6	6.5176	4.48	14	1.0838
<i>Pten repeat 1</i>	5.27	56.9	4.4147	6.75	79.1	6.6282	4.84	9.8	0.8238
<i>Pten repeat 1</i>	5.4	58.9	4.6238	6.76	78.6	6.6266	4.81	11.3	0.9425
<i>Pten repeat 1</i>	5.44	59.8	4.7016	6.76	79.1	6.6380	4.85	11.8	0.9918

2.2.4 Comparison with other Biomechanical Methods

In this thesis, both muscle in-levers and jaw out-levers are calculated as the perpendicular distance from the fulcrum to the line of action (muscle force vector or bite force vector) (Throckmorton et al., 1980). This differs from another frequently employed methodology which approximates the lever arm length as a simple linear distance from the fulcrum (mandibular condyle) to a point on the attachment of each relevant muscle; and the bite arm length at the distance from the fulcrum the tip of the incisor (Radinsky, 1985b, Radinsky, 1985a, Radinsky, 1981a, Swiderski and Zelditch, 2010, Thorington and Darrow, 1996, Velhagen and Roth, 1997). The vast majority of studies employing the latter methodology have carried out these analyses in two dimensions, whilst calculation of mechanical advantage within the present thesis is based upon three dimensional linear measurements.

As methodological differences in the approach to calculating mechanical advantage may have an impact on the results of such investigations, a comparison of three different methods of assessing the function of the masticatory complex in terms of mechanical advantage was carried out. Swiderski and Zelditch (2010) examine jaw lever arm lengths in 23 species of sciurine tree squirrels, reporting isometry of the masseter moment arm in relation to the output arm, a result consistent with that of Velhagen and Roth (1997). In the present study the two dimensional methodology described by Swiderski and Zelditch (2010) (Method A), a three dimensional version of this methodology (Method B), and three dimensional methodology devised for this thesis (Method C) were applied to a subsection of the brachymorph, pten and C57 samples. Results were then compared to those published by Swiderski and Zelditch (2010).

Ten specimens from each strain (pten, C57 and brachymorph) were selected at random to form a subset of the overall sample on which to carry out the three methods. All three methods were carried out on all 30 individuals.

2.2.4.1 *Method A*

Method A is a replication of that detailed in Swiderski and Zelditch (2010). In order to generate two-dimensional lateral images of the mandibles of the sample, three-dimensional mandibular surface files (for details of surface generation see **Section 2.2.3.1**) were imported into 3D modelling and animation software Autodesk 3D Studio Max (Autodesk, 2013). Surfaces were orientated using three separate interfaces to ensure that alignment was consistent in the X, Y and Z direction. A scale bar was placed alongside each mandible, and a virtual orthographic camera was then used to capture and render a two dimensional image of the lateral surface of each mandible. Images were saved and imported into TPSDig2 software where two dimensional linear measurements were taken.

Five two dimensional linear distances from the mandibular condyle (**Figure 2.2.10**) were collected for each specimen (based upon the work of Swiderski and Zelditch (2010)). Lever arm lengths were calculated as the distance from the condyle to the following points: T1 – tip of the coronoid process, proximal end of temporalis insertion (temporalis muscle in-lever arm); T2 – base of the coronoid process; distal end of temporalis insertion (temporalis muscle in-lever arm; SM1- posterolateral corner of angular process, posterior end of superficial masseter insertion (superficial masseter muscle in-lever arm); AM – anterior end of the deep masseter insertion (deep masseter muscle in-lever arm); INC – tip of the incisor (jaw out-lever arm).

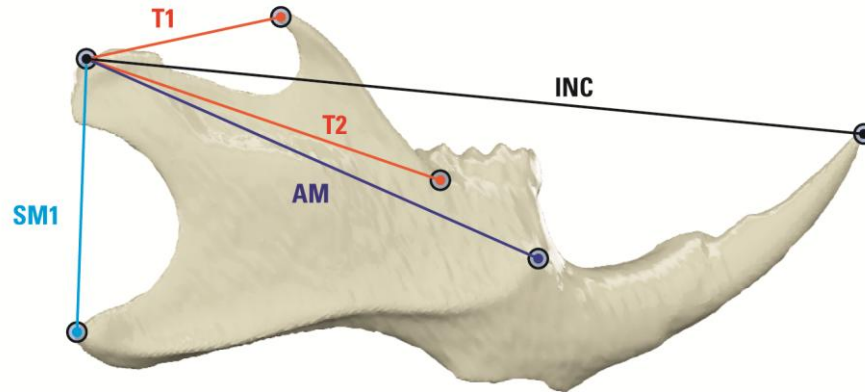


Figure 2.2.10: Depicting alternative linear in- and out- lever measurements based upon work of Swiderski and Zelditch (2010). Jaw out-lever length is defined as the distance from the mandibular condyle to the incisor tip (INC). In-lever lengths are defined as the distance from the mandibular condyle to: for temporalis, the tip of the coronoid process (T1) and the proximal end of temporalis insertion (T2); for superficial masseter, the angular process (SM1); for deep masseter, the most anterior point of the insertion of the deep masseter (AM).

2.2.4.2 *Method B*

Method B is a replication of that detailed in Swiderski and Zelditch (2010), with the difference of being carried out in three dimensions rather than two dimension. Three dimensional mandibular surface files (for details of surface generation see **Section 2.2.3.1**) were imported into three dimensional visualisation software Amira (VisageImaging, 2008). Five three dimensional linear distances from the mandibular condyle (**Figure 2.2.10**) were collected for each specimen. Descriptions of these five measurements are the same as those detailed in Method A.

2.2.4.3 *Method C*

Method C is that described in **Section 2.2.3.7.**, where three dimensional surfaces were created for each muscle origin and insertion for each individual. Attachment surface files were used to generate a centroid for each muscle origin and insertion. A centroid MFV was taken as a line passing through the centroid point of the muscle origin and the centroid point of the muscle insertion The anterior MFV was taken as a line passing through the most anterior point of the muscle origin and the most anterior point of the muscle insertion. Finally, the posterior MFV was taken as a line passing through the most posterior post of the muscle origin and the most posterior point of the muscle insertion. Muscle in-lever (MiL) lengths were calculated as the perpendicular distance from the centre of the mandibular condyle (the fulcrum) to the muscle force vector (MFV). The jaw out-lever (JoL) was calculated as the perpendicular distance from the centre of the mandibular condyle (the fulcrum) to the bite force vector (BFV).

2.2.4.4 *Results*

Result from the three different methods for the three mouse strains were compared against those of Swiderski and Zelditch (2010). For each strain for each method, average jaw out-lever length for was plotted against average muscle in-lever length (**Figure 2.2.11; Table 2.2.3**). Little difference was observed between results of the two-dimensional (Method A) and corresponding three-dimensional (Method B) measurements for the mouse strains. Results of the latter two methods also showed a tendency to largely follow trends set in the 23 species of sciurine tree squirrels (Swiderski and Zelditch, 2010). As RMA regression lines showed neither a gradient of 1 or an intercept of 0 for any muscles however it could be argued that the jaw lever analysed here do not show true isometric scaling. Results of Method C (that employed in this thesis) does however show substantial differences to those of either Method A and/or Method B. This finding indicates that simplification of muscle in-lever and jaw out-lever lengths demonstrated in Methods A and B may generate different results to methods in which lever lengths are taken as the perpendicular line from the fulcrum to the muscle or bite force vector.

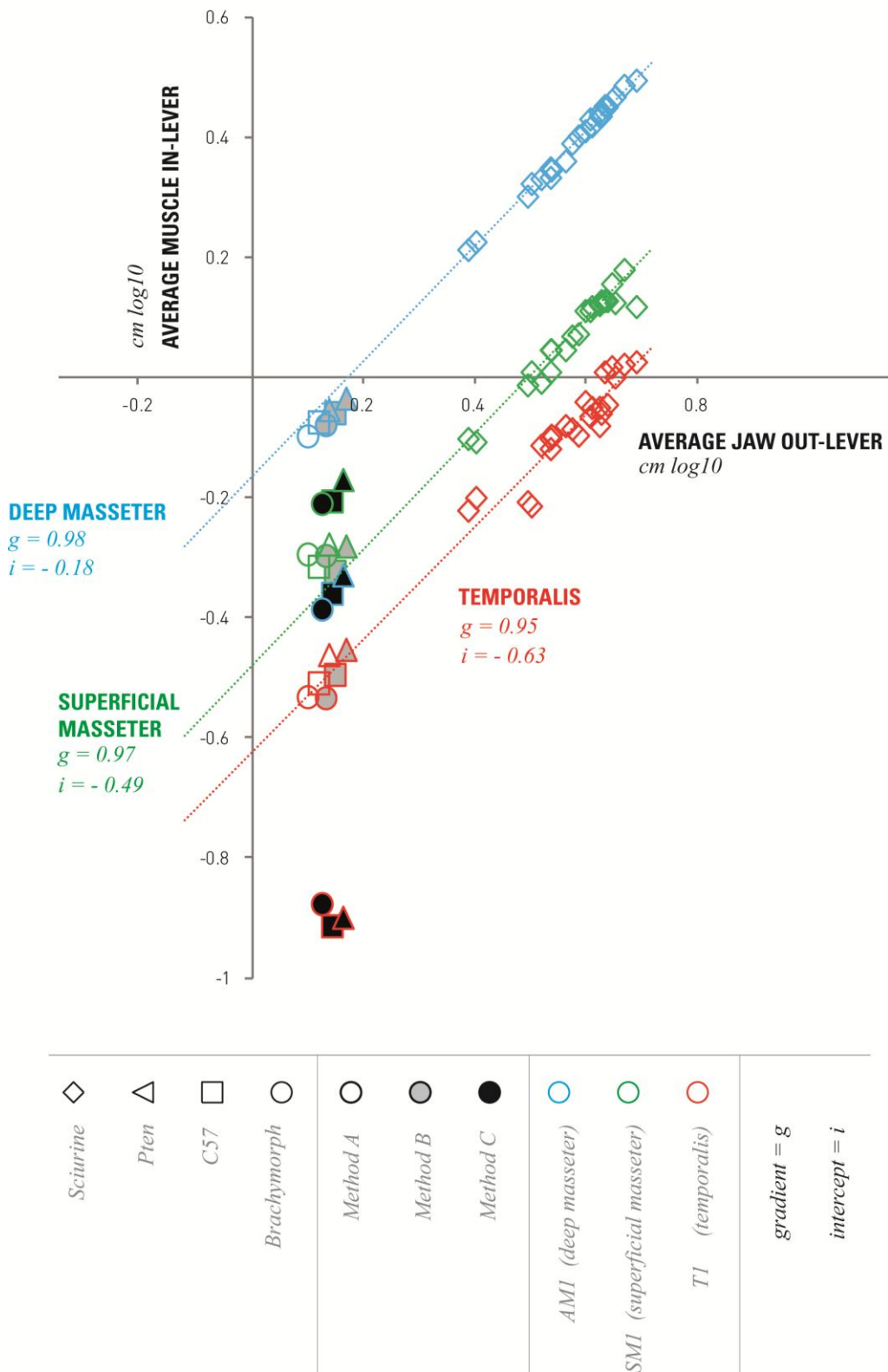


Figure 2.2.10: Average jaw out-lever length plotted against average in-lever length for 23 species of sciurine tree squirrels (diamond markers) (Swiderski and Zelditch 2010), and brachymorph (circular markers), C57 (square markers) and pten (triangular markers) mouse strains; for three muscles; deep masseter (blue outline) superficial masseter (green outline) and temporalis (red outline). Results of three methodologies, Method A (no fill), Method B (grey fill) and Method C (black fill) are shown for the three mouse strains.

**COMPARISON OF IN- AND OUT-LEVER LENGTHS DETERMINED VIA
THREE DIFFERENT METHODOLOGIES**

Table 2.2.3

Average lever arm lengths (cm LOG10) for each species and strain					
Methodology	Species / Strain	Jaw out-lever (INC)	Superficial masseter muscle in-lever (SM1)	Temporalis muscle in-lever (T1)	Deep masseter muscle in-lever (AM)
Method A (results taken from Swiderski and Zelditch (2010))	<i>M. alfari</i>	0.39	-0.10	-0.22	0.21
	<i>M. flaviventer</i>	0.40	-0.11	-0.20	0.23
	<i>T. hudsonicus</i>	0.49	-0.01	-0.21	0.30
	<i>T. douglasi</i>	0.50	0.01	-0.21	0.32
	<i>S. alberti</i>	0.63	0.13	-0.06	0.43
	<i>S. alleni</i>	0.59	0.07	-0.10	0.40
	<i>S. arizonensis</i>	0.63	0.13	0.01	0.45
	<i>S. aureogaster</i>	0.62	0.12	-0.08	0.43
	<i>S. carlinensis</i>	0.61	0.12	-0.05	0.42
	<i>S. colliaei</i>	0.62	0.12	-0.05	0.44
	<i>S. deppei</i>	0.54	0.05	-0.10	0.34
	<i>S. granatensis</i>	0.54	0.05	-0.10	0.35
	<i>S. griseus</i>	0.67	0.18	0.02	0.49
	<i>S. ignitus</i>	0.52	-0.01	-0.11	0.33
	<i>S. igniventris</i>	0.65	0.12	0.00	0.47
	<i>S. lis</i>	0.54	0.01	-0.12	0.33
	<i>S. nayaritensis</i>	0.65	0.16	0.02	0.46
	<i>S. niger</i>	0.64	0.13	-0.05	0.45
	<i>S. spadiceus</i>	0.69	0.12	0.03	0.49
	<i>S. stramineus</i>	0.60	0.11	-0.04	0.41
<i>S. variegatoides</i>	0.61	0.11	-0.07	0.43	
<i>S. vulgaris</i>	0.56	0.05	-0.08	0.36	
<i>S. yucatanensis</i>	0.57	0.07	-0.09	0.39	
Method A	<i>M. musculus</i> - C57 'wild-type'	0.15	-0.32	-0.50	-0.06
	<i>M. musculus</i> - Pten mutant	0.17	-0.28	-0.45	-0.04
	<i>M. musculus</i> - Brachymorph mutant	0.13	-0.30	-0.53	-0.08
Method B	<i>M. musculus</i> - C57 'wild-type'	0.12	-0.32	-0.51	-0.07
	<i>M. musculus</i> - Pten mutant	0.14	-0.28	-0.46	-0.05
	<i>M. musculus</i> - Brachymorph mutant	0.10	-0.29	-0.53	-0.10
Method C	<i>M. musculus</i> - C57 'wild-type'	0.14	-0.21	-0.91	-0.36
	<i>M. musculus</i> - Pten mutant	0.16	-0.17	-0.90	-0.33
	<i>M. musculus</i> - Brachymorph mutant	0.12	-0.21	-0.88	-0.39

2.2.5 Visualisations

All figures were generated with Adobe illustrator (Adobe, 2012). Graphical exports from programs specified in methodologies were imported into Adobe illustrator in order to create high resolution infographics and diagrams.

2.3 CONCLUSION TO MATERIALS AND METHODS

Chapter 2 gives an introduction to the materials and methods used throughout this thesis, alongside analyses exploring the sample in question. Three strains of mice make up the sample utilised in this work, two mutant strains (pten and brachymorph) and a comparable wild-type strain (C57). The pten mutant phenotype is characterised by an elongated cranium whilst the brachymorph mutant phenotype is characterised by a reduction in cranial length. Both mutant strains share the same background strain as the wild-type control mouse (C56BL/6J). As both mutations selectively effect chondrocranial growth, influence of both are expected to be limited to crania, with any morphological adaptation seen in the mandibles of the pten and brachymorph strains expected to be as a result of epigenetic plastic adaptation.

In order to determine whether statistically significant differences in cranial length between the three strains were present, linear measurements were taken on both crania and mandibles. Significant differences between all three strain were found in terms of both overall cranial length and overall mandibular length. In the cranium however it was found that the pten strain achieved an increase in cranial length predominantly by an elongation in the anterior region, while the brachymorph strain achieved a decrease in cranial length predominantly by a reduction in the posterior region. Conversely, in the mandible, the anterior region of the brachymorph mandible was found to be particularly reduced in length, while the posterior region of the pten mandible was found to be particularly elongated.

To undertake geometric morphometric analyses, firstly surface files of all individuals within the sample were required. A thresholding comparison was carried out to ascertain whether a general threshold value could be applied to all individuals of all strains without introducing significant error. As error introduced by differing thresholding values was no greater than the error involved in landmark digitisation a consistent threshold value was selected to apply to all individuals. A cranial landmark set and a mandibular landmark set were then developed. Cranial landmarks were symmetrised to remove any asymmetry which was shown to partially veil patterns of variation in the crania. Mandibular landmarks were divided into left and right landmark sets retaining midline landmarks in order to remove the effect of the left and right hemi-mandibles shifting relative to each other due to the weak ligamentous symphysis present in mice.

Principal component analyses were carried out on both a cranial and mandibular set of three-dimensional landmark coordinates for all individuals of all three strains in order to explore patterns of shape variance both within and between strains. Key patterns of shape variance showed the *pten* phenotype to be characterised by an increase in cranial length alongside a decrease in cranial height and width while the brachymorph phenotype is characterised by a decrease in cranial length alongside an increase in cranial height and width. The wild-type strain was shown to fall between the two mutant strains in terms of this key pattern of shape variance, but with greater overlap with the *pten* than brachymorph strain. Intra-strain principal component analyses indicated the presence of common patterns of shape variance in both the cranium and mandible of the three strains.

In order to carry out biomechanical analyses, first cranial and mandibular surface files were realigned to meet incisal occlusion. So that three dimensional analyses could be carried out the jaw out-lever was calculated via the dot product. A comparison study was then carried out to establish differences between two potential methods of determining the muscle force vector from which to calculate the muscle in-lever. As no significant difference was found in the variance of the two methods, the 'attachment areas' method was selected as this method incorporated more biological information. Methods of calculating both jaw out-lever and muscle in-lever were also compared with similar published work by other authors (Swiderski

and Zelditch, 2010). While little difference was found between comparable three-dimensional and two dimensional methods; methods of defining muscle force vectors from three dimensional muscle attachment areas developed and used in this thesis were found to generate significantly different results to alternative published methods. The latter result may be due to differences in the definition of the muscle in-lever arm. Many authors use the term lever-arm and moment -arm interchangeably, and methods developed for this thesis define the muscle in-lever as the perpendicular distance from the fulcrum to the muscle line of action (this length which may also be termed the moment-arm). Other authors however define the muscle in-lever as the distance from the fulcrum to the point of force application (lever arm), (Flanagan, 2014) or provide a surrogate measure of the moment arm. When cases where the lever arm is taken as the distance from the fulcrum to the point of force application are compared to cases where the lever arm is taken as the perpendicular distance from the fulcrum to the muscle line of action, these two distances will only be the same when the force is acting perpendicular to the lever arm (Flanagan, 2014)

CHAPTER 3 THE MORPHOLOGY OF THE MOUSE MASTICATORY MUSCULATURE

This thesis chapter is published as: BAVERSTOCK, H., JEFFERY, N. S. & COBB, S. N. 2013. The morphology of the mouse masticatory musculature. *Journal of anatomy*, 223, 46-60. (DOI: 10.1111/joa.12059)

3.1 INTRODUCTION

The house mouse (*Mus musculus*) has dominated work on the development, genetics and evolution of the mammalian skull and associated soft-tissue for decades. During this time the emphasis has shifted from one of general qualitative description of changes at the cellular level and to a lesser extent at the organ system level; to the quantification and investigation of morphological outcomes following genetic and/or experimental manipulation, from dietary regimes through to surgical interventions (Kyrkanides et al., 2007, Yamada et al., 2006, Byron et al., 2004, Byron et al., 2008, Maedaa, 1987). As detailed knowledge of mouse craniofacial anatomy is a prerequisite to such work it is generally assumed that this essential knowledge base is well established. Authors have focussed attention on the anatomy of the brain (Klintworth, 1968), limbs (Pomikal and Streicher, 2010), internal organs (Berry, 1900, Roberts, 1975), and the embryology (Kaufman and Bard, 1999, Kaufman, 1992, Brune et al., 1999) of the mouse, with very few detailed descriptions of mouse musculature or craniofacial skeletal anatomy, and no accurate description of the masticatory musculature of this species is available in the literature.

While mouse models have been widely used in many scientific disciplines for decades there has been a recent resurgence in the use of mice to explore morphological questions, and this species is proving extremely valuable in understanding craniofacial development, morphology, function and evolution. Several authors have employed the mouse in studies of craniofacial morphological development and variation (Boughner et al., 2008, Cray et al., 2011, Hallgrimsson and Lieberman, 2008, Lieberman et al., 2008, Vecchione et al., 2007, Willmore et

al., 2006a, Byron et al., 2004, Klingenberg, 2002, Leamy, 1993, Morriss-Kay and Wilkie, 2005). Contemporary investigation of integration and modularity has also often focused on the mouse as a model (Hallgrímsson et al., 2006, Hallgrímsson et al., 2004b, Hallgrímsson et al., 2004a, Klingenberg et al., 2003, Mezey et al., 2000) and this species has played a significant role in the understanding of the adaptive evolution of morphology and the function of genetics in such evolution (Renaud et al., 2010, Klingenberg and Leamy, 2001, Cheverud et al., 1991, Atchley et al., 1985a, Atchley et al., 1988, Atchley et al., 1985b, Ravosa et al., 2008b, Willmore et al., 2006b). Additionally, medical and dental science has benefited from the mouse as a model through the investigation of pathological conditions affecting craniofacial morphology (*Cleft lip*: (Chai and Maxson, 2006, Parsons et al., 2008); *Down Syndrome*: (Hill et al., 2007, Richtsmeier et al., 2002); *Craniosynostosis*: (Perlyn et al., 2006); *Midfacial Retrusion*: (Lozanoff et al., 1994); *Craniofacial Dysmorphology*: (Tobin et al., 2008)). As the mouse has in the past, and continues to play such a crucial role in the advancement of understanding of craniofacial development, morphology and evolution it is surprising that very little published data exists regarding the anatomy, and in particular the muscular anatomy of the craniofacial complex of *Mus musculus*.

Despite the paucity of published descriptive mouse anatomy, a significant amount of literature exists regarding rodent masticatory anatomy in general (Ball and Roth, 1995, Cox and Jeffery, 2011, Druzinsky, 2010a, Druzinsky, 2010b, Greene, 1936, Hautier and Saksiri, 2009, Hiiemae and Houston, 1971, Janis, 1983b, Offermans and De Vree, 1989, Olivares et al., 2004, Satoh, 1997, Satoh and Iwaku, 2004, Satoh and Iwaku, 2006, Satoh and Iwaku, 2009, Turnbull, 1970, Weijs and Dantuma, 1975b, Weijs, 1973, Woods and Howland, 1979, Woods and Hermanson, 1985, Yoshikawa and Suzuki, 1969) as well as bite force and feeding mechanics in rodents (Freeman and Lemen, 2008a, Freeman and Lemen, 2008b, Gorniak, 1977, Hiiemäe and Ardran, 1968, Robins, 1977, Mosley and Lanyon, 1998, Nies and Young Ro, 2004, Satoh, 1998, Satoh, 1999, Williams et al., 2009). Patel (1978) presents a paper regarding the bone-muscle complex of the masticatory apparatus of *Mus musculus*. This study however was investigated through dissection alone and given the size of the mouse it is appreciably incomplete and provides little detail of the origins and

insertions of the muscles. To the best of the authors' knowledge no other literature exists regarding either the muscular anatomy or the bite force and feeding mechanics of *Mus musculus*.

In this study we present, for the first time, a detailed description of the masticatory apparatus of *Mus musculus*. Using contemporary high resolution micro-computed tomography (micro-CT) with iodine staining, complemented by more traditional dissection techniques we provide a comprehensive description of mouse masticatory musculature that will enable this model organism to be utilised further in an array of disciplines and fields. The methodology of using contrast enhanced micro-CT imaging coupled with reconstruction techniques is the same as that used by Cox and Jeffery (2011), based upon the work of Jeffery et al (2011) and Metscher (2009). While micro-CT imaging methods have been employed in quantitative studies of variation (Hallgrímsson et al., 2007) and development (Parsons et al., 2008) in the craniofacial region of mice, the use of contrast-enhanced micro-CT imaging to document non-invasively and incorporate muscular architecture in such studies thus far remains a little utilised technique. Such contrast-enhanced scanning techniques are more commonly utilised in vascular and cardiac research, both in humans (Aslanidi et al., 2012) and other mammals including mice (Badea et al., 2008), and even to image arthropod circulatory systems (Wirkner and Prendini, 2007, Wirkner and Richter, 2004). These techniques have also been used to investigate jaw muscle anatomy in the alligator (Tsai and Holliday, 2011). The reporting of accurate three dimensional reconstructions of mammalian post-natal craniofacial musculature from contrast-enhanced micro-CT imaging to provide valuable detail for comparative, developmental, functional and quantitative studies of morphology is however so far limited to the rat, squirrel, guinea-pig and spiny rat (Cox et al., 2012, Cox and Jeffery, 2011, Hautier et al., 2012). This present study sits alongside the work of Cox and Jeffery (2011) providing a direct comparison with those three rodents that have currently been described using the same technique as presented here.

The ongoing status of the mouse as an ideal model organism for investigation and understanding craniofacial development, morphology, function and evolution; combined with exciting and fast moving developments in the field of comparative

anatomy and morphology results in the urgent need for an excellent description of mouse masticatory anatomy.

This study constructs the foundation for a series of future investigations of form and function. Many authors have taken advantage of the versatility of the mouse in the investigation of variance, canalisation, modularity, integration, functional significance and other fundamental areas of focus in the exploration of form, function and evolution. This large body of studies has included comparative work of different strains, species (Auffray et al., 1996, Macholán et al., 2008, Macholán, 2008, Cordeiro-Estrela et al., 2006), geographic populations (Renaud and Michaux, 2007, Macholán et al., 2008, Corti and Rohlf, 2001), hybrids (Debat et al., 2006) and mutant (Hallgrímsson et al., 2006, Perlyn et al., 2006, Kawakami and Yamamura, 2008) mice. While the present study is limited to one species, the detailed and precise anatomical investigation of *Mus musculus* provided here will be utilised in future investigations characterising functionally significant variations in morphology among both different mutant strains and rodent species. Not only will this current work allow the investigation of the functional significance of variation and the role of mechanical forces on the development of the craniomaxillary complex through computational mechanical modelling techniques such as finite element analysis (FEA) and multibody dynamic modelling (MDA), but it will also serve as an invaluable reference for phenotypic comparison with other strains and species of mice.

3.2 MATERIALS AND METHODS

3.2.1 Dissection

Detailed dissection was carried out on four *Mus musculus* specimens. These specimens were acquired from Newton Resources, Jarrow UK. Using a micro-dissection kit each specimen was carefully dissected to reveal muscle insertions, attachments and morphology. Superficial muscles were firstly retracted to reveal deep muscles, and later removed. Individual muscle masses from one specimen of *Mus musculus* were then collected using digital scales. The dissection was documented and photographed using a Canon G9 digital camera (Figure. 3.3.2).

3.2.2 3D Skull and Muscle Reconstruction

Contrast enhanced micro-CT data for one adult specimen of *Mus musculus* (adult, BALB/c background strain) was carried out by one of us (NSJ; see Jeffery et al., 2011). This specimen was acquired post-mortem from Charles River UK Ltd.

A solution of iodine potassium iodide (I₂KI) was used as the contrast agent to increase the differential attenuation of X-rays among the soft tissues. This technique has been shown not only to effectively differentiate between individual muscles and bone, but also to demonstrate patterns of muscle fibres and fascicles alongside connective tissues (Jeffery et al., 2011, Cox and Jeffery, 2011).

The specimen was fixed in a phosphate-buffered formal saline solution (polymerized formaldehyde dissolved as a 4% solution in phosphate buffered saline, allowing for the long-term storage with limited tissue shrinkage) and then placed in 3.75% I₂KI contrast agent for a period of 7 days. Although it is possible that muscle shrinkage may occur with this technique the effect is likely to be relatively small given the low concentration of I₂KI used and consistent across all muscles and thus has no effect on the relative proportions reported or qualitative muscle descriptions. The specimen

was then imaged with the Metris X-Tek custom 320kV bay system at the EPSRC funded Henry Moseley X-ray Imaging Facility at the University of Manchester. Imaging parameters were optimised for the individual specimen to maximise the spatial and contrast resolution (kV 75; μ A 105). Voxel resolution was isotropic with vertices of 0.033mm (Jeffery et al., 2011).

The contrast enhanced micro-CT images were viewed using Aviso 6.3, 3D visualisation software designed for visualisation, analysis and modelling of scientific data (Avizo6, 2009).

A three-dimensional reconstruction of the masticatory musculature of *Mus musculus* was carried out using the segmentation function of Aviso 6.3.

Each masticatory muscle, major masticatory tendon and the craniofacial skeleton and mandible were individually reconstructed. The techniques of contrast enhancement of muscles prior to scanning results in clarity and distinction of individual muscles, yet this has the disadvantage of reducing the contrast difference between muscle and bone. As iodine as a contrast agent reduces the contrast resolution between bone and the surrounding tissues, a scan is produced in which greyscale values are not sufficiently different between muscles and bone and thus automated division of these two different materials that is usually possible with a CT scan (through use of a threshold function available in visualisation software such as Aviso 6.3) is not possible here. Consequently all muscle and bone reconstructions were built manually. The contrast enhanced micro-CT scan was loaded into Aviso6.3, and muscles of interest was carefully identified and painted. Where appropriate an interpolation function was used to insert material between two selected areas approximately ten slices apart in order to improve the efficiency of the process. A smoothing function was applied to reduce the blocky appearance of the reconstruction.

Attachments areas of the muscles were established through segmentation of the contrast enhanced micro-CT scan independent of that of the muscle volumes. While muscle boundaries on the scan are distinguished via the appearance of a darker greyscale band between the muscle in question and adjacent structures, attachment areas were determined as regions of the scan in which no darker band was present

between muscle and bone, and instead a merging of the greyscale appearance of the two was observable. The authors acknowledge that the subjective nature of this method may introduce some error.

Following completion of the 3D reconstruction an output of each individual muscle volume was calculated by Aviso6.3. Assuming a muscle density of 1.0564 g/cm³, individual muscle masses were calculated (mass = volume x density) (Murphy and Beardsley, 1974). Volumes, masses and percentages of muscles are outlined in **Table 3.3.1**.

The masticatory musculature revealed through both dissection and three dimensional muscle reconstructions was compared to that of previous literature. The literature consulted was as follows: Ball and Roth, 1995 (*Sciurus, Microsciurus, Sciurillus, Tamiasciurus, Tamias, Glaucomys*); Byrd, 1981 (*Cavia*); Cox and Jeffery, 2011 (*Sciurus, Cavia, Rattus*); Druzinsky 2010a (*Aplodontia, Cynomys, Tamias, Marmota, Ratufa, Sciurus, Thomomys*); Gorniak, 1977 (*Mesocricetus*); Greene, 1935 (*Rattus*); Hautier and Saksiri, 2009, (*Laonastes*); Hautier, 2010 (*Ctenodactylus*); Offermans and De Vree, 1989 (*Pedetes*); Olivares et al., 2004 (*Aconaemys, Octomys, Tympanoctomys, Spalacopus, Octodon, Octodontomys*); Rinker, 1954 (*Sigmodon, Oryzomys, Neotoma, Peromyscus*); Rinker and Hooper, 1950 (*Reithrodontomys*); Satoh, 1997, 1998, 1999 (*Apodemus, Clethrionomys*); Satoh and Iwaku, 2004 (*Mesocricetus, Cricetulus, Tscherkia, Phodopus*); Satoh and Iwaku, 2006 (*Onychomys*); Satoh and Iwaku, 2009 (*Neotoma, Peromyscus*); Turnbull, 1970 (*Sciurus, Rattus, Hystrix*); Weijs, 1973 (*Rattus*); Wood, 1965 (*Marmota, Myocastor, Ondatra*); Woods, 1972 (*Proechimys, Echimys, Isothrix, Mesomys, Myocastor, Octodon, Ctenomys, Erethizon, Cavia, Chinchilla, Dasyprocta, Thryonomys, Petromus*); Woods and Howland, 1979 (*Capromys, Geocapromys, Plagiodontia, Myocastor*); Woods and Hermanson, 1985 (*Capromys, Geocapromys, Plagiodontia, Myocastor, Echimys, Octodon, Erethizon, Coendou, Dasyprocta, Atherurus, Thryonomys, Petromus*).

3.2.3 Nomenclature

Despite there being very little published work regarding the craniofacial anatomy and musculature in *Mus musculus*, a number of publications exist detailing the masticatory anatomy of species in the rodent order, including the rat (Greene, 1936, Hiiemae and Houston, 1971, Weijs, 1973, Cox and Jeffery, 2011); capromyid rodents (Woods and Howland, 1979); hystricognath rodents (Woods and Hermanson, 1985); new world squirrels (Ball and Roth, 1995); old world hamsters (Satoh and Iwaku, 2004); northern grasshopper mouse (Satoh and Iwaku, 2006); Loatian rock rat (Hautier and Saksiri, 2009); mountain beaver (Druzinsky, 2010a, Druzinsky, 2010b) and many more. A number of different nomenclatures currently exist throughout this body of literature as regards both rodent and general mammalian craniofacial muscular anatomy (Druzinsky et al., 2011). In this paper we will follow the system of a number of authors, with three layers of the masseter observed and identified as the superficial masseter, the deep masseter, and the zygomaticomandibularis. The temporalis is also divided into two parts, the lateral- and medial- temporalis as reflects their anatomical relationship. The pterygoids are referred to in reference to their origin on and in and pterygoid fossa, as the internal- and external- pterygoid muscles (Cox and Jeffery, 2011, Turnbull, 1970, Weijs, 1973, Ball and Roth, 1995).

Other authors have opted for different nomenclatures: some authors have named the three layers of the masseter as the superficial-, lateral- and medial- masseter (Hautier and Saksiri, 2009; Wood, 1965; Woods, 1972); others use a combination of the latter system and that used in this paper (Satoh and Iwaku, 2004, Satoh and Iwaku, 2006, Satoh and Iwaku, 2009, Offermans and De Vree, 1989, Druzinsky, 2010a, Druzinsky, 2010b) . An additional variation found is in the naming of the rostral expansion of the innermost layer of the masseter, referred to here as the infra-orbital zygomaticomandibular, it is sometimes referred to as the maxillomandibularis (Coldiron, 1977, Janis, 1983a).

The sole published work specifically regarding the anatomy of the masticatory muscles of *Mus musculus* (Patel, 1978) combines a number of the nomenclatures described above. Patel (1978) differentiates and classifies the masticatory muscles of the mouse as the superficial masseter, deep masseter (consisting of an anterior deep masseter, infraorbital part of the anterior deep masseter, and posterior deep masseter), temporalis (anterior fasciculus, posterior fasciculus and zygomaticus fasciculus) and the pterygoids (external and internal).

The nomenclature elected in this paper has been chosen for its consistency with that of used in the literature regarding most other mammalian groups (Storch, 1968, Coldiron, 1977, Janis, 1983a, Druzinsky et al., 2011); and for its uniformity with Cox and Jeffery (2011) who have applied the same techniques reported here to other rodent taxa. This system is also favoured as it clearly reflects the anatomical relationships and positions of the musculature.

3.3. RESULTS

Figure 3.3.1 illustrates the bony anatomy of the cranium and mandible of *Mus musculus*. Enhanced photographic images of dissection results are given in **Figure 3.3.2**, whilst **Figures 3.3.3, 3.3.4, 3.3.5 and 3.3.6** show the enhanced micro-CT three dimensional reconstructions of the muscles of mastication in *Mus musculus*. **Table 3.3.1** gives the corresponding muscle volumes, masses and percentages.

KEY ANATOMICAL REGIONS ON THE CRANIUM AND MANDIBLE

Figure 3.3.1

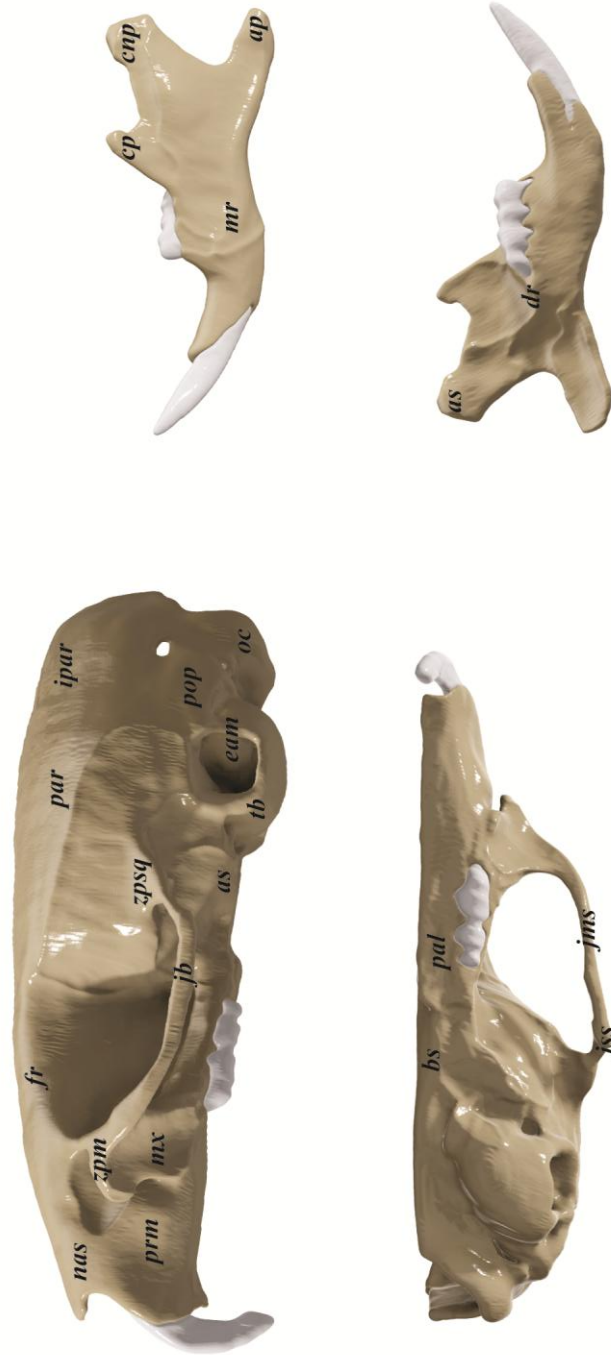
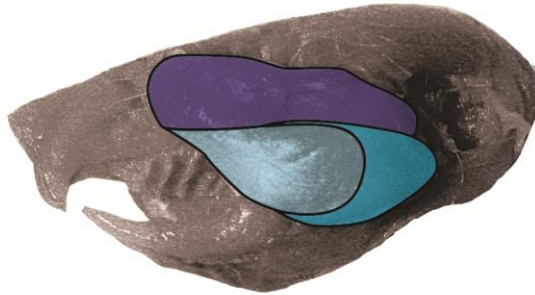


Figure 3.3.1: Key anatomical regions on the cranium and mandible in *Mus musculus*: as, articular surface; cnp, condyloid process; ap, angular process; mr, masseteric ridge; cp, coronoid process; dr, dental ridge; prm, premaxilla; nas, nasal; fr, frontal; aef, anterior ethmoidal foramen; mx, maxilla; zpm, zygomatic process of maxilla; bs, basosphenoid; par, parietal; zpsq, zygomatic process of squamosal bone; ipar, interparietal; eam, external auditory meatus; tb, tympanic bulla; pop, paraoccipital process; oc, occipital condyle; pal, palatine; as, alisphenoid; jb, jugal bone; jss, jugosquamosal suture; jms, jugomaxillary suture.

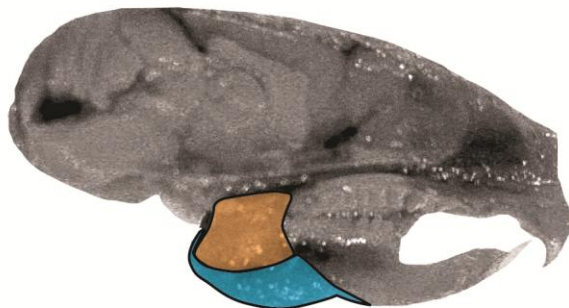
a.



b.



c.



SUPERFICIAL MASSETER

 muscle

 tendon

DEEP MASSETER



ZYGOMATICOMANDIBULARIS

 infraorbital

 anterior

 tendon

TEMPORALIS

 medial

PTERYGOID

 internal

Figure 3.3.2: Graphically enhanced photographs of *Mus musculus* dissection, highlighting major masticatory muscles. (A) Lateral view with skin removed to reveal the temporalis, deep masseter and superficial masseter muscles; (B) Lateral view with skin removed and both superficial and deep masseter muscles retracted to reveal the zygomaticomandibularis muscle with its infraorbital and anterior regions alongside its tendon; (C) Bisected sagittally to reveal the medial surface of the mandible, with the internal pterygoid and the reflected portion of the superficial masseter.

The superficial masseter muscle is clearly distinguished both on micro-CT and through dissection. A significant unipennate masticatory muscle, the superficial masseter and its tendon account for 19% of the total muscle mass (**Table 3.3.1**).

Alongside its tendinous sheet that covers in the region of one third of the lateral surface, the superficial masseter runs obliquely from the anterior portion of the cranium to the posterior portion of the mandible. Roughly triangular in shape and passing obliquely this muscle directly overlies approximately half of the deep masseter which lies immediately medial to the superficial muscle (**Figure 3.3.2a; Figure 3.3.3**).

The tendinous origin of the superficial masseter attaches to a small process on the maxillary bone of the cranium, immediately medioventral to the infraorbital foramen. Fibres originating from the tendinous sheet run posteriorly following the oblique path of the tendon and muscle to insert onto the body of the mandible on both the lateral and medial surfaces (**Figure 3.3.6a**).

The superficial masseter has a slender yet lengthy insertion along the ventral border of the mandible. This attachment area lays both on the ventromedial and ventrolateral surfaces. On the lateral surface, directly beneath the attachment of the deep masseter this attachment runs from the angle of the mandible to a position ventral to the first molar (**Figure 3.3.4e**). Similarly, on the medial surface reflected fibres run from the angle of the mandible to a position ventral to the first molar, with the height of the attachment area increasing in the portion beneath the third molar (**Figure 3.3.4f**).

A dorsal elongation of the reflected part of the superficial masseter onto the medial surface of the mandible is present. This pars reflexa (Druzinsky et al., 2011, Turnbull, 1970, Woods, 1972, Weijs, 1973, Cox and Jeffery, 2011) attaches along a clearly defined ridge just anterior to the attachment of the internal pterygoid (**Figure 3.3.3; Figure 3.3.4f**).

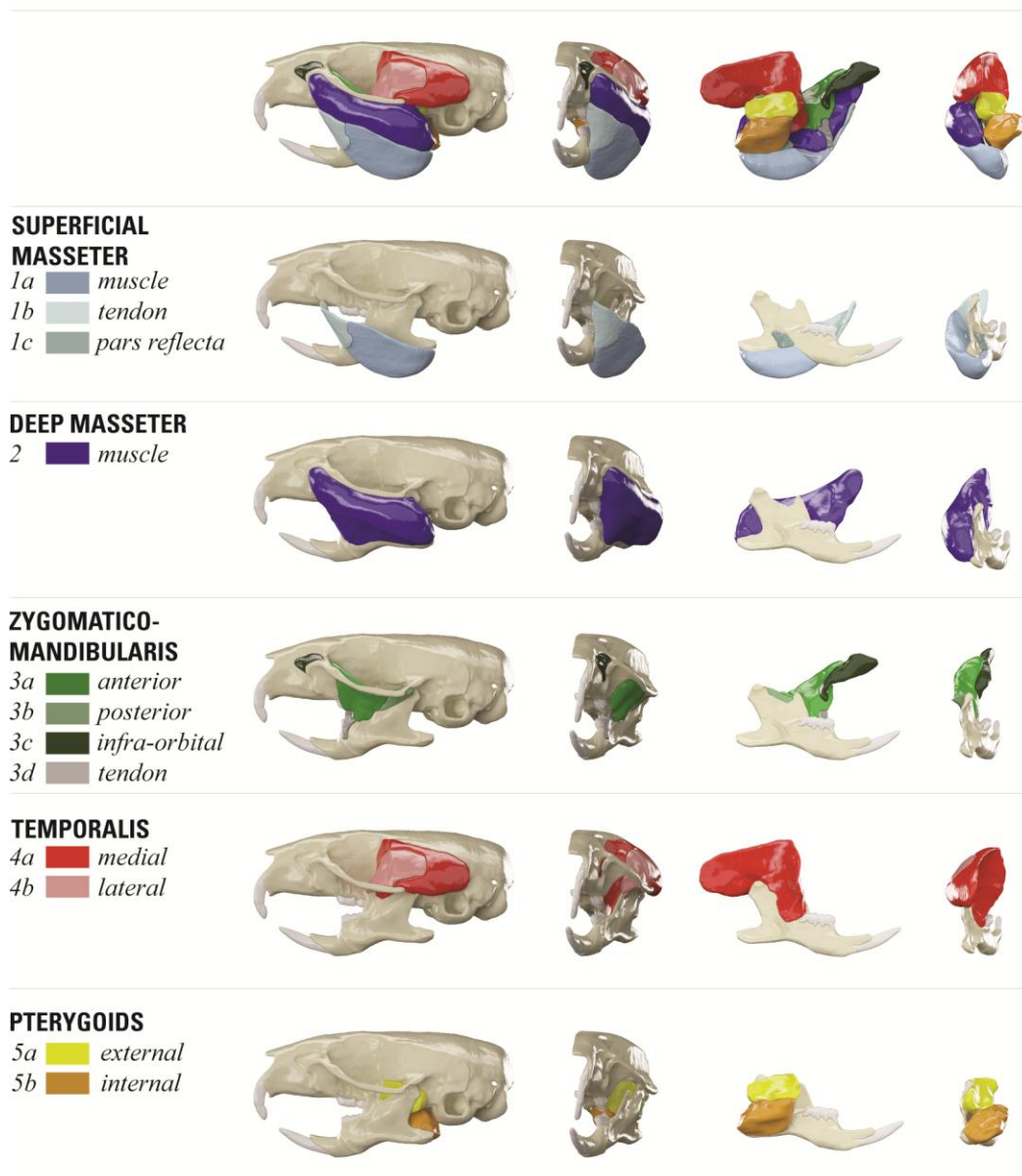


Figure 3.3.3: Three-dimensional reconstruction of masticatory apparatus, with insets showing individual muscles positioning on the cranium and mandible.

Table 3.3.1 **VOLUMES, MASSES AND PERCENTAGES OF MASTICATORY MUSCLES**

	Muscles volumes estimated from dissection, mm ³	Muscle volumes outputted from segmentation, mm ³	Muscle masses calculated from segmentation, g	Percentage of overall muscle mass or volume, %	Percentage of volume of composite parts to individual muscle, %
Superficial masseter (total)	64	58.50	0.062	19.13	
Muscle		52.83	0.056		91.82
Tendon		4.71	0.005		8.18
Pars reflecta		0.96	0.001		1.67
Deep masseter (total)	100	101.89	0.108	33.32	
Zygomatichandibularis (total)	25	26.92	0.028	8.80	
Anterior		15.71	0.017		58.38
Posterior		3.52	0.004		13.07
Infraorbital		7.17	0.008		26.63
Tendon		0.52	0.001		1.92
Temporalis (total)	60	68.63	0.073	22.44	
Lateral		15.98	0.017		23.28
Medial		52.65	0.056		76.72
Pterygoid (total)	42	49.87	0.053	16.31	
External	10	14.49	0.015	4.74	29.06
Internal	32	35.38	0.037	11.56	70.94

3.3.2 Deep Masseter

The deep masseter is the largest masticatory muscle in the mouse, accounting for 33% of the overall muscle mass (**Table 3.3.1**). This large muscle which lies medial to the superficial masseter takes the form of a broad parallelogram, spanning the length of the jugal bone and covering the majority of the mandible (**Figure 3.3.3**).

Whilst in other rodents a clear division of the deep masseter into anterior and posterior parts is reported (Cox and Jeffery, 2011) in the mouse no clear distinction between two such regions was found on either dissection or segmentation of micro-CT images. A number of septa within the deep masseter are visible on micro-CT yet none of these are fully discernible as an anterior-posterior divide and no variation in fibre direction suggestive of such a separation were observed (**Figure 3.3.6**). The deep masseter is thus reported as a single muscle in the present study.

The deep masseter originates from the ventrolateral surface of the jugal bone. This attachment spans almost the entire length of this bone, running anteriorly from the anterior most point on the rim of the zygomatic process of the maxilla, to the jugosquamosal suture (**Figure 3.3.4**). Muscle fibres run from their origin on the jugal bone, posteroventrally to meet their attachment area on the surface of the mandible (**Figure 3.3.6**).

The deep masseter inserts onto the lateral surface of the mandible with an attachment area so great that it covers a large proportion of this surface. This attachment sits directly above that of the superficial masseter and below that of the anterior and posterior zygomaticomandibularis, stretching across the surface of the mandible from the angle to a point ventral to the first molar. The inferior border of this attachment runs from the angular process, along the masseteric ridge, to a point ventral to the anterior border of M1. The anterior border of this attachment begins at the point of greatest curvature between the angular process and the condylar process, runs anterodorsally to meet the inferior border of the attachment of the posterior zygomaticomandibularis, and then passes posteroventrally to the most anterior point on the masseteric ridge, ventral to the anterior border of M1 (**Figure 3.3.4e**).

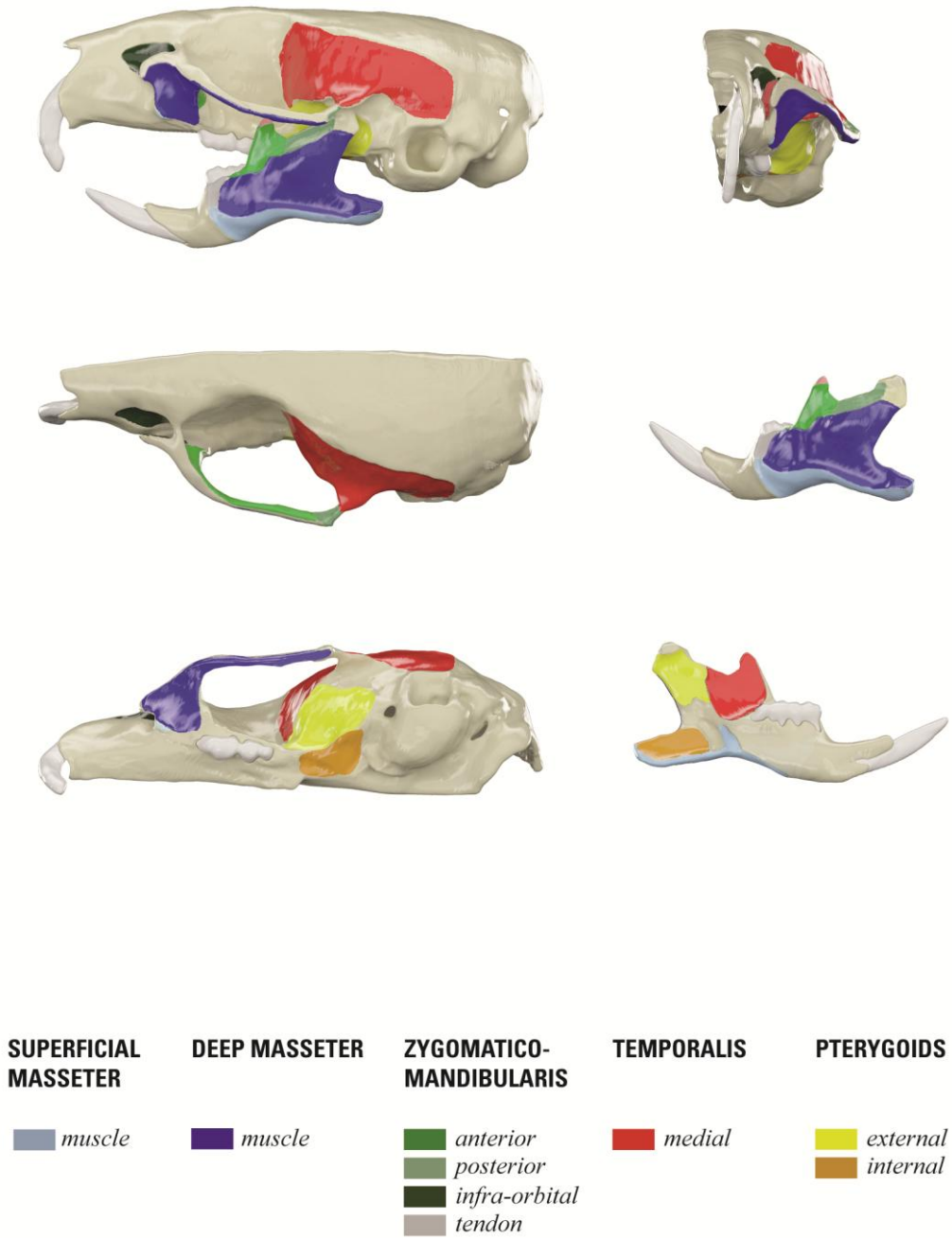


Figure 3.3.4: Depiction of masticatory muscle attachment areas.

3.3.3 Zygomaticomandibularis

The zygomaticomandibularis is a muscle less acknowledged in the literature and less conventional in its morphology. Several authors do not recognise the zygomaticomandibularis as a separate muscle from the deep masseter in rodents (Hiemae and Houston, 1971, Byrd, 1981, Satoh, 1998, Satoh, 1997, Satoh, 1999). In contrast we found that on micro-CT there is a clear distinction between the deep masseter and the zygomaticomandibularis in the mouse, as is also found in the squirrel, rat and guinea pig (Cox and Jeffery, 2011). A clear division between an anterior and posterior part of this muscle, as well as a rostral expansion termed the infra-orbital zygomaticomandibularis are also found here in the mouse.

Viewed as a whole, the zygomaticomandibularis begins anteriorly as a small bulb-like muscle sitting in a fossa in the maxillary bone anterodorsal to the infraorbital foramen. This muscle then passes posteriorly through the infraorbital foramen, attaching along the length of the jugal bone on the mediodorsal surface. The zygomaticomandibularis then travels ventrally, medial to the jugal bone to attach onto the dorsolateral surface of the mandible (**Figure 3.3.3**). Despite the length of the entire zygomaticomandibularis being greater than that of the deep masseter this is a slim and relatively short muscle which viewed as a whole still accounts for only 9% of the total masticatory muscle mass in the mouse (**Table 3.3.1**). Below we approach and describe this muscle as its three constituent parts: the infra-orbital zygomaticomandibularis, the anterior zygomaticomandibularis and the posterior zygomaticomandibularis.

MICRO-CT SLICES HIGHLIGHTING MASTICATORY MUSCULATURE

Figure 3.3.5

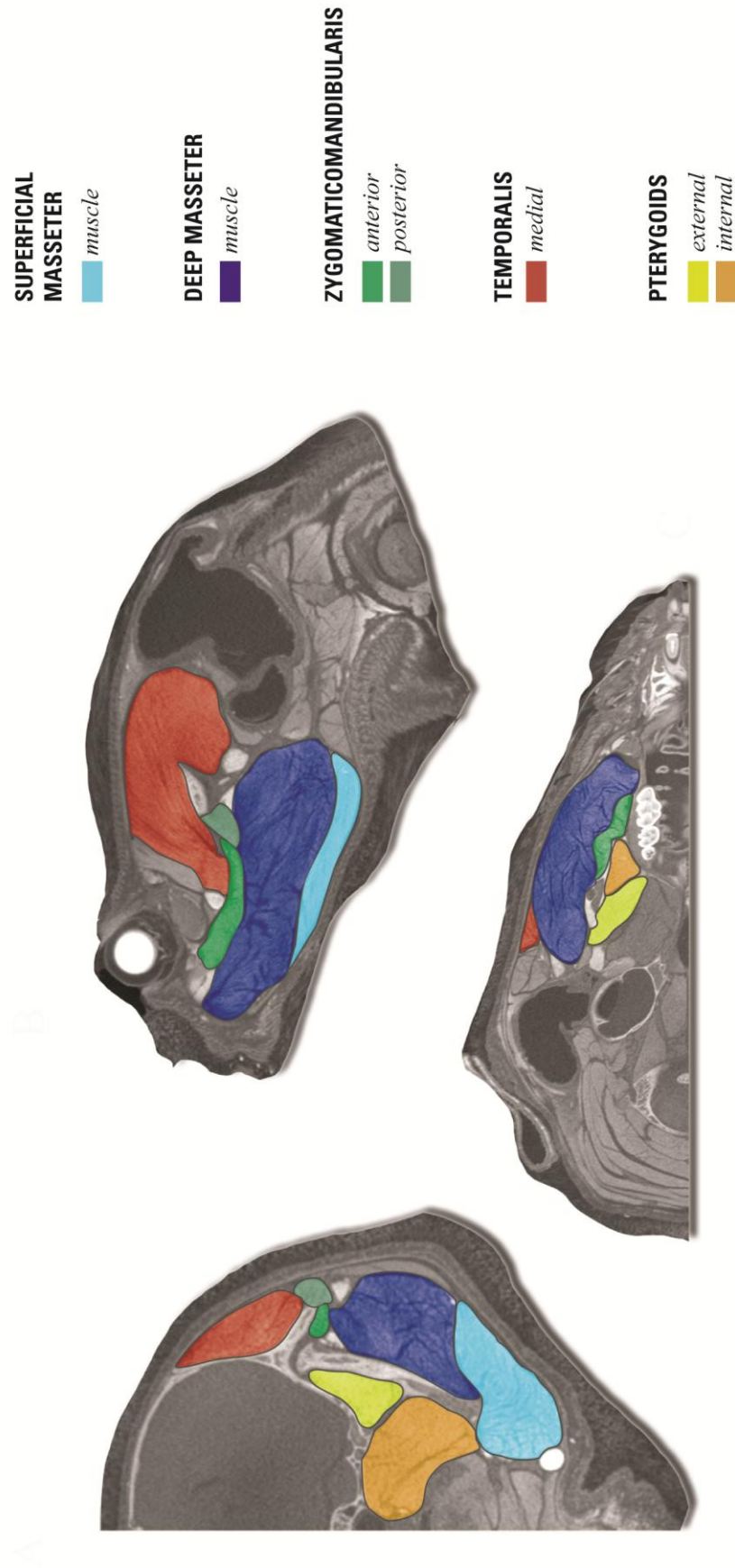


Figure 3.3.5: Contrast enhanced micro-CT slices, graphically enhanced to visualise masticatory muscles. (A) coronal section; (B) sagittal section; (C) transverse section.

3.3.3.1 Anterior zygomaticomandibularis

The anterior zygomaticomandibularis is the largest part of this muscle, accounting for 58% of the total muscle mass of the zygomaticomandibularis.

This muscle originates from the dorsomedial surface of the zygomatic arch, anteriorly from the point of greatest curvature on the medial surface of the zygomatic process of the maxilla, to the jugosquamosal suture of the jugal bone (**Figure 3.3.4b**). There is also a small attachment area of this muscle on the maxillary bone, posteroventral to the zygomatic process of the maxilla (**Figure 3.3.4a**). Muscles fibres run ventrally to attach onto the lateral surface of the mandible.

The anterior zygomaticomandibularis inserts onto the lateral surface of the mandible, with an attachment area that encompasses almost the entirety of the coronoid. Sitting directly dorsal to the attachment of the deep masseter this attachment runs obliquely from a point ventral to the first molar towards the coronoid process, sparing the very tip of this coronoid where the lateral temporalis attaches. The anterior zygomaticomandibularis attachment continues posterior of the coronoid, finishing at the point of greatest curvature between the coronoid process and the condylar process where it meets the attachment of the posterior zygomaticomandibularis (**Figure 3.3.4e**).

The zygomaticomandibularis also has a thick tendinous band that inserts onto the lateral surface of the mandible, ventral to the anterior border of M1 and anterior to the attachment of the deep masseter (**Figure 3.3.3, Figure 3.3.4e**). In addition to its attachment area on the lateral surface of the coronoid, fibres from the anterior zygomaticomandibularis inset onto this tendon.

3.3.3.2 Posterior zygomaticomandibularis

Accounting for just 13% of the total mass of the zygomaticomandibularis, the posterior section is the smallest of the three parts of the zygomaticomandibularis

(**Table 3.3.1**). This small muscle forms a bridge between the very posterior portion of the jugal bone and the mandible.

The posterior zygomaticomandibularis originates from a small area of bone on the lateral posterior border of the jugal bone, at the point where the squamosal bones extends to meet the jugosquamosal suture. This slim attachment area lies directly posterolateral to the lateral expansion of the attachment of the medial temporalis onto the squamosal bone.

Fibres of the posterior zygomaticomandibularis pass anteroventrally, lateral to the jugal bone, to insert onto the lateral surface of the mandible. Again this is a relatively small attachment area, extending from the posterior border of the attachment of the anterior zygomaticomandibularis at the point of greatest curvature between the coronoid process and the condylar process, to a point just anterior of the condylar process. This attachment area lies directly dorsal to the attachment of the deep masseter (**Figure 3.3.4e**).

3.3.3.3 Infraorbital zygomaticomandibularis

The infraorbital zygomaticomandibularis is again a relatively small masticatory muscle in the mouse, accounting for 27% of the muscle mass of the zygomaticomandibularis, but only 2.4% of the overall muscle mass. This is a distinctive muscle, lying in a fossa on the maxilla anterior to the infraorbital foramen, passing posteriorly through the infraorbital foramen and then ventrally, medial to the jugal bone to attach onto the lateral surface of the mandible.

The infraorbital zygomaticomandibularis originates from a concavity in the maxilla, ventral to the nasal bone, medial to the zygomatic process of the maxilla, anterior to the orbit, and posterior to the premaxillomaxillary suture. The infraorbital zygomaticomandibularis attaches onto the lateral border of this concavity and also onto the medial surface of the zygomatic process of the maxilla (**Figure 3.3.4**)

Fibres of the infraorbital zygomaticomandibularis pass posteriorly through the infraorbital foramen, and then once through the foramen immediately descend ventrally, medial to the jugal bone, to insert onto the lateral surface of the mandible. This insertion is via a thick tendinous band that has a relatively small attachment area directly ventral to the anterior border of M1, anterior to the attachment of the deep masseter and immediately dorsal to the attachment area of the superficial masseter (**Figure 3.3.4e**). Fibres of the infraorbital zygomaticomandibularis are joined by fibres of the anterior zygomaticomandibularis in their attachment to this tendinous band. While it is difficult to determine on the micro-CT images and, due to the small size of these muscles, on dissection, fibres from the infraorbital zygomaticomandibularis may also attach to the medial border of the jugal bone or join those of the anterior zygomaticomandibularis as these two muscles run ventrally together to attach to the tendon.

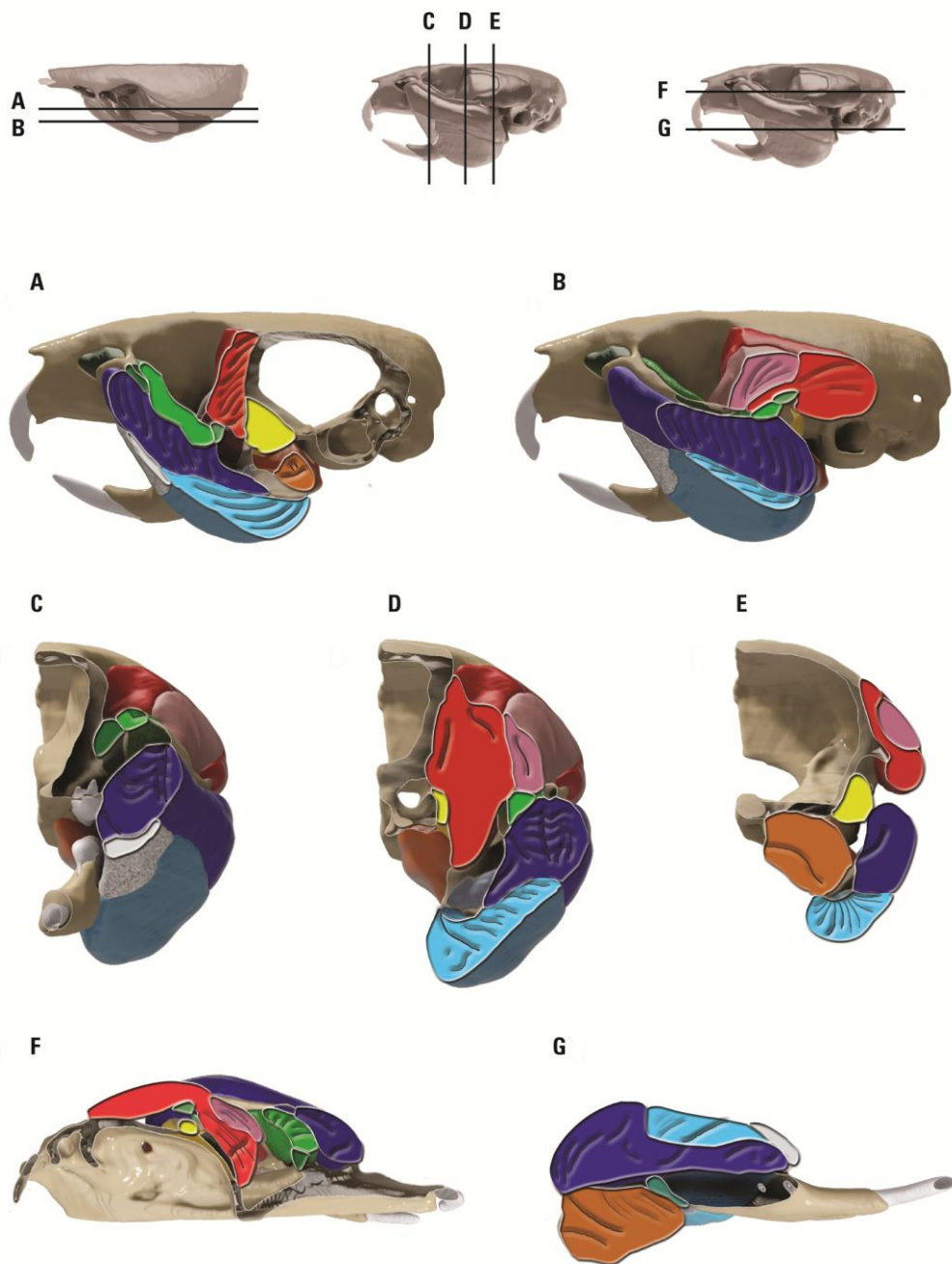


Figure 3.3.6: Cross sections of the three dimensional reconstruction of *Mus musculus* craniofacial anatomy, with fibre orientations highlighted. (A) and (B) sagittal sections moving mediolaterally; (C) (D) and (E) coronal sections moving anteroposteriorly; (F) and (G) transverse sections moving dorsoventrally. See **Figure 3.3.3** for colour key.

3.3.4 Temporalis

The temporalis muscle is a major masticatory muscle, accounting for 22% of the overall muscle mass, and is thus the second largest masticatory muscle in the mouse. In rats (Cox and Jeffery, 2011) a clear division of the temporalis into lateral and medial parts is reported. A similar separation of the temporalis is reported in many rodents and other Glires, although various terminology is used throughout the literature, and this muscle is most often described as consisting of anterior and posterior parts (Druzinsky et al., 2011, Gorniak, 1977, Turnbull, 1970, Druzinsky, 2010a, Woods and Howland, 1979, Hiimae and Houston, 1971) A division into lateral and medial parts is apparent in the mouse, however the exact boundaries of this division are equivocal on the micro-CT scan utilised in this study, especially as regards the superior region of the margin between the two parts. In this investigation we therefore report the temporalis muscle as medial and lateral parts but are cautious about the precise boundary and attachment points of the lateral temporalis (**Figure 3.3.3**). It is estimated that the lateral temporalis is the smaller portion accounting for 23% of the overall temporalis muscle mass, whilst the medial portion accounts for 77% (**Table 3.3.1**).

3.3.4.1 Medial temporalis

The medial temporalis originates from a large area on the lateral surface of the cranium. This broad attachment to the floor of the temporal fossa extends as far posteriorly as the occipitoparietal suture and as far anteriorly as the posterior boundary of the first molar. There also appears to be a lateral expansion of the attachment of the medial temporalis onto the zygomatic process of the squamosal bone. This attachment is seen to extend as far laterally as the jugosquamosal suture (**Figure 3.3.4**).

Fibres of the medial temporal muscle run anteroventrally from the posterior margin of the origin until the anterior border of the attachment on the temporal fossa, where

they pass ventrally down the deepest and most medial part of the frontal bone, medial to the jugal bone to insert onto the medial surface of the mandible. The attachment area of the medial temporalis is a large region directly dorsal to that of the *pars reflecta* of the superficial masseter and anterior to that of the external pterygoid. Encompassing the medial surface of the coronoid process, this insertion extends ventrally to the dental ridge and posteriorly to the point of greatest curvature between the coronoid and condyloid processes (**Figure 3.3.4f**).

3.3.4.2 Lateral temporalis

It is estimated that the lateral temporalis originates from the lateral surface of the medial temporalis. The true origin of this lateral portion is likely to be an aponeurosis or fascia overlying the medial temporalis although this is difficult to determine with any clarity on micro-CT. Micro-CT images do show a septa between the lateral and medial parts of the temporalis, and fibre orientation differs slightly between the two parts, yet a fascial layer cannot be ascertained via this methodology (**Figure 3.3.5**). On dissection no comprehensive and significant fascia could be found overlying the temporalis muscle, and possibly due to the small size of the muscle no clear division between a lateral and medial part could be found.

Fibres of the lateral temporalis run anteroventrally, passing medial to the jugal bone, alongside but lateral to the fibres of the medial temporalis. This small muscle then attaches to the tip and a small area of the lateral surface of the coronoid process (**Figure 3.3.4e**)

3.3.5 Pterygoids

The pterygoid muscles jointly account for 16% of the overall masticatory muscle mass. Of this 16% the external pterygoid accounts for 29% and the larger internal pterygoid for 71% (**Table 3.3.1**).

Fibre orientation in the pterygoids is difficult to resolve via micro-CT, yet significant septa were apparent in both the internal and external muscles.

3.3.5.1 *External pterygoid*

The external pterygoid is a relatively small muscle when compared to other masticatory muscles such as the deep masseter, accounting for just 5% of the overall muscle mass (**Figure 3.3.3**).

The external pterygoid originates from the cranial base, with an attachment area that lies just anterior to the tympanic bulla, extends laterally from the palatine process to the alisphenosquamosal suture (**Figure 3.3.4c**).

This small muscle then passes ventrolaterally to insert onto the medial surface of the condylar process, just ventral to the articular surface of the mandible (**Figure 3.3.4f**).

3.3.5.2 *Internal pterygoid*

The internal pterygoid is the larger of the two pterygoid muscles, accounting for 12% of the overall masticatory muscle mass in the mouse, giving this muscle a greater mass than that of the total zygomaticomandibularis muscle.

The internal pterygoid originates from the cranial base, with an attachment area that surprisingly is approximately half the size of that of its external counterpart. This attachment area runs medially from the palatine process to the pterygoid process,

lying medial to the attachment of the external pterygoid (**Figure 3.3.2c; Figure 3.3.4c**).

The internal pterygoid muscle then passes posteroventrally as well as medially to insert onto the medial surface of the angle of the mandible, directly dorsal to the reflected attachment of the superficial masseter. This attachment area spans almost the entirety of the angle of the mandible as well as projecting anteriorly to nearly meet the attachment of the *pars reflecta* of the superficial masseter (**Figure 3.3.4f**).

3.4 DISCUSSION

The bony anatomy of the craniofacial complex is diverse in mammals, and as follows so is muscle architecture. The high diversity of masticatory morphology has in turn lead to diversity in nomenclature. With masticatory muscles particularly unique when compared to other mammalian groups, rodent morphology has been the focus of many investigations over the years (Druzinsky et al., 2011, Cox and Jeffery, 2011). Despite numerous studies attending to the masticatory anatomy of rodents in general, nomenclature and muscle division are incompatible and inconsistent between authors.

Following the terminology of Cox and Jeffery (2011) distinct muscles were determined through both dissection and detailed 3D segmentation and reconstruction of one *Mus musculus* individual with six well-defined muscles identified and described.

As in all other published studies using the same methodology (Cox and Jeffery, 2011, Tsai and Holliday, 2011, Hautier et al., 2012) only one individual of the species had its craniofacial musculature reconstructed from a contrast enhanced micro-CT scan, however initially both left and right sides were reconstructed for intra-individual comparative purposes. This approach was coupled with classical dissection techniques to control for intraspecific variation. While classical dissection methods are still valid and can provide highly detailed and accurate anatomical knowledge, for very small species such as the mouse this methodology can be problematic. Small yet highly significant reflections of muscles, such as the pars reflecta that has previously been used to define the hystricognathous condition of the jaw (Woods, 1972), are almost impossible to determine with confidence or accuracy by means of dissection but are revealed using reconstruction techniques. Reconstruction of contrast enhanced micro-CT is not only advantageous in the anatomical investigation of small species, but also provides a non-destructive method where soft-tissue and muscle layers can be examined in situ providing accurate information regarding their relationships to one-another without the need to remove or retract superficial layers of tissue. This technique also holds the

advantage that greater time and consideration can be given to the segmentation of structures, and if detectable errors are made these can be re-examined and corrected as many times as required without the need to start anew. However boundaries between closely integrated muscles, such as the lateral and medial parts of the same muscles are not always clearly visible on these scans. In this study the boundary and precise attachment of the lateral temporalis were indistinct. While the medial temporalis clearly originates from the bone of the temporal fossa it is difficult to distinguish if any fibres of the lateral temporalis take their origin from the skull, or whether lateral temporalis fibres take their origin from an aponeurosis overlying the medial temporalis. Cox and Jeffery (2011) describe the latter arrangement in both the rat and squirrel, with the origin of the lateral temporalis extending over a large surface of the medial temporalis in the rat in comparison to a much more limited origin in the squirrel. These authors also describe difficulty resolving clear medial and lateral parts to the temporalis in the guinea pig (Cox and Jeffery, 2011). Additionally, although it is possible that muscle shrinkage may occur with the iodine contrast enhanced micro-CT technique there is no discernible bias when comparing muscle volumes established by this technique against those measured following dissection (**Table 3.3.1**) and thus it may be assumed that any effect of muscle shrinkage is less than that of intraspecific variation.

Combining the results of both classical dissection and the contemporary method of contrast-enhanced micro-CT reconstruction provides a highly accurate and clear anatomical investigation of this thus-far largely undescribed region.

A unique finding of this study is the lateral expansion of the medial temporalis onto the zygomatic process of the squamosal bone in the mouse. Many previous studies regarding the masticatory musculature of rodents do not note such an attachment of the temporalis muscle onto the dorsal surface of the posterior portion of the jugal bone (Cox and Jeffery, 2011, Satoh and Iwaku, 2009, Turnbull, 1970, Patel, 1978). Satoh and Iwaku (2006) do however make reference to a suprazygomatic portion of the temporalis muscle in *Onychomys leucogaster*, and a number of authors describe a third division of the temporalis by distinguishing out the ventral most fibres of this muscle, often those fibres taking origin from the zygomatic process of the squamosal (Woods, 1972, Weijs, 1973, Druzinsky, 2010a, Hautier and Saksiri, 2009, Satoh and

Iwaku, 2006). Hautier (2010) describes a unique arrangement of a third temporalis division in *Ctenodactylus*, though it is suggested that this is not universal amongst rodents but instead results from the distal position of the eye in this species leading to a lateral displacement of the temporalis (Hautier, 2010, Cox and Jeffery, 2011).

Recently renewed attention has been given to a possible function of the temporal fascia in primates being to aid the zygomatic arch in resisting the tensions of the masseter muscle exerted during biting (Eisenberg and Brodie, 1965, Curtis et al., 2011b). Curtis et al. (2011b) suggest the substantial temporal fascia found in primates plays a critical role in stabilising the arch during biting. During biting, the bulge of the contracted temporalis results in a tensioned temporalis fascia shown to generate force great enough to oppose the downwards pull of the masseter (Curtis et al., 2011b).

In this current study no temporal fascia of substance was found in the mouse either through dissection or segmentation. Little to no attention is given to, or observation made of the temporalis fascia in literature regarding rodent masticatory apparatus (Cox and Jeffery, 2011, Satoh and Iwaku, 2009, Turnbull, 1970, Patel, 1978, Satoh and Iwaku, 2006). We might therefore conclude that despite both the sizeable deep masseter and the anterior and posterior regions of the zygomaticomandibularis attaching onto the zygomatic arch, in the mouse, and likely also in rodents, the temporal fascia plays no role in stabilising the arch during mastication. The lateral expansion of the attachment of temporalis onto the posterodorsal region of the zygomatic arch extending as far as the zygomatico-squamosal suture found in this investigation however could be hypothesised to show an analogous biomechanical solution in rodents to that seen in primates where the temporalis fascia may play an important role in stabilising the arch during downwards loading. Fibre direction in this region is not consistently clear on the contrast enhanced micro-CT, however in regions where some direction does become apparent this does appear to be consistent with a counter-balancing function. Such a discovery could prove to be a critical consideration when modelling mouse craniofacial anatomy for techniques such as FEA. Further investigation is needed to determine more precisely the nature and effect of this attachment and additionally whether such an arrangement is extended to other rodent species.

Other findings of this investigation provide interesting comparison with other rodents and mammals. A dorsal elongation of the reflected part of the superficial masseter onto the medial surface of the mandible was identified in this investigation. This masseteric extension, termed the pars reflexa is reported in the rat and other rodents (Druzinsky et al., 2011, Turnbull, 1970, Woods, 1972, Weijjs, 1973, Cox and Jeffery, 2011, Hautier and Saksiri, 2009). Such an extension is found to be present in both rodents and lagomorphs but not in primates, with carnivores and ungulates also possessing masseteric extensions. The latter suggests that extensions of the masseter may have evolved independently several times in mammals to aid production of large forces at the anterior dentition (Druzinsky et al., 2011).

Perhaps the greatest implication of this current work is the potential for future applications in biomechanical modelling to further the utility of the mouse, and of other myomorph rodents including the rat in the understanding of form-function relationships in evolution and other fields. For instance, in order to carry out FEA, accurate data regarding muscle origin, attachment, mass, fibre orientation and general anatomy is required. In the past ten years FEA has been engaged as a modelling technique capable of answering questions in vertebrate biomechanics and evolution that were not previously feasible and thus remained largely unexplored. With the advent and availability of superb 3D imaging and robust computing power, morphologists may now address questions using engineering tools such as FEA that allow the construction of highly controlled *in silico* experiments. These techniques not only provide great benefit to the field of biomechanics in general (Amin et al., 2011, Chegini et al., 2009, Elkins et al., 2011) but are also playing an ever increasing and central role in craniofacial biomechanics, allowing detailed and precise descriptions and comparisons of mechanical performance in different species and morphologies (Chalk et al., 2011, Gröning et al., 2011a, Gröning et al., 2011b, Koolstra et al., 1988, Moazen et al., 2008, Moreno et al., 2008, Nakashige et al., 2011, Panagiotopoulou et al., 2011, Reed et al., 2011, Tseng, 2009).

Computational simulations require of a vast assortment of accurate data to produce biologically meaningful models of the craniofacial skeleton. Such necessary data includes the precise anatomical description relevant craniofacial tissues, data concerning the material properties of these tissues, and information regarding

feeding mechanics that may be established through *in vivo* electromyography and kinematics (Gorniak, 1977, Cobb, 2011). Whilst traditionally knowledge of feeding patterns and mechanics was ascertained through electromyographical work, accessibility of such techniques as well as ethical considerations has meant that there is a paucity of such important data. Where electromyography is not available or suitable, MDA is now a possible technique for the prediction of muscle activation patterns (Alfaro et al., 2004, Bates and Falkingham, 2012, Curtis et al., 2010b, Curtis, 2011, Curtis et al., 2008, Grubich and Westneat, 2006, Moazen et al., 2009b, Moazen et al., 2009a, Moazen et al., 2008, Westneat, 2003, Westneat, 2004, Koolstra and van Eijden, 1992, de Zee et al., 2007). Still a relatively uncommon method in mammalian taxa, MDA may be used to model the movements and forces between structures such as the cranium and mandible; and in turn allows the prediction of muscle activation during feeding, modelling of jaw motion, and the investigation of the function of muscle parameters such as fibre length and muscle tension (Peck et al., 2000, Langenbach and Hannam, 1999, Hannam et al., 2008). As with FEA, MDA requires as a prerequisite detailed and accurate anatomical descriptions of the relevant craniofacial tissues such as the muscles of mastication, and it is this which, in regard to the mouse, this study provides.

This study forms the preliminary basis for a series of future experimental applications. In prospective studies mouse models will be used to address questions regarding modularity, integration and plasticity in the craniofacial complex. These and other concepts key to our understanding of evolution may be elegantly explored through the use of the mouse as a model organism, with the use of knockout mice allowing valuable experimental models to be created. The detailed and precise anatomical knowledge acquired in the current study permits the precise construction of biologically accurate representations of relevant anatomy and as such allows questions of biological and functional significance to be accurately addressed.

CHAPTER 4: CRANIOMANDIBULAR INTEGRATION AND ADAPTIVE PLASTICITY IN THE MURINE SKULL

4.1 INTRODUCTION

The craniofacial skeleton is a complex structure that is required to perform many vital dynamic functions such as respiration, food acquisition and processing; as well as housing major sensory structures. Despite the demanding functional requirements of the skull this is not a static region but an intricate skeletal construct subject to many changes in form. Complexly patterned morphological changes during development, adaptation in response to numerous internal and external stimuli, and mutational phenotypic variance, makes the continuous modification of form a fundamental and potentially unremitting feature of craniofacial skeletal morphology. The skull must however remain cohesive despite ongoing modification to its form if essential functions are to be maintained. In order to achieve such maintenance of morphological and functional integrity a high degree of correlation between composite parts of the whole is expected. As such, while the cranium and mandible may be considered relatively independent skeletal structures, in the absence of extensive integration between these two parts, change to the shape or size of one resulting from either development or mutational variance could potentially result in malocclusion and thus reduction to or loss of functional performance.

All biological systems are composed of elements or regions that are recognisable and relatively distinct from other such parts due to strong internal interactions and relative autonomy (Schlosser and Wagner, 2004, Wagner et al., 2007a, Breuker et al., 2006b, Wagner, 1996, Klingenberg, 2005a). The division of composite structures into highly connected subsets of semi independent modules, though abstract in concept, is considered a fundamental aspect of biological organisation (West-Eberhard, 2003, Wagner et al., 2007a). Different types of modules have been established, those which are developmental in nature and those which are functional in nature, but all share the defining quality of being more tightly connected internally than externally connected with other semi-independent parts (Cheverud, 1996b, Raff,

1996, Wagner, 1996, Wagner et al., 2007a, Wagner and Altenberg, 1996, Klingenberg, 2008). Although integration within modules is greater than that between modules, integration between modules may not be unsubstantial, and thus modularity is a hierarchical concept. In a complex, multifaceted region such as the skull, levels of connectivity and integration between composite parts form a hierarchical network of interactions where modules may exist within modules such that modules at one level may be the traits that make up modules at a higher level of organisation (Klingenberg, 2005a).

The hierarchical connectivity and integration of parts of a skeletal complex such as the skull may provide the necessary framework for the maintenance of form and thus function when substantial variation to components of morphology occurs. Such variation of parts occurs throughout ontogeny when the skull changes substantially in both size and shape, but may also be present during microevolutionary change when mutation may result in the isolated variance of parts of a skeletal complex. Integration within and between semi-independent regions such as the cranium and the mandible, whether developmental or functional in nature, may provide a necessary connection between composite parts of a whole so as that modification to the form of one of these structures is reflected in the other, and thus cohesion of overall morphology and function is maintained.

Integration manifests itself as the covariation among morphological traits, and as such may be statistically analysed by means of morphometric data. Both analysis of correlations among distance measurements (Olson and Miller, 1958, Cheverud, 1982a, Leamy and Atchley, 1984, Zelditch, 1987, Cheverud, 1995) and in more recent years the correlation among the positions of morphological landmark points (Klingenberg et al., 2003, Klingenberg and Zaklan, 2000, Bookstein et al., 2003, Bastir and Rosas, 2005, Bastir and Rosas, 2006, Bastir et al., 2005a, Ackermann, 2005, Burgio et al., 2009, Cobb and Baverstock, 2009b, Goswami, 2006, Goswami, 2007, Kulemeyer et al., 2009, Makedonska et al., 2012, Meloro et al., 2011) have been used to gain important insight into patterns of covariance. Establishing such patterns of covariance between skeletal structures and traits revealed can provide information about the presence of integration and thus modularity. Set of traits which are highly integrated internally yet relatively independent of other traits may be

considered modular, whereas a high degree of covariance of all parts of an overall structure is indicative of strong integration of that whole (Klingenberg, 2005a).

Patterns of morphological integration and modularity within mammalian crania are reasonably well investigated. Following concepts of integrated craniofacial growth (Enlow et al., 1971, Enlow and Hans, 1996a, Enlow and Azuma, 1975) and the spatial packing model developed by Biegert (1963), correlates of major cranial dimensions within the hominoid and primate cranium have been examined by numerous authors (Lieberman et al., 2000b, Lieberman et al., 2000a, Lieberman et al., 2002, Mitteroecker and Bookstein, 2008, Ross and Henneberg, 1995, Marroig et al., 2003, Marroig and Cheverud, 2001, Ross and Ravosa, 1993, Bookstein et al., 2003). The influence of the basicranium, and particularly flexion at the cranial base, on the morphology and spatial positioning of other regions of the cranium is the key focus of many of these studies (Bookstein et al., 2003, Lieberman et al., 2000b, Lieberman et al., 2000a); with results indicating the cranium is a highly integrated structure in which variations in overall form may in part derive from variation in basicranial morphology. Additionally, studies examining integration of the cranium at an evolutionary level in primates find that developmentally and functionally related traits are integrated in terms of genetic and environmental correlations as well as in terms of phenotypic correlations (Cheverud, 1996b, Cheverud, 1995, Cheverud, 1988, Ackermann and Cheverud, 2000). The underlying connections and interactions of composite parts of the mammalian cranium have also been examined using samples of mutant mice (Lieberman et al., 2008, Hallgrímsson et al., 2004b, Hallgrímsson et al., 2007, Hallgrímsson and Lieberman, 2008, Hallgrímsson et al., 2009, Hallgrímsson et al., 2006). Results of these studies support previous studies (Cheverud, 1995, Cheverud, 1982a, Lieberman et al., 2002, Bookstein et al., 2003, Ackermann, 2005, González-José et al., 2004, Enlow, 1990) showing that the cranium is a strongly integrated unit, characterised by complex covariation both within and between constituent parts. Work by Hallgrímsson and colleagues investigating cranial integration in mutant mouse strains also provides an indication of the patterns and processes that generate both canalisation and covariation in the skull (Hallgrímsson et al., 2007, Hallgrímsson and Lieberman, 2008, Hallgrímsson et al., 2009, Hallgrímsson et al., 2006).

Patterns of morphological integration and modularity have also been extensively studied within the mandible of rodents (Klingenberg et al., 2003, Klingenberg et al., 2001, Cheverud et al., 1997, Zelditch et al., 2008, Mezey et al., 2000, Monteiro et al., 2005, Ehrich et al., 2003, Leamy, 1993, Atchley et al., 1985b, Atchley et al., 1985a). Fewer analyses investigating covariation between the mammalian cranium and mandible have been undertaken. Counterpart analyses in humans suggest variation in the angle of the middle cranial fossa may be a primary determinant of ramus breadth (Enlow et al., 1982, Bhat and Enlow, 1985). Following on from this work, Bastir et al., (2004, 2005b) show that the mandibular ramus and the bilateral middle cranial fossa form a morphologically integrated unit in humans. Based upon the work of Olson and Miller (1958), Zelditch (1988) use linear measurements on both the cranium and mandible of lab rats to examine the influence of developmental interactions upon observed morphological integration.

Concepts extensively discussed by Enlow (Enlow et al., 1971, Enlow and Hans, 1996a) highlight how for balance of form, the enlargement or displacement of one part of a complex should lead to an equivalent change in connected parts. Experimental investigation of coordinated reaction of the mandible in response to changes in cranial form has however thus far been neglected. This may in part be due to the complex nature of the skull which poses many challenges for understanding the intrinsic arrangements and relationships between underlying parts that determine its form. Multifaceted evolutionary, genetic and developmental processes shape the morphology of these structures, and thus unpicking the ability of the mandible to respond to changes in cranial form in a coordinated and correlated manner is problematic in traditional skeletal samples. The increasing use and availability of model organisms such as mice (Hallgrímsson and Lieberman, 2008) however now permits the specific investigation of phenotypic covariance between the cranium and mandible when variance occurs in one. Such a model sample of mice is employed in the present study to address this gap in the literature, examining the ability of the mandible to covary appropriately with the cranium when an isolated mutation, directly effecting one parameter of form, is introduced to the crania early on in development.

Craniomandibular variance and covariance are explored in three phenotypically distinct strains of mice. A control wild-type mouse is compared to two mutant strains which share the same background strain as the control. The two mutant strains display extremes of cranial length generated via specific *pten* (Sansal and Sellers, 2004) and *brachymorph* (ul Haque et al., 1998, Kurima et al., 1998) mutations affecting chondrocranial growth alone. The *pten* mutation results in an increased cranial length the, *brachymorph* mutation a decreased cranial length when compared to the control. As cartilage growth alone is targeted, and the early mandible is formed by intramembranous rather than endochondral ossification (Ramaesh and Bard, 2003), increased growth in the case of the *pten* strain, and decreased growth in the *brachymorph* strain should only occur in the chondrocranium (Hallgrimsson and Lieberman, 2008). There may however be some contribution of Meckel's cartilage to the morphogenesis of the mandible (Bhaskar et al., 1953, Glasstone, 1971, Ramaesh and Bard, 2003). Meckel's cartilage forms at approximately day 12.5 of pre-natal growth (E12.5) as a rostral process and two lateral rods that fuse together and grow (Chai et al., 1994, Miettinen et al., 1999) , influencing jaw lengthening (Kurihara et al., 1994) prior to disintegration of this cartilage at approximately E16 (Ramaesh and Bard, 2003). However, there appears to be no direct evidence that Meckel's cartilage regulates mandibular morphogenesis (Ramaesh and Bard, 2003) and while the contribution of this cartilage may be real, it is transient and does not appear to be a significant growth cartilage or play an appreciable role in either the length or the width of the mandible directly by its endochondral ossification (Frommer and Margolies, 1971). In addition, while the mandibular condyle of the mouse develops through the method of endochondral ossification, this particular ossification may not be that of classical endochondral ossification (Silbermann and Frommer, 1972). It may therefore be reasonably assumed in the present sample that, if not all, at least the the vast majority of change in mandibular form in the two mutant strains when compared to the control is, a secondary effect of variation in cranial length, which we infer to be a result of an epigenetic plastic adaptation. Establishing patterns of covariance between the cranium and mandible of these three strains of mice can therefore provide important information regarding the strength of integration within craniomandibular complex in the absence of genetic basis for any such integration. Determining covariance between these two semi-independent structures may show

the potential ability of the complex to epigenetically respond in a coordinated, plastic and appropriate manner to substantial regional variation in form such that overall cohesion and function are maintained.

The ability of an organism or skeletal structure to respond to an altered environmental condition is encompassed by the term adaptive plasticity. The “environment” which is altered may refer to and include both the organism’s external surroundings and internal conditions, and thus may encompass a vast array of kinds of variability (Ravosa et al., 2008a, West-Eberhard, 2003). Plasticity has the ability to facilitate phenotypic change via immediate correlated shifts in related traits. An isolated alteration in one skeletal element may initiate a series of compensatory responses in surrounding structures, thereby effecting major change in overall morphology. Complex, coordinated and adaptive phenotypes may therefore rapidly originate with little genetic change once an initiating variation occurs (West-Eberhard, 2003, West-Eberhard, 1989, West-Eberhard, 2005).

The sample utilised in the present study has the potential to demonstrate the capability of the craniomandibular complex to plastically adapt in a coordinated and integrated manner in response to isolated morphological variance. Alteration in cranial length as modelled by the sample is a key morphological variant seen both during development and evolution. The presence of integrated, adaptive mutant phenotypes would indicate the capacity of the cranium and mandible to epigenetically produce complex coordinated and cohesive overall morphology in response to a relatively simple morphological change. Such a result would have substantial implications for the evolvability of this dynamic skeletal region.

Integration enables the skull and associated soft tissues to maintain cohesive form and function both within individuals during ontogeny and among individuals across a range of size and shape phenotypic variants. Covariation structure is thus essential in complex organisms due to the need to preserve suitable size and shape relationships among structures. As such structuring reflects the organisation of organism into sets of traits that have common developmental, functional or genetic influences, modularity is the determinant of such covariation structuring (Hallgrímsson et al., 2007). The modular organisation and integrated variance

between related parts are likely fundamental determinants of the evolvability of a structure. The partitioning of an organism or structure into modules reduces the probability that a mutation that is beneficial for one trait is deleterious for others, while integration can allow coordinated variation within a group of traits or regions enabling preferred directions for evolutionary change (Hallgrímsson et al., 2009, Hallgrímsson et al., 2007).

This study addresses two key questions. As both of these mutant mouse strains have a known specific mutation that selectively effects chondrocranial growth, cranial morphology should alone be directly altered. As such, neither the morphology of the masticatory musculature or the mandible are likely to be directly influenced by the *pten* or *brachymorph* mutation. Despite this lack of primary influence on mandibular morphology, it is predicted that underlying covariance structure between the cranium and mandible will lead to secondary epigenetic changes in mandibular morphology, such that patterns of mandibular morphology in the two mutant strains will correspond to patterns of variance observed in their relevant crania. Thus strong craniomandibular integration in combination with adaptive plasticity is expected to lead to strong correlation between cranial and mandibular form in the *pten* and *brachymorph* stains. Previous studies have shown the *pten* and *brachymorph* mutation to result in both increased cranial variance and a suite of unique cranial features in each strain (Hallgrímsson and Lieberman, 2008, Hallgrímsson et al., 2006), thus some degree of difference between strains both in strength and pattern of covariance between the crania and mandible may be present. However, as underlying covariance structure between the cranium and mandible is likely developmental and/or functional in nature, patterns of covariance between these two semi-independent structures are expected to show common elements across all three strains. This study firstly addresses the question: do patterns of mandibular morphology in the *pten* and *brachymorph* strains correspond to patterns of observed variance in their respective crania? and secondly: do shared common patterns of covariance between crania and mandibles exist between the three strains?

4.2 MATERIALS AND METHODS

4.2.1 Sample

The sample utilised in this study consists of a total of 75 *Mus musculus* specimens. Within this sample there are two mutant strains (brachymorph and pten) and a wild-type strain, all from similar genetic backgrounds (C57BL/6J). Mutations in both the brachymorph and pten strains cause perturbations that influence chondrocranial and endocranial growth early on in the development of the craniofacial skeleton (Hallgrímsson et al., 2006). 28 wild-type, 24 brachymorph and 23 pten individuals make up the sample of this study, micro-CT scans of which were kindly provided by Benedikt Hallgrímsson, University of Calgary.

Brachymorph (bm) mutants (C57/BL/6J background, the Jackson Laboratory, Bar Harbor, ME, USA) have a relatively short-faced morphology that results from an autosomal recessive mutation in the phosphoadenosine-phosphosulfate synthetase 2 gene (*Papss2*) (Kurima et al., 1998). The *Papss2* gene mutation in the brachymorph mouse results in an extracellular matrix alteration that leads to a dramatically reduced growth of cartilage, thus all skeletal elements that rely upon cartilage are abnormally small (Hallgrímsson et al., 2006, Kurima et al., 1998, Orkin et al., 1976, Lane and Dickie, 1968, Ford-Hutchinson et al., 2005). As the growth of dermatocranial elements does not directly depend upon cartilage growth in the skull the direct effects of this mutation should be confined to the chondrocranium (Kaufman and Bard, 1999, Hallgrímsson et al., 2006). The brachymorph mutant phenotype is characterised by a shortened yet complex craniofacial morphology with a distinctive dome-shaped cranium (Ford-Hutchinson et al., 2005). Further details of the *Papss2* gene mutation in the brachymorph mouse are given in Hallgrímsson et al. (2006) and Ford-Hutchinson et al (2005).

Pten mutants have a relatively long-faced morphology that results from crossing mice with floxed Pten alleles with transgenic mice on a C57BL/6J background, a technique referred to as conditional gene deletion.

Conditional gene deletion is often approached via the Cre/LoxP system, this being a technique which allows the creation of tissue-specific knockout mice. Cre- and loxP-containing strains are developed independently and then crossed to generate offspring that carry both additions. The first strain contains a targeted gene flanked by two loxP sites, this commonly being termed a 'floxed' gene. The second strain is a conventional transgenic mouse line (one in which cloned genetic material has been transferred) expressing Cre recombinase under the control of a tissue- or cell-specific promoter. Cre recombinase of the P1 bacteriophage efficiently catalyses two of its consensus DNA recognition sites (*loxP* sites). Offspring generated via the crossing of the floxed strain and the Cre-expressing strain may inherit both the floxed gene and the Cre- transgene. In such individuals, tissues in which the Cre recombinase is expressed the floxed DNA segment will be excised and hence rendered inactive, whilst cells and tissues in which the Cre recombinase is not expressed the floxed gene will remain active (Kos, 2004, Rajewsky et al., 1996, Gassmann and Hennet, 1998, Rossant and McMahon, 1999, Orban et al., 1992, Nagy, 2000, Hamilton and Abremski, 1984).

PTEN (phosphatase and tensin homolog deleted on chromosome 10) is a tumour suppressor gene (Sansal and Sellers, 2004) that negatively regulates the phosphatidylinositol 3' kinase signalling pathway. Phosphatidylinositol 3' kinase enzymes are involved in cellular functions such as growth, proliferation, differentiation and survival (Sansal and Sellers, 2004, Hallgrímsson et al., 2007). The transgenic mice used in combination with mice with floxed *Pten* alleles express Cre recombinase under control of the relatively cartilage-specific *Col2al* gene promoter (Hallgrímsson et al., 2007). *Col2al* refers to the pro α 1(II) collagen gene which encodes Type II collagen, the latter being a principal marker of chondrocyte differentiation (Ovchinnikov et al., 2000, Mayne, 1990).

Through the breeding of floxed *pten* mice with *Col2al-Cre* mice individuals are developed that carry both the floxed gene and the Cre- transgene. In these individuals the negative regulation of the phosphatidylinositol 3' kinase signalling pathway is blocked and thus cellular functions such as the growth and proliferation is increased, and this increase is specific to type II collagen. Only homozygous (Cre fl/fl) individuals were included in the sample.

4.2.2 Data Acquisition

Micro-CT scans of all three strains of mice were provided by Benedikt Hallgrímsson, University of Calgary. 40 cranial (**Figure 4.2.1; Table 4.2.1**) and 39 mandibular (**Figure 4.2.2; Table 4.2.2**) three-dimensional landmarks were defined and digitised for each individual. Landmark collection was carried out in Amira 5.2 following the generation of an isosurface for each specimen.

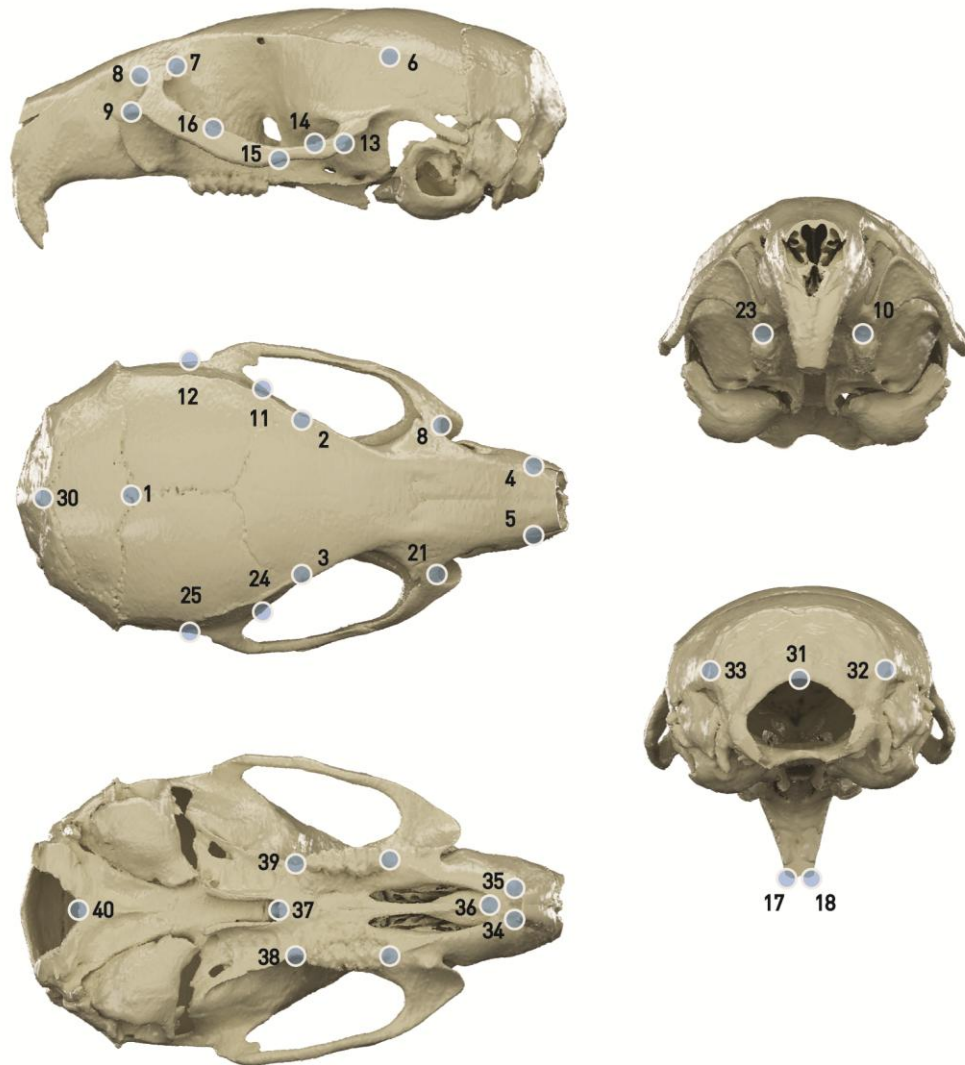


Figure 4.2.1: Depiction of cranial landmarks. Landmark definitions are given in **Table 4.2.1**.

Table 4.2.1

left	Landmark number		Landmark description
	right	midline	
		1	Lambda - the midline intersection of the sagittal and lambdoidal sutures
2	3		Fronto-temporal-parietal junction (anterior projection of parietal in superior view)
4	5		Anterior most point at the intersection of the premaxillae and nasal bones
6	19		Central point on the squamoso-parietal suture
7	20		Intersection of fronto maxillary suture with orbital rim
8	21		Superior most border of infraorbital foramen
9	22		Anterior most post along inferior zygomatic rim of the maxilla
10	23		Anterior edge of the alveolus of the first maxillary molar
11	24		Point of greatest curvature along anterior edge of zygomatic process of temporal bone
12	25		Point of greatest curvature along posterior edge of zygomatic process of temporal bone
13	26		Postero-ventral temporal-zygomatic junction on zygomatic arch
14	27		Postero-dorsal temporal-zygomatic junction on zygomatic arch
15	28		Antero-ventral temporal-zygomatic junction on zygomatic arch
16	29		Antero-dorsal temporal-zygomatic junction on zygomatic arch
17	18		Central point on tip of maxillary incisor
		30	Intersection of interparietal and occipital bones at the midline
		31	Dorsal midline border of foramen magnum
33	32		Most lateral inferior point on the occipital bone
34	35		Posterior edge of the alveolus of the maxillary incisor
		36	Anterior midline margin of incisive foramen
		37	Midline junction between palate and presphenoid
38	39		Posterior edge of the alveolus of the third maxillary molar
		40	Ventral midline border of foramen magnum

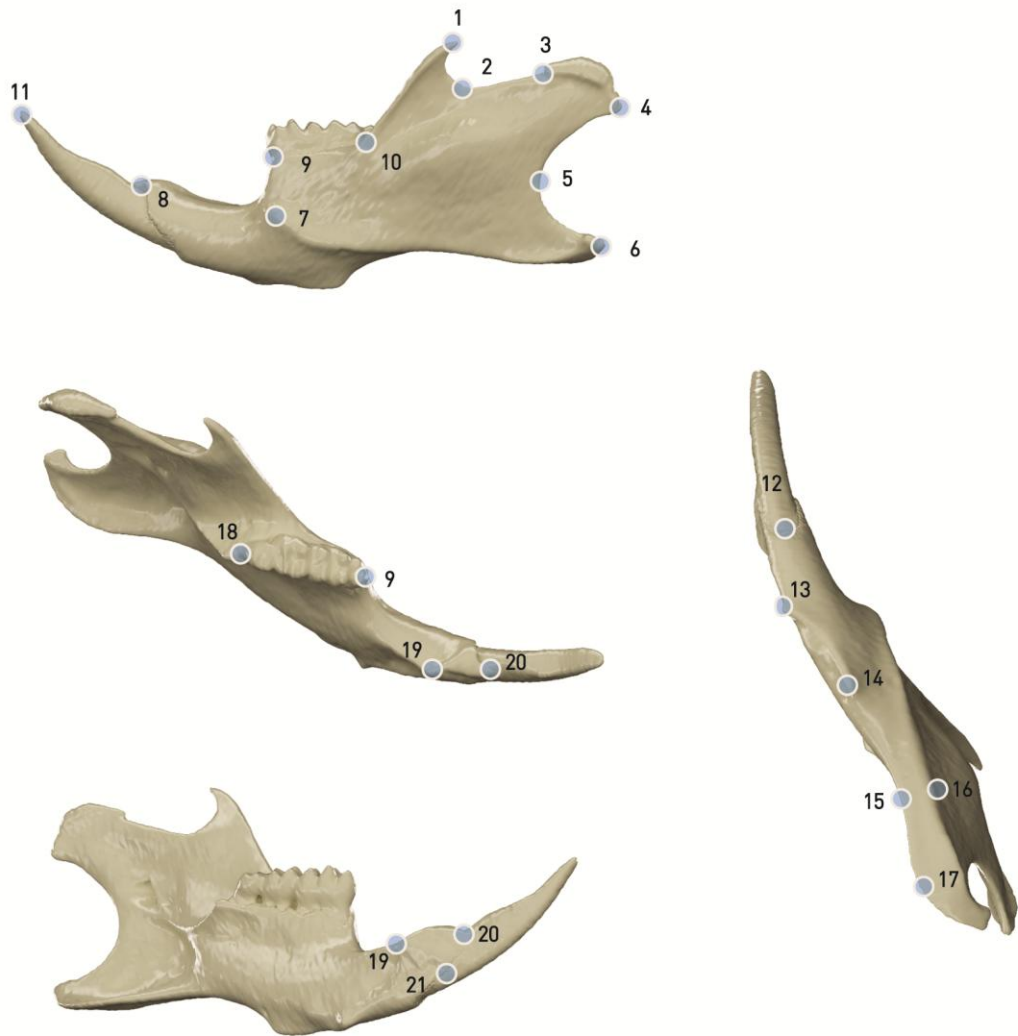


Figure 4.2.2: Depiction of mandibular landmarks. Landmark definitions are given in **Table 4.2.1**.

Table 4.2.2

Mandibular Landmark Definitions

Landmark number		Landmark description
left	right	
1	1	Tip of coronoid process
2	2	Most inferior point on mandibular notch
3	3	Anterior most point on condyloid process
4	4	Posterior inferior most point on condyloid process
5	5	Point of greatest curvature
6	6	Posterior most point on angular process
7	7	Anterior most point on the masseteric ridge
8	8	Superior most point on incisor alveolar rim in the midline
9	9	Anterior edge of the alveolus of the mandibular third molar
10	10	Intersection of molar alveolar rim and base of the coronoid process
11	11	Tip of mandibular incisor
12	12	Ventro-posterior edge of the alveolus of the mandibular incisor
13	13	Anterior most point on the tuberoisty of the insertion site of mandibular transverse muscle
14	14	Posterior most point on the tuberoisty of the insertion site of mandibular transverse muscle
15	15	Narrowest point on ventral surface of mandible, buccal surface
16	16	Narrowest point on ventral surface of mandible, lingual surface
17	17	Point of greatest curvature on the ventral surface of the angle of the mandible, buccal surface
18	18	Posterior edge of the alveolus of the mandibular third molar
19	19	Posterior most border of symphysis on dorsal surface of mandible
20	20	Anterior most border of symphysis on dorsal surface of mandible
21	21	Anterior inferior most point of symphysis, ventral surface of mandible

Cranial landmarks for each specimen were symmetrised following results of a pilot study which revealed a degree of asymmetry in the sample that veiled patterns of variation and covariation. The object symmetry procedure involves creating a reflected copy of the landmark configuration such that two landmark configurations now exist but with X coordinates for each landmark that are positive in one set, and negative in the other. Landmarks on the left and right side of the median axis of the reflected copy are relabelled. A mean of the original and reflected relabelled configurations is then calculated to give the new symmetric dataset (Klingenberg et al., 2002, Mardia et al., 2000, Burgio et al., 2009).

As the mouse jaw has a weak ligamentous symphysis joining the left and right hemi-mandibles the relative position of these two halves is variable. To remove the effect of shifting of the left and right parts relative to each other, mandibular landmarks were divided into left and right hemi-mandible configurations, retaining mid-line landmarks in each set (**Figure 4.2.2**). A data set was then produced containing landmarks pertaining to only the right hemi-mandible and the midline. Results reported in this chapter use the latter data, analysing the right hemi-mandible alone.

To validate results of partial least squares analyses between a full (symmetric) cranium and the right hemi-mandible two additional data sets were produced and analysed. Firstly, a cranial data set where the cranial landmark configuration (**Figure 4.2.1**) was divided into left and right parts, retaining midline landmarks in each, with the separate left and right configurations treated as individual specimens contained in one data file. Secondly, a mandibular data set where the separate left and right hemi-mandibles with midline landmarks in each (**Figure 4.2.2**) were treated as individual specimens contained in one data file. The latter two data files were exposed to the same partial least squares analyses as the key data file, and results are given in the supplementary material for this chapter (**Figure S 4.3.4; Figure S 4.3.6; Table S 4.3.1; Table S 4.3.2; Table S 4.3.3**).

4.2.3 Geometric Morphometric Methods

Geometric morphometric methods were used to analyse and describe patterns of variation and covariation in the sample, these methods providing a quantitative approach to addressing shape comparisons (Zelditch et al., 2004a).

Digitisation of landmarks to describe the morphology of specimens produces Cartesian coordinates, the latter which will vary according to the location and orientation of each specimen in respect to the axis in which the data was collected. Generalised Procrustes Analysis (GPA) is a commonly used method that registers a series of specimen forms, translating and rotating each specimen to minimise the squared, summed distances between corresponding landmarks on each configuration and an iteratively computed mean specimen (Gower, 1975, Goodall, 1991, Rohlf and Slice, 1990). Specimen size is accounted for by the calculation of centroid size, a measure of size that is mathematically independent of shape, calculated as the squared root of the sum of squared distances of the landmarks in the configuration to their average location (Slice, 2007, Zelditch et al., 2004a, O'Higgins, 1997). Generalised procrustes analysis results in the landmark configurations of all specimens in the analysis lying in a common coordinate system, with differences in landmark coordinate values reflecting differences in configuration shapes (Slice, 2007).

Shape data derived from generalised procrustes superimposition lies in a non-linear, hyper-hemispherical shape space, first described by Kendall (1984) (Kendall, 1984). Each landmark configuration is represented by a single point within this multidimensional shape space. As the shape data lies in a non-linear space in order to perform common statistical methods based on linearity, data is projected onto a Euclidean (linear) tangent space (Rohlf, 1996, O'Higgins, 1997, Slice, 2001, Zelditch et al., 2004a).

4.2.4 Principal Component Analysis

Principal component analysis (PCA) uses tangent space coordinates to extract eigenvectors, these being the principal components of shape variation. As the specimens are represented on a tangent plane, principal components (PC) may be plotted orthogonally to each other with each PC representing a statistically independent mode of variation.

To carry out PCA on the sample data was first subjected to generalised procrustes superimposition.

4.2.5 Partial least squares analysis

Partial least squares analysis (also referred to as singular warp analysis) is a method used to explore patterns of covariation between blocks of variables , allowing analysis of hypotheses of morphological integration (Zelditch et al., 2004a).

2-block partial least squares (PLS) models the covariation between the two separate sets of variables of interest by identifying linear combinations (singular axes) between the two sets. The mathematical technique of singular value decomposition (SVD) extracts these singular axes from the variance/covariance matrix. As in regression, PLS examines the relationship between two sets of variables, however while in regression one set of variables is assumed to be dependent on the other, PLS treats variables equally, viewing both sets as jointly related to an underlying cause. Linear combinations of these variables that are assumed to reflect responses to underlying variables are referred to as latent variables. Latent variables present in one block that show the highest correlation to latent variables in the other block are paired (Rohlf and Corti, 2000, Bookstein et al., 2003, Bastir and Rosas, 2006, Bastir and Rosas, 2005, Zelditch et al., 2004a, Klingenberg, 2009, Klingenberg et al., 2003).

PLS resembles PCA in the definition of axes. In PLS an inter-block variance-covariance matrix is decomposed into mutually orthogonal axis, with components ordered according to the amount of covariance between block explained by each one. Where PCA aims to maximise low-dimensional representation of the total sample variance, SVD in PLS aims to maximise low-dimensionality representation of the between-block covariance (Bastir and Rosas, 2004, Bastir and Rosas, 2006, Bastir and Rosas, 2005).

Statistical significance of the covariation between the two landmark configurations (blocks) is established by means of a permutation test, simulating the null hypotheses of complete independence between the two (Manly, 2007). Quantification for the covariance between the two landmark configurations is provided by the RV coefficient. This is a scalar measure of the strength of association between two sets of variables, and in the context of PLS is used as a measure of the total amount of covariation between the variables (Escoufier, 1973). Taking values between zero and one, the RV coefficient infers at zero that the two blocks are completely uncorrelated with each other, and at one that one block differs from the other only in its rotation, reflection, scaling or translation (Klingenberg, 2009).

When carrying out an inter-specific or inter-strain PLS analysis the presence of different populations or strains may be corrected for by using a pooled within group covariation matrix. In this type of analysis the deviations of the observations of the group averages of the variables are used instead of deviations from the grand mean (Klingenberg, 2009, Klingenberg et al., 2003, Mitteroecker and Bookstein, 2008). This methodology makes the assumption that the covariation observed between the two blocks of variables is the same in the different groups (Klingenberg, 2009).

4.2.6 Vector direction comparison

PLS axes correspond to directions in shape tangent spaces, and thus to assess how similar two or more PLS axis are the angles between such vectors may be computed. The methodology may be applied to principal component and regression vectors as

well as PLS axes, and has been utilised in both traditional and geometric morphometrics (Klingenberg and Zaklan, 2000, Klingenberg and McIntyre, 1998, Klingenberg and Zimmermann, 1992, Cheverud, 1982b). The angle between two column vectors is calculated as the arc-cosine of the inner product of the two vectors after both are scaled to unit length (Hunt, 2007, Gómez-Robles and Polly, 2012). Statistical assessment of the calculated angles may be computed either via simulation of angles between pairs of random vectors in the multivariate space of interest, or via a closed-form formula (Li, 2011).

Angles between vectors within the multivariate space range between 0° and 90° , where an angle of 0° is present when the directions of two vectors are identical, and an angle of 90° is given when the directions of the two vectors are disparate. Angles varying from approximately 20° to 60° with significant P-values imply a correspondence between vectors, indicating similarity in patterns of covariance observed on the axis in question (Gómez-Robles and Polly, 2012, Renaud et al., 2009).

To ensure PLS axes being compared lie within the same multivariate space, all data of interest is analysed together in one GPA. Following registration, the data set is subdivided into groups such as strain and an individual PLS analysis carried out on each strain. Angles between PLS axes/vectors for each individual strain may now be calculated to assess similarity of vectors and thus patterns of covariance between the strains.

4.2.7 Calculation of percentage of overall variance

While most software offering PLS analysis provides a quantification of the percentage total covariance between the two blocks of variables alongside a measure of the overall association between the two blocks (the RV coefficient), no quantification is given of the percentage of total variance in the sample accounted for by the percentage of covariance. A calculation of the percentage total variance for each covariance per block can be calculated as the variance of the scores of one PLS

axis for one block of variables, divided by the sum of eigenvalues (following PCA) for the same block.

4.2.8 Visualisation

In the present study all geometric morphometric analyses were carried out in MorphoJ (Klingenberg, 2012). Patterns of variation and covariation elicited through PCA and PLS were visualised as the shape changes produced when warping a 3D surface to the negative and positive extremes of the axis in question. Warped landmark configurations (coordinate files) were exported from MorphoJ at -0.1 and +0.1 of each axis. ‘Landmark’ software (Wiley, 2005) was used to warp and export a surface file for each extreme of each axis (Wiley et al., 2005). Warped surfaces produced in ‘Landmark’ were aligned, scaled and rendered in 3DStudioMax.

4.2.9 Analyses addressing whether patterns of mandibular morphology in the three mouse strains correspond to patterns of observed variance in their respective crania.

To address the first question posed in this study, raw landmark coordinates were first subjected to GPA. PLS analysis was then carried out for the whole sample to determine patterns of covariation between crania and mandibles; firstly assessing deviations of observations from the grand mean and secondly via a pooled-by-group analysis assessing deviations from group means.

4.2.10 Analyses addressing whether shared common patterns of covariance between crania and mandibles exist between the three strains.

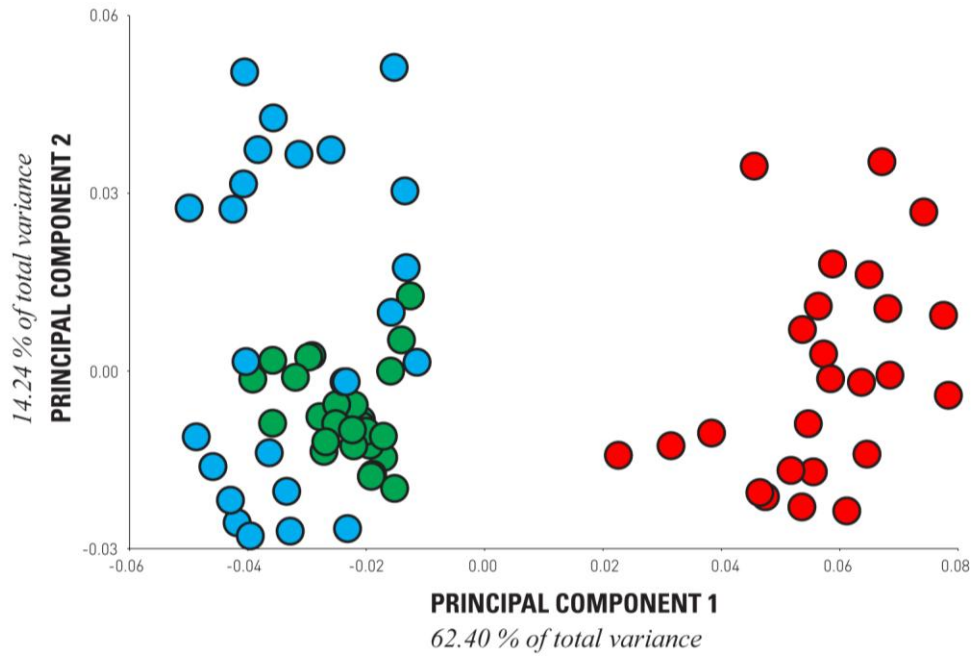
To address the second question posed in this study, the whole sample was subjected to GPA. Data was then divided into that of the three strains and an individual PLS analyses performed for each. Vector directions for each individual strain PLS analysis were then compared to that of a pooled-by-group PLS analysis for the whole sample.

4.3 RESULTS

The three strains show clear inter-strain variance in both cranial and mandibular form. **Figure 4.3.1** shows the first two axes of variance in the cranium, and **Figure 4.3.2** the first two axis of variance in the mandible when principal component analysis is carried out for the whole sample. Corresponding wireframe visualisations are given in supplementary material for this chapter (**Figure S 4.3.1** and **Figure S.4.3.2**).

Cranial variance in the three strains for the first two principal axes is dominated by differences in length (**Figure 4.3.1**). At the positive extremes of the axes (a combined 76.64% of total variance) a decrease in cranial length is seen alongside a relative increase in cranial height and a relative increase in cranial width. Clear separation between the two mutant strains is demonstrated, with the relatively long *pten* crania showing a flattened appearance in comparison to the relatively short *brachymorph* crania which displays a characteristic dome-like appearance. Wild-type crania are seen to fall within the shape range of the *pten* strain, the former also showing a smaller range of variance across these axes.

Mandibular variance in the three strains for the first two principal axes is also dominated by difference in length (**Figure 4.3.2**). At the positive extremes of the axis (a combined 43.44% of total variance) a relative overall decrease in mandibular length is seen alongside a relative increase in mandibular height. Variance in mandibular length here is primarily attributable to changes in length of both the mandibular condyle and angle of the mandible, while changes in mandibular height are seen throughout the mandible. All three strains show separation across these axes, with a small overlap between the range of the *pten* and *C57* strains.



PRINCIPAL COMPONENT 1

negative warp -0.1

positive warp 0.1



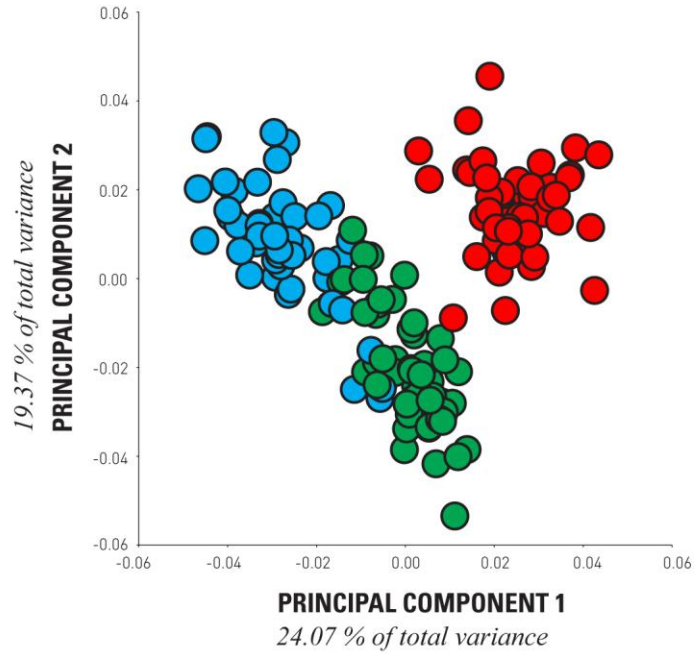
PRINCIPAL COMPONENT 2

negative warp -0.1

positive warp 0.1



Figure 4.3.1: Principal component analysis of brachymorph (red markers); C57 (green markers) and ptn (blue markers) crania. Insets show warps along PC1 (62.40% of total variance) and PC2 (14.24% of total variance), to 0.1 and -0.1 of these axes.



PRINCIPAL COMPONENT 1

negative warp -0.1



positive warp 0.1



PRINCIPAL COMPONENT 2

negative warp -0.1



positive warp 0.1



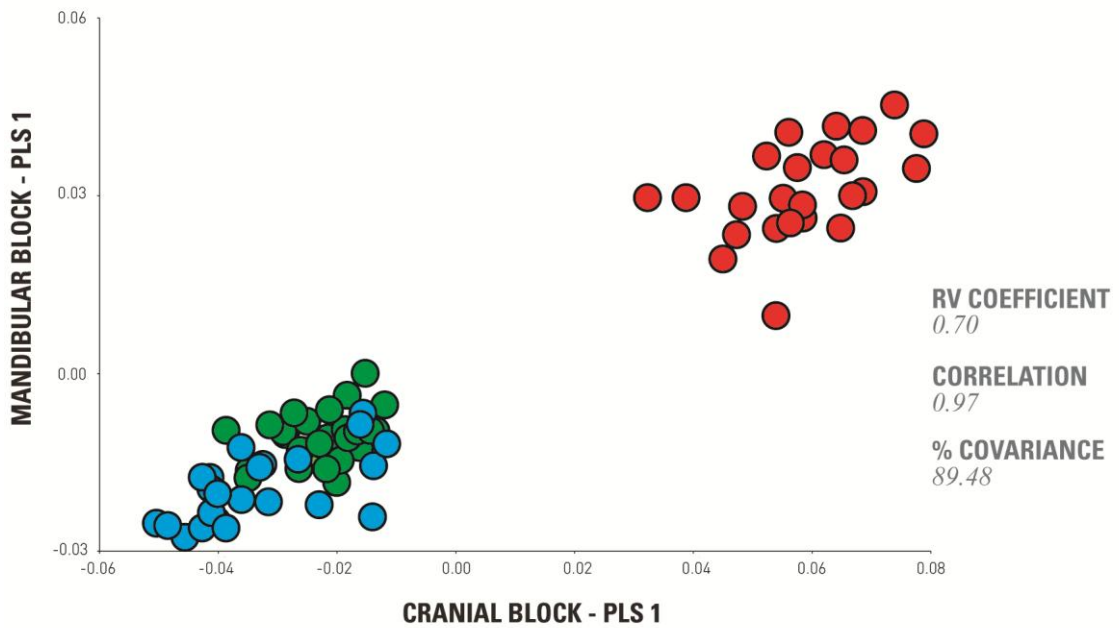
Figure 4.3.2: Principal component analysis of brachymorph (red markers); C57 (green markers) and pten (blue markers) mandibles. Insets show warps along PC1 (62.40% of total variance) and PC2 (14.24% of total variance), to 0.1 and -0.1 of these axes.

4.3.1 Do patterns of mandibular morphology in the three mouse strains correspond to patterns of observed variance in their respective crania?

Partial least squares (PLS) analyses we carried out to assess patterns of covariance between the cranium and mandible within and between the three strains. In order to establish patterns of covariance present in all three strains PLS analyses were both performed on the whole sample (inter-strain PLS analysis), firstly assessing deviations of observations from the grand mean and via a pooled-by-group analysis assessing deviations from group averages.

Figure 4.3.3 shows the first singular axis of covariance (RV: 0.70; covariance: 89.48%; correlation: 0.97) between the cranium and mandible in all three strains when deviations of observations from the grand mean were assessed (**Table 4.3.1**). Corresponding wireframe visualisations are given in supplementary material for this chapter (**Figure S 4.3.3**). Separation of all three strains along a common trajectory is observed, with some overlap between the pten and wild-type strains. Wider spreads of data points and thus variance-in and covariance-between the two blocks is seen in the two mutant strains when compared to the wild-type strain. At the positive extreme of the axis a relative decrease in cranial length alongside a relative increase in cranial height and width is seen to covary with a mandible that also shows a relative decrease in length alongside relative increases in height and width. At the negative extreme of PLS1 a relative increase in cranial length alongside relative decreases in cranial height and width is seen to covary with a mandible that also shows relative increase in length alongside decrease in height and width. Patterns of covariance seen along this axis correspond highly to patterns of variance observed on PC1 for principal component analyses of shape variance in both the cranium and mandible. Such correspondence between PCA and PLS results alongside a RV coefficient of 0.70 indicates a high level of integration between the cranium and mandible in the three strains.

Validation of this result via a comparable PLS analysis of separate hemi-crania and separate hemi-mandibles is given in supplementary material for this chapter (**Figure S 4.3.4; Table S 4.3.1**). See **Section 4.2.2** for details of methodology.



PLS 1 WARP - CRANIUM

negative warp -0.1

positive warp 0.1

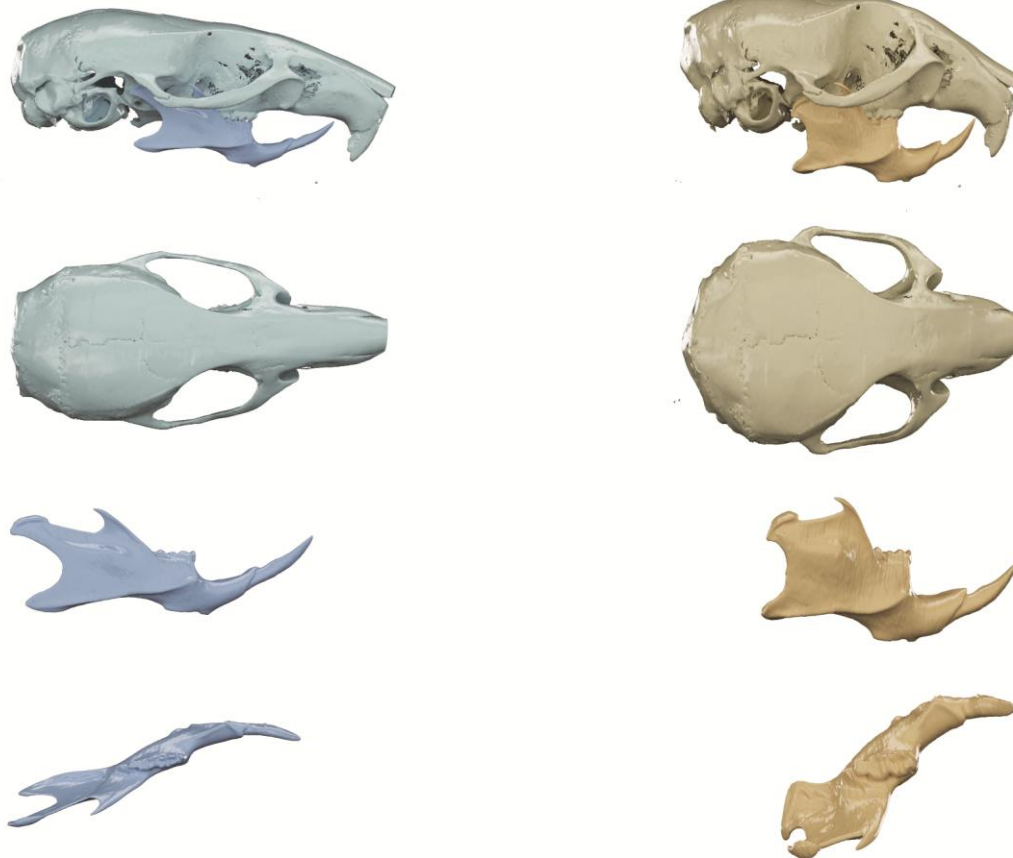
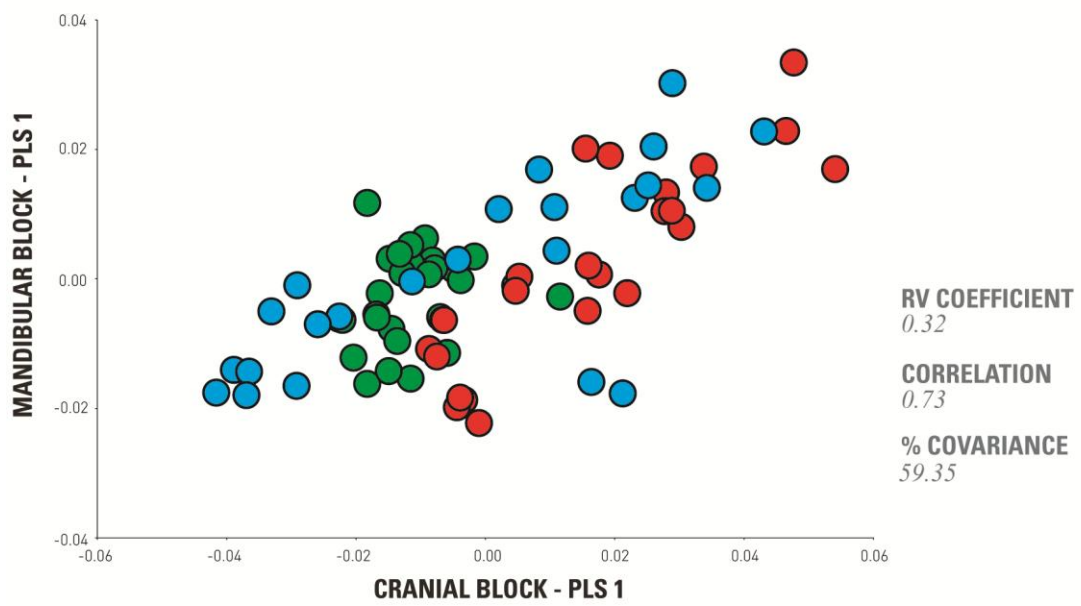


Figure 4.3.3: Partial least squares analysis of brachymorph (red markers); C57 (green markers) and pten (blue markers) crania and mandibles. Insets show positive (0.1) and negative (-0.1) extremes of covariance (89.48% of total covariance) between crania and mandibles for the sample as a whole.

Figure 4.3.4 shows the first singular axis of covariance (RV: 0.32; covariance: 59.35%; correlation: 0.73) between the cranium and mandible in all three strains when deviations of observations from the group means were assessed (**Table 4.3.1**). Corresponding wireframe visualisations are given in supplementary material for this chapter (**Figure S 4.3.5**). A common trajectory is seen in all three strains, again with a greater degree of variance/covariance observed in the two mutant strains. At the positive extreme of the first singular axis (PLS1) an increase in curvature of the cranium (ventral rotation at the rostral and occipital regions) and a decrease in cranial length alongside an increase in cranial height is seen to covary with a mandible that is also decreased in length, has an increase in height at the condyle, and shows ventral rotation at the anterior region. At the negative extreme of the first singular axis a flattened cranium (dorsal rotation at the rostral and occipital regions) with an increased length and decreased height is seen to covary with a mandible that is increased in length, decreased in height at the condyle, and shows a dorsal rotation at the anterior region. Patterns of covariance seen along this axis correspond highly to patterns of variance observed on PC2 for principal component analyses of shape variance in the cranium.

Validation of this result via a comparable PLS analysis of separate hemi-crania and separate hemi-mandibles is given in supplementary material for this chapter (**Figure S 4.3.6; Table S 4.3.1**). See section 4.2.2 for details of methodology.



PLS 1 WARP

negative warp -0.1

positive warp 0.1

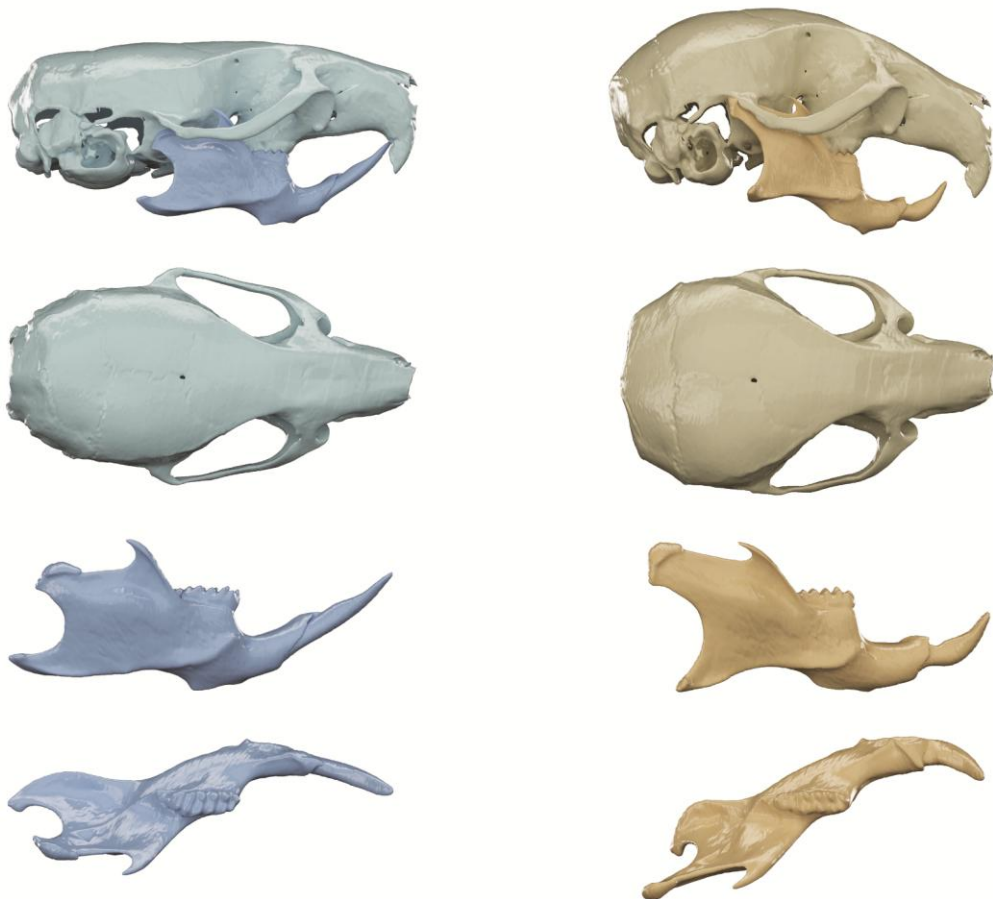


Figure 4.3.4: Partial least squares analysis, pooled by group, of brachymorph (red markers); C57 (green markers) and pten (blue markers) crania and mandibles. Insets show positive (0.1) and negative (-0.1) extremes of covariance (59.35% of total covariance) between crania and mandibles for the sample as a whole.

4.3.2 Do shared common patterns of covariance between crania and mandibles exist between the three strains?

Individual PLS analyses were carried out for each strain (intra-strain analysis), assessing patterns of covariance between the cranium and mandible in each group. Patterns and vectors of covariance in each strain were then compared to common patterns of covariance in all three strains (**Table 4.3.2; Table 4.3.3**). **Figure 4.3.5** shows the first axis of common (inter-strain) patterns of covariance (pooled by group) compared to the first singular axis of covariance in the brachymorph and pten strains. Corresponding wireframe visualisations are given in supplementary material for this chapter (**Figure S 4.3.7**). A high correspondence between patterns of covariance on PLS1 in the two mutant strains when compared to patterns seen on PLS1 of the common (inter-strain) analysis is observed, and a shared pattern of covariance is confirmed by comparison of vectors of covariance. For inter-strain (RV:0.32; covariance: 59.35%; correlation: 0.73), brachymorph (RV: 0.58; covariance: 61.49%; correlation: 0.88) and pten (RV: 0.39; covariance: 72.03%; correlation 0.80) PLS1 axes, an increase in curvature of the cranium (ventral rotation at the rostral and occipital regions) and a decrease in cranial length alongside an increase in cranial height is seen to covary with a mandible that is also decreased in length, has an increase in height at the condyle, and shows ventral rotation at the anterior region (**Table 4.3.1**). At the opposite extreme of landmark configurations warps a flattened cranium (dorsal rotation at the rostral and occipital regions) with an increased length and decreased height is seen to covary with a mandible that is increase in length, decreased in height at the condyle, and shows a dorsal rotation at the anterior region. Patterns of covariance observed on the first singular axis for the wild-type strain do not correspond so highly to common patterns on PLS, with vector analysis confirming lack of correspondence with the general patterns of covariance.

Further detail and visualisation of PLS analyses for individual strains are given in supplementary material for this chapter (brachymorph: **Figures S 4.3.8 and S 4.3.9**; pten: **Figures S 4.3.10 and S 4.3.11**). Validation of vectors of covariance by means of comparable PLS analyses of separate hemi-crania and separate hemi-mandibles

are also given in supplementary material for this chapter (**Table S 4.3.2; Table S 4.3.3**). See section 4.2.2 for details of methodology.

PLS ANALYSIS - VECTOR AND WARP COMPARISON

Figure 4.3.5

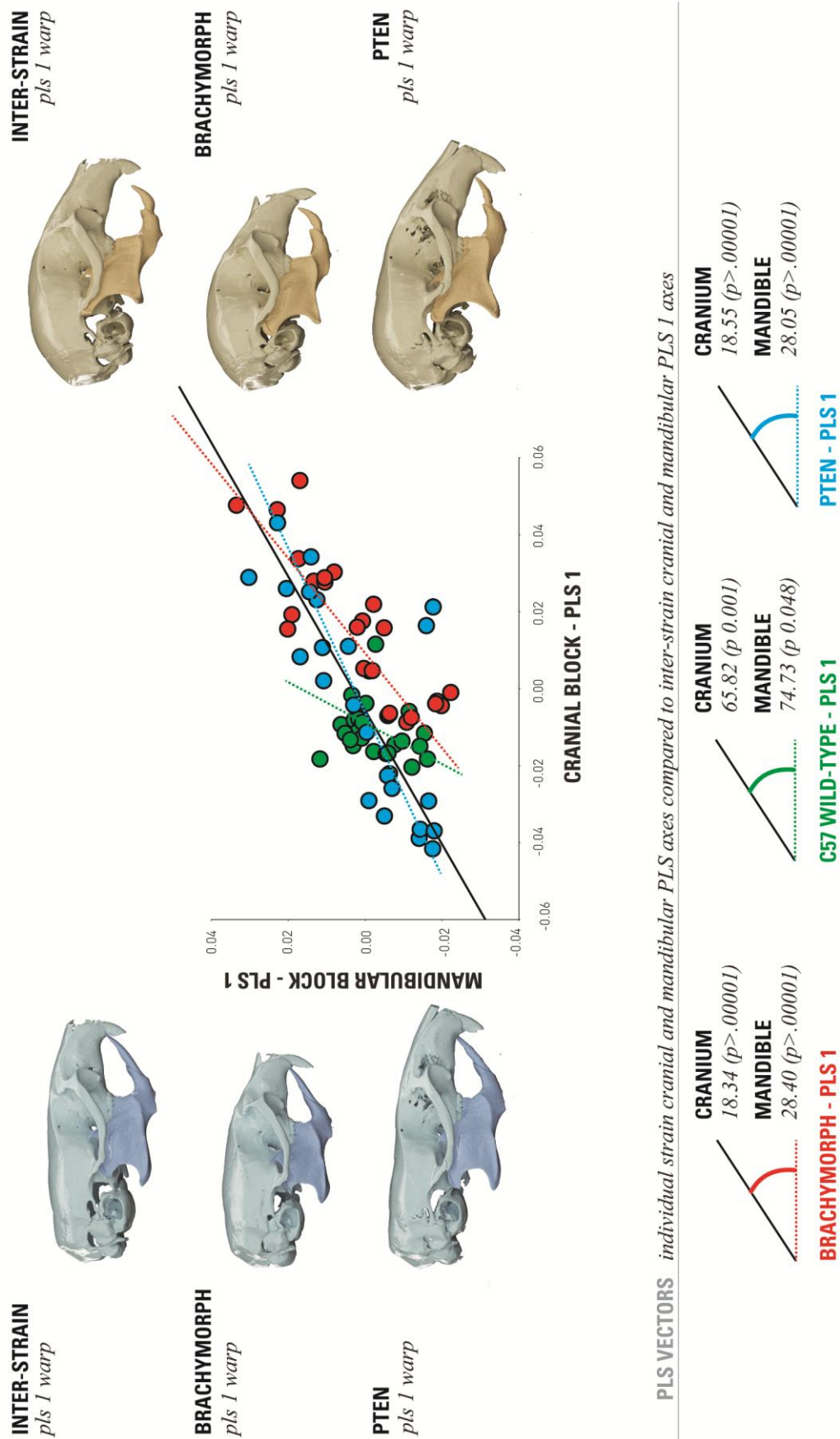


Figure 4.3.5: Comparison of PLS vectors and warps for the PLS analyses: Insets show positive (0.1) and negative (-0.1) warps along PLS1 of the whole sample; PLS1 of brachymorph strain, and PLS1 of pten strain. Graph shows plot of PLS1 of cranial block and PLS1 of mandibular block for inter-strain analysis pooled by group (brachymorph (red markers) C57 (green markers) and pten (blue markers)). Black solid line depicts vectors for inter-strain analysis, coloured dashed lines (brachymorph (red) C57 (green) and pten (blue)) depict PLS vectors for PLS analyses of individual strains. PLS vectors are shown to be comparable between inter-strain, brachymorph and pten PLS analyses.

**RV COEFFICIENTS, SINGULAR VALUES AND PAIRWISE CORRELATIONS OF
PLS SCORES BETWEEN CRANIAL AND MANDIBULAR BLOCKS**

Table 4.3.1

Analysis	PLS axis	RV coefficient		singular value		percentage	correlation	p-value
		RV coefficient	p-value	singular value	p-value	total covariance		
Inter-strain	PLS 1	0.70	<.0001	0.00092	<.0001	89.48	0.97	<.0001
	PLS 2			0.00025	<.0001	6.80	0.79	<.0001
Inter-strain pooled by group	PLS 1	0.32	<.0001	0.00017	<.0001	59.35	0.73	<.0001
	PLS 2			0.00010	<.0001	21.15	0.76	<.0001
Brachymorph	PLS 1	0.58	<.0001	0.00029	<.0001	61.49	0.88	0.00
	PLS 2			0.00014	0.04	15.28	0.82	0.02
C57 (wild-type)	PLS 1	0.48	<.0001	0.00016	0.00	59.65	0.86	0.00
	PLS 2			0.00008	0.04	15.16	0.85	0.00
Pten	PLS 1	0.39	0.00	0.00036	0.01	72.03	0.80	0.01
	PLS 2			0.00012	0.56	7.71	0.75	0.16

Figure 4.3.6 shows the second axis of common (inter-strain) patterns of covariance (pooled by group) compared to the second singular axis of covariance in the brachymorph (RV: 0.58; covariance: 15.28%; correlation: 0.82) and pten (RV: 0.39; covariance: 7.71%; correlation: 0.75) strains and the first singular axis of covariance in the wild-type strain (RV: 0.48; covariance: 59.65%; correlation: 0.86) (**Table 4.3.1**). Corresponding wireframe visualisations are given in supplementary material for this chapter (**Figure S 4.3.12**). High correspondence between patterns of covariance on PLS2 in the two mutant strains and PLS1 in the wild-type strain are revealed when compared to patterns seen on PLS2 of the common (inter-strain) analysis. This shared pattern of covariance confirmed by comparison of vectors of covariance (**Table 4.3.2; Table 4.3.3**). An increase in cranial length is seen alongside a decrease in cranial width and a relative flaring of the zygomatic arches is seen to covary with an increase in mandibular length and a medial rotation of the two hemi mandibles such that mandibular width is decreased. Conversely a decrease in cranial length and increase in cranial width is seen to covary with a decrease in mandibular length and a lateral rotation of the two hemi mandibles such that overall mandibular width is increased.

Correspondence between PLS1 of the brachymorph and pten strains and PLS2 of the wild-type strain is likely due to the highly spherical distribution of individual data points for the wild-type strain, rendering the order of the singular axes in this strain more arbitrary.

Further detail and visualisation of PLS analyses for all strains, and individual strains are given in supplementary material for this chapter (inter-strain: **Figures S 4.3.13** and **S 4.3.14**; brachymorph: **Figures S 4.3.15** and **S 4.3.16**; C57 (wild-type): **Figures S 4.3.17** and **S 4.3.18**; pten: **Figures S 4.3.19** and **S 4.3.20**). Validation of vectors of covariance by means of comparable PLS analyses of separate hemi-crania and separate hemi-mandibles are also given in supplementary material for this chapter (**Table S 4.3.2; Table S 4.3.3**). See section 4.2.2 for details of methodology.

Figure 4.3.6

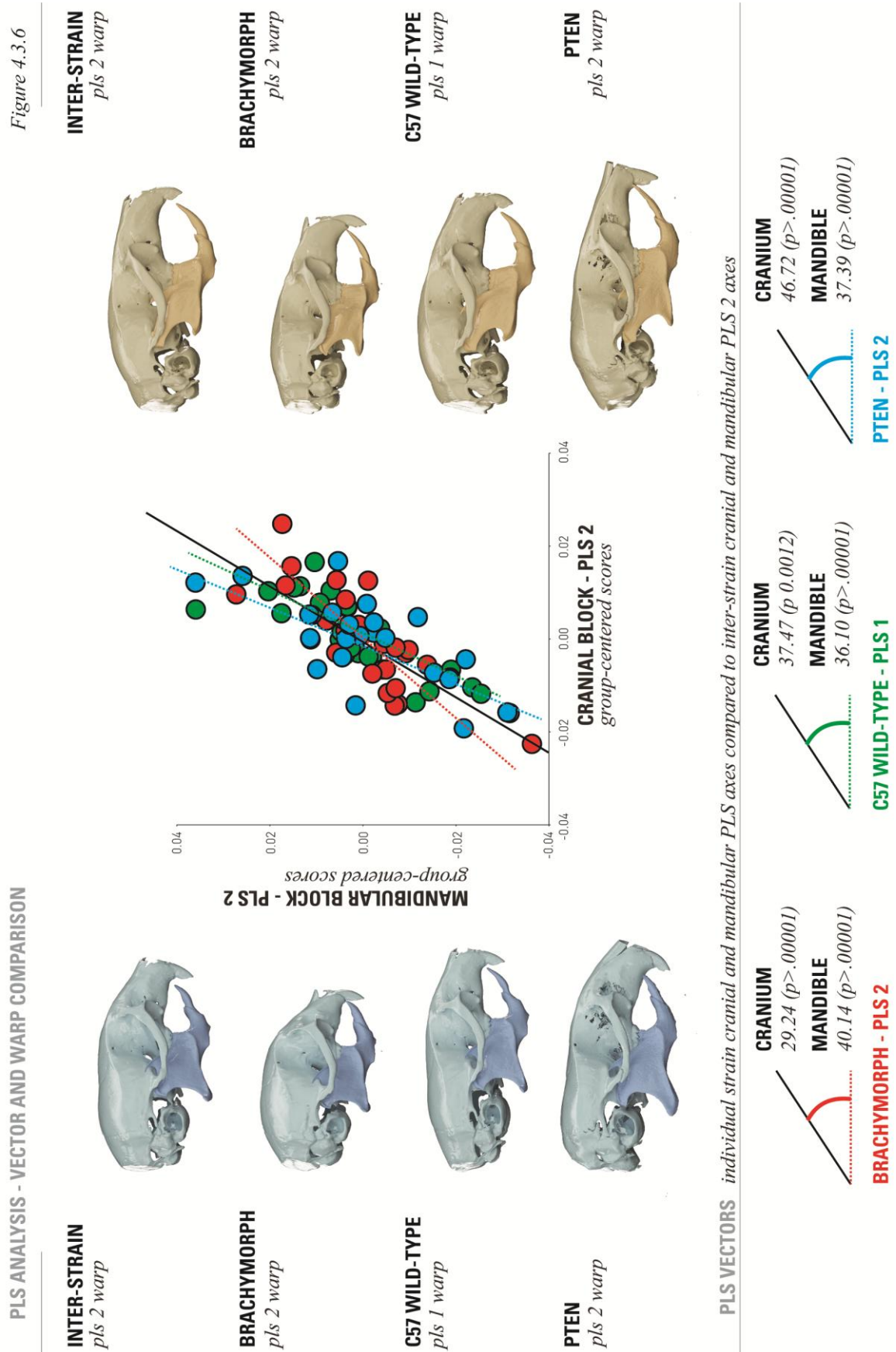


Figure 4.3.6: Comparison of PLS vectors and warps for the PLS analyses: Insets show positive (0.1) and negative (-0.1) warps along PLS2 of the whole sample; PLS2 of brachymorph strain, PLS2 of pten strain, and PLS1 of C57 strain. Graph shows plot of PLS2 of cranial block and PLS2 of mandibular block for inter-strain analysis pooled by group (brachymorph (red markers) C57 (green markers) and pten (blue markers)). Black solid line depicts vector for inter-strain analysis, coloured dashed lines (brachymorph (red) C57 (green) and pten (blue)) depict PLS vectors for PLS analyses of individual strains. PLS vectors are shown to be comparable between inter-strain, brachymorph and pten PLS2 analyses and C57 PLS1 analysis.

**VECTOR COMPARISON BETWEEN INDIVIDUAL PLS SCORES
AND INTER-STRAIN PLS SCORES FOR CRANIAL BLOCK**

Table 4.3.2

	Brachymorph cranium			Plen cranium			C57 cranium					
	PLS1	PLS2		PLS1	PLS2		PLS1	PLS2				
	vector	p-value	vector	p-value	vector	p-value	vector	p-value	vector			
Inter-strain cranium pooled by group PLS1	18.34	< 00001	83.43	0.38	18.55	< 00001	80.97	0.23	65.82	0.00	87.22	0.71
Inter-strain cranium pooled by group PLS2	82.09	0.29	29.24	< 00001	76.53	0.07	46.72	< 00001	37.47	< 00001	87.09	0.70

**VECTOR COMPARISON BETWEEN INDIVIDUAL PLS SCORES
AND INTER-STRAIN PLS SCORES FOR MANDIBULAR BLOCK**

Table 4.3.3

	Brachymorph mandible			Plen mandible			C57 mandible					
	PLS1	PLS2		PLS1	PLS2		PLS1	PLS2				
	vector	p-value	vector	p-value	vector	p-value	vector	p-value	vector			
Inter-strain mandible pooled by group PLS1	28.40	< 00001	79.56	0.18	28.05	< 00001	72.96	0.03	74.73	0.05	86.55	0.66
Inter-strain mandible pooled by group PLS2	77.23	0.10	40.14	< 00001	69.74	0.01	37.39	< 00001	36.10	< 00001	78.52	0.14

4.4 DISCUSSION

The ability of the craniomandibular skeleton to adapt appropriately to changes in both the size and shape of components of its own form is vital for the maintenance of cohesive morphology and thus functional performance. Mutational variance, morphological change throughout ontogeny, and environmental adaptation expose the skull to significant variation in form, and yet vital functions such as mastication must be consistently achieved and maintained.

A number of studies have investigated the functional performance of the craniomandibular complex during ontogenetic changes in form (Tanner et al., 2010, La Croix et al., 2011a, La Croix et al., 2011b, Erickson et al., 2003, Binder and Van Valkenburgh, 2000), yet less is known about the general potential and mechanisms by which this region may achieve maintenance of function in the face of variance in form. This study was designed to confront this gap and investigate the ability of the skull to adapt in a cohesive and appropriate manner when faced with variation in one region. The capacity of the craniomandibular complex to remain cohesive in terms of form in two mutant mouse strains in which cranial length alone was altered early on in development was investigated. Patterns of variance and covariance within the skull of the two mutant strains were compared to those of a control of the same background strain.

Two hypotheses were posed, firstly that patterns of mandibular morphology would correspond to patterns of variance in the craniomandibular skeletons of the three strains, and secondly that all three strains would show common patterns of covariance between the craniofacial and mandibular skeletons.

Strong patterns of covariance between crania and mandibles were revealed when partial least squares analysis was carried out for the whole sample, indicating a high degree of integration in the craniomandibular complex. This result is supported by a high correspondence between patterns of variance in crania and mandibles revealed via principal component analysis and patterns of covariance between these two structures revealed via partial least squares analysis. In all three strains an increase in cranial length is seen to covary with an increase in mandibular length, and

conversely a decrease in cranial length is found to covary with a decrease in mandibular length. Additional parameters of form such as width and height show tight coherence in both crania and mandibles. Such strong correlation of form between these two structures indicates the capacity of the cranium and mandible to maintain cohesion in its overall form despite genetically induced variance in one component that is absent in other regions of the complex.

While the cranium and mandible are easily identifiable as two separate structures, association of form revealed between these two semi-independent parts reveals a substantial degree of coordination within the craniomandibular complex as a whole. Such conflict between the simultaneous coordination and relative independence of composite parts of a skeletal complex is described by the concepts of integration and modularity (Klingenberg, 2008, Olson and Miller, 1958, Pigliucci and Preston, 2004). Modularity describes the division of a system into partially dissociated components, while integration refers to the coordinated variation of functionally and developmentally related parts of an organism. Modules themselves are integrated, made both coherent and semi-independent of other surrounding structures due to strong interactions between their component parts (Klingenberg et al., 2003), such that integration between modules is less manifold and firm than integration within modules. Integration between modules is however often not insubstantial, with developmental and functional links between semi-independent parts providing the necessary coordination for a cohesive whole. Thus in a highly complex structure composed of numerous semi-independent parts, a hierarchical network of interactions between features is present. While there is no agreement on how isolated a character must be to be counted as a module (Hansen, 2003, Raff and Raff, 2000, Griswold, 2006), with unique structural identities the cranium and mandible of vertebrates would generally be considered distinct modules, and yet the high degree of covariance of these structures revealed here is indicative of strong integration of the whole complex (Klingenberg, 2005a).

In all three strains a relatively lengthened cranium is seen to covary with a relatively lengthened mandible, and conversely a relatively shortened cranium is seen to covary with a relatively shortened mandible. Both pten and brachymorph mutations affect cartilage development and growth, and thus, cranial growth alone, in both

cases the causal factor/s in these covariances are almost certainly epigenetic. Thus, as mandibular morphology observed in the two mutant strains is unlikely to be a heritable trait, the tight coherence between cranial and mandibular form in these mice is proposed to be the consequence of substantial plastic adaptation occurring within a highly integrated system. This result indicates the potential of the craniomandibular complex to respond to regional changes in skeletal morphology with appropriate plastic adaptation in other linked regions. In the absence of such a plastic response, mutationally derived morphological variance in a semi-independent region such as the cranium could be expected to result in poor occlusion with the mandible and potentially deleterious functional consequences. Instead, results of this study point to a global integration throughout the craniomandibular complex, such that an alteration to morphology in one semi-independent region such as the cranium results in appropriate plastic adaptation in other semi-independent but globally integrated regions such as the mandible. This result thus indicates the capacity for an integrated system and plastic mechanism to lead to appropriate global adaptation throughout the entire complex when variance occurs in one region, retaining suitable size relations between parts and therefore functionality.

Such a potential globally adaptive system not only requires a hierarchical organisation of parts such that individual regions have both semi-independence and global coordination throughout the complex, but also requires the ability of skeletal regions to morphologically adapt in the absence of genetic instruction. Phenotypic adaptive plasticity describes the ability of an organism to react and respond to altered environmental conditions during the course of its ontogeny, conferring the ability of a single genotype to produce more than one alternative form of morphology (West-Eberhard, 1989, Ravosa et al., 2008a). A small genetic alteration may initiate a series of plastic compensatory responses in surrounding structures, thereby effecting major change in overall form. Thus in the absence of major genetic change, plasticity may produce complex, coordinated and adaptive phenotypes (West-Eberhard, 2003, West-Eberhard, 1989). The strong correlation and coordination between cranial and mandibular form found in the two mutant strains demonstrates the ability of adaptive plasticity to produce appropriate and integrated phenotypes in the absence of genetic patterning.

Not only are patterns of mandibular morphology found to correspond aptly to cranial morphology, but common patterns of both cranial and mandibular morphology are found in all three strains. Results of this study show that not only does adaptation occur in the mandible of both mutant strains such that cranial and mandibular morphology are tightly correlated with appropriate size relations between the two maintained; but also that patterns of observed covariance are common to both mutant strains and share elements of covariance with the wild-type strain. Analysis of patterns of covariance between the cranium and mandible reveal the same trajectory and morphological relationships between the cranium and mandible in all three strains (intra-strain analyses), with these patterns and trajectories being consistent with patterns revealed when all three strains were subjected to a global (inter-strain) analysis. This result is suggestive of common integrating factors across all three strains.

The covariation and integration of semi independent skeletal elements such as the cranium and mandible may be viewed as functional, developmental, genetic and/or evolutionary in origin (Klingenberg, 2008, Cheverud, 1996b). As morphological structures are produced via developmental processes, epigenetic developmental interactions between parts can mutually influence each other achieving coordinated development of the whole complex and organism (Hallgrímsson et al., 2007, Hall, 1999, Klingenberg, 2003). Pleiotropic effects of genes on morphological traits may result in patterns of genetic modularity and integration (Klingenberg, 2008, Wagner, 1996, Wagner et al., 2007a). Shared function may act as an integrating factor with direct mechanical forces produced during mastication alongside other dynamic functions such as capture and processing of prey, leading to coordination between semi-independent regions of the whole (Breuker et al., 2006b). Finally, structured associations between the evolutionary divergence of different traits results in evolutionary modularity (Klingenberg, 2008). These processes are however not isolated. Development mediates the expression of both genetic and environmentally induced phenotypic variance via the transmission of effects across different traits, linking genetic and developmental integration (Klingenberg, 2008, Klingenberg, 2005b). Developmental processes also form the morphology of functional components, connecting developmental modularity and functional modularity

(Breuker et al., 2006a); while functional modularity can influence developmental modularity via plastic processes such as bone remodelling in which the rates and directions of tissue growth are influenced by mechanical loading (Klingenberg, 2008, West-Eberhard, 2003, Enlow and Hans, 1996a, Herring, 1993). Genetic and functional modularity both influence evolutionary modularity, as genetic variation is a critical determinant for evolutionary change via selection and drift (Felsenstein, 1988), and as the modular structure of morphological traits is linked to selection on functional performance (Klingenberg, 2008). Common patterns of covariation between the cranium and mandible found in all three strains analysed in this study may be indicative of common integrating factors in the three. As mandibular morphology observed in both the brachymorph and pten strains is unlikely to be directly affected by the respective brachymorph and pten mutations, the cause of such tight covariance is likely epigenetic and thus integrating factors developmental and/or functional in nature. While clarification of the integrating factors responsible for these results is beyond the remit of this work, we may hypothesise that function may play a key role in the plastic adaptation of the mandible such that cranial and mandibular form are correlated in the three strains. While genes undoubtedly play a crucial role in determining the morphology of a skeletal structure, these may be up- or down- regulated by mechanical stimuli prior to translation into macroscopic growth (Mao and Nah, 2004). Common functional requirements, such as mastication, across the three strains may lead to common features of cranial and mandibular covariation. As masticatory muscle stimulation plays a significant role in stresses placed upon the craniomandibular complex, and such mechanical forces play a critical role in the regulation of chondrogenesis and osteogenesis (Herring and Lakars, 1981, Lanyon, 1984, Frost, 1987, Atchley et al., 1991, Thorogood, 1993, Huiskes, 2000, Skerry et al., 2000, Rauch and Schoenau, 2001, Mao and Nah, 2004, Carter et al., 1998, Mao, 2002, van der Meulen and Huiskes, 2002), essential functions such as mastication may result in common morphological adaptation across the three strains in order to maximise performance potential.

In all three strains a suite of cranial features are seen alongside both an increase and decrease in cranial length. As cranial length increases, cranial width and height decrease and a dorsal rotation at the rostrum and occiput results in a

characteristically flattened cranial appearance. Conversely a decrease in cranial length is seen alongside and increase in cranial width and height and a ventrally rotated rostrum and occiput, giving a distinctive dome like appearance to the cranium. As discussed above, such a common suite of morphological features may indicate strong developmental and functional integration both within and between cranium and mandible, providing the necessary coordinated variance of the upper and lower jaws to ensure that proper occlusion and thus support for function such as mastication are achieved. This common suite of features may also however be indicative of common constraints to adaptation in all three strains. The craniomandibular complex is a highly dynamic region that performs many vital functions additional to mastication, as well as housing critical organs. Results of this study show not only the potential of the mandible to epigenetically plastically adapt in a coordinated manner to morphological changes in the cranium, but also suites of common morphological characteristic within the cranium and within the mandible of each strain. As cranial length is seen to increase, cranial height and width are consistently seen to be reduced across all three strains. Conversely as cranial length is seen to decrease, cranial height and width are consistently seen to be increased across all three strains. Patterns of mandibular morphology are found to correspond with these cranial extremes across all three strains, such that a reduced cranial length with increased width and height covaries with a mandible also reduced in length and increased in width and height. This finding may be due to constraints present in the complex as a result of the necessity to maintain other vital organ size dimensions and functions. The requirement to maintain brain volume and respiratory function may explain why a reduction in cranial length results in increased width and height, with mandibular proportions following so as that masticatory function may also be maintained.

Suites of morphological characteristic attributed to integration have been reported in other species. In humans dolicho- and brachycephalic skull patterns form an integrated suite of morphological character traits associated with facial height variation (Bastir and Rosas, 2004, Enlow and Hans, 1996a, Zollikofer and Ponce de Leon, 2002, Lieberman et al., 2000a, Moss and Salentijn, 1971, Bhat and Enlow, 1985, Enlow and McNamara, 1973). These craniofacial integrative patterns in

humans are found to hold some similarity with patterns of morphological covariance in the chimpanzee skull (Bastir and Rosas, 2004, Bastir et al., 2005a). While dolicho- and brachycephalic skull patterns characterise the extremes of an integrated suite of feature in humans, in the great apes analogous craniofacial extremes of variation have been termed airo- and klinorhynch. The latter two archetypal forms may also be attributed to strong integration within the skull, where angulation of the palate covaries with a whole suite of related morphological features (Baverstock and Cobb – unpublished data).

Results of the present study indicate strong, common patterns of epigenetic integration in the craniomandibular skeleton presumably such that functional maintenance may be achieved. Global coordination of such a pertinent structure has implications for the evolvability of this complex. Evolvability, the ability (for example in terms of speed) to respond to a selective change, requires the capacity to produce suitable variation for selection to act upon (Hansen, 2003, Griswold, 2006). It is generally hypothesised that modular organisation and thus relative independence of constituent parts of a whole may allow for adaptation of individual regions without deleterious effects on other parts (Hansen, 2003, Wagner and Altenberg, 1996, Riedl, 1977, Hallgrímsson et al., 2009, Raff, 1996, Wagner and Mezey, 2004, Wagner et al., 2007a), and that strong covariation may constitute an evolutionary constraint (Klingenberg, 2005a). It has also however been posited that modularity may hamper evolvability by reducing mutational target size (Hansen, 2003, Wagner, 1996, Wagner and Altenberg, 1996), and that, as integration results in the expression of coordinated variation that preferred directions for evolutionary change may be created (Hallgrímsson et al., 2009, Hallgrímsson et al., 2007, Klingenberg, 2005a).

There is general consensus that an increase in pleiotropy reduces evolvability (Griswold, 2006) due to a lower probability that a mutation will have beneficial effects on all characters (Orr, 2000). However, while the probability that a mutation may have a deleterious effect on at least one character may increase with pleiotropy or global integration, equally the probability that a mutation will also have beneficial effect on at least one character should also increase in such a scenario (Griswold, 2006). Additionally pleiotropy or strong integration may result in a mutation having beneficial effects on two or more characters providing a larger overall benefit even if

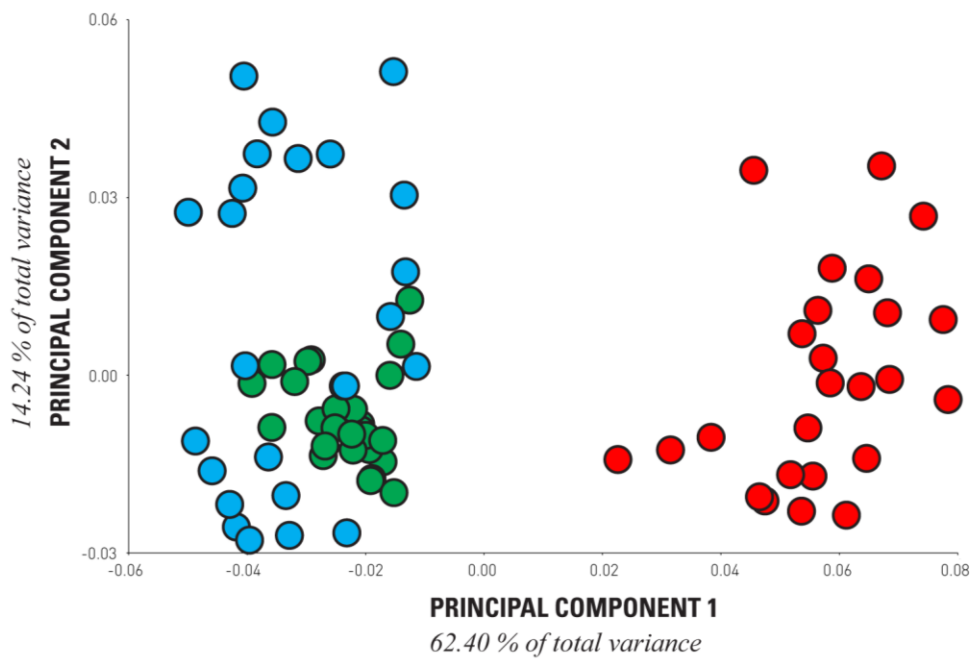
the acting mutation has deleterious effects on other characters. As such, the selective effects of such a mutation may be greater than those which are limited to a single character (Griswold, 2006).

In the present study an isolated variance in cranial length in two mutant mice strains is seen to result in a common pattern of global integration in the craniofacial complex. Compensatory and epigenetically coordinated plastic adaptation is induced in the mandible such that a suite of correlated phenotypic features ensues. Such a covariance structure is necessary in complex skeletal systems such as a skull in order to maintain appropriate size and shape relationships when faced with phenotypic variation. However, although the maintenance of appropriate size and shape relationship between the upper and lower jaws as revealed here is beneficial in terms of achieving correct occlusion and thus preserved fitness in this respect, the resulting alteration to craniomandibular length influences other parameters of function. If muscle attachment sites remain static, an increase in skull length and thus jaw out-lever length has the effect of reducing the mechanical advantage of the masticatory system, while conversely reducing skull length in the absence of changes to muscle in-lever lengths will increase mechanical advantage (Smith and Savage, 1956, Crompton and Hiimae, 1969). However, as a suite of integrated phenotypic changes were found here alongside the change in cranial length it is possible that muscle attachment sites and positioning of the mandibular condyle may also undergo coordinated changes compensatory for change to jaw out-lever length. Additional parameters of performance such as speed would also be altered with a change in jaw length. Although an increase in jaw length may result in reduced mechanical advantage of the masticatory system, this increase in length would also have the effect of increasing speed of bite (Smith and Savage, 1956, Reduker, 1983). Smaller mechanical advantages typically result in the faster movement of the mandible yet at the expense of force (Reduker, 1983), while an increase in condyle height may improve leverage for certain masticatory muscles (Smith and Savage, 1956, Crompton and Hiimae, 1969, Cassini and Vizcaíno, 2012). There is also the potential for coordinated changes to masticatory muscle positioning and size, which may not only influence mechanical advantage but also bite force capacity (Raadsheer et al., 1999).

Like pleiotropy, the multifaceted effect of strong craniomandibular integration and plastic adaptation in response to an isolated phenotypic change revealed here may decrease the probability that any such mutation will have beneficial effect on all characters. Equally such a coordinated system where vital size and shape relationships show maintenance may have the potential to maintain some critical functions while increasing the performance of other parameters. An integrated yet concurrently modular and hierarchical system may also allow for a coordinated maintenance of overall form in response to variance in one region, and yet the independent modular adaptation of individual traits facilitating rapid and parsimonious evolution of morphological traits.

Further work is required to establish the functional performance of the sample used in this study, such that the potential of the skull to not only coordinate and maintain form in response to isolated variance, but also to maintain functional performance.

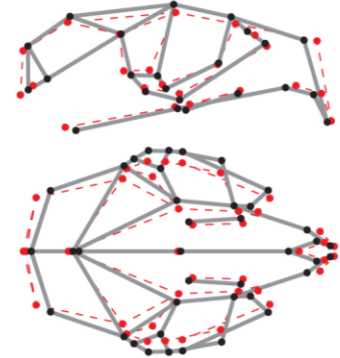
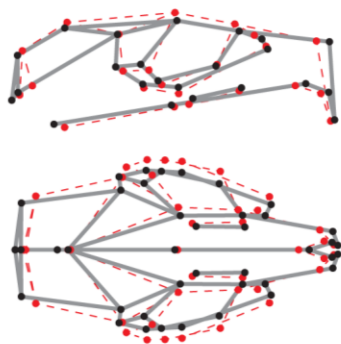
CHAPTER 4 - SUPPLEMENTARY MATERIAL



PRINCIPAL COMPONENT 1

negative warp -0.1

positive warp 0.1



PRINCIPAL COMPONENT 2

negative warp -0.1

positive warp 0.1

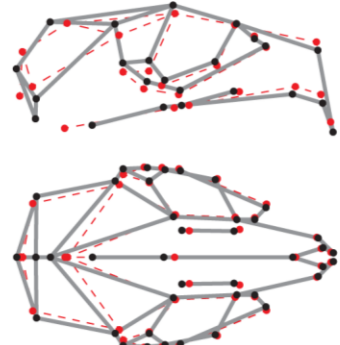
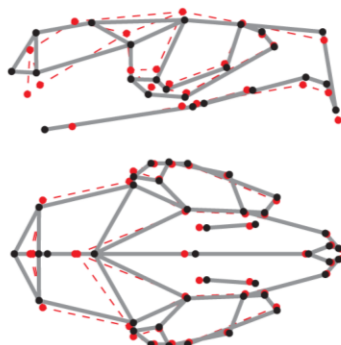
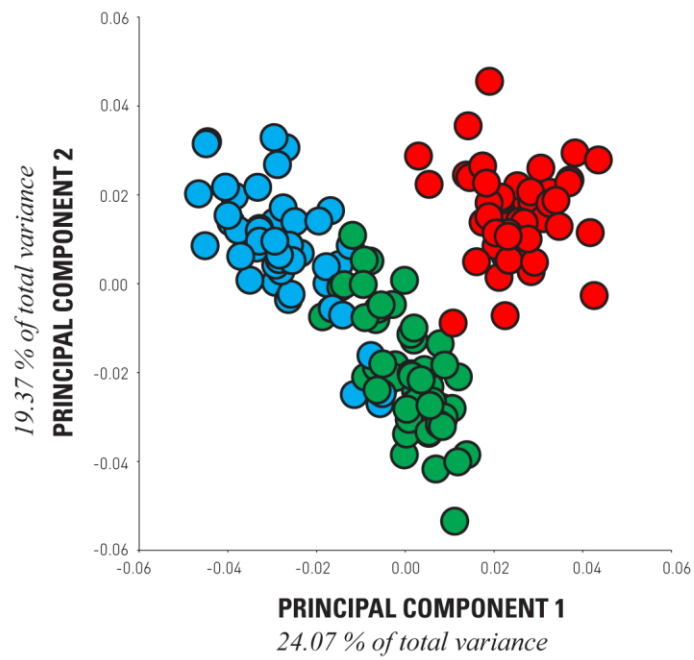


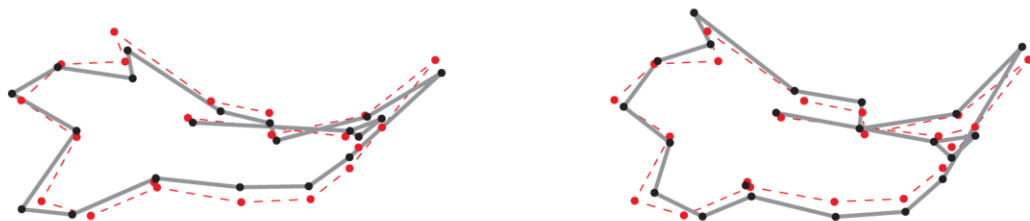
Figure S 4.3.1: Principal component analysis of brachymorph (red markers); C57 (green markers) and pten (blue markers) crania. Insets show wireframes and landmark positions at the 0.1 and -0.1 extremes of PC1 (62.40% of total variance) and PC2 (14.24% of total variance). Red landmarks and dashed lines depict the mean shape of the sample, black landmarks and lines depict landmark positions at each extreme.



PRINCIPAL COMPONENT 1

negative warp -0.1

positive warp 0.1



PRINCIPAL COMPONENT 2

negative warp -0.1

positive warp 0.1

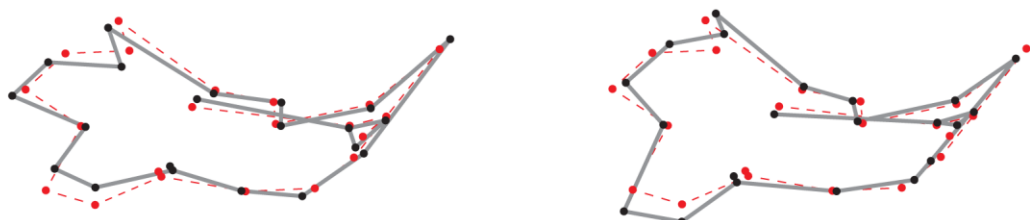
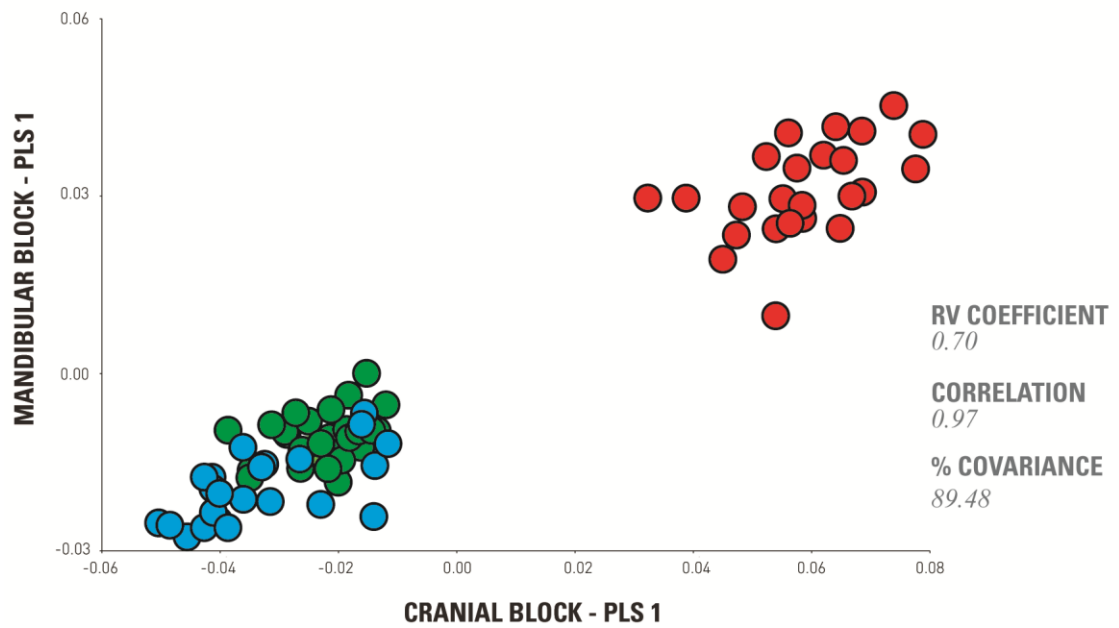


Figure S 4.3.2: Principal component analysis of brachymorph (red markers); C57 (green markers) and pten (blue markers) mandibles. Insets show wireframes and landmark positions at the 0.1 and -0.1 extremes of PC1 (62.40% of total variance) and PC2 (14.24% of total variance). Red landmarks and dashed lines depict the mean shape of the sample, black landmarks and lines depict landmark positions at each extreme.



PLS 1 WARP - CRANIUM

negative warp -0.1

positive warp 0.1

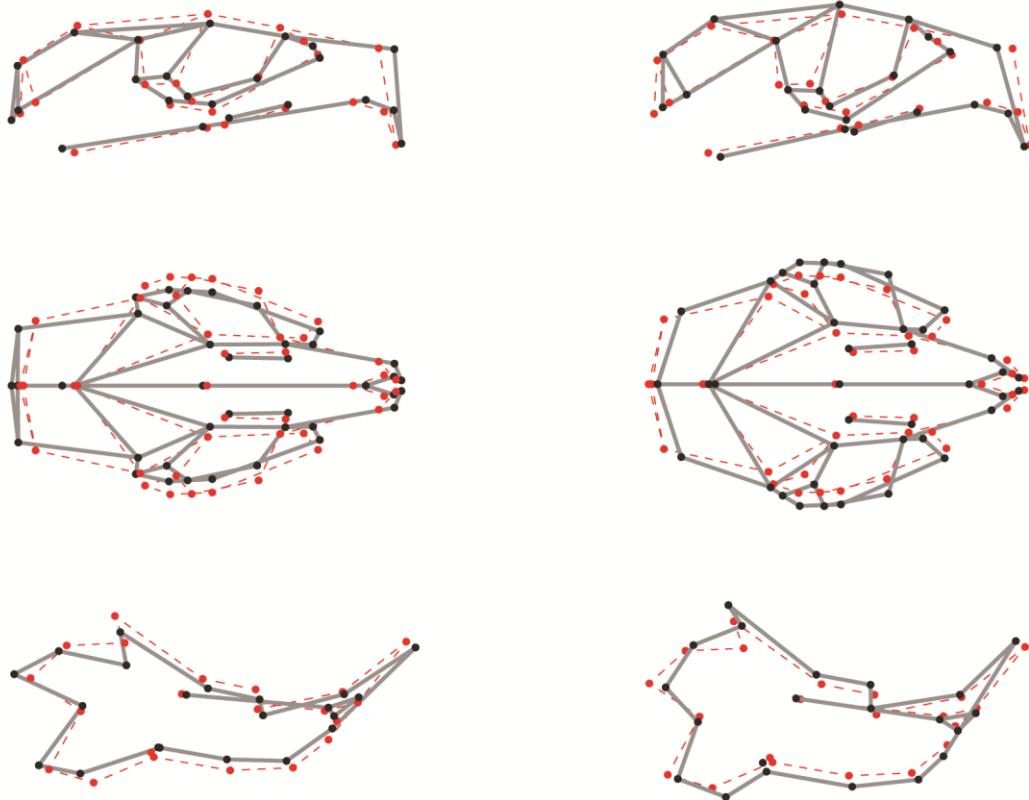
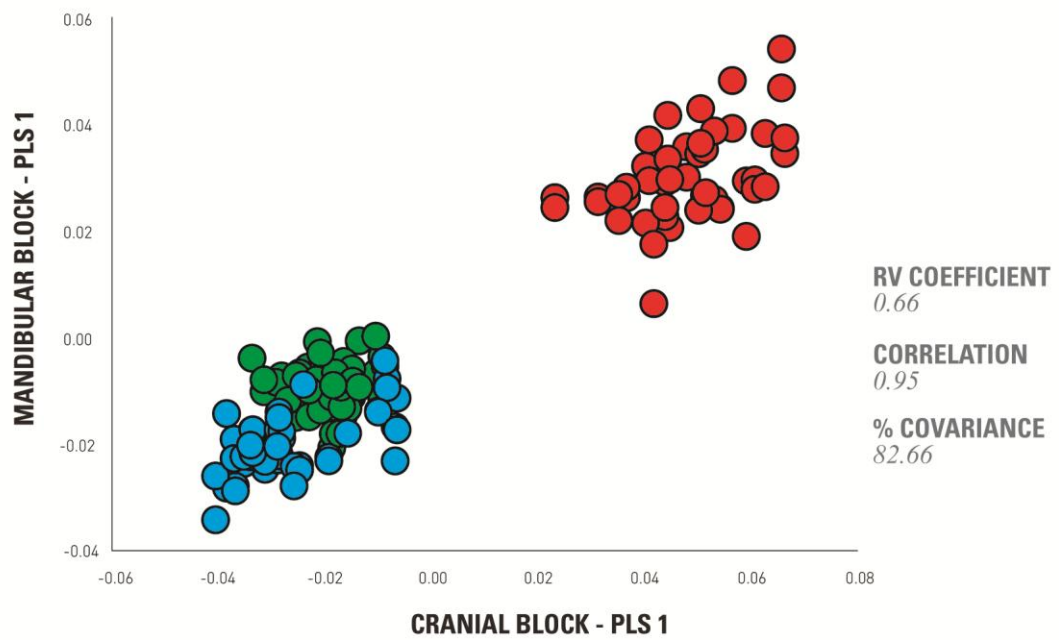


Figure S 4.3.3: Partial least squares analysis of brachymorph (red markers); C57 (green markers) and pten (blue markers) crania and mandibles. Insets show wireframes and landmark positions at the positive (0.1) and negative (-0.1) extremes of covariance (89.48% of total covariance) between crania and mandibles for the sample as a whole. Red landmarks and dashed lines depict the mean shape of the sample, black landmarks and lines depict landmark positions at each extreme.



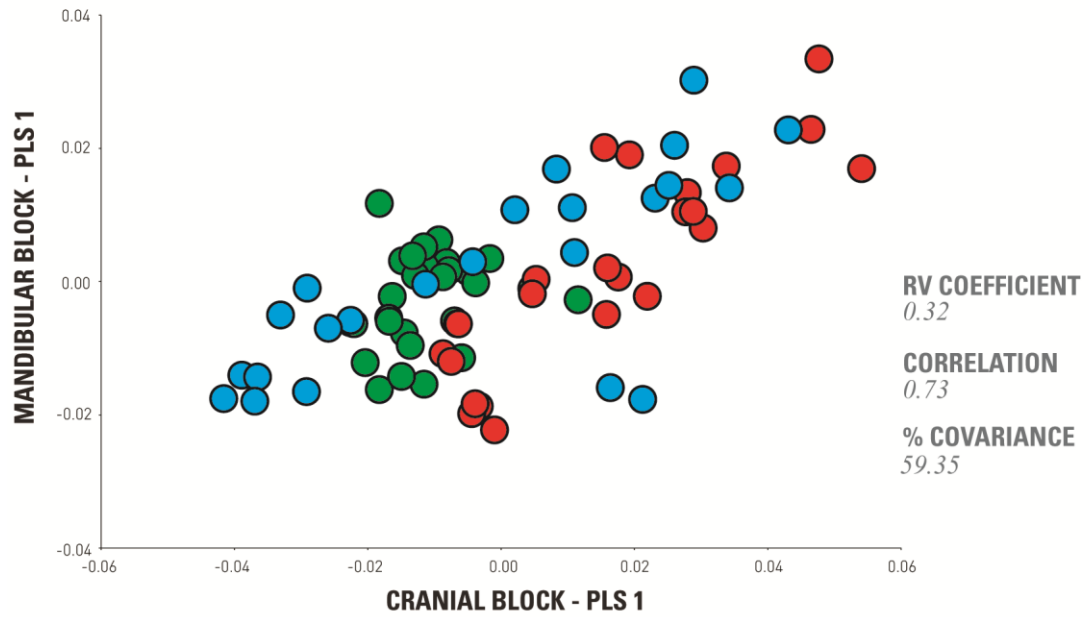
PLS 1 WARP

negative warp -0.1

positive warp 0.1



Figure S 4.3.4: Partial least squares analysis of brachymorph (red markers); C57 (green markers) and ptn (blue markers) left and right hemi crania and left and right hemi mandibles. Insets show warps to the positive (0.1) and negative (-0.1) extremes of covariance (82.66% of total covariance) for PLS1.



PLS 1 WARP

negative warp -0.1

positive warp 0.1

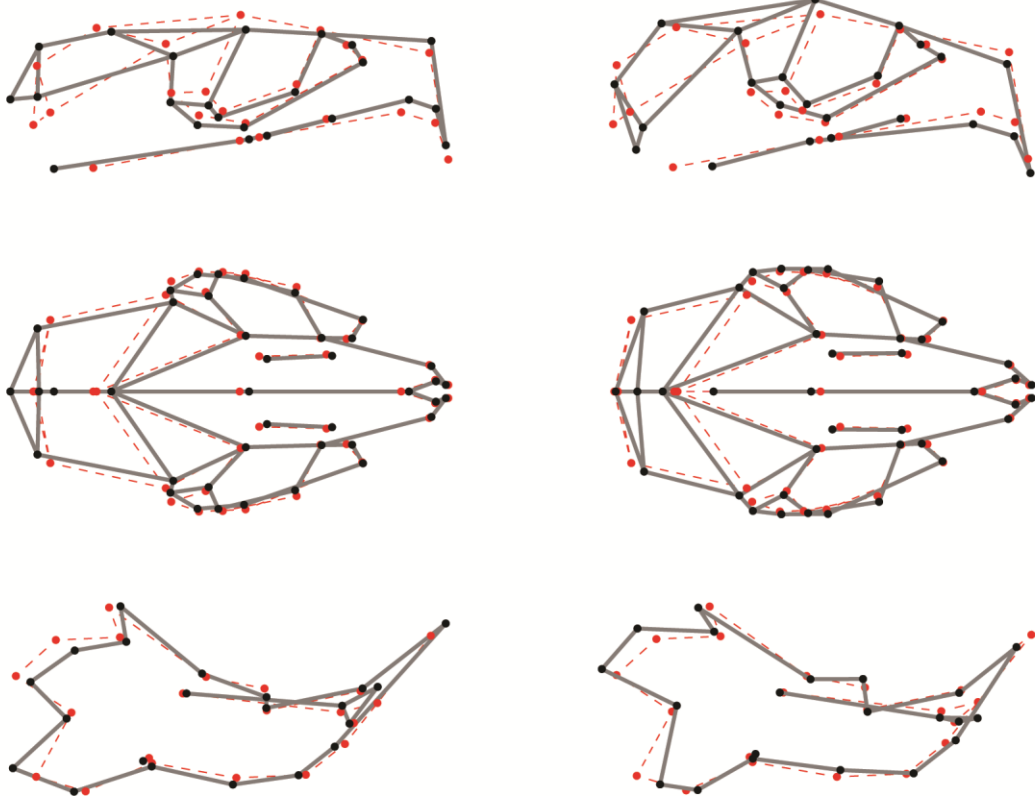
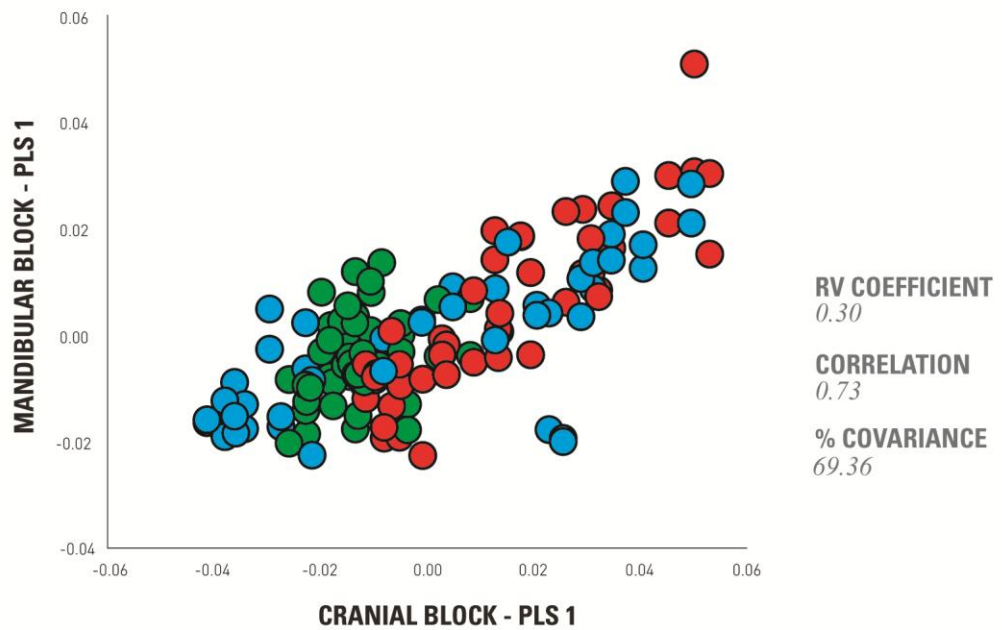


Figure S 4.3.5: Partial least squares analysis, pooled by group, of brachymorph (red markers); C57 (green markers) and pten (blue markers) crania and mandibles. Insets show wireframes and landmark positions at the positive (0.1) and negative (-0.1) extremes of covariance (59.35% of total covariance) between crania and mandibles for the sample as a whole. Red landmarks and dashed lines depict the mean shape of the sample, black landmarks and lines depict landmark positions at each extreme.



PLS 1 WARP

negative warp -0.1

positive warp 0.1

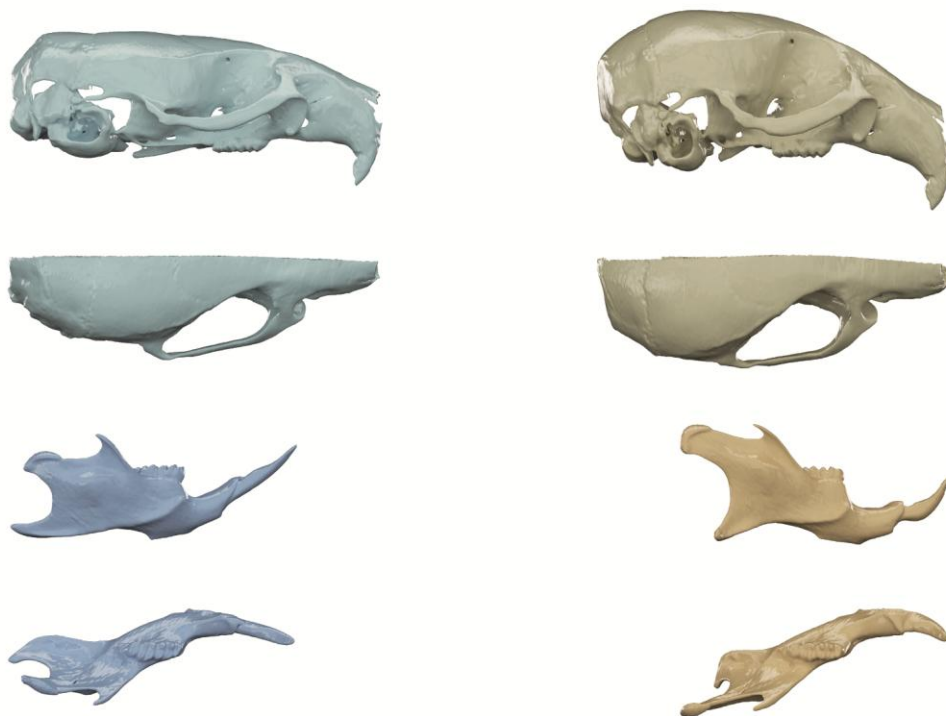


Figure S 4.3.6: Partial least squares analysis, pooled by group, of brachymorph (red markers); C57 (green markers) and pten (blue markers) left and right hemi crania and left and right hemi mandibles. Insets show warps to the positive (0.1) and negative (-0.1) extremes of covariance (69.36% of total covariance) for PLS1.

Figure S 4.3.7

PLS ANALYSIS - VECTOR AND WARP COMPARISON

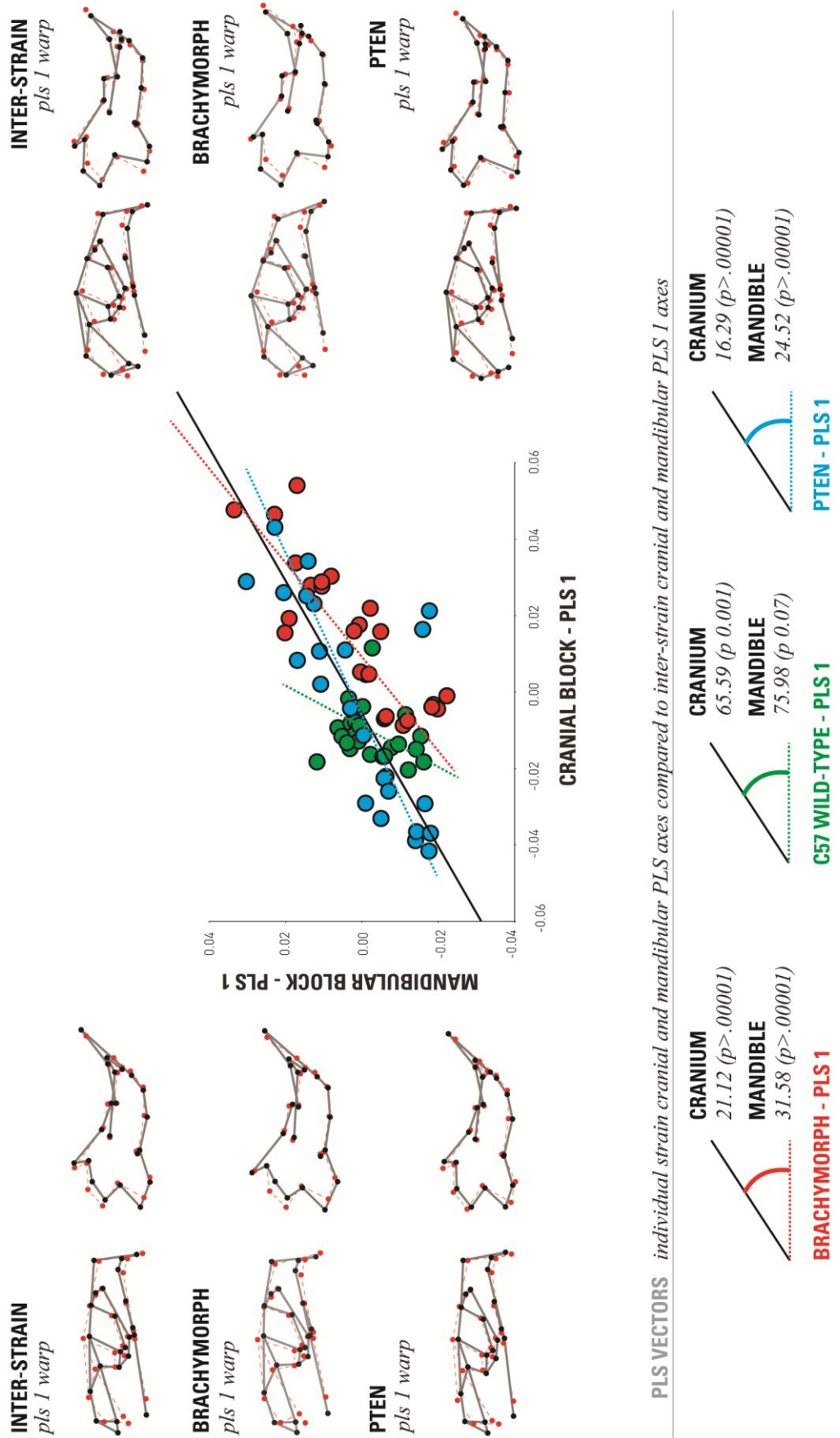


Figure S 4.3.7: Comparison of PLS vectors and warps for the PLS analyses: Insets show wireframes and landmark positions at the positive (0.1) and negative (-0.1) warps along PLS1 of the whole sample; PLS1 of brachymorph strain, and PLS1 of pten strain. Red landmarks and dashed lines depict the mean shape of the sample, black landmarks and lines depict landmark positions at each extreme. Graph shows plot of PLS1 of cranial block and PLS1 of mandibular block for inter-strain analysis pooled by group (brachymorph (red markers) C57 (green markers) and pten (blue markers)). Black solid line depicts vectors for inter-strain analysis, coloured dashed lines (brachymorph (red) C57 (green) and pten (blue)) depict PLS vectors for PLS analyses of individual strains. PLS vectors are shown to be comparable between inter-strain, brachymorph and pten PLS analyses.

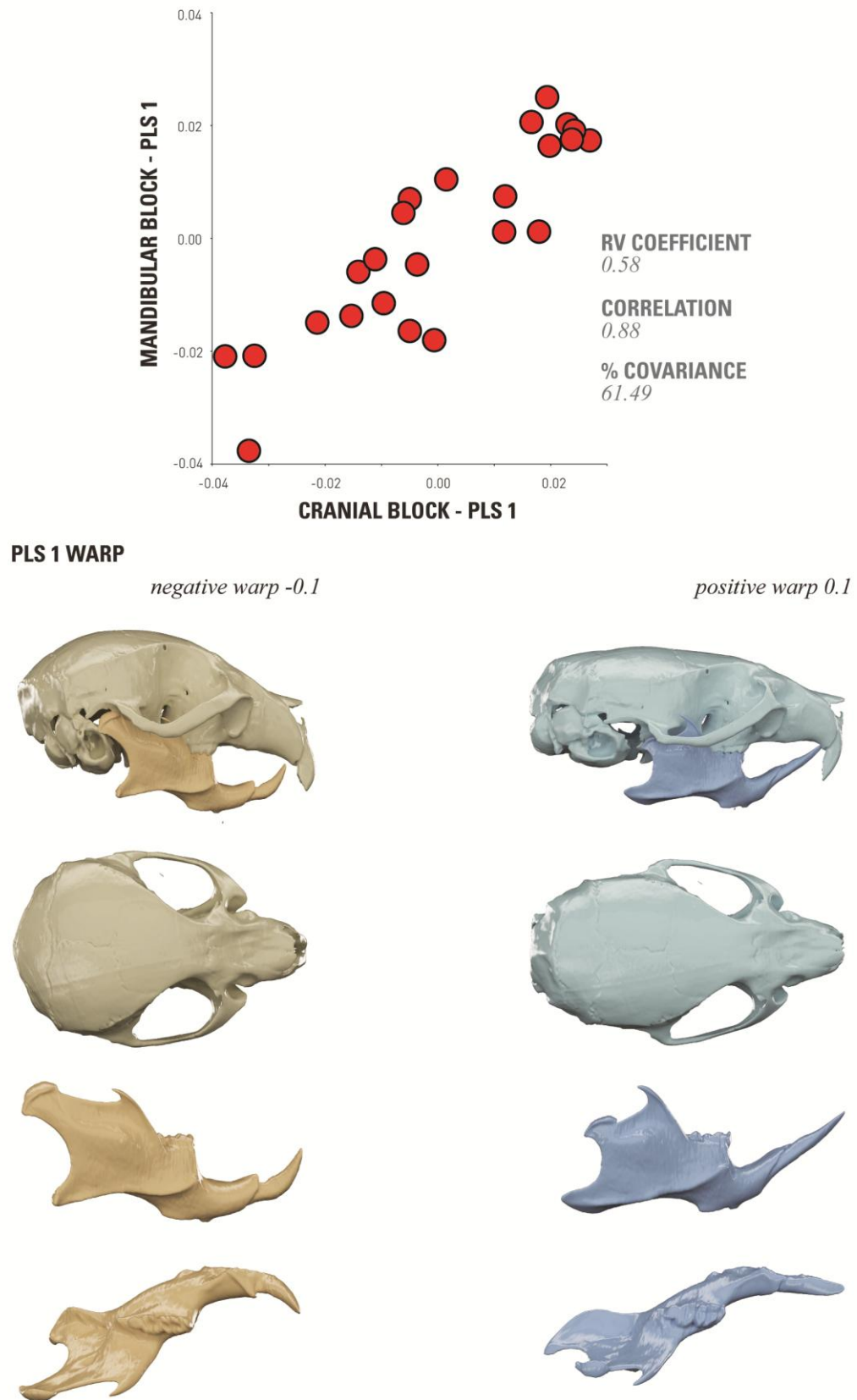


Figure S 4.3.8: Partial least squares analysis of brachymorph crania and mandibles (intra-strain analysis). Insets show warps to the positive (0.1) and negative (-0.1) extremes of covariance (61.49% of total covariance) for crania and mandibles for PLS1.

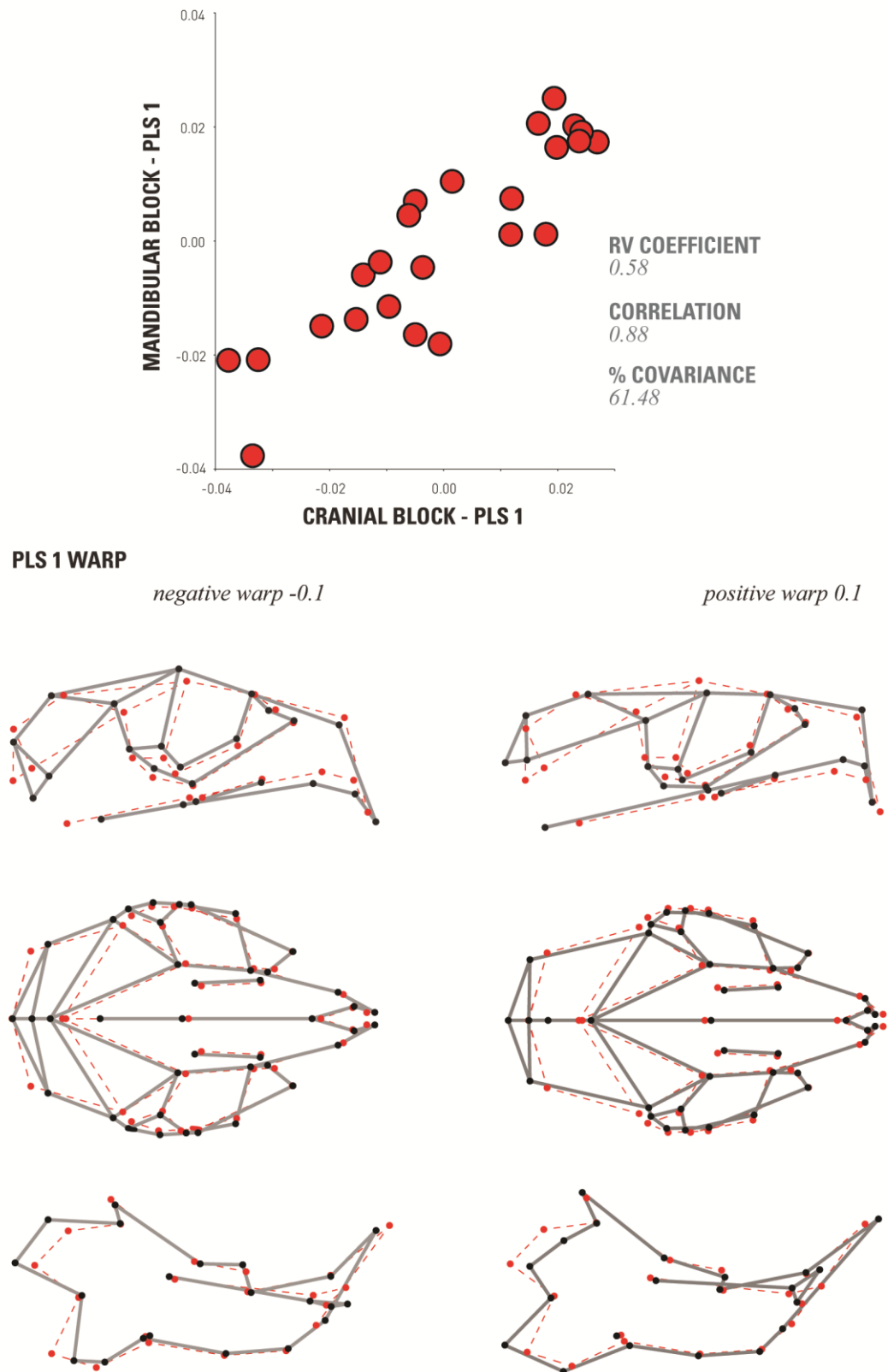


Figure S 4.3.9: Partial least squares analysis of brachymorph crania and mandibles (intra-strain analysis). Insets show wireframes and landmark positions for the positive (0.1) and negative (-0.1) extremes of covariance (61.49% of total covariance) for crania and mandibles for PLS1. Red landmarks and dashed lines depict the mean shape of the sample, black landmarks and lines depict landmark positions at each extreme.

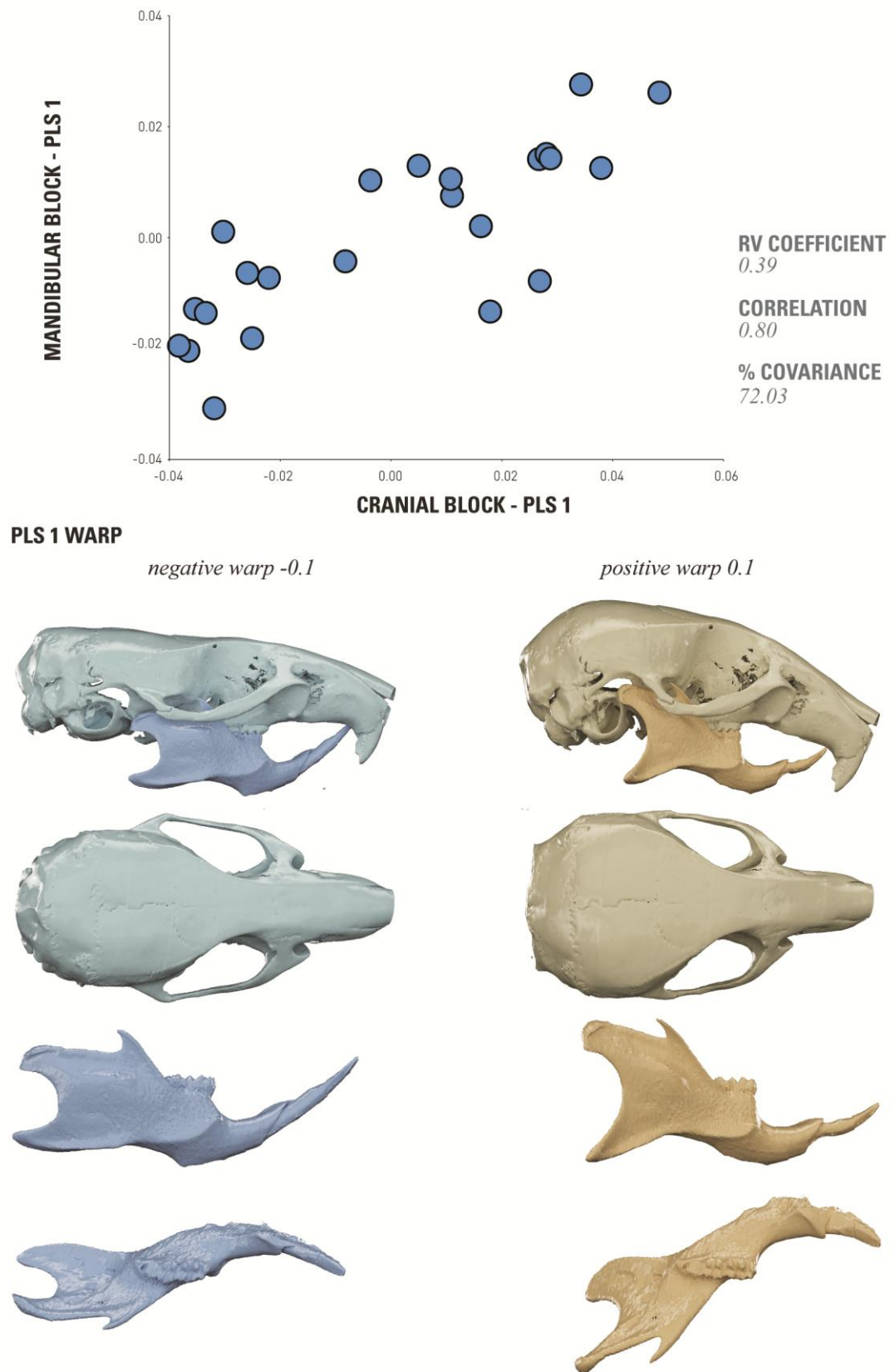


Figure S 4.3.10: Partial least squares analysis of pten crania and mandibles (intra-strain analysis). Insets show warps to the positive (0.1) and negative (-0.1) extremes of covariance (72.03% of total covariance) for crania and mandibles for PLS1.

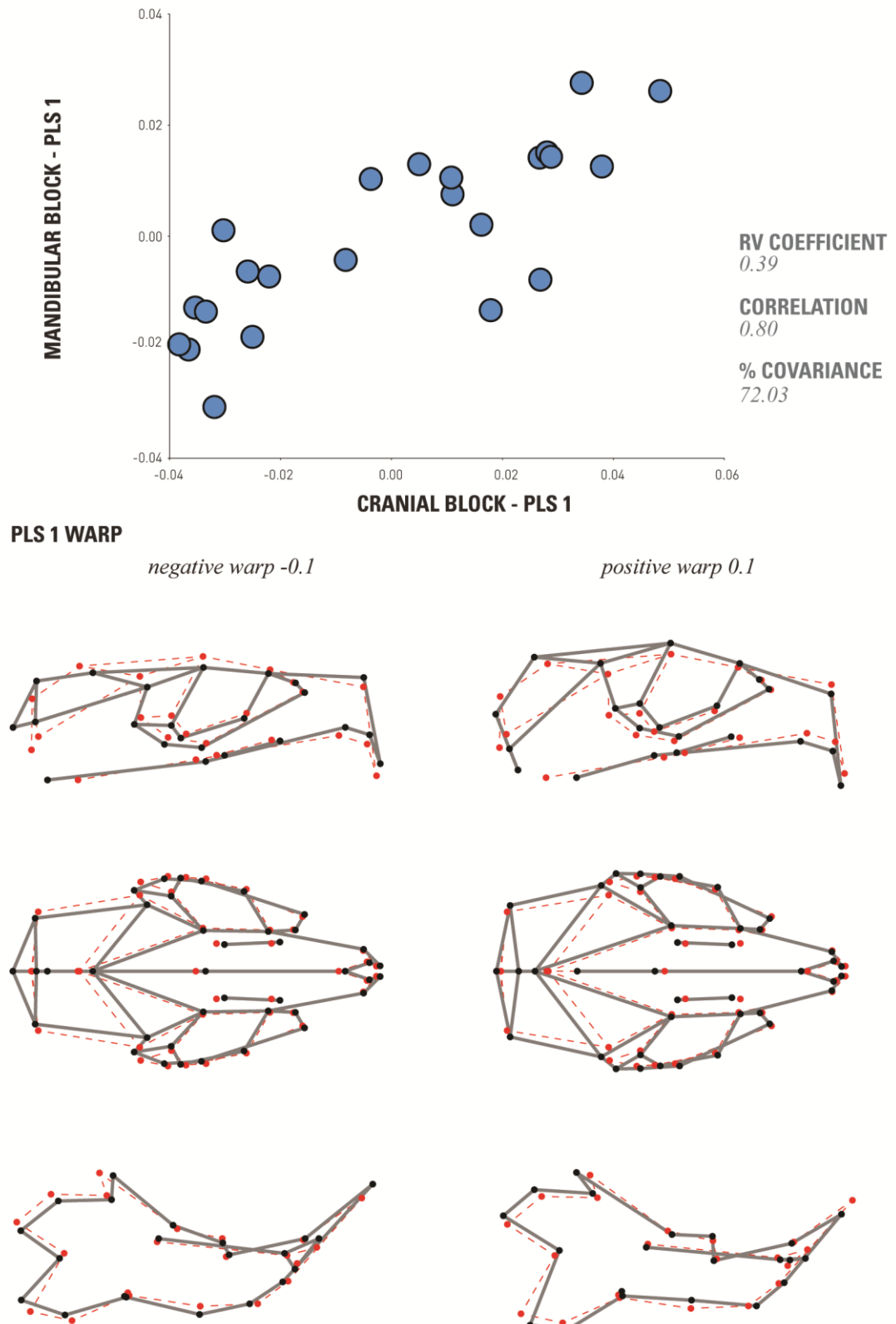


Figure S 4.3.11: Partial least squares analysis of PTEN crania and mandibles (intra-strain analysis). Insets show wireframes and landmark positions for the positive (0.1) and negative (-0.1) extremes of covariance (72.03% of total covariance) for crania and mandibles for PLS1. Red landmarks and dashed lines depict the mean shape of the sample, black landmarks and lines depict landmark positions at each extreme.

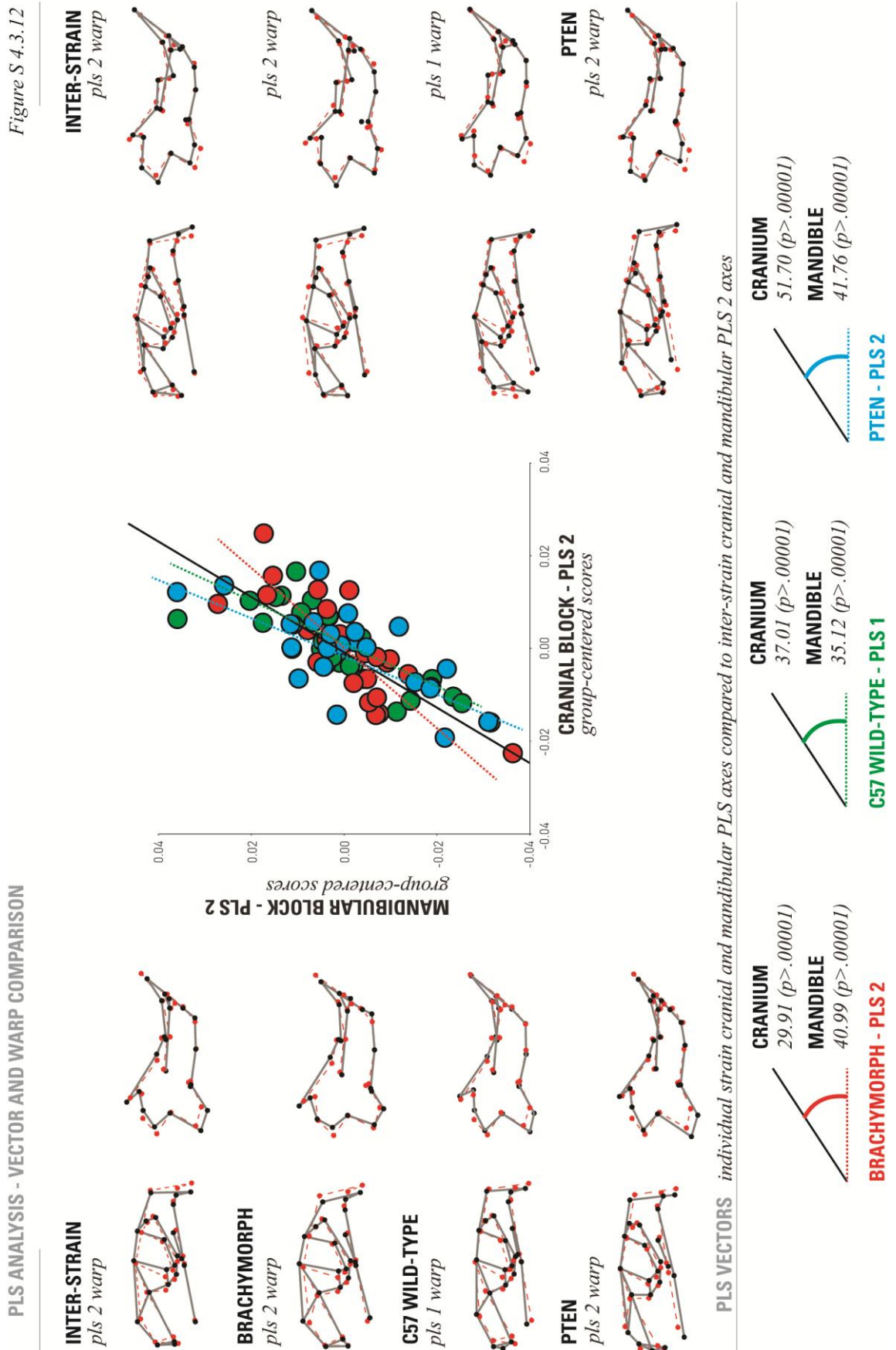


Figure S 4.3.12: Comparison of PLS vectors and warps for the PLS analyses: Insets show wireframes and landmark positions at the positive (0.1) and negative (-0.1) warps along PLS2 of the whole sample; PLS2 of brachymorph strain, PLS2 of PTEN strain, and PLS1 of C57 strain. Red landmarks and dashed lines depict the mean shape of the sample, black landmarks and lines depict landmark positions at each extreme. Graph shows plot of PLS2 of cranial block and PLS2 of mandibular block for inter-strain analysis pooled by group (brachymorph (red markers) C57 (green markers) and PTEN (blue markers)). Black solid line depicts vector for inter-strain analysis, colored dashed lines (brachymorph (red) C57 (green) and PTEN (blue)) depict PLS vectors for PLS analyses of individual strains. PLS vectors are shown to be comparable between inter-strain, brachymorph and PTEN PLS2 analyses and C57 PLS1 analysis.

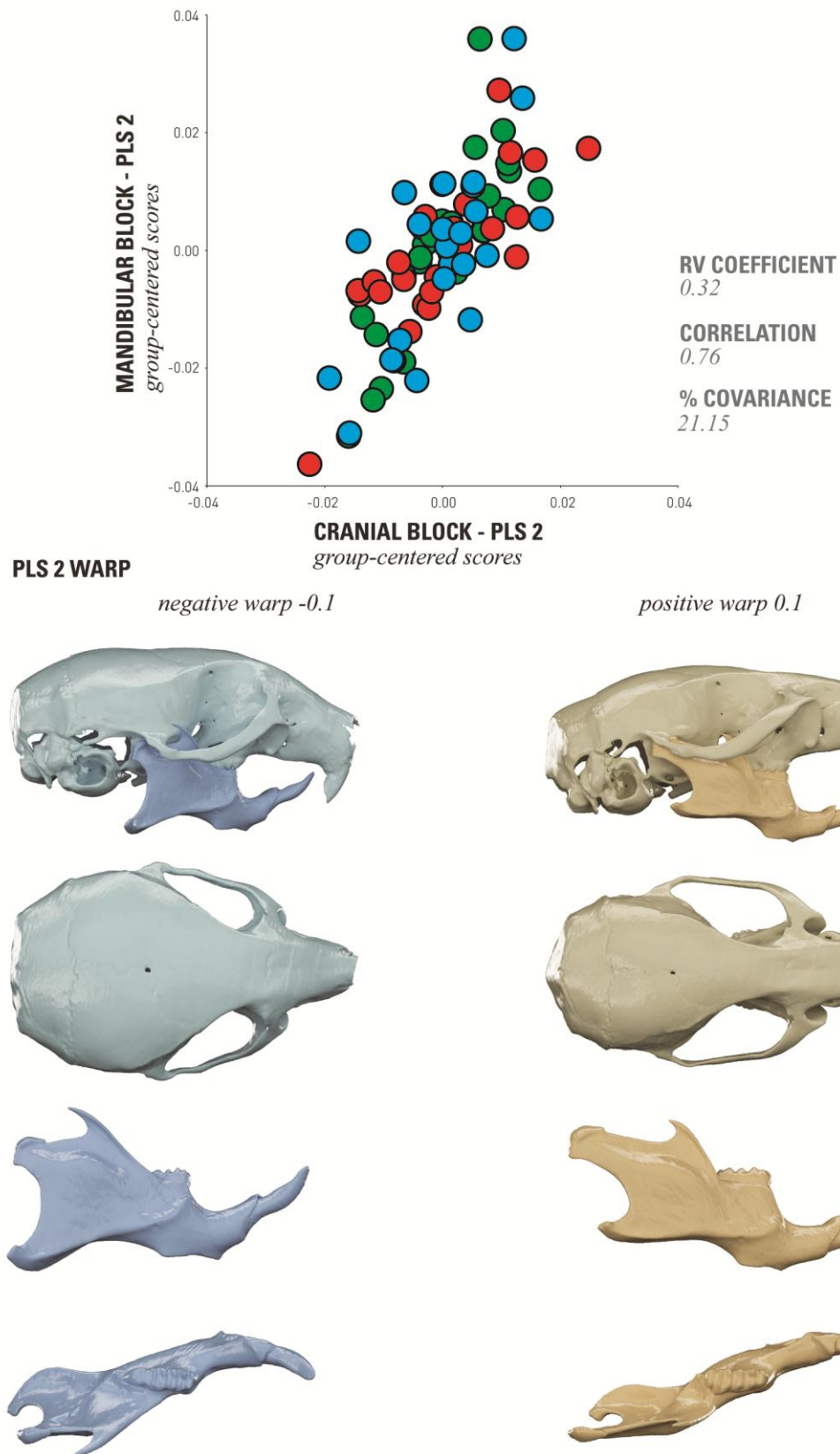


Figure S 4.3.13: Partial least squares analysis (PLS2) of brachymorph (red markers); C57 (green markers) and pten (blue markers) crania and mandibles. Insets show warps to the positive (0.1) and negative (-0.1) extremes of PLS2 covariance (21.15 % of total covariance) between crania and mandibles for the sample as a whole.

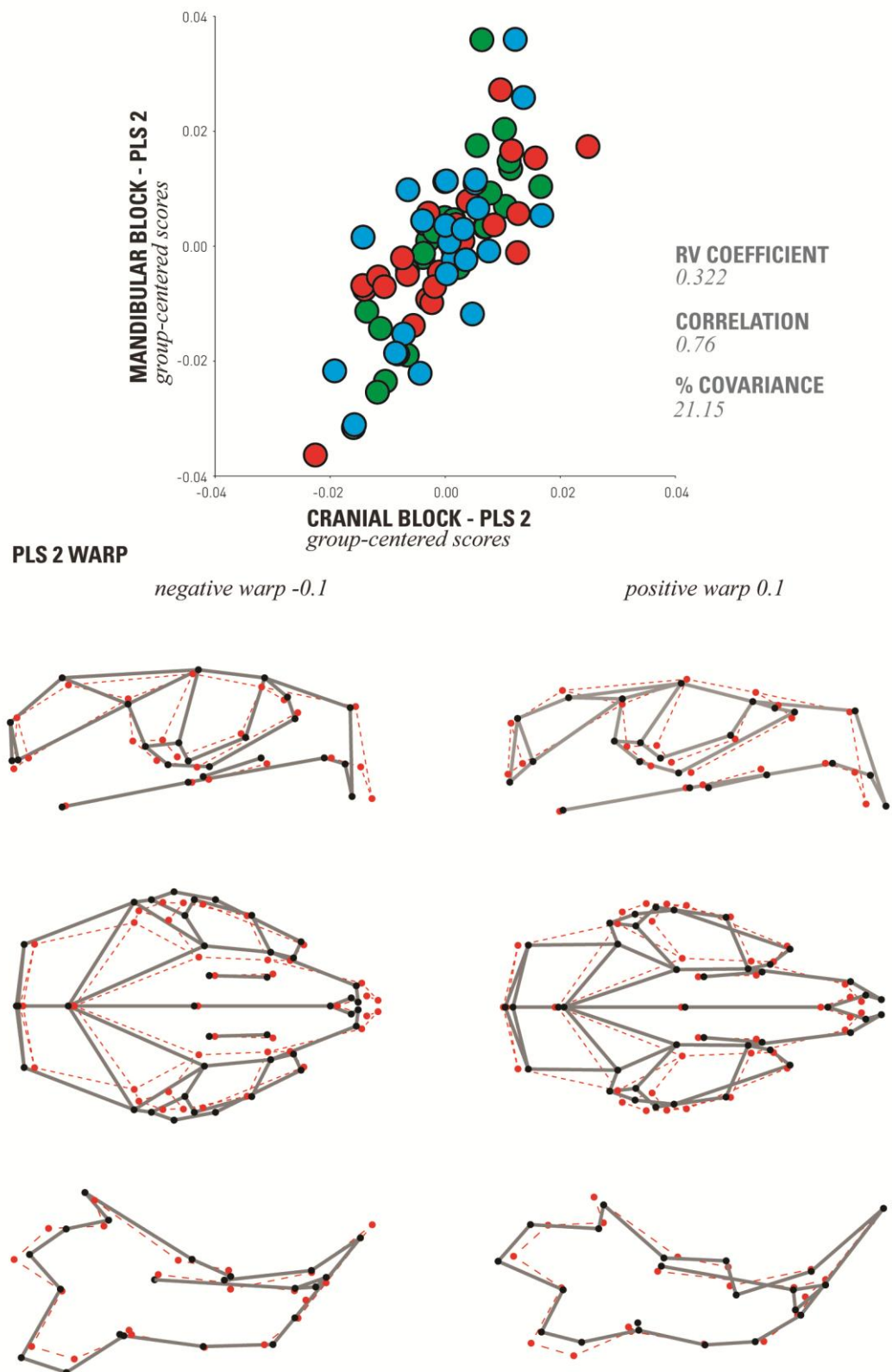


Figure S 4.3.14: Partial least squares analysis (PLS2) of brachymorph (red markers); C57 (green markers) and pten (blue markers) crania and mandibles. Insets show wireframes and landmark positions at the positive (0.1) and negative (-0.1) extremes of PLS2 covariance (21.15% of total covariance) between crania and mandibles for the sample as a whole. Red landmarks and dashed lines depict the mean shape of the sample, black landmarks and lines depict landmark positions at each extreme.

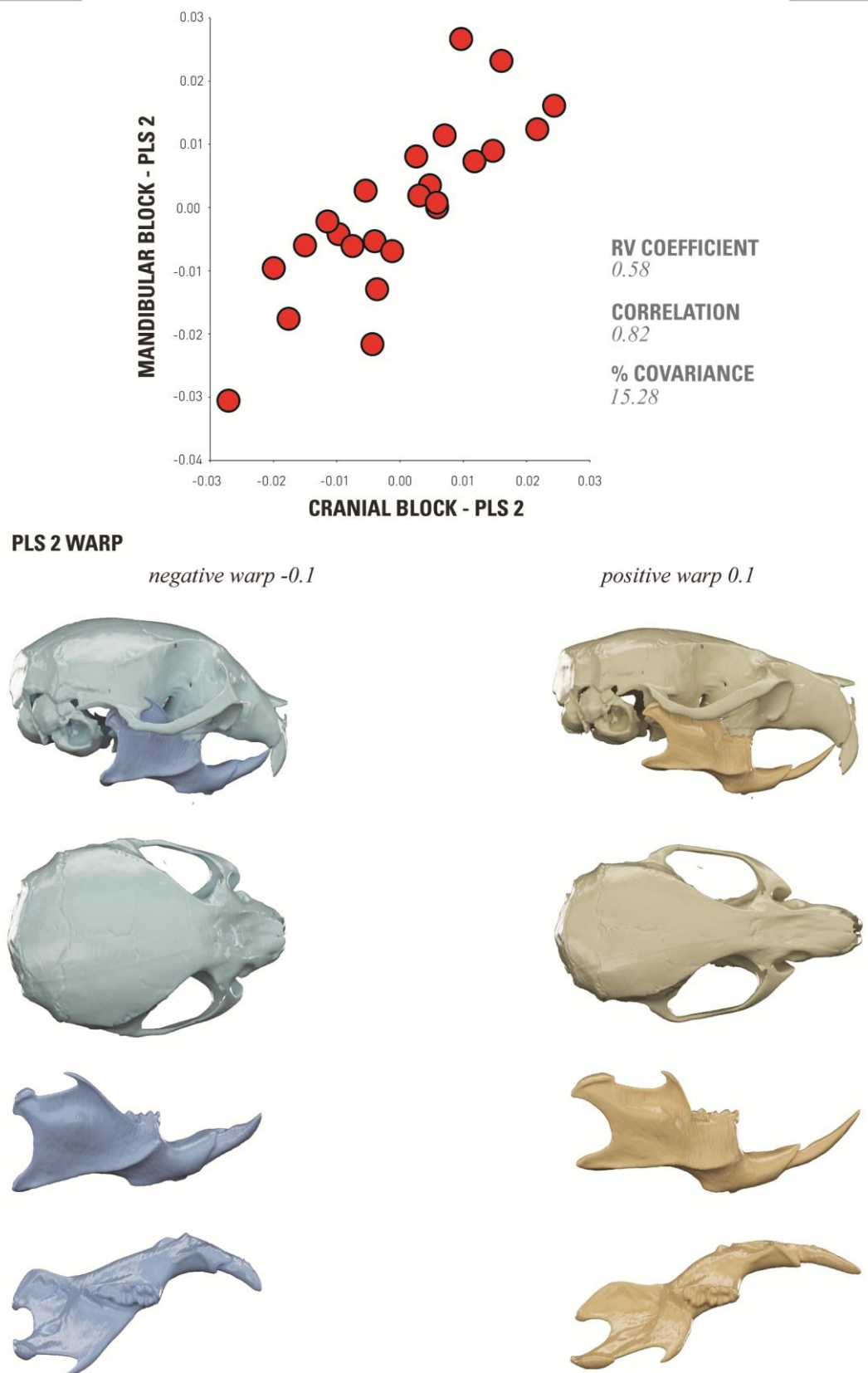


Figure S 4.3.15: Partial least squares analysis of brachymorph crania and mandibles (intra-strain analysis). Insets show warps to the positive (0.1) and negative (-0.1) extremes of covariance (15.28 % of total covariance) for crania and mandibles for PLS2.

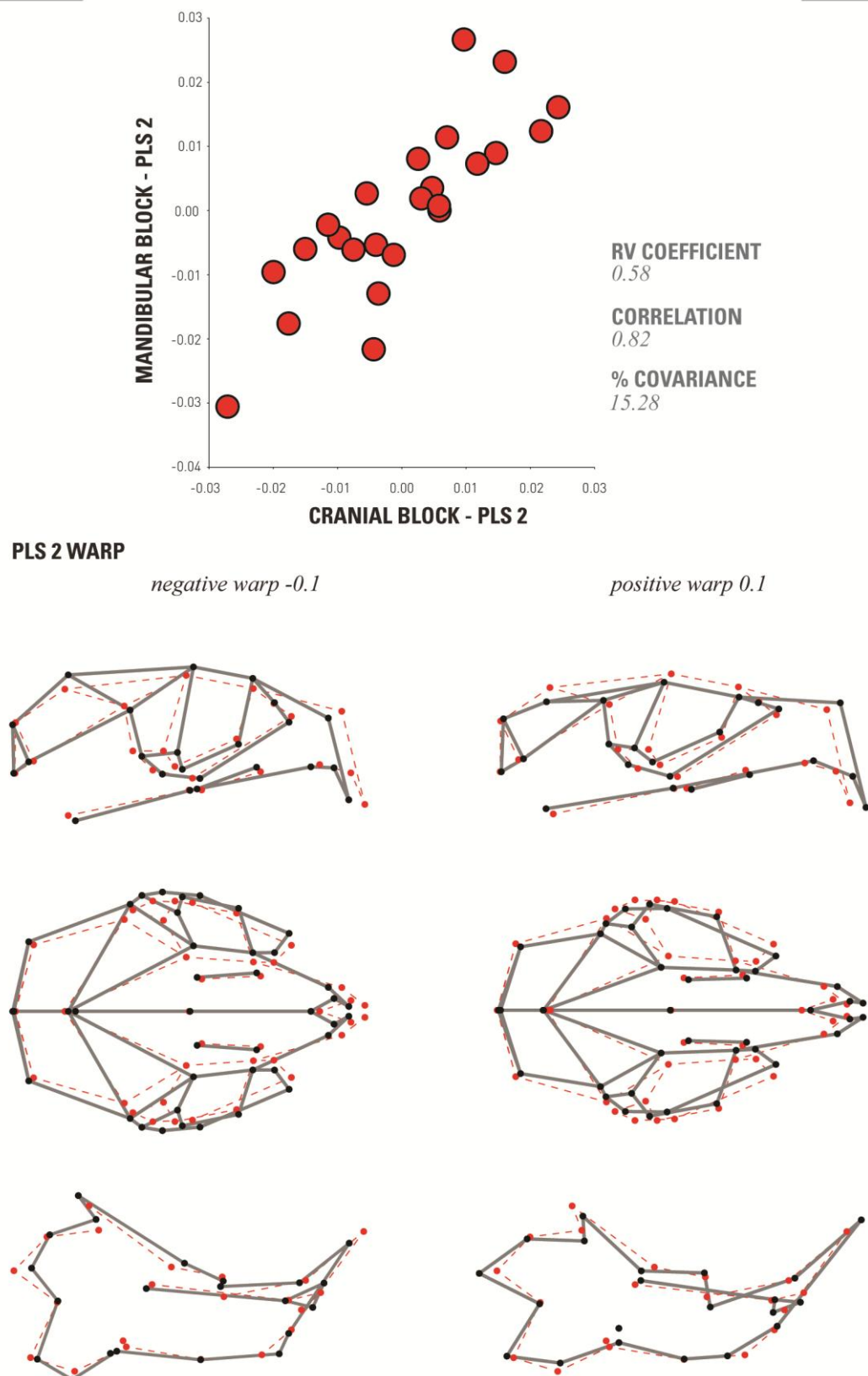


Figure S 4.3.16: Partial least squares analysis of brachymorph crania and mandibles (intra-strain analysis). Insets show wireframes and landmark positions for the positive (0.1) and negative (-0.1) extremes of covariance (15.28% of total covariance) for crania and mandibles for PLS2. Red landmarks and dashed lines depict the mean shape of the sample, black landmarks and lines depict landmark positions at each extreme.

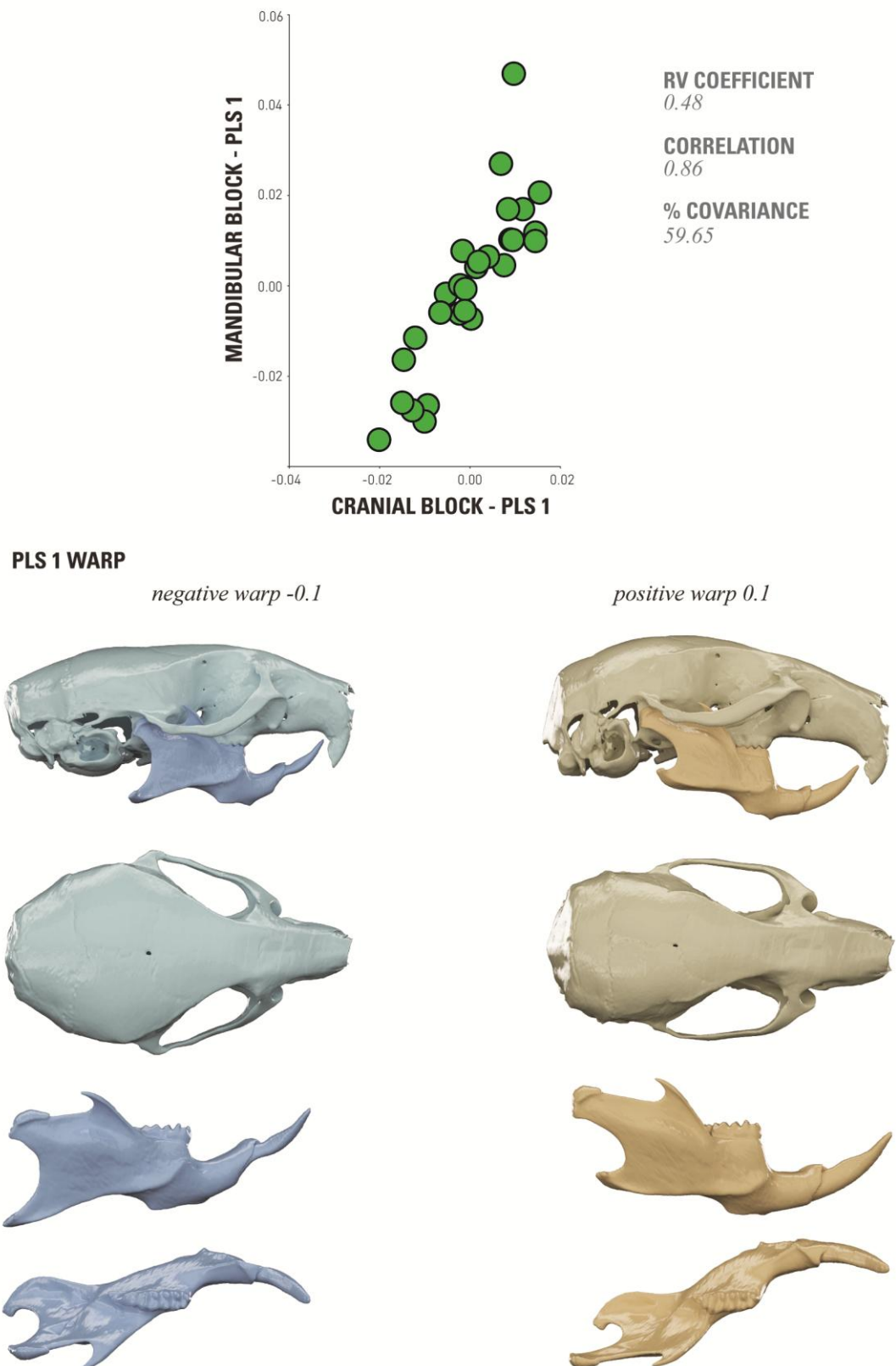


Figure S 4.3.17: Partial least squares analysis of C57 (wild-type) crania and mandibles (intra-strain analysis). Insets show warps to the positive (0.1) and negative (-0.1) extremes of covariance (59.65 % of total covariance) for crania and mandibles for PLS1.

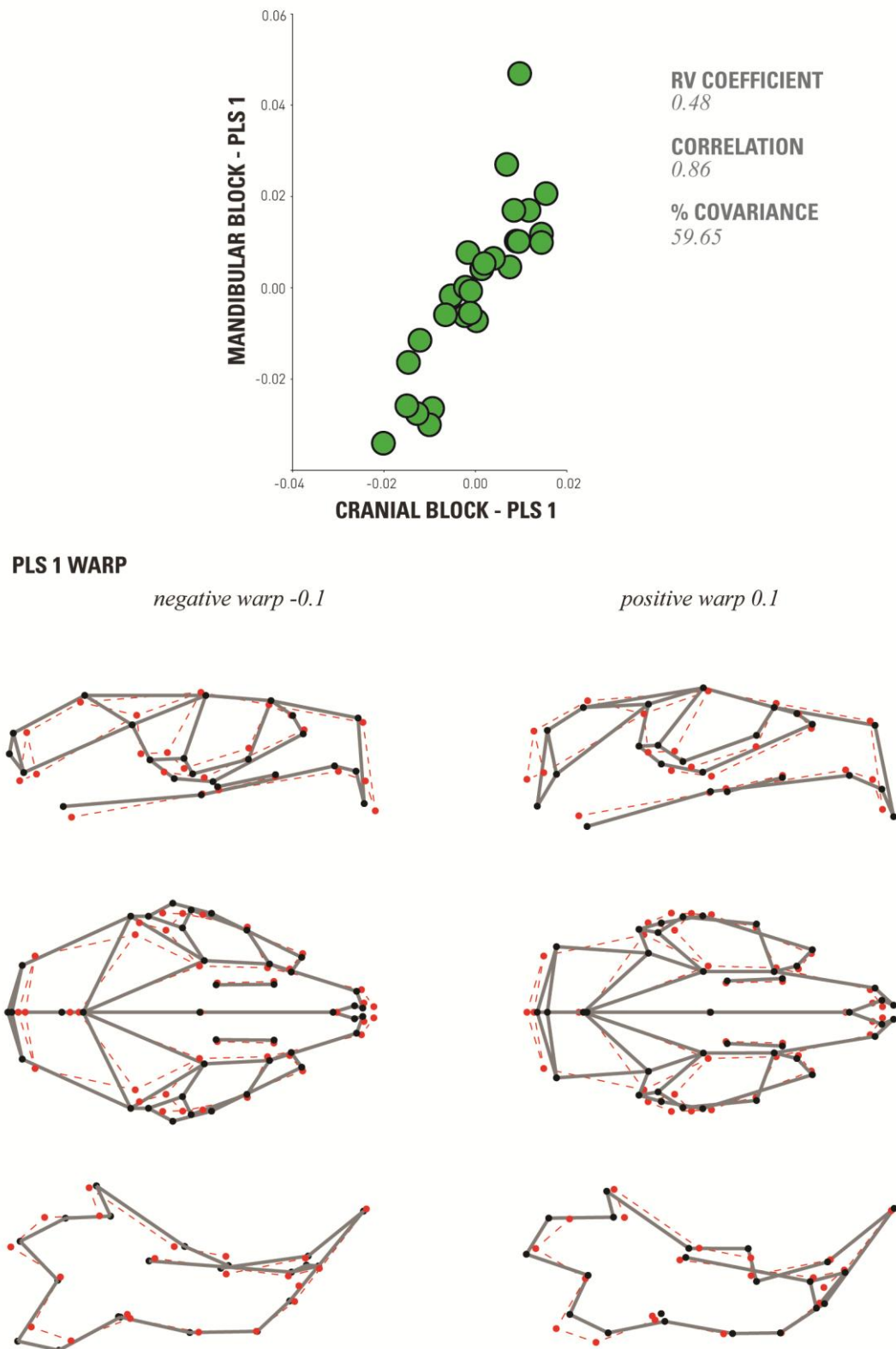
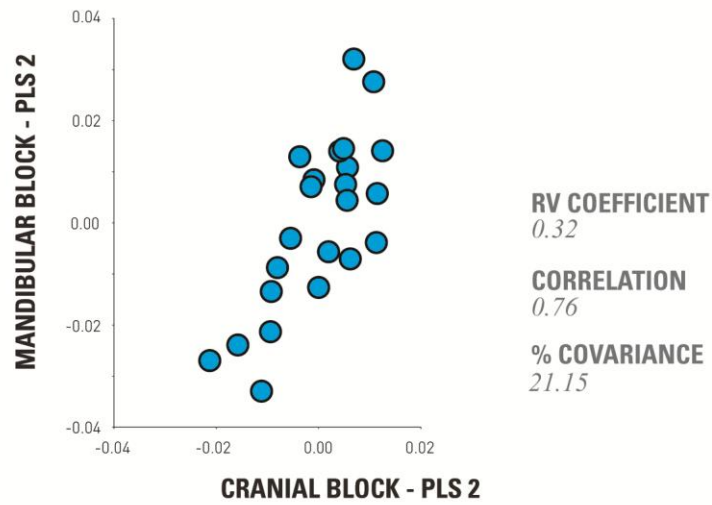


Figure S 4.3.18: Partial least squares analysis of C57 (wild-type) crania and mandibles (intra-strain analysis). Insets show wireframes and landmark positions for the positive (0.1) and negative (-0.1) extremes of covariance (59.65% of total covariance) for crania and mandibles for PLS1. Red landmarks and dashed lines depict the mean shape of the sample, black landmarks and lines depict landmark positions at each extreme.



PLS 2 WARP

negative warp -0.1

positive warp 0.1

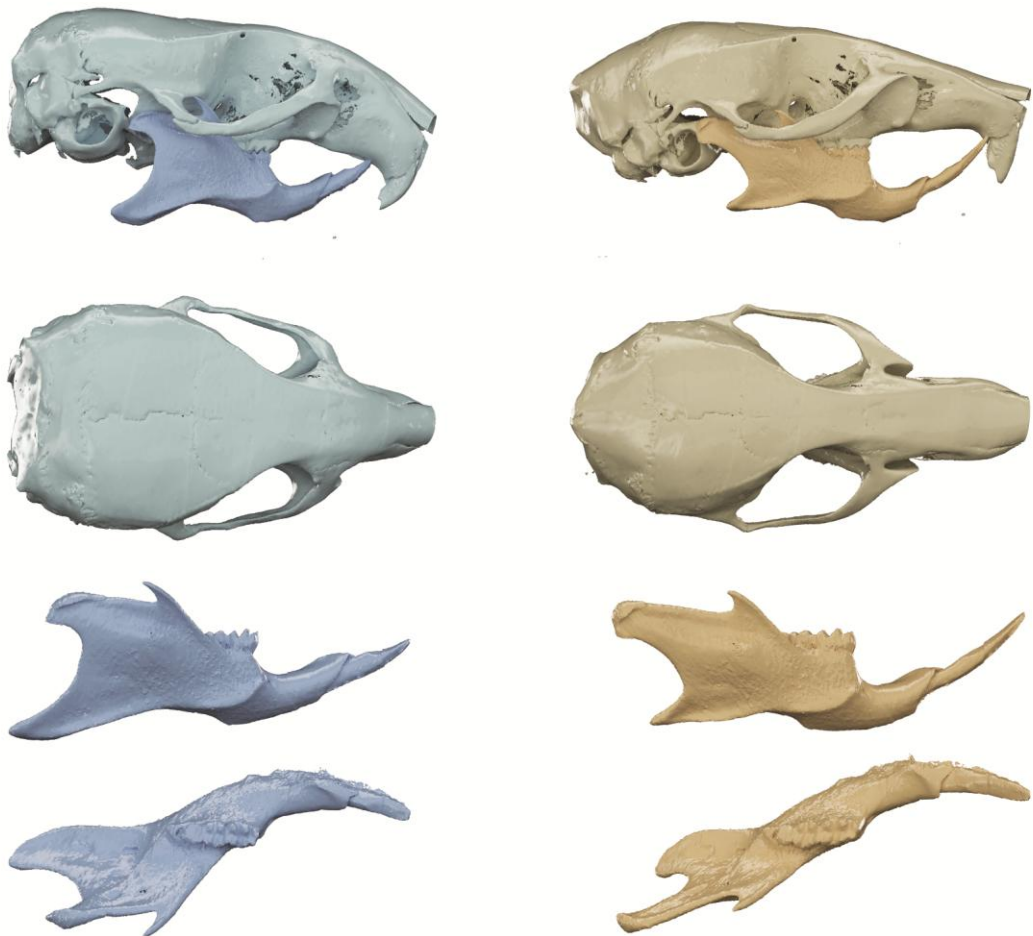


Figure S 4.3.19: Partial least squares analysis of pten crania and mandibles (intra-strain analysis). Insets show warps to the positive (0.1) and negative (-0.1) extremes of covariance (21.15 % of total covariance) for crania and mandibles for PLS2.

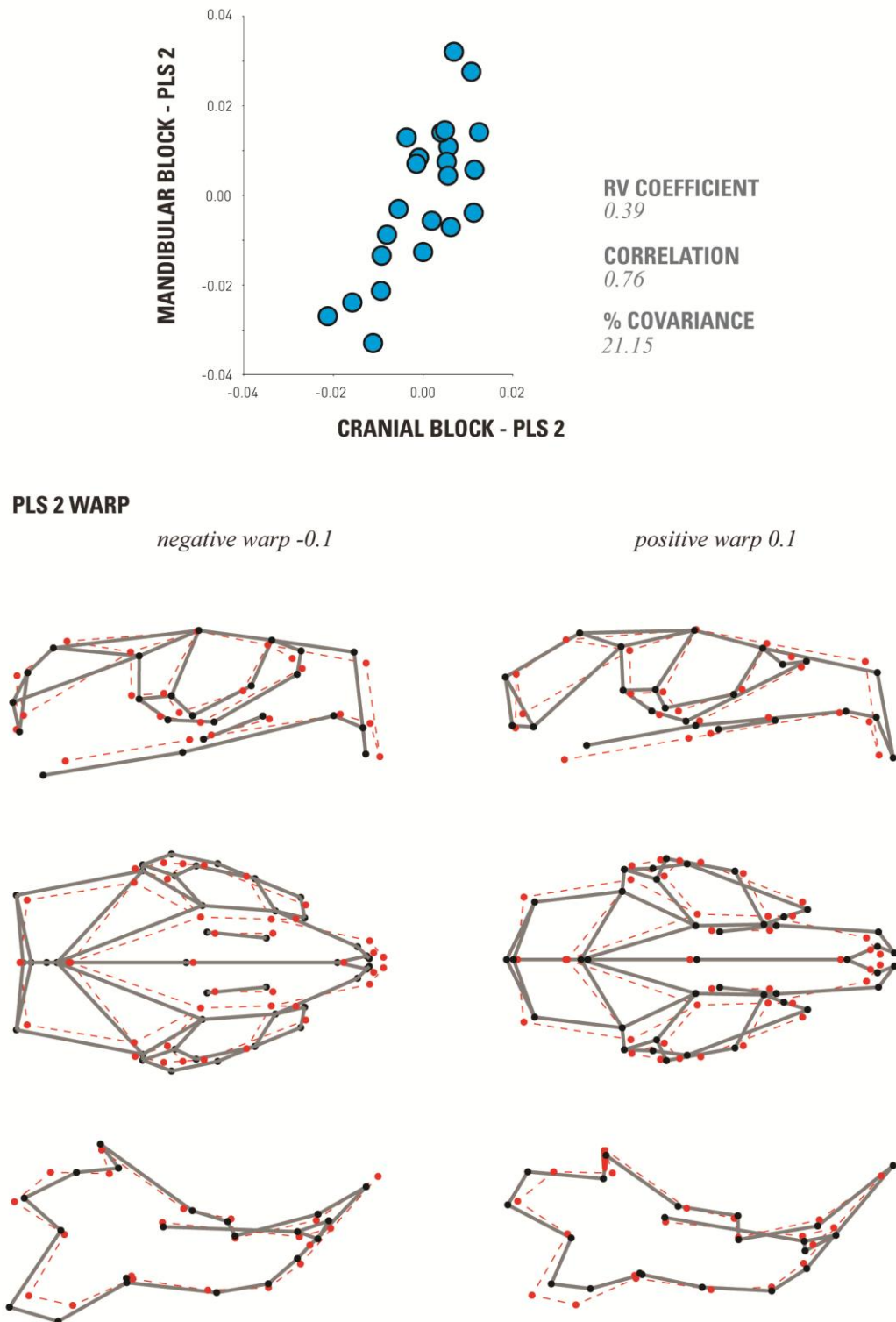


Figure S 4.3.20: Partial least squares analysis of pten crania and mandibles (intra-strain analysis). Insets show wireframes and landmark positions for the positive (0.1) and negative (-0.1) extremes of covariance (21.15% of total covariance) for crania and mandibles for PLS2. Red landmarks and dashed lines depict the mean shape of the sample, black landmarks and lines depict landmark positions at each extreme.

**RV COEFFICIENTS, SINGULAR VALUES AND PAIRWISE CORRELATIONS OF
PLS SCORES BETWEEN CRANIAL AND MANDIBULAR BLOCKS**

Table S 4.3.1

Analysis	PLS axis	RV coefficient	RV coefficient <i>p</i> -value	singular value	singular value <i>p</i> -value	percentage total covariance	correlation	correlation <i>p</i> -value
Inter-strain	PLS 1	0.66	<.0001	0.00072	<.0001	82.66	0.95	<.0001
	PLS 2			0.00028	<.0001	12.16	0.77	<.0001
Inter-strain pooled by group	PLS 1	0.30	<.0001	0.00019	<.0001	69.36	0.73	<.0001
	PLS 2			0.00008	<.0001	14.21	0.74	<.0001
Brachymorph	PLS 1	0.58	<.0001	0.00003	<.0001	69.59	0.88	0.00
	PLS 2			0.00011	0.01	9.02	0.80	0.00
C57 (wild-type)	PLS 1	0.43	<.0001	0.00014	<.0001	57.65	0.86	<.0001
	PLS 2			0.00008	<.0001	17.37	0.73	0.00
Pten	PLS 1	0.35	0.00	0.00037	<.0001	76.69	0.80	<.0001
	PLS 2			0.00012	0.01	8.00	0.85	<.0001

**VECTOR COMPARISON BETWEEN INDIVIDUAL PLS SCORES
AND INTER-STRAIN PLS SCORES FOR CRANIAL BLOCK**

Table S 4.3.2

	Brachymorph cranium				Pten cranium				C57 cranium			
	PLS1		PLS2		PLS1		PLS2		PLS1		PLS2	
	vector	p-value	vector	p-value	vector	p-value	vector	p-value	vector	p-value	vector	p-value
Inter-strain cranium pooled by group PLS1	17.60	< 00001	80.12	0.18	17.22	< 00001	82.69	0.32	68.50	0.00	72.26	0.02
Inter-strain cranium pooled by group PLS2	81.54	0.25	33.18	< 00001	77.37	0.09	55.72	< 00001	41.63	< 00001	86.71	0.66

**VECTOR COMPARISON BETWEEN INDIVIDUAL PLS SCORES AND
INTER-STRAIN PLS SCORES FOR MANDIBULAR BLOCK**

Table S 4.3.3

	Brachymorph mandible				Pten mandible				C57 mandible			
	PLS1		PLS2		PLS1		PLS2		PLS1		PLS2	
	vector	p-value	vector	p-value	vector	p-value	vector	p-value	vector	p-value	vector	p-value
Inter-strain mandible pooled by group PLS1	21.41	< 00001	80.40	0.21	23.75	< 00001	74.71	0.05	74.54	0.05	85.89	0.60
Inter-strain mandible pooled by group PLS2	78.28	0.13	44.42	< 00001	72.33	0.02	41.62	< 00001	33.98	< 00001	85.13	0.53

CHAPTER 5 FUNCTIONAL MAINTENANCE AND VARIATION IN CRANIAL LENGTH OF THE MOUSE MASTICATORY SYSTEM

5.1 INTRODUCTION

The concept of adaptive evolution by selection on heritable variation underpins every evolutionary analysis of form and function (West-Eberhard, 2003). The evolution of a novel trait by means of natural selection is initiated by the recurrent development of a new environmentally or genetically induced phenotypic variant. For such adaptive evolution to succeed and produce a functionally viable phenotype, particularly in the case of a complex structure, the complex must display both integration and semi-independence (West-Eberhard, 2003, Lewontin, 1978). Semi-independence of subsets of the whole may allow for variance to occur in one region without deleterious effects on others, whereas integration may lead to coordinated adaptation of the whole in response to isolated variance such that overall integrity is maintained.

Variation in regions of a skeletal complex is not however confined to those initiated via genetic or environmental changes. The craniofacial skeleton is a complex dynamic structure that is continually required to adapt to changes in regions of its form. The skull is both subject to both an elaborate pattern of morphological change during ontogeny and the requirement to adapt and respond to its internal and external environment during postnatal life. As vital performances such as mastication must be reliably and effectively achieved in spite of any variation in form of elements of the functional system, viability of the complex is reliant on the ability to manage any regional modifications. Clues to how the skull achieves the maintenance of coordinated size and shape relationships and thus appropriate functional performance when faced with phenotypic variation may be found in the underlying arrangement and relationships between parts of the whole.

Any complex structure may reasonably be considered a composite of numerous highly connected subsets, termed modules, which are recognisable and relatively distinct from other regions (Schlosser and Wagner, 2004, Wagner, 1996, Wagner et

al., 2007a, Klingenberg, 2008, Klingenberg, 2005a). While there is little agreement on how isolated a character must be to be counted as a module (Raff and Raff, 2000, Hansen, 2003, Griswold, 2006), modules share the defining quality of having more tight internal connections than external connections with other regions (Cheverud, 1996b, Raff, 1996, Wagner, 1996, Wagner and Altenberg, 1996, Wagner et al., 2007a, Klingenberg, 2008). Internal connections termed integration, may be developmental, functional, genetic and/or evolutionary in origin and nature (Cheverud, 1996b, Klingenberg, 2008). Modularity however is not a stand-alone concept. While integration within modules may be high, differing levels of connectivity within and between regions gives rise to a hierarchical network of interactions (Klingenberg, 2005a).

Integration, manifest as the covariation of morphological traits such that variation in one region is associated with variation in another connected region, is necessary for complex skeletal systems such as the skull to maintain appropriate size and shape relationships when faced with phenotypic variation (West-Eberhard, 2005, Lewontin, 1978). There is however a question regarding whether such strong integration is detrimental to the evolvability of a skeletal structure or organism. While a modular arrangement of parts may allow mutation or variation to occur in one element without deleterious effects on other regions, strong integration may reduce the probability that a mutation will have beneficial effects on all characters. Conversely, modularity may hamper evolvability by reducing mutational target size (Wagner, 1996, Wagner and Altenberg, 1996, Hansen, 2003), and there is the potential for pleiotropy or global integration to increase evolvability by having beneficial effects on two or more characters (Griswold, 2006). Strong cranial integration revealed in previous work was found to preserve appropriate size and shape relationships between the upper and lower jaws such that suitable occlusion is maintained when variation occurred in one region (see Chapter 5: Craniomandibular integration and adaptive plasticity in the murine skull). Such an integrated response affecting a suite of characteristics throughout the complex however may have implications for numerous functions.

One method of assessing the ability of the craniomandibular complex to maintain morphological and functional coordination while shape changes occur in both the

cranium and mandible to is examine these parameters during ontogeny. A developing individual must retain cohesion of the craniomandibular complex, meeting and maintaining functions such as the ability to process food despite often profound changes in both size and shape of functional components of the complex (Koehl, 1996). Not only must a degree of function be maintained, but the required performance ability of a juvenile may often be comparable to adults of the species (Herrel and Gibb, 2006, La Croix et al., 2011a, La Croix et al., 2011b, Monteiro et al., 1999). A number of authors have assessed the functional performance of the skull during ontogeny (La Croix et al., 2011a, La Croix et al., 2011b, Tanner et al., 2010, Binder and Van Valkenburgh, 2000, Christiansen and Adolfssen, 2005) with some reporting maintenance of measure of functional performance despite ongoing changes in morphology. La Croix et al (2011b) report an early achievement of adult mechanical advantage measurements in juvenile coyotes, with maintenance of the proportions of jaw in- and out- levers found throughout a developmental period in which dramatic changes in the size and shape of both the cranium and mandible occur (La Croix et al., 2011b, La Croix et al., 2011a). Adult length equivalence was found for the jaw out-lever at 12 weeks and the muscle in-lever at 21 weeks, whilst full skull and feeding performance maturity was not reached until approximately 36 weeks (La Croix et al., 2011b). Maintenance of mechanical advantage of the masseter muscle throughout ontogeny is also reported in the spotted hyena, with mechanical advantage of the temporalis muscle in this species found to reach maturity prior to skull shape maturity (Tanner et al., 2010). Such early maturity of mechanical advantage may be essential for juveniles in accomplishing adequate feeding performance during the challenging period immediately after weaning (La Croix et al., 2011b).

While functional performance during ontogeny has received recent attention, the potential of the system to maintain function while shape changes associated with development or evolution occur remains largely unexplored. This study aims to test the potential of the skull to maintain one measure of function when one parameter of form is altered early on in development. A model sample is employed, consisting of two mutant *Mus musculus* strains and one control wild-type mouse of the same background strain (C57/BL/6J) as the two mutants. Both mutant strains have a

known specific mutation affecting chondrocranial growth. The *pten* strain has a cranium increased in length when compared to the control that results from the crossing of mice with floxed *pten* alleles with transgenic C57/BL/6J mice, the consequence of which is an increase in collagen II growth and proliferation (Hallgrímsson et al., 2007). In the brachymorph strain (C57/BL/6J background, the Jackson Laboratory, Bar Harbor, ME, USA) an autosomal recessive mutation in the phosphoadenosine-phosphosulphate synthetase 2 (*Paps2*) gene (Kurima et al., 1998) results in dramatic reduction in the growth of cartilage (Lane and Dickie, 1968, Orkin et al., 1976, Kurima et al., 1998, Ford-Hutchinson et al., 2005, Hallgrímsson et al., 2006) decreasing cranial length when compared to the control. As both *pten* and brachymorph mutations affect cartilage growth alone, direct phenotypic changes are largely confined to the cranium and any changes seen in the morphology of the mandibles of these two strains when compared to the control can reasonably be assumed to be due to functionally or developmentally integrated plastic adaptation. This sample may therefore be exploited to assess the potential of the craniomandibular complex to maintain functional performance via integrated plastic adaptation when faced with variation in the size and shape of constituent parts of the whole.

Previous work shows that the mandibles of the two mutant strains plastically adapt to maintain size and shape relationships with the upper jaw, preserving appropriate occlusion (see Chapter 5: Craniomandibular integration and adaptive plasticity in the murine skull). The brachymorph mandible is thus decreased in length and the *pten* mandible increased in length when compared to the control. While such tight integration within the skull may be beneficial in terms of achieving appropriate occlusion and thus support for mastication, variation in length of the two mutant strains may influence other parameters of the masticatory systems such as the ability to produce an effective bite at the dentition.

One method of assessing the masticatory functional potential of the craniomandibular complex is to model the jaw as a lever and calculate the mechanical advantage of the system. Jaws act as third class levers, with the input force crossing the lever between the pivot and the point at which an output force is produced. The temporomandibular joint acts as a pivot with the masticatory muscles

supplying the input force and the dentition acting on food providing the output force (Smith and Savage, 1956, Crompton and Hiiemae, 1969, Greaves, 1974, Hildebrand, 1988). Analysis of the lever arm system of the skull, and the relationship between the input and output levers allows the calculation of mechanical advantage. Mechanical advantage is a measure of the efficiency of the system, and thus the amount of force transferred through the lever (Anderson, 2008). Proportional to the ratio of the in-lever (distance from the fulcrum to the point at which force is applied to the lever) to the out-lever (distance from the fulcrum to the point where the force is applied by the lever), mechanical advantage is a one useful method of assessing the underlying performance capabilities of functional morphologies.

The potential of the craniofacial complex to plastically adapt in a correlated manner such that adequate functional performance is maintained is investigated via the calculation of mechanical advantage of the masticatory system. The sample utilised in this study models variance in cranial length, and previous investigation has shown mandibular length in the three strains corresponds to cranial length (see Chapter 5: Craniomandibular integration and adaptive plasticity in the murine skull). In functional terms a short craniomandibular complex confers a reduced distance between the temporomandibular joint (TMJ) and the bite point at the dentition, a decrease in the length of the out-lever, and an increase in mechanical advantage and thus the production of force at the dentition. Conversely a long craniomandibular complex will give increased distance between the TMJ and the bite point at the dentition, an increase in out-lever length, and a reduction in mechanical advantage and force production at the dentition (Reduker, 1983). As mechanical advantage is a ratio of the in- and out- lever however, efficiency of the system at producing force at the dentition is also determined by the positioning and length of the in-lever, and therefore the anatomy and location of masticatory muscle origins and insertions. Muscles whose line of actions pass close to the TMJ will have a shorter in-lever length and thus will give a reduced mechanical advantage in comparison to muscles whose line of action are distant from the pivot and therefore a relatively long in-lever conferring a larger mechanical advantage (Smith and Savage, 1956). Consequently, coordinated plastic adaptation throughout the craniomandibular complex in response to mutational variation in length has the potential to compensate for changes to jaw

out-lever lengths. Alterations to regions such as muscle attachment sites and the mandibular condyle, and to phenotypic characteristics such as width and height of the skull, have the capacity to modify in-lever lengths. This study assesses whether in an integrated complex system such as the skull, modification to the form of one region early on in development initiates a suite of integrated adaptive responses in other regions which may not only retain the integrity of the overall structure in terms of form, but could also counterbalance any changes to functionally significant parameters such that performance and fitness of the whole is maintained.

5.2 MATERIALS AND METHODS

5.2.1 Sample

A sample of 71 *Mus musculus* individuals was analysed, composed of one wild-type and two mutant strains, all from similar genetic backgrounds (C57BL/6J). Mutations in both the brachymorph and pten strains cause perturbations that predominantly influence chondrocranial growth early on in the development (Hallgrímsson et al., 2006). 25 wild-type, 24 brachymorph and 22 pten specimens were analysed, micro-CT scans of which were provided by Benedikt Hallgrímsson, University of Calgary.

The brachymorph mutant (C57/BL/6J background, the Jackson Laboratory, Bar Harbor, ME, USA) have a relatively short-faced morphology that results from an autosomal recessive mutation in the phosphoadenosine-phosphosulfate synthetase 2 gene (*Paps2*) (Kurima et al., 1998, ul Haque et al., 1998). This gene mutation results in an extracellular matrix alteration that leads to a dramatically reduced growth of cartilage, and thus all skeletal elements that rely upon cartilage are abnormally small (Hallgrímsson et al., 2006, Kurima et al., 1998, Orkin et al., 1976, Lane and Dickie, 1968, Ford-Hutchinson et al., 2005). As the growth of dermatocranial elements does not directly depend upon cartilage growth in the skull the direct effects of this mutation should be confined to the chondrocranium (Kaufman and Bard, 1999, Hallgrímsson et al., 2006).

The Pten mutant has a relatively long-faced morphology, resulting from the crossing of mice with floxed Pten alleles with transgenic mice (C57BL/6J background) expressing Cre recombinase under control of the relatively cartilage-specific *Col2al* gene (Ovchinnikov et al., 2000, Hallgrímsson et al., 2007). *Pten* negatively regulates phosphatidylinositol 3' kinase signalling pathways responsible for controlling cell proliferation and size as well as differentiation and survival (Sansal and Sellers, 2004). In *Pten*^{flox/flox} mice crossed with *Col2al*-Cre mice the negative regulation of the phosphatidylinositol 3' kinase signalling pathway is blocked, and thus growth and proliferation specific to type II collagen is amplified and chondrocranial bone

growth increased (Hallgrímsson et al., 2007). Only homozygous (Cre fl/fl) individuals were included in the sample.

5.2.2 Data Acquisition

5.2.2.1 *Processing and preparing data*

Micro-CT data was processed using Amira v5.2 image analysis software (VisageImaging, 2008). Automatic thresholding was used to capture the full geometry of each individual, and subsequent manual segmentation was conducted to create individual cranial and mandibular surfaces for each specimen. Cranial and mandibular surfaces were re-orientated and aligned such that incisal occlusion was met. Realignment was carried out in Amira v5.2 (VisageImaging, 2008) initially by means of the placement of two sets of three-dimensional landmarks onto the surfaces, with corresponding landmarks on mandibular and cranial surfaces. A landmark surface warp was performed, aligning the two landmark sets and thus the two surfaces. Following this alignment process fine manual reorientation was conducted to ensure that in each individual the mandibular condyle was in contact with the articular surface of glenoid fossa and that incisor tips were in direct occlusion. All subsequent methods were applied to only the right hand side of the craniomandibular skeleton.

5.2.2.2 *Lever arm data collection*

A traditional approach to assessing cranial masticatory function is to model the jaw as a lever, calculating mechanical advantage as ratio of two levers; the jaw out-lever and the muscle in-lever (Thomason, 1991b, Tanner et al., 2010, Greaves, 2000, Radinsky, 1985a, Davis, 1961, Turnbull, 1970, Bramble, 1978, Greaves, 1982). Here

mechanical advantage is calculated as a ratio of these levers for three key masticatory muscles; superficial masseter, deep masseter and temporalis.

5.2.2.3 *Muscle in-lever*

The muscle in-lever (MiL) is calculated as the perpendicular distance from the centre of the mandibular condyle (the fulcrum) to the muscle force vector (MFV). This distance is also known as moment-arm (Flanagan, 2014)

Muscle force vector is a vector passing from the muscle insertion on the mandible to the muscle cranial origin. Three muscle force vectors (MFV), and thus three muscle in-levers are calculated for each muscle based upon three lines of action; anterior, posterior and centroid (**Figure 5.2.1**). The anterior MFV (MFVa) is the vector from the anterior border of the muscle insertion to the anterior border of the muscle origin; the posterior MFV (MFVp) is the vector from the posterior border of the muscle insertion to the posterior border of the muscle origin and the central MFV (MFVc) the vector from the centroid of the muscle insertion to the centroid of the muscle origin (**Figure 5.2.1**).

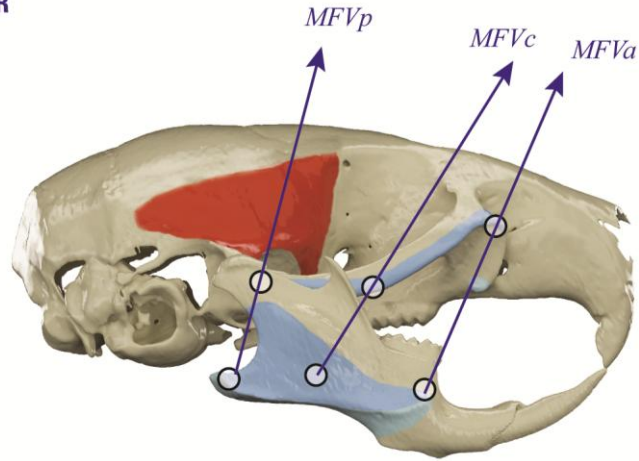
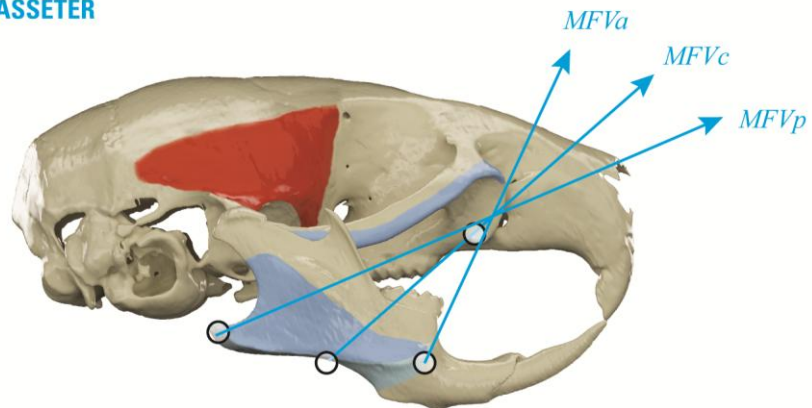
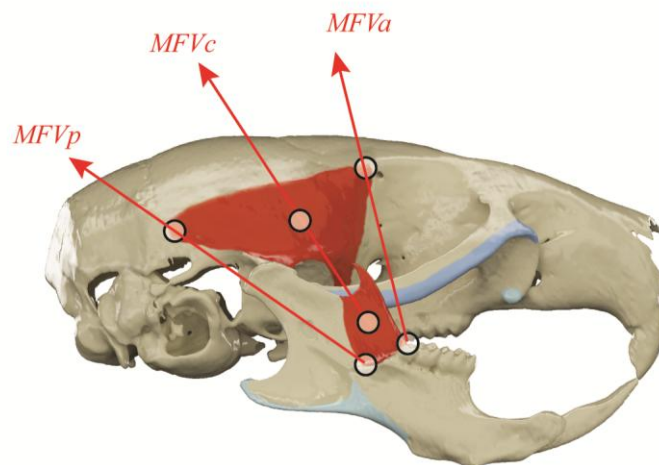
DEEP MASSETER**SUPERFICIAL MASSETER****TEMPORALIS**

Figure 5.2.1: Depiction of muscle force vectors determined from attachment sites for three key masticatory muscles. An anterior (MFV_a), centroid (MFV_c) and posterior (MFV_p) muscle force vector is established from origin and insertion sites for the deep masseter (dark blue); superficial masseter (pale blue) and temporalis (red).

Muscle origin and insertion centroids were calculated based upon methods reported in Davis et al (2010). In the present study cranial and mandibular OBJ surface files were imported into 3DStudioMax (Autodesk, 2013) and attachment areas defined based upon anatomical knowledge from dissection and contrast-enhanced micro-CT reconstruction of *Mus musculus* masticatory anatomy (Baverstock et al., 2013). Surface polygons pertaining to each attachment area were selected and isolated, such that an individual mesh one polygon in depth was created for each origin or insertion. Six attachment areas (superficial masseter origin; superficial masseter insertion; deep masseter origin; deep masseter insertion; temporalis origin; temporalis insertion) were saved as individual STL surface files for each specimen. Attachment surface files were imported into AreaCentroid (Matlab program (Mathworks); Area_Centroids_From_STL, available upon requests) where the centroid of each muscle attachment was calculated. Three dimensional (3D) coordinate outputs describing each area centroid were formatted such that they could be imported into Amira v5.2 as six 3D landmarks from which 3D linear measurement and angles could be gathered.

In order to calculate muscle in-levers, three dimensional linear measurements and angles were collected in Amira v5.2. Measurement of the length between the centre of the condyle and the muscle insertion (anterior, posterior or centroid), and the angle (a) between the muscle insertion (anterior, posterior or centroid) and relevant MFV allows calculation of the MiL via trigonometry (**Figure 5.2.2**).

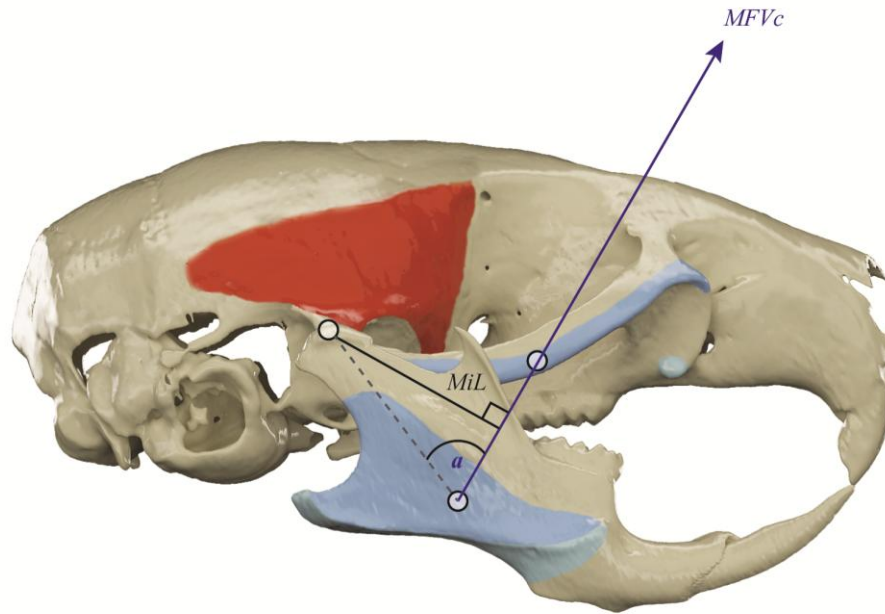


Figure 5.2.2: Calculation of muscle in-lever. Spherical points identify the fulcrum (centre of mandibular condyle), and the centroid of deep masseter's origin and insertion. MFV_c is the centroid line of action (muscle force vector) for the deep masseter. The muscle in-lever length (MiL) for the centroid line of action for the deep masseter is the perpendicular distance from the fulcrum to the MFV_c . MiL may be calculated via trigonometry by establishing the distance from the fulcrum to the centroid of the deep masseter's mandibular insertion; and the angle (a) between the latter line and the MFV_c .

5.2.2.4 *Jaw out-lever*

The jaw out-lever (JoL) is calculated as the perpendicular distance from the centre of the mandibular condyle (the fulcrum) to the bite force vector (BFV).

The BFV is approximated as a vector perpendicular to the occlusal plane (OP) that passes through the tip of the mandibular incisor. **Figure 5.2.3** illustrates a two-dimensional calculation of the JoL, whereby the length CI and angle i can be measured. As both the OP and JoL are perpendicular to the BFV angle ii and angle i are equivalent, and as a consequence length CI and angle ii are known lengths and the JoL may be calculated using trigonometry. However this method makes the assumption of a two dimensional system and does not account for the offset of length CI and the OP in the mediolateral third dimension.

To account for this difference in plane four 3D landmarks were placed on the mandible (**Figure 5.2.4**). These landmarks provide the three dimensional coordinates for the calculation of three 3D lengths, *length ac*; *length bc*, and *length db*. Angles between planes were calculated using the dot product:

$$\Theta = \arccos(\mathbf{n} \cdot \mathbf{m} / |\mathbf{n}| |\mathbf{m}|)$$

where \mathbf{n} and \mathbf{m} are the normal vectors between the two planes and Θ is the angle between them.

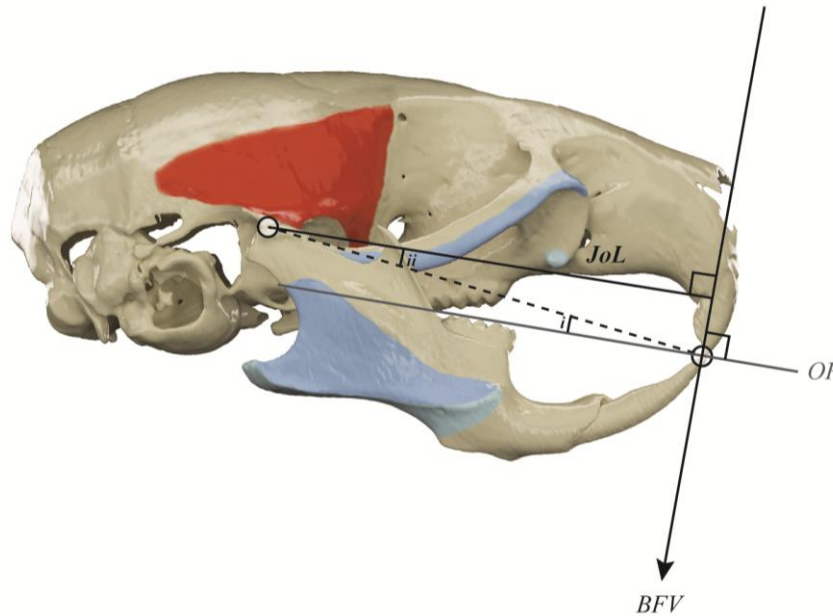


Figure 5.2.3: Calculation of jaw out-lever. Spherical points identify the fulcrum (centre of mandibular condyle), and the tip of the mandibular incisor. The bite force vector (*BFV*) is taken as perpendicular to the occlusal plane, passing through the tip of the mandibular incisor. Jaw out-lever (*JoL*) is the perpendicular distance from the fulcrum to the *BFV*. In a two dimensional analysis *JoL* could be calculated via trigonometry by establishing the distance from the fulcrum to the incisor tip and measuring angle *i* (angle between the latter line and the *OP*), thus also finding angle *ii*.

5.2.3 Statistical analyses

Box-plots were produced and one-way ANOVAs performed to assess whether the three strains showed significant differences in jaw-out lever, muscle in-lever and mechanical advantage. P-values were Bonferroni corrected for questions 1b and 1c to account for multiple comparisons.

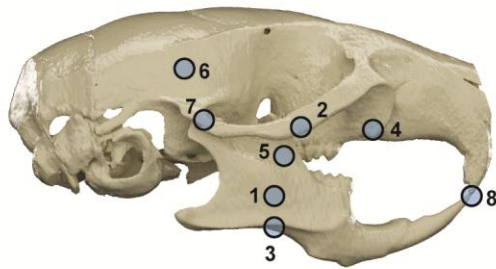
Muscle in-lever (MiL) was plotted against jaw out-lever (JoL) to assess the relationship between the two levers. Reduced Major Axis (RMA) regressions were conducted to measure the gradient and intercept of each slope and correlations (r^2) between the two levers. A gradient of 1 and an intercept of 0 indicates consistent mechanical advantage and a MiL isometric with respect to JoL. ANCOVA tests were performed to assess the homogeneity of slopes between strains for each muscle and in-lever group.

5.2.4 Shape analysis

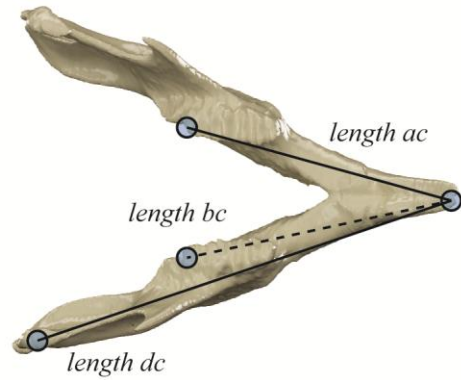
Geometric morphometric methods were used to describe patterns of shape variation within the lever arm system and covariation between the lever arm system and general cranial form. These methods provide a quantitative approach to addressing shape comparisons (Zelditch et al., 2004a)

Eight three-dimensional landmarks (**Figure 5.2.4; Table 5.2.1**) relating to the lever-arm system, and twelve three dimensional landmarks (**Figure 5.2.4; Table 5.2.2**) that described broad cranial morphology yet were independent of regions directly involved in the masticatory lever arm system were identified and digitised in Amira v5.2.

LEVER ARM SYSTEM LANDMARKS



JAW OUT-LEVER LANDMARKS



CRANIAL LANDMARKS

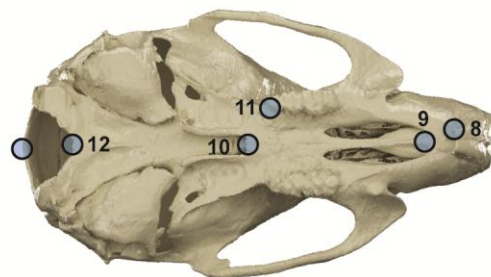
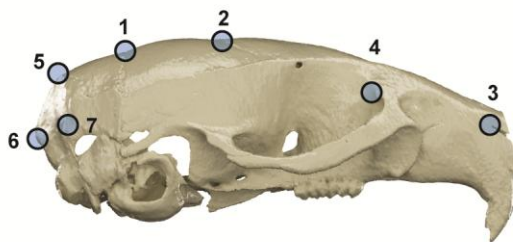


Figure 5.2.4: Position of three-dimensional landmark points for three separate landmark sets: lever arm system landmarks; jaw out-lever calculation landmarks; and cranial landmarks. Corresponding landmark definitions are given in table 5.2.1 and table 5.2.2. Jaw out-lever landmarks and length are utilised in the dot product calculation to determine jaw out-lever length.

Table 5.2.1

LEVER ARM SYSTEM LANDMARKS (RIGHT SIDE)

Landmark number	Landmark description
1	Centroid of deep masseter muscle insertion
2	Centroid of deep masseter muscle origin
3	Centroid of superficial masseter muscle insertion
4	Centroid of superficial masseter muscle origin
5	Centroid of temporalis muscle insertion
6	Centroid of temporalis muscle origin
7	Centre of articular surface of mandibular condyle
8	Tip of mandibular incisor

Table 5.2.2

CRANIAL LANDMARKS (RIGHT SIDE)

Landmark number	Landmark description
1	Lambda - the midline intersection of the sagittal and lambdoidal sutures
2	Fronto-temporal-parietal junction (anterior projection of parietal in superior view)
3	Anterior most point at the intersection of the premaxillae and nasal bones
4	Intersection of fronto maxillary suture with orbital rim
5	Intersection of interparietal and occipital bones at the midline
6	Dorsal midline border of foramen magnum
7	Most lateral inferior point on the occipital bone
8	Posterior edge of the alveolus of the maxillary incisor
9	Anterior midline margin of incisive foramen
10	Midline junction between palate and presphenoid
11	Posterior edge of the alveolus of the third maxillary molar
12	Ventral midline border of foramen magnum

Generalised Procrustes Superimposition was employed to register specimen forms, translating and rotating each specimen to minimise the squared, summed distances between corresponding landmarks on each configuration and an iteratively computed mean specimen (Gower, 1975, Goodall, 1991, Rohlf and Slice, 1990).. Within this superimposition specimen size is accounted for by the calculation of centroid size, a measure of size that is mathematically independent of shape location (Slice, 2007, Zelditch et al., 2004a, O'Higgins, 1997). GPA leads to landmark configurations of all specimens lying in a common coordinate system, with differences in landmark coordinate values reflecting differences in configuration shapes (Gower, 1975, Goodall, 1991, Rohlf and Slice, 1990).

5.2.4.1 *Principal component analysis*

Following GPA of lever-arm system landmarks a principal component analysis (PCA) was performed to assess patterns of shape variance.

During PCA tangent space coordinates are used to extract eigenvectors, these being the principal components of shape variation. The representation of specimens on a tangent plane allows principal components (PC) to be plotted orthogonally to each other, each PC representing a statistically independent mode of variation (O'Higgins and Jones, 1998).

5.2.4.2 *Linear regression*

To assess whether mechanical advantage findings are accounted for by a simple scaling of the lever-arm system with size, lever-arm shape (Procrustes coordinates)

was regressed against centroid size of cranial landmarks. A measure of the percentage of the total shape variance explained by the regression was then calculated.

Landmarks configurations representing shape most correlated with size lying along the linear regression line were exported at different out-lever lengths. Muscle in-lever, muscle out-lever and mechanical advantage were calculated as per the method detailed above for these hypothetical landmark configurations. Muscle in and jaw out levers for these hypothetical skulls were then plotted alongside sample results and slope gradient and intercepts compared.

5.2.4.3 *Partial least squares analysis*

2-block PLS analysis was performed to assess patterns of covariance between general cranial shape and lever-arm system morphology.

Partial least squares analysis (also referred to as singular warp analysis) is a method used to explore patterns of covariation between blocks of variables, allowing analysis of hypotheses of morphological integration (Zelditch et al., 2004a, Rohlf and Corti, 2000). Two-block partial least squares (PLS) models the covariation between the two separate sets of variables of interest by identifying linear combinations (singular axes) between the two sets. As in regression, PLS examines the relationship between two sets of variables, however while in regression one set of variables is assumed to be dependent on the other, PLS treats variables equally, viewing both sets as jointly related to an underlying cause. (Rohlf and Corti, 2000, Bookstein et al., 2003, Bastir and Rosas, 2006, Bastir and Rosas, 2005, Zelditch et al., 2004a, Klingenberg, 2009, Klingenberg et al., 2003). Statistical significance of the covariation between the two landmark configurations (blocks) is established by means of a permutation test, simulating the null hypotheses of complete independence between the two (Manly, 2007). Quantification for the covariance between the two landmark configurations is provided by the RV coefficient. The RV coefficient is a scalar measure of the strength of association between two sets of

variables, and in the context of PLS is used as a measure of the total amount of covariation between the variables (Escoufier, 1973). Taking values between zero and one, a RV coefficient of zero infers that the two blocks are completely uncorrelated with each other, and an RV coefficient of one suggests that the difference between the two blocks is only due to rotation, reflection, scaling or translation (Klingenberg, 2009).

5.2.4.4 *Calculation of percentage of overall variance*

While most software offering PLS analysis provides a quantification of the percentage total covariance between the two blocks of variables alongside a measure of the overall association between the two blocks (the RV coefficient), no quantification is given of the percentage of total variance in the sample accounted for by the percentage of covariance. A calculation of the percentage total variance for each covariance per block can be calculated as the variance of the scores of one PLS axis for one block of variables, divided by the sum of eigenvalues (following PCA) for the same block.

This calculation was carried out to assess the amount of overall variance in the lever arm-system accounted for by covariance between cranial shape and the lever-arm system.

5.2.4.5 *Modularity Hypothesis*

A modularity hypothesis was used to gauge whether the lever arm system shows relative independence of cranial shape. MorphoJ software (Klingenberg, 2012) allows hypotheses of modularity to be addressed, assessing whether hypothetical modules show a low degree of covariation in comparison to alternative partitions of the total structure into parts. A low covariation between selected modules does not

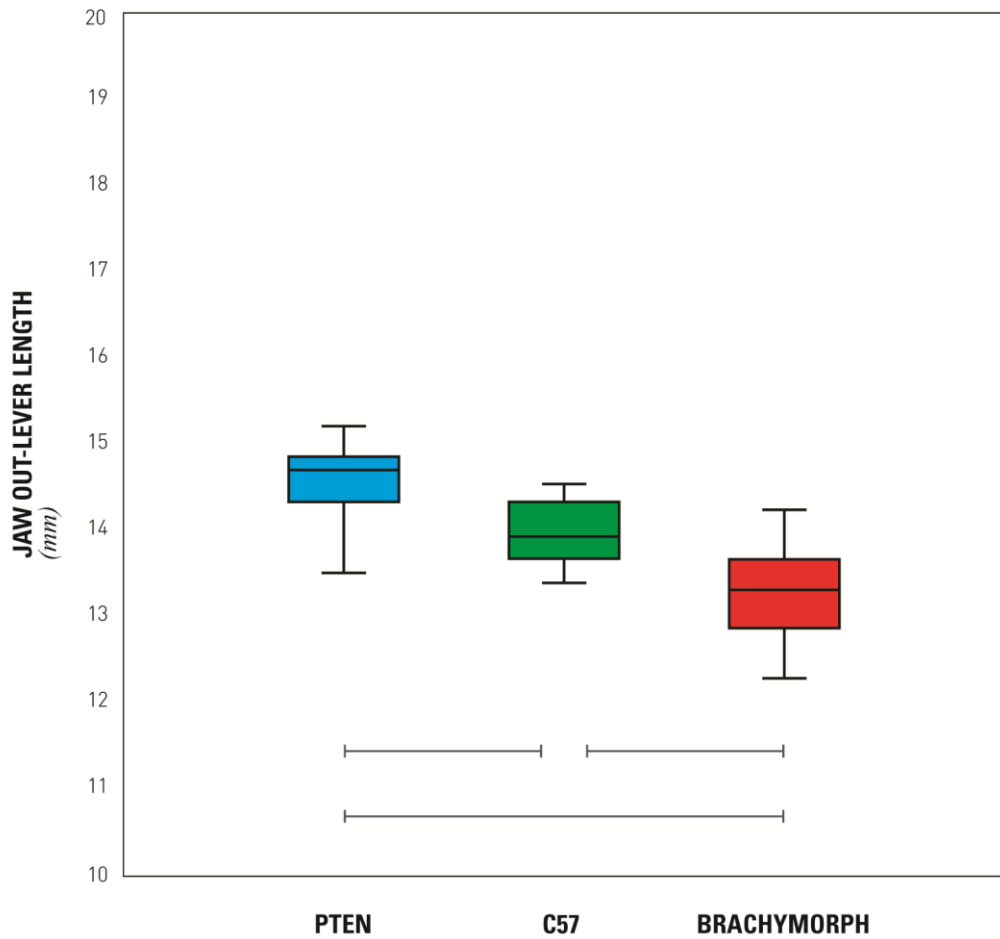
itself imply modularity, but indicates that modularity between selected modules is weaker than the majority of alternative partitions, and thus the hypothesis of modularity cannot be rejected (Drake and Klingenberg, 2010, Klingenberg, 2009, Jarniczky and Hallgrímsson, 2011, Sanger et al., 2012).

Cranial shape landmarks and lever-arm system landmarks (**Figure 5.2.4**) were combined into the same data set, and then within MorphoJ the total landmark set specified as the two original subsets. Strength of association between this subdivision, and a large number of possible alternative partitions consisting of the same number of landmarks were then compared. An RV coefficient is computed for the selected subdivision and compared to RV coefficients for all alternative generated partitions, and a histogram of the distribution of these RV coefficients produced. An RV coefficient for the hypothesised subdivision falling to the left of the histogram indicates that the hypothesis of modularity cannot be rejected (Drake and Klingenberg, 2010, Klingenberg, 2009, Jarniczky and Hallgrímsson, 2011, Sanger et al., 2012).

5.3 RESULTS

5.3.1 Jaw Out Lever Lengths

Jaw out-levers were found to be significantly different (Bonferroni corrected p-value < 0.001852) between all three strains (**Figure 5.3.1**).



—| |— Indicates Bonferroni corrected statistical significance ($p < 0.001852$)

Figure 5.3.1: Box-plots illustrating differences in jaw out-lever lengths between pten (blue), C57 (green) and brachymorph (red) mouse strains. Horizontal lines indicated statistically significant differences between the two strains at the extremes of the line.

5.3.2 Muscle In Lever Lengths

Three lines of action for each muscle were analysed to assess muscle in-lever length and mechanical advantage. Centroid (**Figure 5.3.2**) and anterior (**Figure 5.3.3**) lines of action in general show significant differences between strains for muscle in-lever lengths (**Table 5.3.1**). The posterior line of action however showed little significant difference in muscle in-lever length (**Figure 5.3.4**).

Deep masseter showed significantly different lever arms in all three strains for centroid and anterior muscle lines of action. Superficial masseter also shows significantly different in-lever arms for both centroid and anterior muscle lines of action for all strains with the exception of that between C57 and brachymorph strains for the centroid line of action. Temporalis however only shows significant differences in muscle in-lever length between pten and C57, and pten and brachymorph strains for the anterior lines.

Table 5.3.1

ANOVA SIGNIFICANCES BETWEEN STRAINS IN MUSCLE IN-LEVER

Muscle line of action	Strains compared	Bonferroni corrected p value (p<0.00185)		
		Deep Masseter	Superficial Masseter	Temporalis
Centroid	Pten & C57	0.00023	0.00011	0.70
	Pten & Brachymorph	0.00011	0.00011	0.81
	C57 & Brachymorph	0.00011	0.021	0.98
Anterior Border	Pten & C57	0.00021	0.00012	0.00013
	Pten & Brachymorph	0.00011	0.00011	0.00011
	C57 & Brachymorph	0.00011	0.00011	0.0062
Posterior Border	Pten & C57	0.58	0.00012	0.43
	Pten & Brachymorph	0.74	0.00012	0.98
	C57 & Brachymorph	0.20	0.99	0.32

Table 5.3.2

ANOVA SIGNIFICANCES BETWEEN STRAINS IN MECHANICAL ADVANTAGE

Muscle line of action	Strains compared	Bonferroni corrected p value (p<0.00185)		
		Deep Masseter	Superficial Masseter	Temporalis
Centroid	Pten & C57	0.56	0.035	0.96
	Pten & Brachymorph	0.00082	1.0	0.20
	C57 & Brachymorph	0.016	0.04	0.31
Anterior Border	Pten & C57	0.88	0.85	0.12
	Pten & Brachymorph	0.00083	0.0073	0.092
	C57 & Brachymorph	0.0036	0.032	0.99
Posterior Border	Pten & C57	0.88	0.85	0.12
	Pten & Brachymorph	0.00083	0.0073	0.092
	C57 & Brachymorph	0.0036	0.032	0.99

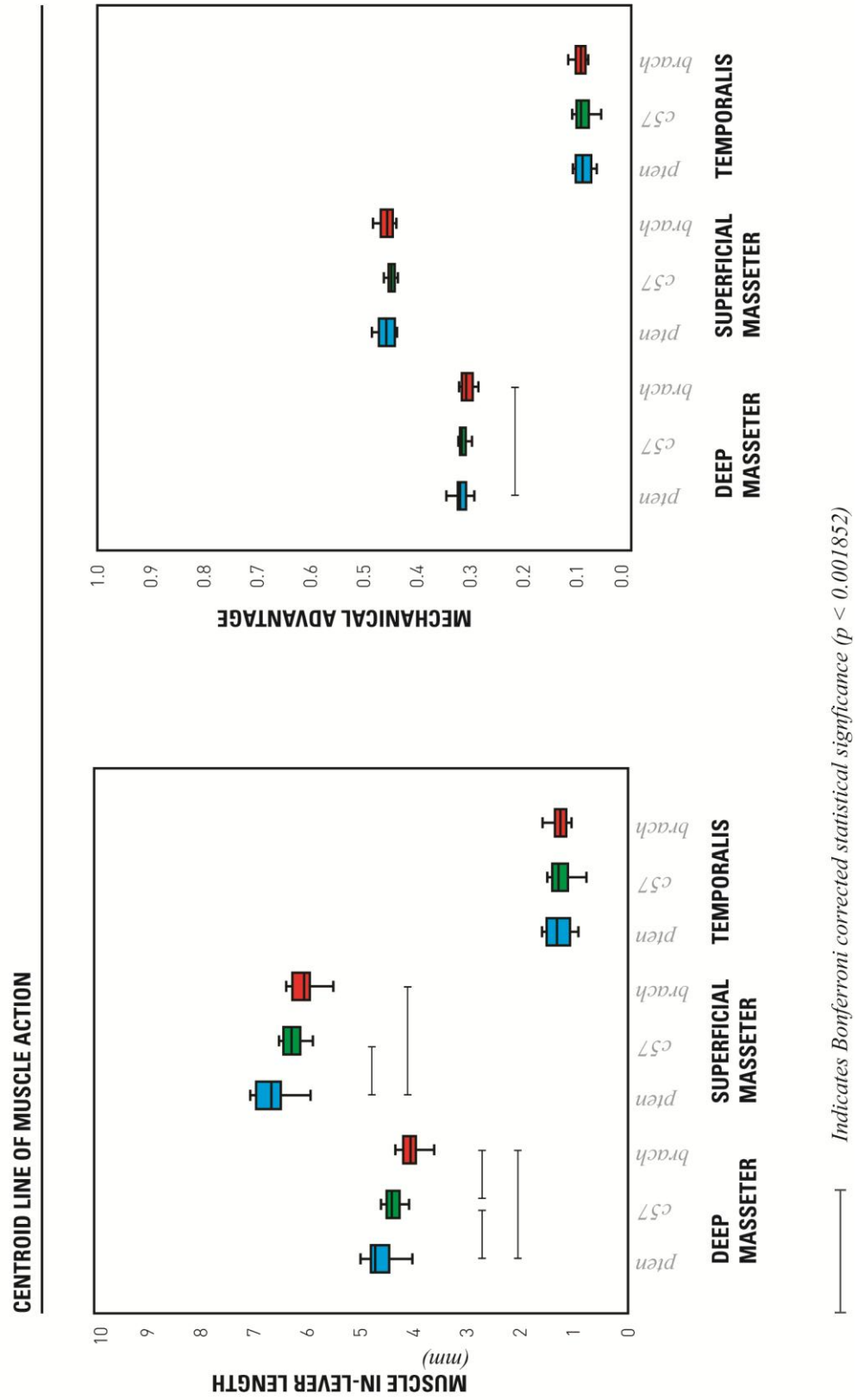
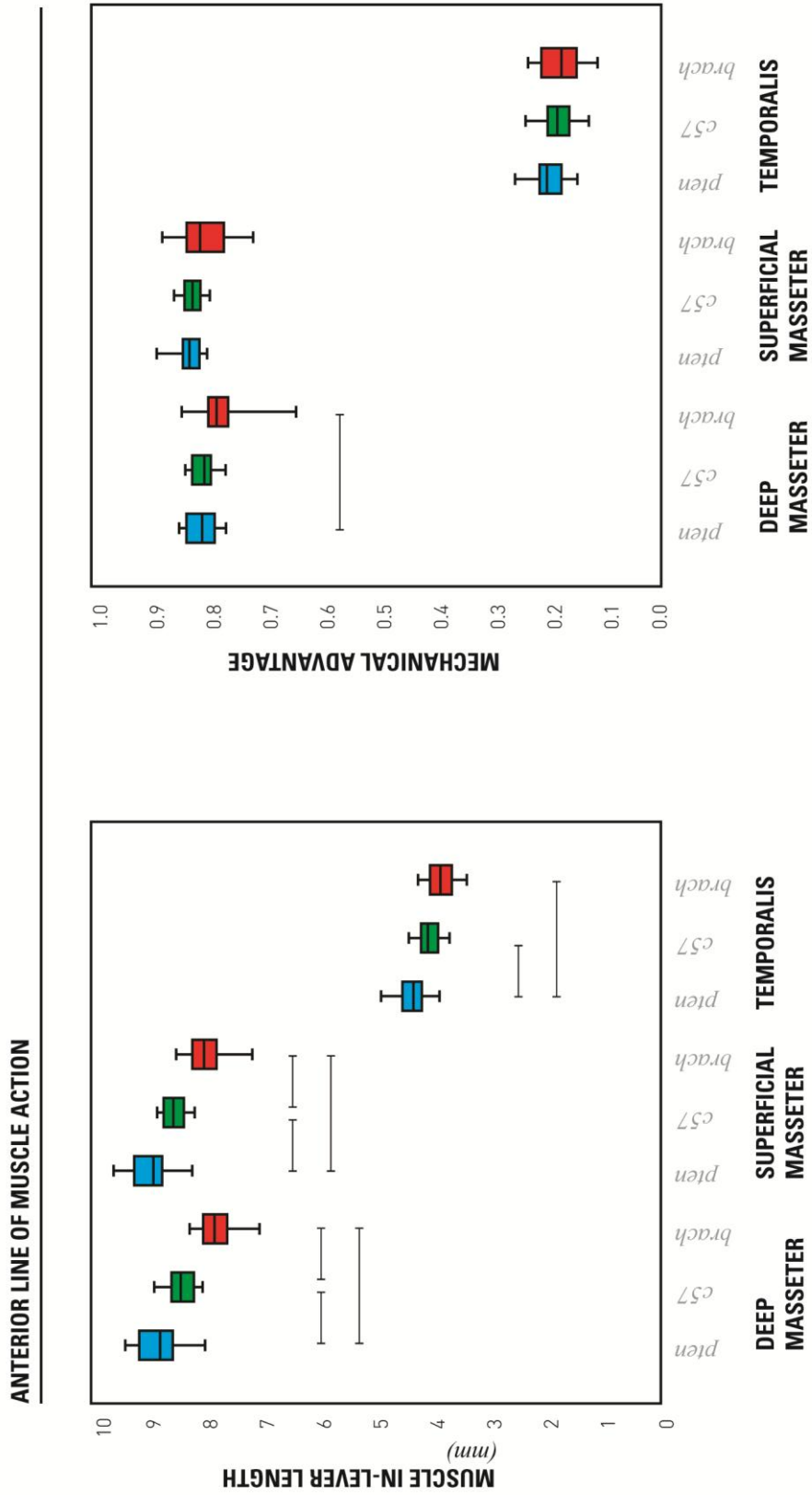


Figure 5.3.2: Box-plots illustrating differences in muscle in-lever lengths for the centroid line of action between ptn (blue), C57 (green) and brachymorph (red) mouse strains. Horizontal lines indicated statistically significant differences between the two strains at the extremes of the line.



Indicates Bonferroni corrected statistical significance ($p < 0.001852$)

Figure 5.3.3: Box-plots illustrating differences in muscle in-lever lengths for the anterior line of action between pten (blue), C57 (green) and brachymorph (red) mouse strains. Horizontal lines indicated statistically significant differences between the two strains at the extremes of the line.

COMPARISON OF MUSCLE IN-LEVER LENGTH AND MECHANICAL ADVANTAGE IN THREE MOUSE STRAINS

Figure 5.3.4

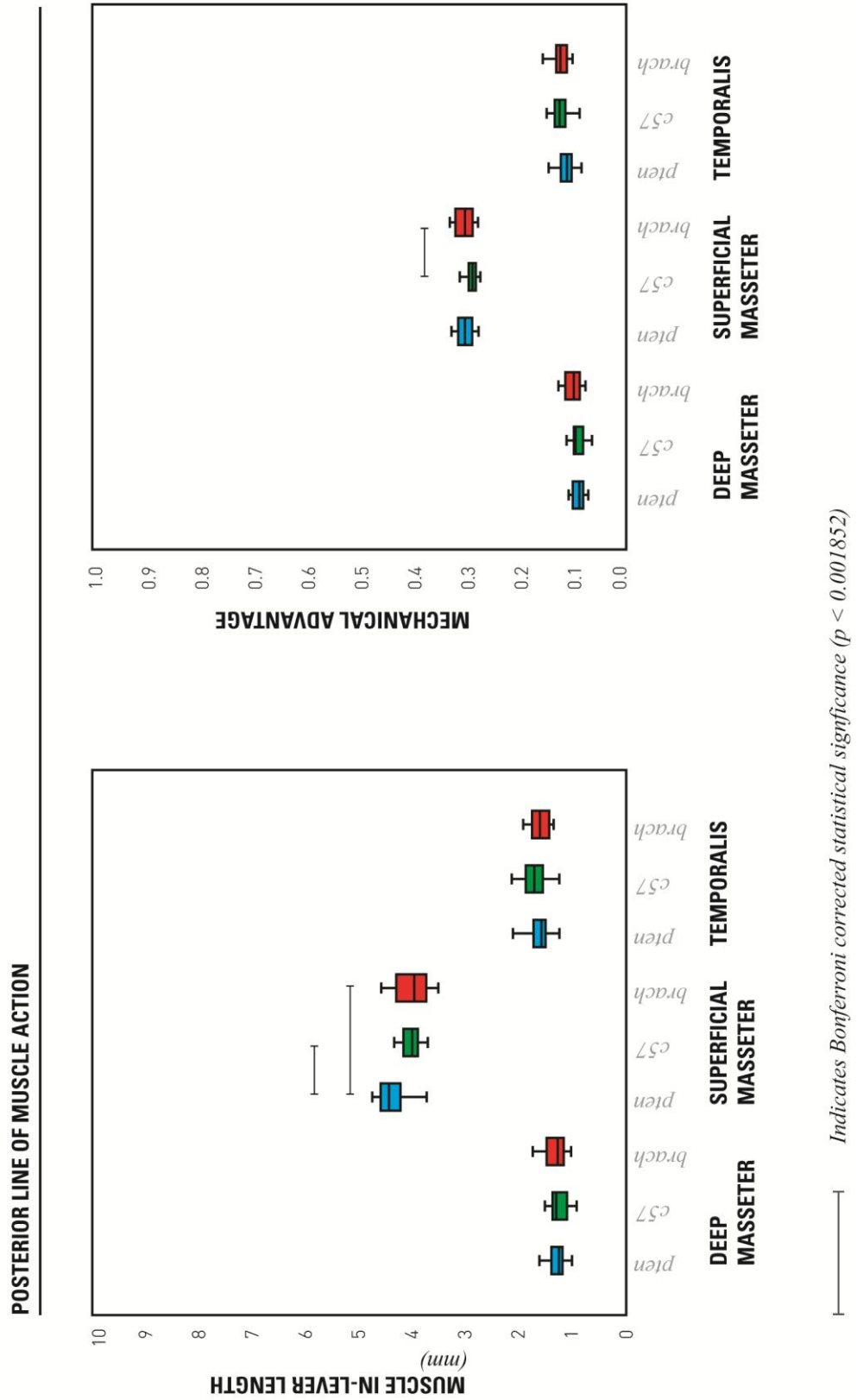


Figure 5.3.4: Box-plots illustrating differences in muscle in-lever lengths for the posterior line of action between pten (blue), C57 (green) and brachymorph (red) mouse strains. Horizontal lines indicated statistically significant differences between the two strains at the extremes of the line.

5.3.3 Mechanical Advantage

Mechanical advantage showed little significant difference for any lines of action between any strains (**Figures 5.3.2; 5.3.3 and 5.3.4**) despite significant differences found in jaw out-lever lengths and the majority of muscle in-lever lengths for centroid and anterior lines of action. Mechanical advantage was only found to be significantly different between pten and brachymorph strains for all three lines of actions for the deep masseter (**Table 5.3.2**).

5.3.4 Assessing the Mechanism of Maintenance of Mechanical Advantage

Plotting jaw out-lever lengths against muscle in-lever lengths shows muscle in-lever lengths to be negatively allometric with respect to jaw out-lever lengths for superficial and deep masseters for both centroid and anterior lines of action (**Figure 5.3.5; Figure 5.3.6**).

Isometric scaling of lever arms would be indicated by a gradient of one with a Y-axis intercept of zero. The only slope showing a gradient that is not significantly different to one is that of the deep masseter for an anterior line of action in the pten strain and this slope has an intercept of -4.4. All other gradients are shown to be significantly different to one, and do not intercept the Y-axis at zero (**Table 5.3.3**).

A gradient of one with a Y-axis intercept of zero would also indicate a fixed mechanical advantage, suggesting that the results here indicate a change in mechanical advantage with increase in out-lever lengths. However, the difference in mechanical advantage indicated by these plots is so small that it is only in the deep masseter that a significant difference is found between the very tail of the data scatter ends (between pten and brachymorph strains).

RELATIONSHIP OF JAW OUT-LEVER LENGTH TO MUSCLE IN-LEVER LENGTH

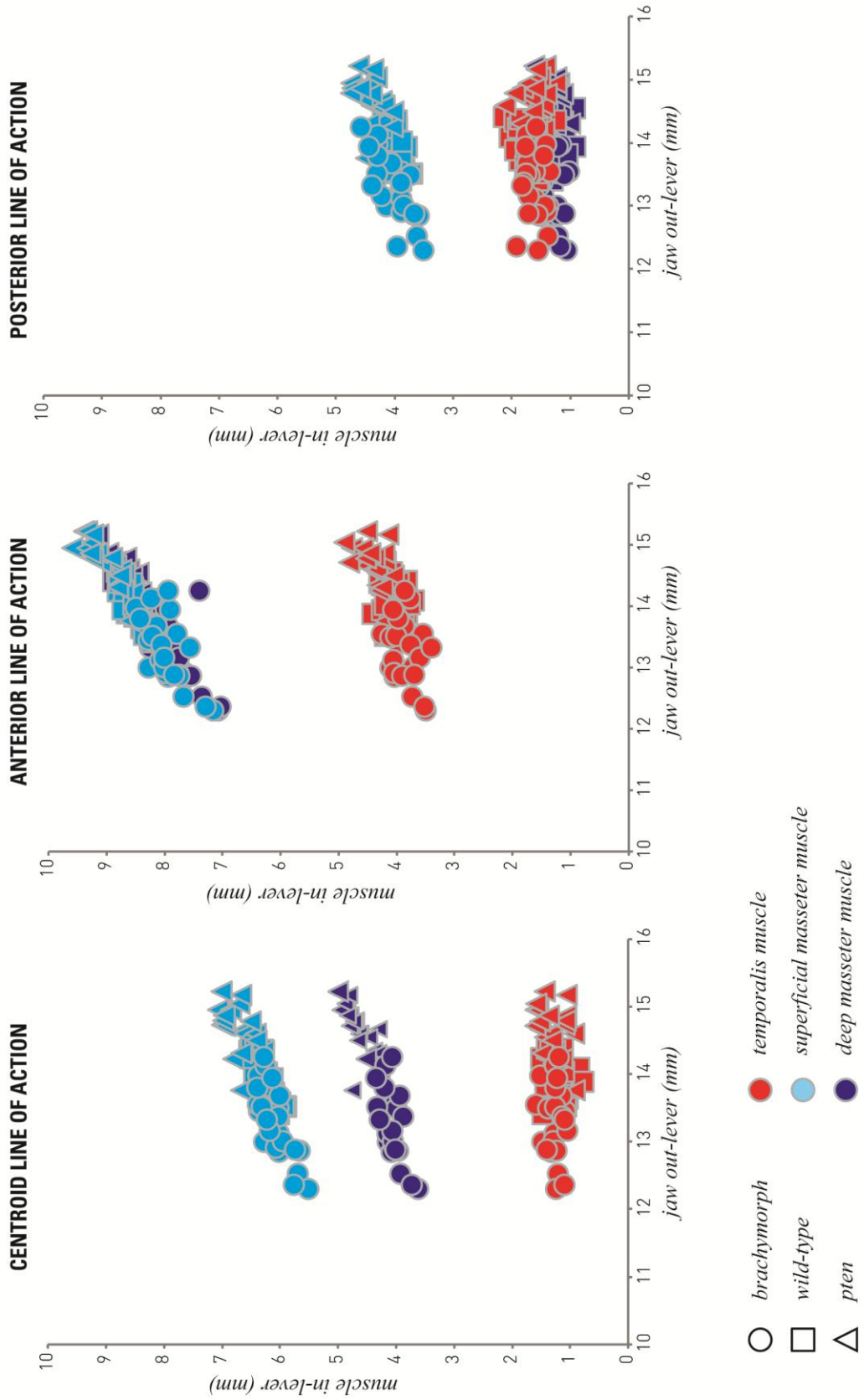


Figure 5.3.5: Plots showing the relationship of jaw out-lever length (mm) to muscle in-lever length (mm) for the centroid; anterior; and posterior lines of action. Circular data points represent the brachymorph strain, square data points the wild-type (C57) strain, and triangular data points the pten strain. Muscle in-lever lengths for the temporalis muscle are represented in red, the superficial masseter muscle in pale blue, and the deep masseter muscle in dark blue.

Figure 5.3.6

RELATIONSHIP OF JAW OUT-LEVER LENGTH TO MUSCLE IN-LEVER LENGTH (LOGARITHMIC SCALE)

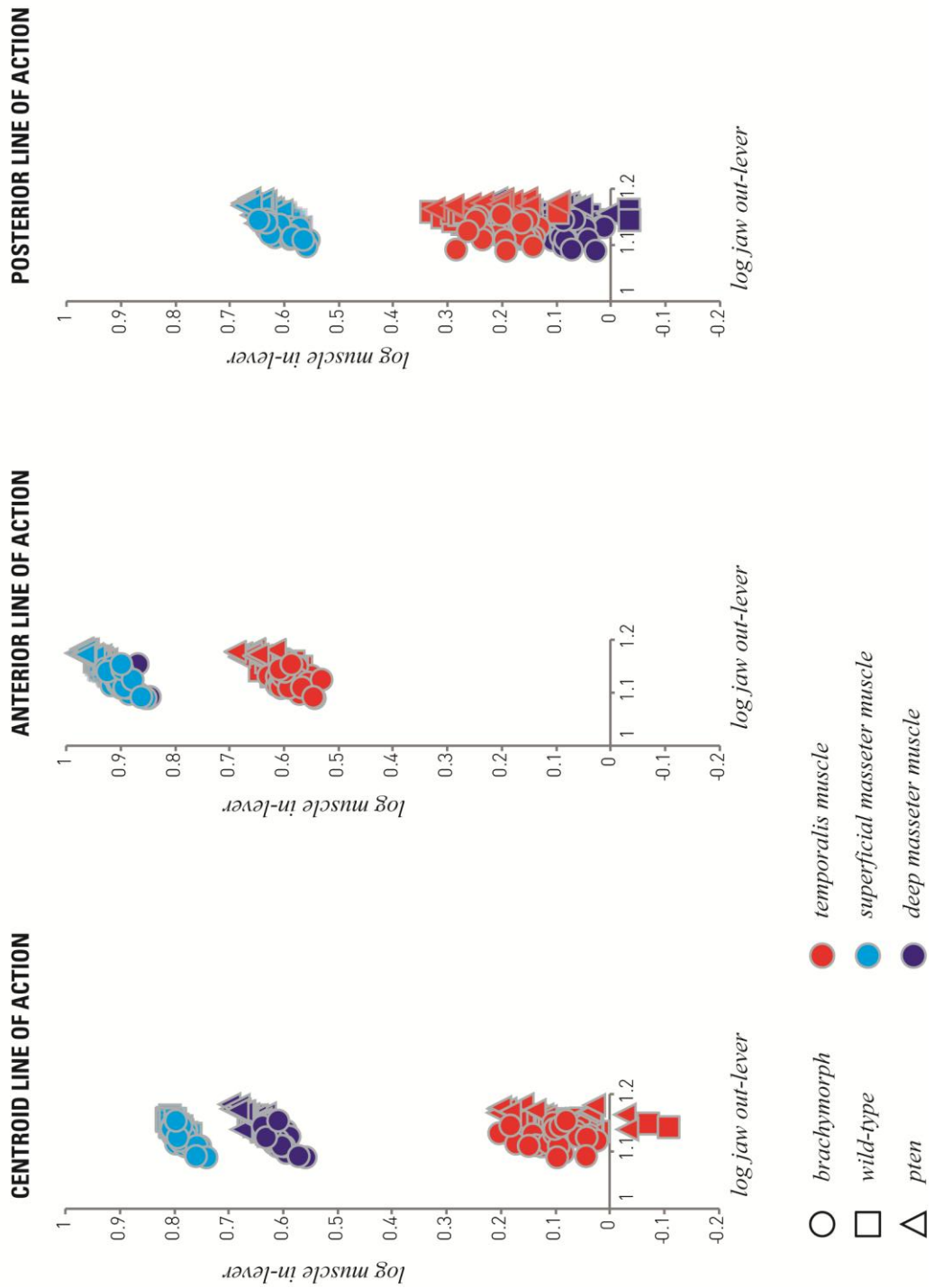


Figure 5.3.6: Plots showing the relationship of jaw out-lever length in logarithmic scale, to muscle in-lever length in logarithmic scale, for the centroid; anterior; and posterior lines of action. Circular data points represent the brachymorph strain, square data points the wild-type (C57) strain, and triangular data points the pten strain. Muscle in-lever lengths for the temporalis muscle are represented in red, the superficial masseter muscle in pale blue, and the deep masseter muscle in dark blue.

Table 5.3.3

SLOPES INTERCEPTS AND CORRELATIONS FOR RMA REGRESSION OF MUSCLE IN-LEVER AND JAW OUT-LEVER LENGTHS

Muscle line of action	Muscle	Strain/s	Intercept of slope		Correlation of X and Y axis (r^2)	p slope is equal to 1 (p a=1)
			Gradient of slope (a)	with Y axis (b)		
Centroid	Deep Masseter	C57	0.42	-1.51	0.57	7.23E-10
		Pten	0.58	-3.86	0.56	0.0001
		Brachymorph	0.34	-0.40	0.43	3.01E-11
		Strains combined	0.44	-1.71	0.77	2.63E-33
	Superficial Masseter	C57	0.61	-2.23	0.77	1.69E-06
		Pten	0.68	-3.28	0.42	1.25E-02
		Brachymorph	0.47	-0.18	0.58	4.81E-08
		Strains combined	0.51	-0.77	0.75	7.80E-25
	Temporalis	C57	0.58	-6.83	0.0038	1.97E-03
		Pten	0.53	-6.50	0.18	3.55E-04
		Brachymorph	0.26	-2.17	0.009	4.40E-12
		Strains combined	0.27	-2.48	0.031	6.80E-34
Anterior	Deep Masseter	C57	0.71	-1.52	0.72	1.25E-03
		Pten	0.91	-4.43	0.57	2.82E-01
		Brachymorph	0.62	-0.43	0.45	8.05E-04
		Strains combined	0.76	-2.22	0.92	6.97E-09
	Superficial Masseter	C57	0.63	-0.26	0.72	2.15E-05
		Pten	0.78	-2.41	0.77	1.55E-02
		Brachymorph	0.61	-0.06	0.45	4.66E-04
		Strains combined	0.72	-1.49	0.83	1.24E-11
	Temporalis	C57	0.56	-3.73	0.01	8.57E-04
		Pten	0.62	-4.68	0.37	2.60E-03
		Brachymorph	0.43	-1.92	0.11	1.65E-06
		Strains combined	0.45	-2.19	0.70	2.86E-22
Posterior	Deep Masseter	C57	0.49	-5.66	0.0035	5.92E-05
		Pten	0.40	-4.48	0.06	8.53E-07
		Brachymorph	0.40	-4.00	0.12	2.03E-07
		Strains combined	0.27	-2.45	0.0056	1.22E-33
	Superficial Masseter	C57	0.45	-2.23	0.23	8.42E-07
		Pten	0.62	-4.66	0.30	3.85E-03
		Brachymorph	0.57	-3.54	0.58	1.62E-05
		Strains combined	0.43	-1.89	0.50	5.84E-24
	Temporalis	C57	0.60	-6.64	0.05	3.15E-03
		Pten	-0.48	8.60	0.02	8.96E-12
		Brachymorph	0.31	-2.55	0.0093	6.89E-10
		Strains combined	0.28	-2.24	0.06	3.60E-32

5.3.5 Scaling of Lever-Arm System with Centroid Size

Principal component analysis (form space) was performed on the lever-arm system landmark configuration (**Figure 5.3.7**). PC1 (43.78% of total variance) describes the shape change in the lever-arm system across the three strains (inter-strain variation). An approximation of the jaw out-lever (condyle to incisor tip length) is seen to increase in length across the strain from brachymorph to C57 to pten. Alongside this change in out-lever length, the origin and insertion points of the three masticatory muscles in question are seen to alter their positions. As out-lever length increases, attachment areas are seen to predominantly move anteriorly, increasing the distance between the temporomandibular joint (TMJ) and the muscle attachment points, this which would have the effect of increasing the muscle in-lever length. Conversely as jaw out-lever length is seen to decrease, attachment areas predominantly move posteriorly, reducing their distance from the TMJ and decreasing muscle in-lever length. This increase in muscle in-lever length alongside an increase in out-lever length, and conversely a decrease in muscle in-lever length alongside a decrease in out-lever length could serve to maintain mechanical advantage. PC2 (17.90% of total variance) describes common patterns shape variation within the three strains (intra-strain variation). At the negative extreme of this axis a ventral rotation of incisor tip relative to the TMJ and a small reduction in jaw out-lever length is seen alongside postero-inferior rotation of masseter origins, anterior movement of masseter insertions, and posterior movement of both the temporalis origin and insertion. At the opposite extreme of the axis a dorsal rotation of incisor tip relative to the TMJ and a small increase in jaw out-lever length is seen alongside antero-superior rotation of masseter origins, posterior movement of masseter insertions and anterior movement of both the temporalis origin and insertion. Key shape changes seen here on PC2 reflect those of previous analyses (Chapter 4), with rotation at the rostrum, alongside changes in cranial length being a common pattern of intra-strain variance in all three strains. Changes seen to muscle origins and insertions alongside a small reduction in out-lever length and a ventral rotation of the incisor tip relative to the TMJ are likely to reduce muscle in-lever length; this being especially pronounced for the deep masseter. Conversely changes seen to muscle origins and

insertions alongside a small increase in out-lever length and a dorsal rotation of the incisor tip relative to the TMJ are likely to increase muscle in-lever length; again this being especially pronounced for the deep masseter. These shape changes seen on PC2 may have the potential to compensate for changes to the out-lever length by modification to muscle attachments which result in changes to muscle in-lever length and maintenance of mechanical advantage.

Viewed together, patterns of shape change seen here on PC1 and PC2 demonstrate movement of deep and superficial masseter origins and insertions such that as jaw out-lever length increases so too does the in-lever length of these two muscles, providing a potential for mechanical advantage maintenance. Conversely a decrease in jaw out-lever length is seen alongside muscle attachment movements consistent with a reduction in masseter in-lever length, and thus a maintenance of mechanical advantage. Modification of temporalis in-lever length alongside jaw out-lever length is less clear .

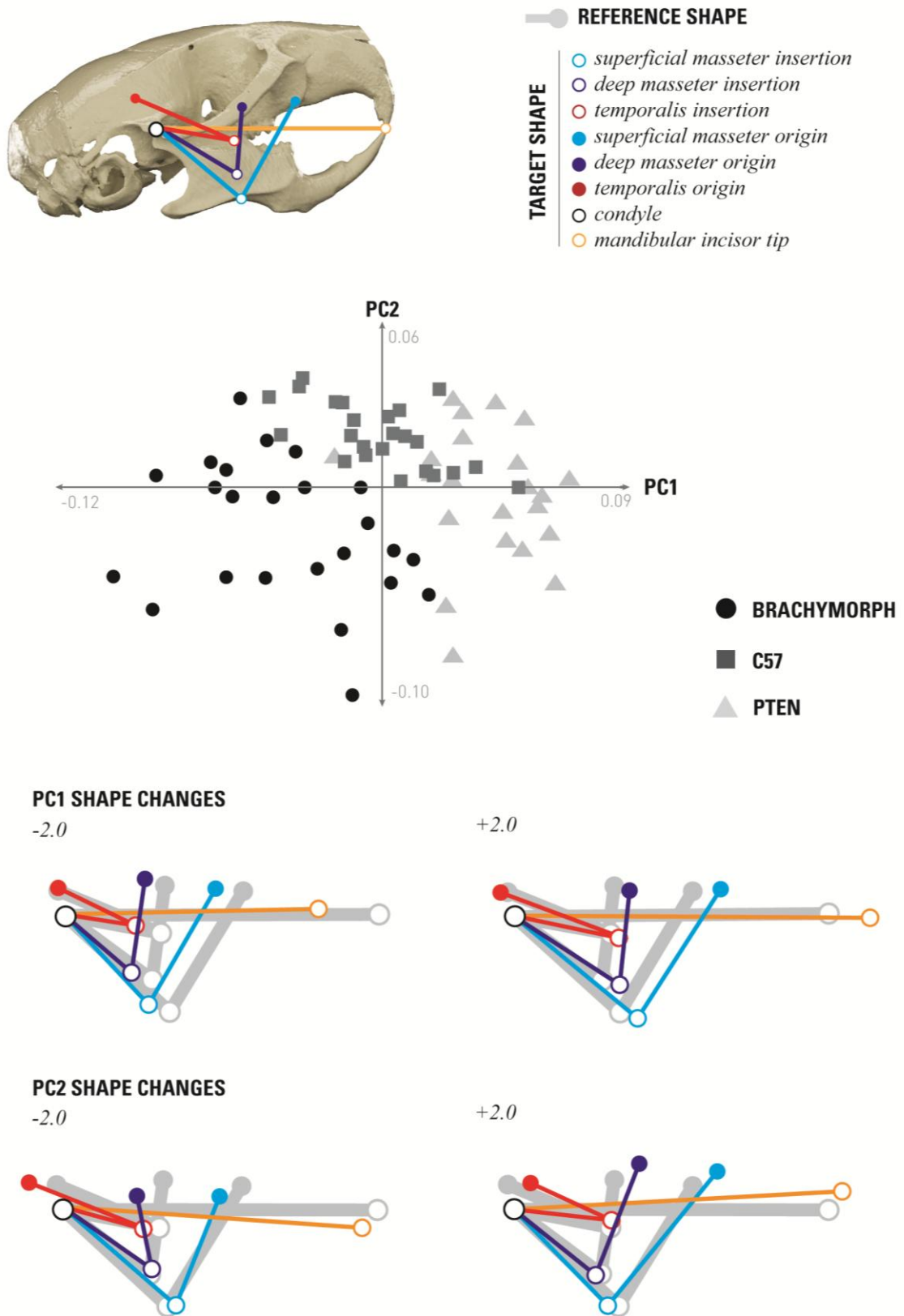


Figure 5.3.7: Principal component analysis of lever-arm system landmark configuration, depicting shape changes along PC1 (43.78% of total variance) and PC2 (17.90% of total variance). Inset shows colour key and landmark positions on the cranium and mandible.

To assess whether mechanical advantage is largely consistent across the three strains due to a simple scaling relationship, shape coordinates of the lever-arm system were regressed against centroid size of a rudimentary cranial shape. Only 18.28% of the total variance of the sample was found to explained by this regression, indicating that the majority shape variance revealed in the lever-arm system landmarks is not simply correlated with size of the overall cranium, and thus adaptation of the lever arm system to maintain a consistent mechanical advantage is not explained by a simple scaling relationship with cranial size.

Partial least squares analysis revealed patterns of covariation between a rudimentary cranial shape and muscle-lever arm system shape. Together PLS1 and PLS2 account for 96.37% of the covariance between these two landmark configurations (RV=0.54; PLS1: 67.75% covariance, 0.88 correlation ($p<0.0001$); PLS2: 28.64% covariance, 0.71 correlation ($p<0.0001$)). However, only 51.98% of the overall shape variance found within the lever arm system with PCA is accounted for by this covariance (PLS1 and PLS2 combined) with cranial shape. This indicates that 48.02% of the shape variance found within the lever arm system is varying independently of cranial shape.

A hypothesis of modularity was applied to a landmark configuration encompassing both a rudimentary cranial form and the lever arm system. A low RV coefficient in comparison to those of a large number of possible alternative partitions histogram indicates that the hypothesis of modularity likely cannot be rejected and that it is possible that the lever-arm system can vary independently of general cranial shape (**Figure 5.3.8**).

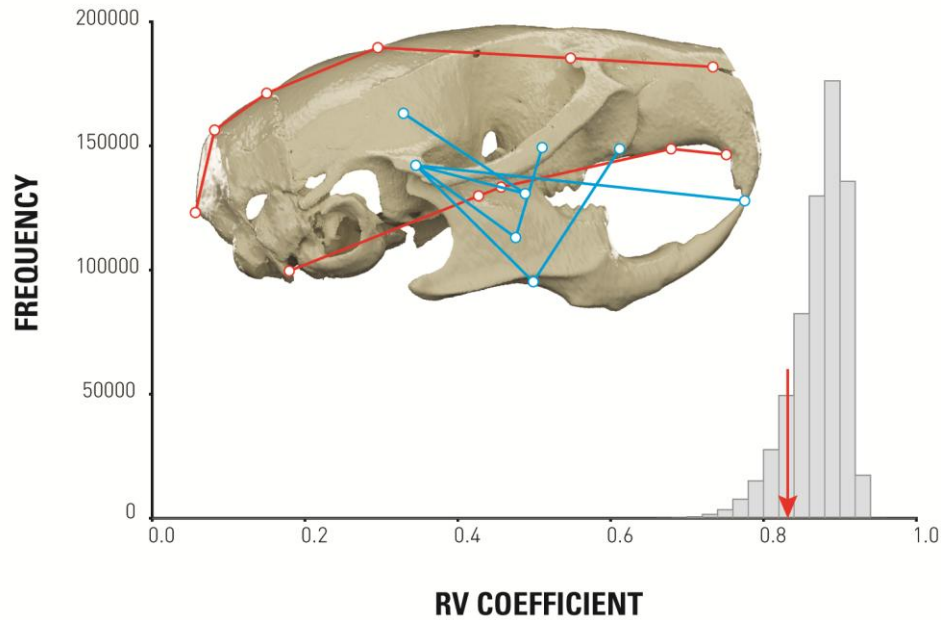


Figure 5.3.8: Depiction of results of a modularity hypothesis when an overall landmark configuration was divided into a simple cranial shape configuration (red lines and points) and a lever arm system configuration (blue lines and points). The red arrow on the histogram indicates the RV coefficient of this division in comparison to randomly generated divisions within the overall landmark configuration. The low RV coefficient of the two hypothetical modules in comparison to other randomly generated partitions (distribution shown in histogram) indicates that a hypothesis of modularity cannot be rejected.

5.4 DISCUSSION

Mechanical advantage of the masticatory complex was calculated as a ratio of the jaw in-lever and the muscle out-lever for three strains of mice showing variation in cranial length. The sample of mice investigated consisted of two mutant strains showing the extremes of cranial length, and a control wild-type mouse of the same background strain. Variance in cranial length in both the *pten* and *brachymorph* mutant are due to increased and decreased chondrocranial growth respectively, thus changes in mandibular morphology in these strains when compared to the control can reasonably be assumed the result of epigenetic plastic adaptation. A previous investigation of patterns of covariation in the three strains indeed found high correspondence between cranial and mandibular form despite the absence of the same genetic influence in the mandible as is present in the cranium (see previous chapter). This investigation follows on from previous work which showed the potential of strong integration within the craniomandibular complex to maintain global coordination in terms of form despite isolated cranial variation (see **Chapter 4**), and aims to assess whether, as form is altered during both evolution and development, such coordinated plastic adaptation has the potential to also maintain parameters of functional performance of the complex.

Non-significant differences in the mechanical advantage of the masticatory complex were found in three strains of mice despite differences in cranial length and thus jaw out-lever length. In the absence of adaptation of muscle in-lever length, variation in out-lever length would result in differences in mechanical advantage, and thus the amount of force produced at the dentition. If all other phenotypic traits remained static, a reduction in craniomandibular length and thus out-lever length as found in the *brachymorph* strain would have the effect of increasing mechanical advantage, while an increase in craniomandibular length as present in the *pten* strain would have the effect of reducing mechanical advantage. However, as mechanical advantage is calculated as a ratio of the in- and out-lever, the ability of the lever arm system to produce force at the dentition is also influenced by the position of the masticatory muscles and thus the length of the muscle in-lever. Muscles whose line of action pass close to the TMJ will have a relatively short in-lever length while muscles

whose lines of action are distant from the pivot will have a relatively long in-lever length (Smith and Savage, 1956).

Significant differences were found in jaw out lever-lengths between the three strains. Despite differences in cranial and mandibular lengths, and thus these differences in jaw out-lever lengths, non-significant differences in the mechanical advantage of the masticatory system were found between the three mouse strains. This maintenance of mechanical advantage despite differences in mandibular and jaw out-lever length looks to be explained by significant differences between the three strains in muscle in-lever lengths. Broadly speaking, significant differences were found in muscle in-lever lengths for the superficial and deep masseter muscles for both the centroid and anterior lines of action. The temporalis muscle in-lever however only showed significant differences between the three strains for the anterior line of action. Overall, significant differences between the three strains in terms of both jaw out-levers and muscle in-levers translated into non significant differences between the three strains in mechanical advantage.

Two possible explanations for this general maintenance of mechanical advantage were considered. Firstly that a simple scaling effect was present such that as craniomandibular length and thus out-lever length increased so too did muscle in-lever length. It has been suggested that, for mechanical reasons, all animals may maintain isometric scaling of linear dimensions of the jaw (Swiderski and Zelditch, 2010). As mechanical advantage, a measure of the functional performance of a jaw, can be revealed by the ratio of a two lever lengths of the same dimensionality (Turnbull, 1970, Greaves, 1982, Bramble, 1978, Davis, 1961) it may be expected that these lengths should scale isometrically with respect to each other such that a functional relationship is maintained (Swiderski and Zelditch, 2010). Stability of jaw lever ratios in 23 species of sciurine tree squirrels has been reported alongside isometry of the masseter moment arm in relation to the output arm (Swiderski and Zelditch, 2010), a result consistent with that of earlier studies (Velhagen and Roth, 1997, Thorington and Darrow, 1996).

Findings of the present study are not in line with that of previous authors who report isometric scaling of such linear dimensions (Swiderski and Zelditch, 2010, Velhagen

and Roth, 1997). Although in the current study maintenance of mechanical advantage is reported, lever arm ratios are not found to scale isometrically for any of the muscles or lines of action investigated. While disparity between findings of the present study and previous work by other authors may be due to species differences, methodological differences in the approach to calculating mechanical advantage may also have had an impact. Although both methods calculate mechanical advantage as a ratio of the jaw out-lever length and muscle in-lever length, the calculation of the latter two lengths is dissimilar. The present study calculates the two lever lengths as the perpendicular line from the fulcrum to the line of action (muscle force vector or bite force vector) (Lieberman, 1997, Smith and Savage, 1956, Throckmorton and Throckmorton, 1985). This differs from another frequently employed methodology which approximates the lever arm length as a simple linear distance from the fulcrum (mandibular condyle) to a point on the attachment of each relevant muscle; and the bite arm length at the distance from the fulcrum the tip of the incisor (Radinsky, 1985b, Radinsky, 1985a, Radinsky, 1981a, Swiderski and Zelditch, 2010, Thorington and Darrow, 1996, Velhagen and Roth, 1997). Additionally, the vast majority of studies employing the latter methodology have carried out these analyses in two dimensions, whilst our calculation of mechanical advantage is based upon three dimensional linear measurements.

In the absence of evidence of isometric scaling of lever arms, the potential of plastic adaptation within a strongly integrated complex to modify regions of the lever-arm system such that in-lever length was suitably proportioned to out-lever lengths was assessed. Partial least squares analysis revealed covariance between a lever arm system landmark configuration and a cranial shape landmark configuration. However, this covariance only accounted for 48% of the overall shape variance seen in the lever arm system, suggesting that half of the total variance found in the form of this system may vary independently of cranial form. Regression analysis showed that only 13% of morphological variance in the lever arm system landmark configuration was explained by the cranial centroid size. Additionally, a modularity hypothesis was performed to assess levels of covariance between the lever arm system shape and cranial shape, with results indicating that covariation between

these two hypothetical modules is weaker than the majority of alternative partitions. Consequently a hypothesis of modularity cannot be rejected (Klingenberg, 2009).

These results imply an underlying hierarchical network of interactions between constituent parts of the complex. While previous results indicate global integration with the craniomandibular complex such that morphological cohesion is maintained (see **Chapter 4**), results of the present study indicate the potential of areas of the complex pertaining to the lever arm system to plastically adapt with relative independence of cranial size and shape.

Any complex system has a notably hierarchical arrangement of parts, that is, there is a complex of subsystems that comprise of subsystems and so forth throughout multiple levels (Callebaut and Rasskin-Gutman, 2005). While individual elements may have a relatively high degree of internal integrity and integration, at the level of the operation or function of the whole organism or structure, individual semi-independent elements are interdependent (Thomas, 2005). This conflict of simultaneous independence and interdependence of parts is encapsulated in the concepts on modularity and integration (Olson and Miller, 1958, Pigliucci and Preston, 2004, Klingenberg, 2008). Modularity refers to the largely abstract division of a structure or system into partially dissociated and internally cohesive elements, while the concept of integration, while difficult to precisely define (Pigliucci, 2003), describes the coordinated variation of parts or traits (Klingenberg, 2008, Klingenberg, 2005a, Pigliucci, 2003). While modules by definition show strong internal integration (Klingenberg et al., 2003), developmental and function connection between these semi-independent regions may not be unsubstantial, providing necessary coordination between parts of the whole structure. Within an organism or structure, when measured at the level of functional groups of characters, some groups may be more or less integrated (Pigliucci, 2003).

The results reported here indicate that while integration throughout the complex is present to the extent that coordination and covariance may be observed between the crania and mandibles, equally regions of the complex may be modified with relative independence. The concept of integration of complex structures is closely tied to another biological phenomenon, phenotypic plasticity (Pigliucci, 2003, Pigliucci,

2001). Plasticity, describes the ability of an organism to respond throughout its development and life to changes to both its internal and external environmental conditions (Ravosa et al., 2008a, West-Eberhard, 1989, Agrawal, 2001, Gotthard and Nylin, 1995, Holden and Vogel, 2002). As such the concept of adaptive plasticity is not only closely linked to that of integration, but also to that of functional adaptation (Ravosa et al., 2008a, Ravosa et al., 2008b). Functional adaptation, at least in a skeletal structure, describes the dynamic coordinated series of modelling and remodelling processes, occurring at a cellular, tissue or biochemical level, in response to routine stresses such that a adequate structure is maintained (Bouvier and Hylander, 1996, Bouvier and Hylander, 1981, Lanyon and Rubin, 1985, Biewener, 1993, Biewener and Bertram, 1993, Biewener et al., 1986, Vinyard and Ravosa, 1998, Hamrick, 1999, Ravosa et al., 2000). Plasticity plays a role in fine-tuning the fit between form and behaviour throughout an organism's life (Ravosa et al., 2008b), and may allow for the accommodation of novelty, providing the capacity for immediate and coordinated shifts in related traits, and the occurrence of condition-sensitive expression of phenotypes (West-Eberhard, 2003, West-Eberhard, 1989, West-Eberhard, 2005).

Results of the present study show the potential of plastic adaptation to occur in regions of the masticatory complex in order to compensate for the presence of a mutationally induced variance which, in the absence of any such adaptive plasticity, would result in an alteration of functional performance.

A key question when assessing patterns of integration within a complex, is whether such covariance amongst characters is an adaptation or constraint (Pigliucci, 2003). On one hand covariance of traits, whether functional, developmental or genetic in origin will limit and channel the evolutionary trajectory of an organism in the short to mid-term future (Pigliucci, 2003, Juenger et al., 2000), while patterns of phenotypic integration may also maintain the internal cohesion of an organism or developmental system (Pigliucci, 2003). Modular organisation of a structure, and thus relative independence of constituents parts is generally hypothesised to permit adaptation of individual regions without detrimental effects on other parts of the whole (Riedl, 1977, Raff, 1996, Wagner and Altenberg, 1996, Wagner and Mezey, 2004, Wagner et al., 2007a, Hansen, 2003, Hallgrímsson et al., 2009), and as such

modularity may increase evolvability. Modularity may however impede evolvability by reduction of the mutational target size (Wagner, 1996, Wagner and Altenberg, 1996, Hansen, 2003). Conversely strong covariation structure has been posited to be an evolutionary constraint (Klingenberg, 2005a), and similarly pleiotropy may lower the probability that a mutation will have beneficial effects on all characters (Griswold, 2006, Orr, 2000). There is also however the potential that a mutation which effects multiple traits, or a highly coordinated system in which a mutation in one region results in a suite of phenotypic changes in other functionally or developmentally linked regions, may have an increased probability of having a beneficial effect on at least one character. In such cases, even if the acting mutation had deleterious effects on some traits, a net benefit could be achieved (Griswold, 2006).

Results of the present study have significant implications for our understanding of the evolvability of the cranial and mandibular complex. This study shows the potential for plastic adaptation to maintain masticatory function when variance in terms of form is present within the craniomandibular skeleton. The plastic capacity of the musculoskeletal system indicated by these findings may buffer variation in terms of form arising from both individual variation occurring during development and/or intraspecific variation between individuals such that function is maintained. A number of authors have shown maintenance of measures of functional performance during ontogeny when substantial variation in terms of both shape and size occurs within individuals (La Croix et al., 2011b, Tanner et al., 2010, Vincent et al., 2007, Meyers et al., 2002, Birch, 1999, Richard and Wainwright, 1995). Intraspecific variation in skull form has also been a common focus of numerous studies (Dalrymple, 1977, Humphrey et al., 1999, Domning and Hayek, 1986, Cheverud, 1989, Bastir and Rosas, 2004, Barahona and Barbadillo, 1998, Hospitaleche and Tambussi, 2006, Dierbach, 1986, Radinsky, 1981b, Freitas et al., 2005). While some of these investigations have concentrated upon dietary and geographic differences between individuals of a species, sexual dimorphism is the key focus of many. However, intra-specific and intra-strain differences in cranial and mandibular form, unrelated to sexual dimorphism and despite dietary and functional overlap, has been documented (Young et al., 2010, Young et al., 2007). Within humans two archetypal

extremes of cranial form, exclusive of sexual dimorphism and termed brachycephalic and dolichocephalic have been described (Enlow and Hans, 1996b, Bastir et al., 2005a, Bastir and Rosas, 2004). Similar patterns of intraspecific shape variation, airohynchy and klinorhynchy, have been described in primates (Bastir and Rosas, 2004, Hofer, 1952) and within other species and strains such as domestic dog breeds (Onar and Güneş, 2003). If these widely documented differences in terms of cranial form within a given species were to equate to significant differences in terms of masticatory function, such intraspecific morphological variance in individuals who exploit the same habitats and dietary resources would perhaps be surprising. Results of the present study may help to explain diversity of cranial and mandibular morphology within species. If plastic adaptation is able to maintain both coordination of form and function when variation occurs in one region of the overall complex, then individual morphological variation may be possible without cost to masticatory performance. Thus within one species perceptible differences in form may be present without significant differences in function, such that all individual possess the same fitness in terms of masticatory ability.

The ability of the masticatory system to plastically adapt to maintain function when variation occurs in form however may also have negative implications for the evolvability of masticatory performance. If the craniomandibular complex is able to plastically adapt in response to variation such that functional performance is maintained, then performance differences between individuals will not occur due to regional a mutational variance. While such a plastic compensatory buffering effect could be beneficial when a change in form would have deleterious effects on functional performance; equally such a mechanism that absorbed functional differences could remove the beneficial effects of an alteration in form that would serve to increase functional performance. Thus the number of mutations within a population that were translated into functional differences upon with selection could act would be decreased, and thus the potential evolvability of the complex would decrease. However, one potential evolutionary advantage of a capacity for plastic adaptation to maintain consistent functional performance despite morphological diversity, is the potential of other regions or functions within the cranium and mandible to modify without deleterious effect on masticatory performance. If

masticatory performance differences do not automatically ensue from individual differences in terms of form, then evolutionary advantageous differences in terms of morphology and subsequent non-masticatory functions may be permitted. For example, if a mutation increased cranial length, leading to increased cranial capacity and brain size, plastic adaptation within the masticatory complex could allow such a beneficial mutation to persist without deleterious effects on the vital function of mastication. Such a compensatory plastic mechanism within the masticatory complex, although not delivering evolutionary advantage in terms of masticatory performance capacity, may allow mutations with other regions or pertaining to other functions to accumulate within a population without deleterious effects on feeding.

The model sample utilised in the present study reveals that not only does global coordination within the craniomandibular complex result in maintenance of crucial size and shape relationships of the upper and lower jaw such that occlusion is maintained when variation is present in an isolated region (see Chapter 5: Craniomandibular integration and adaptive plasticity in the murine skull), but also that the relatively independent adaptation of muscle attachment areas may preserve functional performance in terms of mechanical advantage. Although the plastic ability of the masticatory complex is not documented extensively (Ravosa et al., 2010), early maturity and maintenance of jaw in- and out- levers during post-natal development has been reported in coyotes (La Croix et al., 2011b) and hyenas (Tanner et al., 2010), a time in which considerable changes occur in both the size and shape of the cranium and mandible. In addition, while direct causal links are yet to be established, there is some indication that attachment sites of the jaw-closing masticatory muscles may show evidence of postnatal plasticity in response to muscle hyperplasia (Byron et al., 2004, Byron et al., 2006, Nicholson et al., 2006, Ravosa et al., 2010).

Mechanical advantage, the amount of force transferred through a lever such as the jaw, is not the only consideration when assessing the ability of the complex to be able to effectively capture and process food. A reduction in the mechanical advantage of a lever arm system may favour the development of speed (Cassini and Vizcaíno, 2012). While muscles whose lines of action pass close to the pivot may have a relatively reduced mechanical advantage and thus relatively weak

movements, these movements will be rapid in comparison to the slow by strong movements produced by muscles whose line of action are distant to the pivot (Smith and Savage, 1956, Reduker, 1983). Production of a large force at the dentition is however usually more important than the ability to a rapid movement, this mandibular morphology is usually adapted to give large mechanical advantages of key jaw closing muscles (Smith and Savage, 1956). Additional morphological traits such as condyle height may also influence the functional performance of the complex. A high condyle may result in result in improved leverage for certain key masticatory muscles such as the masseter (Smith and Savage, 1956, Crompton and Hiiemae, 1969, Cassini and Vizcaíno, 2012).

Perhaps the most importance measure of the performance of the craniomandibular complex is bite force. The ability to generate a high bite force is not only vital in determining the dietary range of a vertebrate (Davis et al., 2010, Huber et al., 2005, Aguirre et al., 2003, Herrel et al., 2001, Herrel et al., 2002, Freeman and Lemen, 2007), but also may be decisive in determining territories (Herrel et al., 1999, Lailvaux et al., 2004, Lappin and Husak, 2005, Vanhooydonck et al., 2005) and mates (Huyghe et al., 2005, Lailvaux et al., 2004). While the *in vivo* measurement of bite force is becoming more commonplace (Chazeau et al., 2013, Schaerlaeken et al., 2012, Vanhooydonck et al., 2011, Measey et al., 2011, Aguirre et al., 2002, Dumont et al., 2009, Hylander et al., 1992, Santana and Dumont, 2009, Santana et al., 2010, Williams et al., 2009), prediction of bite force based upon approximations of skull structure and masticatory muscle morphology and physiology are frequently seen (Christiansen and Adolfssen, 2005, Thomason, 1991a, Ellis et al., 2008, Wroe et al., 2005, Davis et al., 2010, Thomason et al., 1990, Christiansen and Wroe, 2007, Curtis et al., 2010b). Such predictions of bite force begin with the modelling of the masticatory complex as a static third-class lever (Crompton, 1963, Greaves, 1978) but in addition requires data regarding muscle force magnitudes, which themselves may be estimated from muscle attachment areas, locations and directions relative to the temporomandibular joint, muscle pennation and muscle mass (Davis et al., 2010, Curtis et al., 2010b, Antón, 1999, Weijs and Dantuma, 1975a, Ross et al., 2005). A standard measure of muscle area is measured physiological cross-sectional area (PCSA) (Herrel et al., 2008, Santana et al., 2010, Taylor et al., 2009, Perry, 2008,

Davis et al., 2010, Curtis et al., 2010b, Antón, 1999) yet a lack of data availability has led to methods of estimating PCSA (Thomason, 1991a, Davis et al., 2010, Kiltie, 1982, Kiltie, 1984). Muscle force magnitude estimates are then determined by multiplication of PCSA with muscle stress (Mendez and Keys, 1960, Van Ruijven and Weijs, 1990).

While yet to be precisely understood, plastic adaptation may occur in not only the general bony structures of the craniomandibular complex and muscle attachment sites (Byron et al., 2004, Byron et al., 2006, Nicholson et al., 2006), but also in the masticatory musculature itself (Ravosa et al., 2010). Throughout ontogeny the masticatory musculature varies in terms of architecture (Herring et al., 1991, Herring and Wineski, 1986, Korfage et al., 2006), fibre-type composition (Maxwell et al., 1979, Shelton et al., 1988, Bredman et al., 1992, Anapol and Herring, 2000, Korfage et al., 2006, Abe et al., 2007, Langenbach et al., 2007), and mechanical advantage (Ravosa, 1991, Ravosa and Daniel, 2010). Long term dietary modification has also been shown to influence physiological cross-sectional area of the masseter muscle (Taylor et al., 2006). As growing mammals begin to adopt an adult-equivalent diet, they may require a greater force-generating capacity conferred by greater numbers of relatively larger type II muscle fibres (Sciote and Morris, 2000) and indeed, analyses of monkeys, mice, dogs and rabbits have all shown postnatal increases in Type II muscle fibre cross sectional area (Korfage et al., 2006, Anapol and Herring, 2000, Maxwell et al., 1979, Shelton et al., 1988, Bredman et al., 1992, Abe et al., 2007, Langenbach et al., 2007). The adaptive potential of the masseter muscle in growing mammal has been shown to adjust to alteration in the material properties of their diet, with a high fracture-resistant diet found to induce physiological variance in both the abundance, type and cross-sectional area of jaw-muscle fibre types (Ravosa et al., 2010).

Limitation of the sample of utilised in the present study includes a current lack of available information regarding muscle anatomy and physiology in the two mutant strains, and thus prevention of both measurement of *in vivo* bite force measurement and estimates of bite force. While measures of mechanical advantage provide some indication of the functional performance of the craniomandibular complex in this model sample, this functional analysis is by no means exhaustive. Results show

maintenance of skeletal size and shape relations (see Chapter 5: Craniomandibular integration and adaptive plasticity in the murine skull) and mechanical advantage when cranial length is altered early on in development, yet the potential for plastic adaptation in jaw muscle fibre type composition (Maxwell et al., 1979, Shelton et al., 1988, Bredman et al., 1992, Anapol and Herring, 2000, Korfage et al., 2006, Abe et al., 2007, Langenbach et al., 2007) and architecture (Herring et al., 1991, Herring and Wineski, 1986, Korfage et al., 2006) could result in divergent bite force capacities in the three strains. Further work is needed to establish muscle anatomy and composition in the three strains of mice, and thus predictions of bite force.

CHAPTER 6 DISCUSSION

6.1 DISCUSSION

This thesis demonstrates the plastic capacity of the cranium and mandible to maintain both coordination of form, and functional performance, when morphological variation occurs in one skeletal region of the complex. Results suggest a hierarchical organisation of composite parts both within and between these skeletal regions, such that units both display semi-independence and interdependence. This juxtaposition of integration and modularity allows some developmentally and/or functionally linked regions to be modified with relative independence of others, while global coordination of parts is still achieved. Adaptive plasticity on top of such hierarchical skeletal organisation is shown to provide both coordination between cranial and mandibular morphology when variation occurs in cranial morphology alone; and maintenance of parameters of functional performance despite both this cranial, and subsequent mandibular, morphological variation.

This assessment of both the morphological and functional response of the craniomandibular complex when variation occurs in cranial length is of great interest as variation is a fundamental feature of both development and evolution. Both the cranium and mandible are exposed to substantial changes in shape and size throughout ontogeny, and are required to adapt to both external and internal stimuli throughout life. Coordination of complex skeletal systems with such ongoing morphological variation is made particularly challenging in regions such as the skull which perform numerous dynamic functions. The cranium and mandible together house major sensory structures as well as performing vital functions such as respiration and food acquisition and processing. The ability to be able to maintain not only coordination between composite parts of these units, but also appropriate functional performance despite variation in the morphology of components is essential to the survival of an individual.

Epigenetic coordination between cranial and mandible was found, preserving appropriate size and shape relationships between these two semi independent

regions. As specific mutations in the model sample alter cranial length alone (Kurima et al., 1998, Sansal and Sellers, 2004, Lieberman et al., 2008, Hallgrímsson and Lieberman, 2008, Hallgrímsson et al., 2006), corresponding mandibular lengths and morphologies found in the two mutant strains are as a result of epigenetic plastic adaptation (Chapter 4). This finding of strong coordination between cranial and mandibular morphology, though achieved via plastic adaptation, is likely facilitated by the presence of strong integration within and between cranial and mandibular units.

Not only are size and shape relationship found to be preserved between the cranium and mandible of all three strains, but functional performance in terms of mechanical advantage is also found to be maintained despite significant differences in cranial and jaw out-lever length (Chapter 5). This maintenance of the mechanical efficiency of the masticatory system in spite of variance in cranial and mandibular length is attributed to plastic adaptation of masticatory muscle attachment sites and thus muscle in-lever lengths.

The coordinated plastic capacity of the cranium and mandible revealed by these investigations indicates the potential of this dynamic complex to minimise the possible deleterious effects of both individual morphological variation, and variation in form occurring during development. Findings of these investigations indicate that adaptive plasticity in association with a hierarchically organised skeletal system may not only buffer variation in terms of form such that necessary size and shape relationships are maintained (for example such that appropriate occlusion is maintained); but that this capacity may extend to the buffering and maintenance of biomechanical measures of function.

This result has substantial implications for our understanding of both intraspecific variation, and the preservation of form and function throughout development. A number of recent investigations have demonstrated maintenance of measures of masticatory functional performance throughout ontogeny and despite the variation in both the size and shape of cranial and mandibular components associated with development (La Croix et al., 2011b, Tanner et al., 2010, Vincent et al., 2007, Meyers et al., 2002, Birch, 1999, Richard and Wainwright, 1995). As cranial length

variation is a key factor in the development of many species, these studies provide an interesting parallel to concepts explored in this work. Results of this thesis not only support results of these studies, but due to the model sample employed indicate that this maintenance is achieved via epigenetic plastic adaptation in regions of the complex.

Intraspecific variation in craniomandibular morphology has been demonstrated in numerous species (Dalrymple, 1977, Humphrey et al., 1999, Domning and Hayek, 1986, Cheverud, 1989, Bastir and Rosas, 2004, Barahona and Barbadillo, 1998, Hospitaleche and Tambussi, 2006, Dierbach, 1986, Radinsky, 1981b, Freitas et al., 2005). The potential of plastic adaptation to buffer variance in form such that function is preserved may help to explain the continued presence of multiple species with large intraspecific differences in cranial and mandibular form. Extremes of integrated spectrums of craniomandibular form, such as the brachycephalic and dolichocephalic conditions found in humans (Enlow and Hans, 1996b, Bastir et al., 2005a, Bastir and Rosas, 2004) and other species including dogs (Wayne, 1986, Haworth et al., 2001, Young and Bannasch, 2006, Drake and Klingenberg, 2010), other carnivores (Wroe and Milne, 2007, Sears et al., 2007) and cats (Künzel et al., 2003); and the airorhynch and klinorhynch conditions found in the great apes (Bastir and Rosas, 2004, Hofer, 1952, Cobb and Baverstock, 2009a) could be expected to have different consequences for masticatory function thus leading a range of performance capacities within one species. If plastic adaptation is able to adapt regions of the craniomandibular complex when individual variation is present however, then it is possible that despite a significant range of morphologies within one species, feeding performance may be maintained within a suitable range for the dietary requirements of that species.

This notable finding not only highlights the capacity of plasticity to adapt skeletal regions such that functional performance is preserved, but also indicates a complex hierarchical arrangement of constituent regions of the craniomandibular complex. All biological systems, including skeletal complexes such as the skull, are composed of parts that may be recognised as relatively distinct of other parts. Such semi-independent regions are termed modules, and are characterised by strong internal interactions and relative independence of other regions (Schlosser and Wagner,

2004, Wagner et al., 2007a, Breuker et al., 2006b, Wagner, 1996, Klingenberg, 2005a). The strong internal interactions found within modules may be referred to as integration. Integration however is not limited to the connections within modules, but degrees of connection exist between modules, and modules may be present within other modules (Klingenberg, 2005a). Where variation is present, integration may be revealed as the covariation and correlation of traits (Hallgrímsson et al., 2009), these correlations tending to be particularly strong in functionally- and developmentally related characters (Olson and Miller, 1958, Atchley, 1984, Atchley, 1983, Atchley et al., 1985b, Atchley et al., 1985a, Cheverud, 1982a, Cheverud, 1984, Cheverud, 1995, Cheverud, 1989, Zelditch and Carmichael, 1989, Zelditch et al., 1990, Cowley and Atchley, 1990, Berg, 1960, Kingsolver and Wiernasz, 1991, Leamy, 1977, Wagner, 1990).

Patterns of covariation revealed between the crania and mandibles of the model sample utilised in this investigation indicate a high level of global integration within the complex. This integration between the cranial and mandibular units is shown to facilitate the preservation of appropriate size and shape relationships between these two semi-independent parts, such that plastic adaptation results in non-heritable mandibular forms that correctly correspond to crania which show mutationally induced variation in length. In addition a suite of morphological features, consistent across the three strains are observed. Such suites of integrated character traits have been reported within a number of species including humans (Bastir and Rosas, 2004, Enlow and Hans, 1996a, Zollikofer and Ponce de Leon, 2002, Lieberman et al., 2000a, Moss and Salentijn, 1971, Bhat and Enlow, 1985, Enlow and McNamara, 1973), other primates (Bastir and Rosas, 2004, Bastir et al., 2005a, Cheverud, 1996a) and dogs (Wayne, 1986, Haworth et al., 2001, Young and Bannasch, 2006, Drake and Klingenberg, 2010). There is relative constancy to variation and covariation patterns for such suites of morphological traits due to the relative constancy of developmental patterns within species and among closely related species (Cheverud, 1996a). Thus in a sample such as that utilised in this investigation, where variation is caused by environmental and genetic factors which perturb a common, relatively invariant developmental system; similar suites of characters and phenotypic variation are both theoretically expected, and commonly observed (Cheverud, 1988,

Cheverud, 1996a). The common suite of integrated traits seen alongside variation in cranial length within both the cranium and mandible of the three strains explored in this thesis is particularly remarkable as observed mandibular morphology is reasonably assumed to be non-heritable in the two mutant mice samples. High levels of integration between the cranial and mandibular units allow plastic adaptation to retain these suites of traits in the brachymorph and pten strains.

The hierarchical organisation of complex skeletal systems however means that this high level of global integration within the craniomandibular complex does not rule out modularity within constituent regions. Findings of maintenance of masticatory functional performance in term of mechanical advantage are attributed to the plastic adaptation of masticatory muscle attachment sites such that muscle in-lever lengths are adapted alongside the induced variance in jaw out-levers. This result implies the ability of such plasticity to adapt some regions of the complex with relative independence of other regions. The latter is supported by results of shape analyses showing relative independence of a basic cranial shape and shape data pertaining to the masticatory lever arm system.

Both global integration, as demonstrated between the cranial and mandibular units, and modularity, as demonstrated between the masticatory lever arm system and general cranial shape have implications for the evolvability of the craniomandibular complex. The extent to which morphological variation observed within and between species may be attributed integration and/or modularity is thought to be a key determinant of evolutionary flexibility (Cheverud, 1984, Wagner and Altenberg, 1996, Klingenberg, 2005a). In some respects strong integration among parts of a skeletal complex may act as an evolutionary constraint, reducing the probability that a mutation will have beneficial effects on all characters (Griswold, 2006). If parts of a complex are under opposing selection regimes, then strong integration between those parts will reduce the capacity of those morphological traits to evolve; whereas a modular arrangement of those parts will increase evolvability by allowing for adaptation of semi-autonomous regions without deleterious effects on other parts (Hansen, 2003, Wagner and Altenberg, 1996, Riedl, 1977, Hallgrímsson et al., 2009, Raff, 1996, Wagner and Mezey, 2004, Wagner et al., 2007a, Drake and Klingenberg, 2010). Such modular organisation of parts however may however reduce mutational

target size, constraining evolution (Hansen, 2003, Wagner, 1996, Wagner and Altenberg, 1996); while covariation may result in an increased probability that a mutation will have a beneficial effect on a least one trait, or an overall net benefit (Griswold, 2006). Indeed, patterns of covariation and thus integration affect the direction of evolution (Arthur, 2001, Schluter, 1996), as the expression of coordinated variation has the potential to channel evolutionary change (Hallgrímsson et al., 2009, Hallgrímsson et al., 2007, Klingenberg, 2005a). This is because covariation determines the extent to which selection on one trait results in correlated responses in other traits (Cheverud, 1982a, Cheverud, 1984, Müller and Wagner, 1996, Wagner et al., 2007b), especially in the case of a complex structure such as the skull (Martínez-Abadías et al., 2009).

The results of this thesis indeed have substantial implications for our understanding of the evolvability of the craniomandibular complex. The capacity of masticatory muscle attachment sites to undergo plastic adaptation relatively independently of other cranial traits, such that muscle-in levers are adapted and mechanical advantage maintained, implies relative modularity of these regions. The resulting preservation of a constant mechanical advantage despite variation in cranial and mandibular length may however be detrimental to the evolvability of masticatory performance. While such plastic adaptation leading to maintenance of function would be beneficial alongside both variation associated with development, and individual genetic variance resulting in morphologies that would otherwise decrease masticatory performance; equally the probability of individual morphological variance resulting in increased masticatory performance would also be removed. As the potential evolvability of the complex relies upon performance differences for selection to act upon, removal of potential performance differences via the plastic buffering of variation in form, may constrain the evolution of the complex.

Mechanical advantage is not however the only determinant of the performance of the masticatory system. While mechanical advantage measures the efficiency of the system in transferring a muscle input force to an output force at the dentition, a trade-off often exists between the capacity of the lever-arm system to produce force at the dentition and other performance determinants. An increase in jaw out-lever length, when all other things remain equal, while reducing mechanical advantage

will increase speed (Westneat, 1994, Richard and Wainwright, 1995). Conversely a reduced out-lever length increases mechanical advantage while reducing speed. However, results of this thesis demonstrate the potential capacity of plasticity adaptation to maintain mechanical advantage via the adaptation of muscle in-lever lengths and despite variation in cranial and mandibular length, thus also maintaining speed.

There is also a trade-off between gape angle and muscle function and thus force production capacity. In general a large gape angle is found to result in increased stretch in the masticatory muscles, thus increased sarcomere excursion and reduction in muscle force production capacity (Williams and Goldspink, 1971, Williams and Goldspink, 1978, Gans, 1982, Eng et al., 2009, Herring and Herring, 1974, Paphangkorakit and Osborn, 1997, Lindauer et al., 1993, Turkawski and Van Eijden, 2001, Dumont and Herrel, 2003). The plastic adaptation to masticatory muscle attachment sites which is found to occur in association with changes in length, such that mechanical advantage is maintained, may affect the degree of stretch of masticatory muscles at high angled gapes, and thus force production capacity. A *stretch factor* may be calculated for a given cranial morphology, determining relative force production capacity of the masticatory apparatus with consideration to muscle stretch and gape angle (Williams et al., 2009, Herring and Herring, 1974). Stretch factor is increased when there is an increase in the difference between the distance between the temporomandibular joint and the muscles insertion, and the temporomandibular joint and the muscle origin. Stretch factor is also decreased when the angle between these two lengths is increased (Herring and Herring, 1974, Williams et al., 2009). Thus while plasticity within the craniomandibular complex may maintain the mechanical advantage of the masticatory system, the modification of masticatory muscle attachment sites occurring to achieve this maintenance may itself result in alteration to force production capacity of the muscles.

Maintenance of masticatory performance despite variance in cranial and mandibular morphology may however be beneficial to evolvability of the complex in terms of other functions. While food acquisition and processing is irrefutably key to the survival of an individual, the skull is required to perform many other vital functions such as respiration, and in addition houses major sensory organs. A capacity of

plastic adaptation to modify regions such as masticatory muscle attachment sites with relative independence of other regions such that masticatory performance was maintained would result in the ability to modify other functionally significant areas of the complex without detrimental effects on feeding. Thus while increased fitness may not be delivered in terms of masticatory function, beneficial effects may be found in other functions.

In conclusion, results of this thesis demonstrate the remarkable plastic capacity of the cranium and mandible. A dynamic and complex region, the craniomandibular skeleton must not only house major sensory structure and perform functions critical to the viability of the organism; but must also be able to manage and respond to ongoing modification and variation. Results of this work establish the potential of this complex to not only plastically adapt to variation in constituent regions in terms of form, but also in terms of function. Findings demonstrate that the introduction of skeletal variation with potential functional consequences leads to plastic epigenetic adaptation in other regions of the complex, such that the potential functional consequences of the initial variation are negated. As skeletal variation, such as that in terms of cranial length, is an integral part of both development and evolution, and is commonly seen between individuals of the same species; these results are highly significant. This thesis demonstrates that individual variation occurring early on in development can initiate coordinated plastic adaptation in other regions of the complex such that functional performance is maintained at a species appropriate level. Such notable plastic buffering of variation in form may not however be without drawbacks. As selection acts upon performance, negation of performance differences when individual skeletal variance occurs will remove the potential of evolution to select upon such variance.

A detailed explanation of the mechanisms behind such plastic potential is beyond the remit of this work, however hypotheses may be drawn. While in part genes determine morphology of a skeletal structure and indeed the phenotype of an organism (Niven, 1933, Murray and Huxley, 1925, Murray, 1936), prior to translation into macroscopic growth genes are up- or down-regulated by mechanical stimuli (Mao and Nah, 2004). Regulation of genetic pathways thus comes from the external environment, specifically in terms of stress (Herring, 1993, Huiskes, 2000,

Skerry et al., 2000, Rauch and Schoenau, 2001, Moore, 2003, Müller, 2003, Lobe et al., 2006). Much of phenotypic variation in terms of skeletal structures is known to be determined by both internal and external stresses which induce the differential and growth of bone cells (Frost, 1987, Huiskes, 2000, Rauch and Schoenau, 2001, Mao and Nah, 2004, Badyaev and Foresman, 2004, Young and Badyaev, 2007, Badyaev et al., 2005). Mechanical forces play a critical role in the regulation of both chondrogenesis and osteogenesis as well as being vital to the processes of bone repair and remodelling (Herring and Lakars, 1981, Lanyon, 1984, Frost, 1987, Atchley et al., 1991, Thorogood, 1993, Huiskes, 2000, Skerry et al., 2000, Rauch and Schoenau, 2001, Mao and Nah, 2004, Carter et al., 1998, Mao, 2002, van der Meulen and Huiskes, 2002). In terms of the craniomandibular and masticatory complex, masticatory muscle stimulation plays a significant role in stress placed on the cranium and mandible, and as such cranial and mandibular development, growth and remodelling (Enlow, 1963, Lanyon and Rubin, 1984, Lanyon, 1993, Frost, 1987). We may therefore hypothesise that a cellular feedback mechanism may exist by which masticatory stresses throughout the developmental period result in the epigenetic growth and remodelling of regions of the complex, such that morphological modifications ensue in order to minimise craniomandibular stress and maximise performance potential.

6.2 LIMITATIONS AND NEED FOR FUTHER INVESTIGATION

Bite force is arguably the key performance measurement when assessing the masticatory potential of the craniomandibular skeleton. High, or at least species appropriate bite force generation is vital not only in determining the dietary range of vertebrates (Davis et al., 2010, Huber et al., 2005, Aguirre et al., 2003, Herrel et al., 2001, Herrel et al., 2002, Freeman and Lemen, 2007), but may also play a role in resolving territories (Herrel et al., 1999, Lailvaux et al., 2004, Lappin and Husak, 2005, Vanhooydonck et al., 2005) and acquiring mates (Huyghe et al., 2005, Lailvaux et al., 2004).

Ideally, contemporary authors are able to take *in vivo* measurement of bite force (Chazeau et al., 2013, Schaerlaeken et al., 2012, Vanhooydonck et al., 2011, Measey et al., 2011, Aguirre et al., 2002, Dumont et al., 2009, Hylander et al., 1992, Santana and Dumont, 2009, Santana et al., 2010, Williams et al., 2009). Where this is not possible methods to predict bite force have been developed, these estimates generated from detailed knowledge of skull morphology, masticatory muscle morphology and architecture (Christiansen and Adolfssen, 2005, Thomason, 1991a, Ellis et al., 2008, Wroe et al., 2005, Davis et al., 2010, Thomason et al., 1990, Christiansen and Wroe, 2007, Curtis et al., 2010b). Initially comparable to measures of mechanical advantage of the masticatory system, these methods involve modelling the jaw as a third-class static lever (Crompton, 1963, Greaves, 1978). Availability of data either giving measures or estimates of muscle force magnitude (Herrel et al., 2008, Davis et al., 2010, Santana et al., 2010) then allow calculation of an estimate of bite force.

Limitation of this thesis largely derive from a lack of available muscle data and anatomy particularly for the brachymorph and pten strains, and generally for all individuals of the sample. The sample utilised in the investigations detailed in Chapters 4 and 5 was in the form of micro-CT scans. Attempts were made to reconstruct masticatory musculature from these scans, but results showed poor validity and repeatability. In the absence of available specimens or scan types or qualities that enable clear differentiation of the masticatory musculature of the sample other measures of masticatory performance such as bite force calculation were unavailable.

In the absence of availability of the necessary sample to measure or calculate an estimation of bite force, mechanical advantage is an appropriate and widely used (Vincent et al., 2007, Dechow and Carlson, 1990, Adams and Rohlf, 2000, Westneat, 2003, Metzger and Herrel, 2005, Stayton, 2006, Oyen et al., 1979, La Croix et al., 2011b, La Croix et al., 2011a, Tanner et al., 2010, Throckmorton and Throckmorton, 1985, Swiderski and Zelditch, 2010, Radinsky, 1985a, Meyers et al., 2002, Birch, 1999, Richard and Wainwright, 1995) measure of performance capacity of the masticatory system. There has been previous suggestion that while mechanical advantage is a widely used measurement of performance capacity among different

species, maintenance of mechanical advantage within species may be due to mechanical advantage being an unreliable intraspecific measure of performance potential (Vincent et al., 2007), although no explanation is given to this assertion. Other authors however have measured mechanical advantage within species (Huber and Motta, 2004).

Necessary muscle data for the brachymorph and pten strains may become available in the future, and if so it may be possible to at least provide estimates of bite force capacity in both these mutant strains and the comparison wild-type strain. This would provide confirmation of whether overall masticatory performance is maintained despite variation in craniomandibular lengths between the three strains. If bite forces were found to be significantly different between the three strains this however would not negate results of this thesis. Plastic adaptation leading to maintenance of mechanical advantage may provide some performance compensation when morphological variation occurs in the craniomandibular complex during either or both development and evolution. Indeed, it was previously found that during ontogeny coyote juveniles attain adult mechanical advantage measurement early in the developmental period despite ongoing changes in the size and shape of the cranium and mandible (La Croix et al., 2011b). These juveniles however show decreased bite force capacity when compared to adults, leading the authors to suggest that early maturity of mechanical advantage helps assist feeding performance in juveniles such that any functional disadvantage is not exacerbated (La Croix et al., 2011b, La Croix et al., 2011a). Thus if differences in bite force were identified between the three mouse strains assessed in this thesis this might imply that maintenance of mechanical advantage despite morphological variance is a strategy to alleviate the impact of other performance differences.

Further work is also needed to establish potential feedback pathways and mechanisms which would allow plasticity to adapt areas such as the masticatory muscle attachment sites such that performance was maintained despite variance in other regions of the craniomandibular complex.

REFERENCES

- ABE, S., MAEJIMA, M., WATANABE, H., SHIBAHARA, T., AGEMATSU, H., SAKIYAMA, K., USAMI, A., GOJYO, K., HASHIMOTO, M. & YOSHINARI, M. 2002. Muscle-fiber characteristics in adult mouse-tongue muscles. *Anatomical Science International*, 77, 145-148.
- ABE, S., SAKIYAMA, K. & IDE, Y. 2007. Muscle plasticity: changes in oral function of muscle fiber characteristics. *Journal of Oral Biosciences*, 49, 219-223.
- ACKERMANN, R. R. 2005. Ontogenetic integration of the hominoid face. *Journal of Human Evolution*, 48, 175-97.
- ACKERMANN, R. R. & CHEVERUD, J. M. 2000. Phenotypic covariance structure in tamarins (genus *Saguinus*): a comparison of variation patterns using matrix correlation and common principal component analysis. *American Journal of Physical Anthropology*, 111, 489.
- ADAMS, D., CARDINI, A., MONTEIRO, L., O'HIGGINS, P. & ROHLF, F. 2011. Morphometrics and phylogenetics: principal components of shape from cranial modules are neither appropriate nor effective cladistic characters. *Journal of Human Evolution*, 60, 240.
- ADAMS, D. C. & ROHLF, F. J. 2000. Ecological character displacement in *Plethodon*: biomechanical differences found from a geometric morphometric study. *Proceedings of the National Academy of Sciences*, 97, 4106-4111.
- ADOBE 2012. Adobe Illustrator CS6. 26.0.0. ed.: Adobe Systems Incorporated.
- AERTS, P., D'AOÛT, K., HERREL, A. & VAN DAMME, R. 2002. Scaling of morphology, bite force and feeding kinematics in an iguanian and a scleroglossan lizard.
- AGRAWAL, A. A. 2001. Phenotypic plasticity in the interactions and evolution of species. *Science*, 294, 321-326.
- AGUIRRE, L., HERREL, A., VAN DAMME, R. & MATTHYSEN, E. 2003. The implications of food hardness for diet in bats. *Functional Ecology*, 17, 201-212.
- AGUIRRE, L. F., HERREL, A., VAN DAMME, R. & MATTHYSEN, E. 2002. Ecomorphological analysis of trophic niche partitioning in a tropical savannah bat community. *Proceedings of the Royal Society of London. Series B: Biological Sciences*, 269, 1271-1278.
- ALBERCH, P. 1982. Developmental constraints in evolutionary processes. *Evolution and Development*. Springer.
- ALFARO, M. E., BOLNICK, D. I. & WAINWRIGHT, P. C. 2004. Evolutionary dynamics of complex biomechanical systems: an example using the four-bar mechanism. *Evolution*, 58, 495-503.
- ALFARO, M. E., BOLNICK, D. I. & WAINWRIGHT, P. C. 2005. Evolutionary consequences of many-to-one mapping of jaw morphology to mechanics in labrid fishes. *The American Naturalist*, 165, E140-E154.
- AMIN, S., KOPPERDHAL, D. L., MELTON, L. J., ACHENBACH, S. J., THERNEAU, T. M., RIGGS, B. L., KEAVENY, T. M. & KHOSLA, S. 2011. Association of hip strength estimates by finite-element analysis with

- fractures in women and men. *Journal of Bone and Mineral Research*, 26, 1593-1600.
- ANAPOL, F. & HERRING, S. W. 2000. Ontogeny of histochemical fiber types and muscle function in the masseter muscle of miniature swine. *American Journal of Physical Anthropology*, 112, 595-613.
- ANDERSON, P. S. 2008. Shape variation between arthropod morphotypes indicates possible feeding niches. *Journal of Vertebrate Paleontology*, 28, 961-969.
- ANTÓN, S. C. 1999. Macaque masseter muscle: internal architecture, fiber length and cross-sectional area. *International Journal of Primatology*, 20, 441-462.
- ARTHUR, W. 2001. Developmental drive: an important determinant of the direction of phenotypic evolution. *Evolution & Development*, 3, 271-278.
- ASLANIDI, O., NIKOLAIDOU, T., ZHAO, J., SMAILL, B., GILBERT, S., JARVIS, J., STEPHENSON, R., HANCOX, J., BOYETT, M. & ZHANG, H. 2012. Application of micro-computed tomography with iodine staining to cardiac imaging, segmentation and computational model development. *IEEE Transactions on Medical Imaging*, 32, 8-17.
- ASZÓDI, A., F. BATEMAN, J., GUSTAFSSON, E., BOOT-HANDFORD, R. & FÄSSLER, R. 2000. Mammalian skeletogenesis and extracellular matrix: what can we learn from knockout mice? *Cell Structure and Function*, 25, 73-84.
- ATCHLEY, W. 1983. A genetic analysis of the mandible and maxilla in the rat. *Journal of Craniofacial Genetics and Developmental Biology*, 3, 409.
- ATCHLEY, W. R. 1984. Ontogeny, timing of development, and genetic variance-covariances structure. *The American Naturalist*, 123, 519-540.
- ATCHLEY, W. R. 1993. Genetic and developmental aspects of variability in the mammalian mandible. In: HANKEN, J. & HALL, B. K. (eds.) *The Skull*. Chicago: The University of Chicago Press.
- ATCHLEY, W. R. & HALL, B. K. 1991. A model for development and evolution of complex morphological structures. *Biological Reviews*, 66, 101-157.
- ATCHLEY, W. R., LOGSDON, T., COWLEY, D. E. & EISEN, E. 1991. Uterine effects, epigenetics, and postnatal skeletal development in the mouse. *Evolution*, 891-909.
- ATCHLEY, W. R., NEWMAN, S. & COWLEY, D. E. 1988. Genetic divergence in mandible form in relation to molecular divergence in inbred mouse strains. *Genetics*, 120, 239-253.
- ATCHLEY, W. R., PLUMMER, A. A. & RISKA, B. 1985a. Genetic analysis of size-scaling patterns in the mouse mandible. *Genetics*, 111, 579-595.
- ATCHLEY, W. R., PLUMMER, A. A. & RISKA, B. 1985b. Genetics of mandible form in the mouse. *Genetics*, 111, 555-577.
- AUFFRAY, J. C., ALIBERT, P., LATIEULE, C. & DOD, B. 1996. Relative warp analysis of skull shape across the hybrid zone of the house mouse (*Mus musculus*) in Denmark. *Journal of Zoology*, 240, 441-455.
- AUTODESK, I. 2013. Autodesk 3ds Max 2013.
- AVIZO6 2009. Avizo6. Berlin: Visualisation Sciences Group.
- BADEA, C. T., DRANGOVA, M., HOLDSWORTH, D. W. & JOHNSON, G. A. 2008. In vivo small-animal imaging using micro-CT and digital subtraction angiography. *Physics in Medicine and Biology*, 53, R319.

- BADYAEV, A. V. 2005. Stress-induced variation in evolution: from behavioural plasticity to genetic assimilation. *Proceedings of the Royal Society B: Biological Sciences*, 272, 877-886.
- BADYAEV, A. V. & FORESMAN, K. R. 2004. Evolution of Morphological Integration. I. Functional Units Channel Stress-Induced Variation in Shrew Mandibles. *The American Naturalist*, 163, 868-879.
- BADYAEV, A. V., FORESMAN, K. R. & YOUNG, R. L. 2005. Evolution of morphological integration: developmental accommodation of stress-induced variation. *The American Naturalist*, 166, 382-395.
- BALL, S. S. & ROTH, V. L. 1995. Jaw muscles of new-world squirrels. *Journal of Morphology*, 224.
- BARAHONA, F. & BARBADILLO, L. J. 1998. Inter-and intraspecific variation in the post-natal skull of some lacertid lizards. *Journal of Zoology*, 245, 393-405.
- BASTIR, M. 2008. A systems-model for the morphological analysis of integration and modularity in human craniofacial evolution. *Journal of Anthropological Sciences*, 86, 37-58.
- BASTIR, M. & ROSAS, A. 2004. Facial heights: Evolutionary relevance of postnatal ontogeny for facial orientation and skull morphology in humans and chimpanzees. *Journal of Human Evolution*, 47, 359-381.
- BASTIR, M. & ROSAS, A. 2005. Hierarchical nature of morphological integration and modularity in the human posterior face. *American Journal of Physical Anthropology*, 128, 26-34.
- BASTIR, M. & ROSAS, A. 2006. Correlated variation between the lateral basicranium and the face: A geometric morphometric study in different human groups. *Archives of Oral Biology*, 51, 814-824.
- BASTIR, M., ROSAS, A. & KUROE, K. 2004. Petrosal orientation and mandibular ramus breadth: Evidence for an integrated petroso-mandibular developmental unit. *American Journal of Physical Anthropology*, 123, 340-350.
- BASTIR, M., ROSAS, A. & SHEETS, D. H. 2005a. The morphological integration of the hominoid skull: a partial least squares and PC analysis with implications for European middle Pleistocene mandibular variation. In: SLICE, D. E. (ed.) *Modern Morphometrics in Physical Anthropology. Developments in Primatology: Progress and Prospects*. New York: Kluwer Academic/Plenum Publishers.
- BASTIR, M., ROSAS, A. & SHEETS, H. 2005b. The morphological integration of the hominoid skull: a partial least squares and PC analysis with implications for European Middle Pleistocene mandibular variation. *Modern morphometrics in physical anthropology*, 265-284.
- BASTIR, M., SOBRAL, P. G., KUROE, K. & ROSAS, A. 2008. Human craniofacial sphericity: A simultaneous analysis of frontal and lateral cephalograms of a Japanese population using geometric morphometrics and partial least squares analysis. *Archives of Oral Biology*, 53, 295-303.
- BATES, K. T. & FALKINGHAM, P. L. 2012. Estimating maximum bite performance in *Tyrannosaurus rex* using multi-body dynamics. *Biology Letters*.
- BAVERSTOCK, H., JEFFERY, N. S. & COBB, S. N. 2013. The morphology of the mouse masticatory musculature. *Journal of Anatomy*, 223, 46-60.

- BECHT, G. Comparative biologic-anatomical researches on mastication in some mammals. *Proc Kon Ned Akad Wet, Ser C*, 1953. 508-527.
- BERG, R. 1960. The ecological significance of correlation pleiades. *Evolution*, 171-180.
- BERNAYS, E. 1986. Diet-induced head allometry among foliage-chewing insects and its importance for graminivores. *Science*, 231, 495-497.
- BERRY, R. J. A. 1900. The true caecal apex, or the vermiform appendix: its minute and comparative anatomy. *Journal of Anatomy and Physiology*, 35, 83-100.
- BHASKAR, S., WEINMANN, J. & SCHOUR, I. 1953. Role of Meckel's cartilage in the development and growth of the rat mandible. *Journal of Dental Research*, 32, 398-410.
- BHAT, M. & ENLOW, D. H. 1985. Facial variations related to headform type. *The Angle Orthodontist*, 55, 269-280.
- BIEGERT, J. 1963. The evaluation of characteristics of the skull, hands and feet for primate taxonomy. *Classification and Human Evolution*, 116-145.
- BIEWENER, A. A. 1993. Safety factors in bone strength. *Calcified Tissue International*, 53, S68-S74.
- BIEWENER, A. A. & BERTRAM, J. 1993. Skeletal strain patterns in relation to exercise training during growth. *Journal of Experimental Biology*, 185, 51-69.
- BIEWENER, A. A., SWARTZ, S. M. & BERTRAM, J. E. 1986. Bone modeling during growth: dynamic strain equilibrium in the chick tibiotarsus. *Calcified Tissue International*, 39, 390-395.
- BIKNEVICIUS, A. R. 1996. Functional discrimination in the masticatory apparatus of juvenile and adult cougars (*Puma concolor*) and spotted hyenas (*Crocuta crocuta*). *Canadian Journal of Zoology*, 74, 1934-1942.
- BINDER, W. J. & VAN VALKENBURGH, B. 2000. Development of bite strength and feeding behaviour in juvenile spotted hyenas (*Crocuta crocuta*). *Journal of Zoology*, 252, 273-283.
- BIRCH, J. M. 1999. Skull allometry in the marine toad, *Bufo marinus*. *Journal of Morphology*, 241, 115-126.
- BLACK, B. L., CROOM, J., EISEN, E., PETRO, A. E., EDWARDS, C. L. & SURWIT, R. S. 1998. Differential effects of fat and sucrose on body composition in AJ and C57BL/6 mice. *Metabolism*, 47, 1354-1359.
- BLANGA-KANFI, S., MIRANDA, H., PENN, O., PUPKO, T., DEBRY, R. W. & HUCHON, D. 2009. Rodent phylogeny revised: analysis of six nuclear genes from all major rodent clades. *BMC Evolutionary Biology*, 9, 71.
- BOOKSTEIN, F. L. 1991. *Morphometric Tools for Landmark Data: Geometry and Biology*, Cambridge, Cambridge University Press.
- BOOKSTEIN, F. L., CHERNOFF, B., ELDER, R. L., HUMPHRIES, J., SMITH, G. R. & STRAUSS, R. E. 1985. *Morphometrics in evolutionary biology: the geometry of size and shape change, with examples from fishes*, Academy of Natural Sciences of Philadelphia Philadelphia.
- BOOKSTEIN, F. L., GUNZ, P., MITTEROECKER, P., PROSSINGER, H., SCHÆFER, K. & SEIDLER, H. 2003. Cranial integration in *Homo*: singular warps analysis of the midsagittal plane in ontogeny and evolution. *Journal of Human Evolution*, 44, 167-187.
- BOUGHNER, J. C., WAT, S., DIEWERT, V. M., YOUNG, N. M., BROWDER, L. W. & HALLGRÍMSSON, B. 2008. Short-faced mice and developmental

- interactions between the brain and the face. *Journal of Anatomy*, 213, 646-662.
- BOURKE, J., WROE, S., MORENO, K., MCHENRY, C. & CLAUSEN, P. 2008. Effects of gape and tooth position on bite force and skull stress in the dingo (*Canis lupus dingo*) using a 3-dimensional finite element approach. *PLoS ONE*, 3, e2200.
- BOUVIER, M. & HYLANDER, W. 1996. Strain gradients, age, and levels of modeling and remodeling in the facial bones of *Macaca fascicularis*. *The Biological Mechanisms of Tooth Movement and Craniofacial Adaptation*, 407-412.
- BOUVIER, M. & HYLANDER, W. L. 1981. Effect of bone strain on cortical bone structure in macaques (*Macaca mulatta*). *Journal of Morphology*, 167, 1-12.
- BRAMBLE, D. M. 1978. Origin of the mammalian feeding complex: models and mechanisms. *Paleobiology*, 271-301.
- BRANDT, J. 1855. Untersuchungen über die craniologischen Entwicklungsstufen und Classification der Nager der Jetztwelt. *Mém Acad Imp Sci St Pétersbourg, Sér*, 6, 1-365.
- BREDMAN, J., WEIJS, W., KORFAGE, H., BRUGMAN, P. & MOORMAN, A. 1992. Myosin heavy chain expression in rabbit masseter muscle during postnatal development. *Journal of Anatomy*, 180, 263.
- BREUKER, C. J., DEBAT, V. & KLINGENBERG, C. P. 2006a. *Trends Ecol. Evol.*, 21, 488.
- BREUKER, C. J., DEBAT, V. & KLINGENBERG, C. P. 2006b. Functional evo-devo. *Trends in Ecology & Evolution*, 21, 488-492.
- BRUECKNER, J. K., ITKIS, O. & PORTER, J. D. 1996. Spatial and temporal patterns of myosin heavy chain expression in developing rat extraocular muscle. *Journal of Muscle Research & Cell Motility*, 17, 297-312.
- BRUNE, R. M., BARD, J. B. L., DUBREUIL, C., GUEST, E., HILL, W., KAUFMAN, M., STARK, M., DAVIDSON, D. & BALDOCK, R. A. 1999. A three-dimensional model of the mouse at embryonic day 9. *Developmental Biology*, 216, 457-468.
- BUONANNO, A., CHENG, J., VENEPALLY, P., WEIS, J. & CALVO, S. 1998. Activity-dependent regulation of muscle genes: repressive and stimulatory effects of innervation. *Acta physiologica scandinavica*, 163, S17.
- BUONANNO, A. & ROSENTHAL, N. 1996. Molecular control of muscle diversity and plasticity. *Developmental Genetics*, 19, 95-107.
- BURGER, E. H. & KLEIN-NULEND, J. 1999a. Mechanotransduction in bone--role of the lacuno-canalicular network. *The FASEB journal : official publication of the Federation of American Societies for Experimental Biology*, 13 Suppl, S101-12.
- BURGER, E. H. & KLEIN-NULEND, J. 1999b. Mechanotransduction in bone—role of the lacuno-canalicular network. *The FASEB Journal*, 13, S101-S112.
- BURGIO, G., BAYLAC, M., HEYER, E. & MONTAGUTELLI, X. 2009. Genetic analysis of skull shape variation and morphological integration in the mouse using interspecific recombinant congenic strains between c57bl/6 and mice of the *mus spretus* species. *Evolution*, 63, 2668-2686.
- BYRD, K. E. 1981. Mandibular movement and muscle activity during mastication in the guinea pig (*Cavia porcellus*). *Journal of Morphology*, 170, 147-169.

- BYRON, C. D., BORKE, J., YU, J., PASHLEY, D., WINGARD, C. J. & HAMRICK, M. 2004. Effects of increased muscle mass on mouse sagittal suture morphology and mechanics. *The Anatomical Record Part A: Discoveries in Molecular, Cellular, and Evolutionary Biology*, 279A, 676-684.
- BYRON, C. D., HAMRICK, M. W. & WINGARD, C. J. 2006. Alterations of temporalis muscle contractile force and histological content from the myostatin and *Mdx* deficient mouse. *Archives of Oral Biology*, 51, 396-405.
- BYRON, C. D., MANESS, H., YU, J. C. & HAMRICK, M. W. 2008. Enlargement of the temporalis muscle and alterations in the lateral cranial vault. *Integrative and Comparative Biology*, 48, 338-344.
- CALLEBAUT, W. & RASSKIN-GUTMAN, D. 2005. *Modularity: understanding the development and evolution of natural complex systems*, Cambridge, USA, MIT Press.
- CARTER, D. R., BEAUPRÉ, G. S., GIORI, N. J. & HELMS, J. A. 1998. Mechanobiology of skeletal regeneration. *Clinical Orthopaedics and Related Research*, 355, S41-S55.
- CASSINI, G. H. & VIZCAÍNO, S. F. 2012. An approach to the biomechanics of the masticatory apparatus of early Miocene (Santacrucian Age) South American ungulates (Astrapotheria, Litopterna, and Notoungulata): moment arm estimation based on 3D landmarks. *Journal of Mammalian Evolution*, 19, 9-25.
- CHAI, Y., MAH, A., CROHIN, C., GROFF, S., BRINGAS JR, P., LE, T., SANTOS, V. & SLAVKIN, H. C. 1994. Specific transforming growth factor- β subtypes regulate embryonic mouse Meckel's cartilage and tooth development. *Developmental Biology*, 162, 85-103.
- CHAI, Y. & MAXSON, R. E. 2006. Recent advances in craniofacial morphogenesis. *Developmental Dynamics*, 235, 2353-2375.
- CHALK, J., RICHMOND, B. G., ROSS, C. F., STRAIT, D. S., WRIGHT, B. W., SPENCER, M. A., WANG, Q. & DECHOW, P. C. 2011. A finite element analysis of masticatory stress hypotheses. *American Journal of Physical Anthropology*, 145, 1-10.
- CHAMPY, M.-F., SELLOUM, M., ZEITLER, V., CARADEC, C., JUNG, B., ROUSSEAU, S., POUILLY, L., SORG, T. & AUWERX, J. 2008. Genetic background determines metabolic phenotypes in the mouse. *Mammalian Genome*, 19, 318-331.
- CHAZEAU, C., MARCHAL, J., HACKERT, R., PERRET, M. & HERREL, A. 2013. Proximate determinants of bite force capacity in the mouse lemur. *Journal of Zoology*.
- CHEGINI, S., BECK, M. & FERGUSON, S. J. 2009. The effects of impingement and dysplasia on stress distributions in the hip joint during sitting and walking: A finite element analysis. *Journal of Orthopaedic Research*, 27, 195-201.
- CHEN, D., ZHAO, M. & MUNDY, G. R. 2004. Bone morphogenetic proteins. *Growth Factors*, 22, 233-241.
- CHEVERUD, J. 1996a. Quantitative genetic analysis of cranial morphology in the cotton-top (*Saguinus oedipus*) and saddle-back (*S. fuscicollis*) tamarins. *Journal of Evolutionary Biology*, 9, 5-42.

- CHEVERUD, J. M. 1982a. Phenotypic, genetic, and environmental morphological integration in the cranium. *Evolution*, 36, 499-516.
- CHEVERUD, J. M. 1982b. Relationships among ontogenetic, static, and evolutionary allometry. *American Journal of Physical Anthropology*, 59, 139-149.
- CHEVERUD, J. M. 1984. Quantitative genetics and developmental constraints on evolution by selection. *Journal of Theoretical Biology*, 110, 155-171.
- CHEVERUD, J. M. 1988. A comparison of genetic and phenotypic correlations. *Evolution*, 958-968.
- CHEVERUD, J. M. 1989. A comparative analysis of morphological variation patterns in the Papionins. *Evolution*, 43, 1737-1747.
- CHEVERUD, J. M. 1995. Morphological Integration in the Saddle-Back Tamarin (*Saguinus fuscicollis*) Cranium. *The American Naturalist*, 145, 63-89.
- CHEVERUD, J. M. 1996b. Developmental Integration and the Evolution of Pleiotropy. *American Zoologist*, 36, 44-50.
- CHEVERUD, J. M., EHRICH, T. H., VAUGHN, T. T., KOREISHI, S. F., LINSEY, R. B. & PLETSCHER, L. S. 2004. Pleiotropic effects on mandibular morphology II: differential epistasis and genetic variation in morphological integration. *Journal of Experimental Zoology Part B: Molecular and Developmental Evolution*, 302, 424-435.
- CHEVERUD, J. M., HARTMANN, D., RICHTSMIEIER, J. T. & ATCHLEY, W. R. 1991. A quantitative genetic analysis of localized morphology in mandibles of inbred mice using finite element scaling analysis. *Journal of Craniofacial Genetic Developmental Biology*, 11, 122-137.
- CHEVERUD, J. M., ROUTMAN, E. J. & IRSCHICK, D. J. 1997. Pleiotropic effects of individual gene loci on mandibular morphology. *Evolution*, 2006-2016.
- CHINWALLA, A. T., COOK, L. L., DELEHAUNTY, K. D., FEWELL, G. A., FULTON, L. A., FULTON, R. S., GRAVES, T. A., HILLIER, L. W., MARDIS, E. R. & MCPHERSON, J. D. 2002. Initial sequencing and comparative analysis of the mouse genome. *Nature*, 420, 520-562.
- CHRISTIANSEN, P. 2007. Evolutionary implications of bite mechanics and feeding ecology in bears. *Journal of Zoology*, 272, 423-443.
- CHRISTIANSEN, P. & ADOLFSEN, J. S. 2005. Bite forces, canine strength and skull allometry in carnivores (Mammalia, Carnivora). *Journal of Zoology*, 266, 133-151.
- CHRISTIANSEN, P. & WROE, S. 2007. Bite forces and evolutionary adaptations to feeding ecology in carnivores. *Ecology*, 88, 347-358.
- COBB, S. N. 2011. Craniofacial biomechanics: in vivo to in silico. *Journal of Anatomy*, 218, 1-2.
- COBB, S. N. & BAVERSTOCK, H. Integrated variation in facial orientation and the craniomandibular skeleton in the extant great apes. *American Journal of Physical Anthropology*, 2009a S48, 107.
- COBB, S. N. & BAVERSTOCK, H. 2009b. Tooth root and craniomandibular morphological integration in the common chimpanzee (*Pan troglodytes*): alternative developmental models for the determinants of root length. In: KOPPE, T., MEYER, G. & ALT, K. W. (eds.) *Alternative Developmental Models for the Determinants of Root Length: Interdisciplinary Dental Morphology*. Basel: Karger.

- COLDIRON, R. W. 1977. On the jaw musculature and relationships of *Petrodomus tetradactylus* (Mammalia, Macroscelidea). *American Museum Novitates*, 2613, 1-12.
- CORDEIRO-ESTRELA, P., BAYLAC, M., DENYS, C. & MARINHO-FILHO, J. 2006. Interspecific patterns of skull variation between sympatric brazilian vesper mice: geometric morphometrics assessment. *Journal of Mammalogy*, 87, 1270-1279.
- CORTI, M. & ROHLF, F. J. 2001. Chromosomal speciation and phenotypic evolution in the house mouse. *Biological Journal of the Linnean Society*, 73, 99-112.
- COWIN, S. C. 2007. The significance of bone microstructure in mechanotransduction. *Journal of Biomechanics*, 40, S105-S109.
- COWLEY, D. E. & ATCHLEY, W. R. 1990. Development and quantitative genetics of correlation structure among body parts of *Drosophila melanogaster*. *American Naturalist*, 242-268.
- COX, P. G. & JEFFERY, N. 2011. Reviewing the morphology of the jaw-closing musculature in Squirrels, Rats, and Guinea Pigs with contrast-enhanced microCT. *The Anatomical Record*, 294, 915-928.
- COX, P. G., RAYFIELD, E. J., FAGAN, M. J., HERREL, A., PATAKY, T. C. & JEFFERY, N. 2012. Functional evolution of the feeding system in rodents. *PLoS ONE*, 7, e36299.
- CRAY, J., KNEIB, J., VECCHIONE, L., BYRON, C., COOPER, G. M., LOSEE, J. E., SIEGEL, M. I., HAMRICK, M. W., SCIOTE, J. J. & MOONEY, M. P. 2011. Masticatory hypermuscularity is not related to reduced cranial volume in myostatin-knockout mice. *The Anatomical Record: Advances in Integrative Anatomy and Evolutionary Biology*, 294, 1170-1177.
- CROMPTON, A. 1963. The evolution of the mammalian jaw. *Evolution*, 431-439.
- CROMPTON, R. H. & HIIEMAE, K. 1969. How mammalian molar teeth work. *Discovery*, 5, 23-34.
- CURREY, J. D. 2002. *Bones: structure and mechanics*, Woodstock, Princeton University Press.
- CURREY, J. D. 2005. Bone architecture and fracture. *Current Osteoporosis Reports* 3, 52.
- CURTIS, N. 2011. Craniofacial biomechanics: an overview of recent multibody modelling studies. *Journal of Anatomy*, 218, 16-25.
- CURTIS, N., JONES, M. E. H., EVANS, S. E., SHI, J., O'HIGGINS, P. & FAGAN, M. J. 2010a. Predicting muscle activation patterns from motion and anatomy: modelling the skull of *Sphenodon* (Diapsida: Rhynchocephalia). *Journal of The Royal Society Interface*, 7, 153-160.
- CURTIS, N., JONES, M. E. H., LAPPIN, A. K., O'HIGGINS, P., EVANS, S. E. & FAGAN, M. J. 2010b. Comparison between in vivo and theoretical bite performance: Using multi-body modelling to predict muscle and bite forces in a reptile skull. *Journal of Biomechanics*, 43, 2804-2809.
- CURTIS, N., JONES, M. E. H., SHI, J., O'HIGGINS, P., EVANS, S. E. & FAGAN, M. J. 2011a. Functional relationship between skull form and feeding mechanics in *Sphenodon*, and implications for Diapsid skull development. *PLoS ONE*, 6, e29804.
- CURTIS, N., KUPCZIK, K., O'HIGGINS, P., MOAZEN, M. & FAGAN, M. 2008. Predicting skull loading: applying multibody dynamics analysis to a Macaque

- skull. *The Anatomical Record: Advances in Integrative Anatomy and Evolutionary Biology*, 291, 491-501.
- CURTIS, N., WITZEL, U., FITTON, L., O'HIGGINS, P. & FAGAN, M. 2011b. The mechanical significance of the temporal fasciae in *Macaca fascicularis*: an investigation using finite element analysis. *The Anatomical Record: Advances in Integrative Anatomy and Evolutionary Biology*, 294, 1178-1190.
- CURTIS, T. A., ASHRAFI, S. H. & WEBER, D. F. 1985. Canalicular communication in the cortices of human long bones. *The Anatomical Record*, 212, 336-344.
- DAEGLING, D. J. & MCGRAW, W. S. 2007. Functional morphology of the mangabey mandibular corpus: relationship to dental specializations and feeding behavior. *American Journal of Physical Anthropology*, 134, 50-62.
- DALRYMPLE, G. H. 1977. Intraspecific variation in the cranial feeding mechanism of turtles of the genus *Trionyx* (Reptilia, Testudines, Trionychidae). *Journal of Herpetology*, 255-285.
- DARWIN, C. 1859. On the origins of species by means of natural selection. *London: Murray*.
- DAVIS, D. D. 1961. Origin of the mammalian feeding mechanism. *American Zoologist*, 1, 229-234.
- DAVIS, J., SANTANA, S., DUMONT, E. & GROSSE, I. 2010. Predicting bite force in mammals: two-dimensional versus three-dimensional lever models. *The Journal of Experimental Biology*, 213, 1844-1851.
- DE CROMBRUGGHE, B., LEFEBVRE, V. & NAKASHIMA, K. 2001. Regulatory mechanisms in the pathways of cartilage and bone formation. *Current Opinion in Cell Biology*, 13, 721-728.
- DE ZEE, M., DALSTRA, M., CATTANEO, P. M., RASMUSSEN, J., SVENSSON, P. & MELSEN, B. 2007. Validation of a musculo-skeletal model of the mandible and its application to mandibular distraction osteogenesis. *Journal of Biomechanics*, 40, 1192-1201.
- DEBAT, V., MILTON, C. C., RUTHERFORD, S., KLINGENBERG, C. P. & HOFFMANN, A. A. 2006. *Evolution*, 60, 2529.
- DECHOW, P. C. & CARLSON, D. S. 1990. Occlusal force and craniofacial biomechanics during growth in rhesus monkeys. *American Journal of Physical Anthropology*, 83, 219-237.
- DELANY, A., AMLING, M., PRIEMEL, M., HOWE, C., BARON, R. & CANALIS, E. 2000. Osteopenia and decreased bone formation in osteonectin-deficient mice. *Journal of Clinical Investigation*, 105, 915-923.
- DEMES, B. & CREEL, N. 1988. Bite force, diet, and cranial morphology of fossil hominids. *Journal of Human Evolution*, 17, 657-670.
- DIERBACH, A. 1986. Intraspecific variability and sexual dimorphism in the skulls of *Pan troglodytes verus*. *Human Evolution*, 1, 41-50.
- DOMNING, D. P. & HAYEK, L. A. C. 1986. Interspecific and intraspecific morphological variation in manatees (Sirenia: *Trichechus*). *Marine Mammal Science*, 2, 87-144.
- DONAHUE, H. J., MCLEOD, K., RUBIN, C., ANDERSEN, J., GRINE, E., HERTZBERG, E. & BRINK, P. 1995. Cell-to-cell communication in osteoblastic networks: Cell line-dependent hormonal regulation of gap junction function. *Journal of Bone and Mineral Research*, 10, 881-889.

- DRAKE, A. G. & KLINGENBERG, C. P. 2010. Large-scale diversification of skull shape in domestic dogs: disparity and modularity. *The American Naturalist*, 175, 289-301.
- DRAKE, T. A., SCHADT, E., HANNANII, K., KABO, J. M., KRASS, K., COLINAYO, V., GREASER III, L. E., GOLDIN, J. & LUSIS, A. J. 2001. Genetic loci determining bone density in mice with diet-induced atherosclerosis. *Physiological Genomics*, 5, 205-215.
- DRUZINSKY, R. E. 2010a. Functional anatomy of incisor biting in *Aplodontia rufa* and sciuriform rodents - Part 1: masticatory muscles, skull shape and digging. *Cells Tissues Organs*, 191, 510-522.
- DRUZINSKY, R. E. 2010b. Functional anatomy of incisor biting in *Aplodontia rufa* and sciuriform rodents - Part 2: sciuriformity is efficacious for production of force at the incisors. *Cells Tissues Organs*, 192, 50-62.
- DRUZINSKY, R. E., DOHERTY, A. H. & DE VREE, F. L. 2011. Mammalian Masticatory Muscles: Homology, Nomenclature, and Diversification. *Integrative and Comparative Biology*, 51, 224-234.
- DRYDEN, I. & MARDIA, K. 1998. *Statistical analysis of shape*, New York, John Wiley and Sons.
- DUCY, P., DESBOIS, C., BOYCE, B., PINERO, G., STORY, B., DUNSTAN, C., SMITH, E., BONADIO, J., GOLDSTEIN, S. & GUNDBERG, C. 1996. Increased bone formation in osteocalcin-deficient mice. *Nature*, 382, 448-452.
- DUMONT, E., HERREL, A., MEDELLIN, R., VARGAS-CONTRERAS, J. & SANTANA, S. 2009. Built to bite: cranial design and function in the wrinkle-faced bat. *Journal of Zoology*, 279, 329-337.
- DUMONT, E. R. 1997. Cranial shape in fruit, nectar, and exudate feeders: implications for interpreting the fossil record. *American Journal of Physical Anthropology*, 102, 187-202.
- DUMONT, E. R., DAVIS, J. L., GROSSE, I. R. & BURROWS, A. M. 2011. Finite element analysis of performance in the skulls of marmosets and tamarins. *Journal of Anatomy*, 218, 151-162.
- DUMONT, E. R. & HERREL, A. 2003. The effects of gape angle and bite point on bite force in bats. *Journal of Experimental Biology*, 206, 2117-2123.
- DUNCAN, R. L. & TURNER, C. H. 1995. Mechanotransduction and the functional response of bone to mechanical strain. *Calcified Tissue International*, 57, 344-358.
- EASON, J. M., SCHWARTZ, G. A., PAVLATH, G. K. & ENGLISH, A. W. 2000. Sexually dimorphic expression of myosin heavy chains in the adult mouse masseter. *Journal of Applied Physiology*, 89, 251-258.
- EDGERTON, V., ZHOU, M., OHIRA, Y., KLITGAARD, H., JIANG, B., BELL, G., HARRIS, B., SALTIN, B., GOLLNICK, P. & ROY, R. 1995. Human fiber size and enzymatic properties after 5 and 11 days of spaceflight. *Journal of Applied Physiology*, 78, 1733-1739.
- EHRICH, T. H., VAUGHN, T. T., KOREISHI, S. F., LINSEY, R. B., PLETSCHER, L. S. & CHEVERUD, J. M. 2003. Pleiotropic effects on mandibular morphology I. Developmental morphological integration and differential dominance. *Journal of Experimental Zoology Part B: Molecular and Developmental Evolution*, 296, 58-79.

- EISENBERG, N. A. & BRODIE, A. G. 1965. Antagonism of temporal fascia to masseteric contraction. *The Anatomical Record*, 152, 185-192.
- ELDER, S. H., GOLDSTEIN, S. A., KIMURA, J. H., SOSLOWSKY, L. J. & SPENGLER, D. M. 2001. Chondrocyte differentiation is modulated by frequency and duration of cyclic compressive loading. *Annals of Biomedical Engineering*, 29, 476-482.
- ELKINS, J. M., STROUD, N. J., RUDERT, M. J., TOCHIGI, Y., PEDERSEN, D. R., ELLIS, B. J., CALLAGHAN, J. J., WEISS, J. A. & BROWN, T. D. 2011. The capsule's contribution to total hip construct stability – A finite element analysis. *Journal of Orthopaedic Research*, 29, 1642-1648.
- ELLIS, J. L., THOMASON, J. J., KEBREAB, E. & FRANCE, J. 2008. Calibration of estimated biting forces in domestic canids: comparison of post-mortem and in vivo measurements. *Journal of Anatomy*, 212, 769-780.
- EMERSON, S. B. 1985. Skull shape in frogs: correlations with diet. *Herpetologica*, 177-188.
- ENG, C. M., WARD, S. R., VINYARD, C. J. & TAYLOR, A. B. 2009. The morphology of the masticatory apparatus facilitates muscle force production at wide jaw gapes in tree-gouging common marmosets (*Callithrix jacchus*). *The Journal of Experimental Biology*, 212, 4040-4055.
- ENLOW, D. H. 1963. *Principles of bone remodeling*, CC Thomas.
- ENLOW, D. H. 1990. *Facial Growth*, Philadelphia, W B Saunders Co.
- ENLOW, D. H. & AZUMA, M. 1975. Functional growth boundaries in the human and mammalian face. In: BERGSMA, D., LANGMAN, J. & PAUL, N. W. (eds.) *Morphogenesis and Malformations of the Face and Brain*. . New York: Alan R. Liss, Inc.
- ENLOW, D. H. & HANS, M. G. 1996a. *Essential of Facial Growth*, Philadelphia, Saunders.
- ENLOW, D. H. & HANS, M. G. 1996b. *Essentials of Facial Growth*.
- ENLOW, D. H., KURODA, T. & LEWIS, A. B. 1971. The morphological and morphogenetic basis for craniofacial form and pattern. *The Angle Orthodontist*, 41, 161-188.
- ENLOW, D. H. & MCNAMARA, J. A. 1973. The neurocranial basis for facial form and pattern. *The Angle Orthodontist*, 43, 256-270.
- ENLOW, D. H., PFISTER, C., RICHARDSON, E. & KURODA, T. 1982. An analysis of Black and Caucasian craniofacial patterns. *The Angle Orthodontist*, 52, 279-287.
- ERICKSON, G. M., LAPPIN, A. K. & VLIET, K. A. 2003. The ontogeny of bite-force performance in American alligator (*Alligator mississippiensis*). *Journal of Zoology*, 260, 317-327.
- ESCOUFIER, Y. 1973. Le Traitement des Variables Vectorielles. *Biometrics*, 29, 751-760.
- FELSENSTEIN, J. 1988. Phylogenies and quantitative characters. *Annual Review of Ecology and Systematics*, 19, 445-471.
- FIELDS, H., PROFFIT, W., CASE, J. & VIG, K. 1986. Variables affecting measurements of vertical occlusal force. *Journal of Dental Research*, 65, 135-138.
- FITTON, L. 2007. Form-function complex of the primate masticatory apparatus. An investigation into the form-function complex of the Cercopithecinae

- masticatory apparatus using computer modelling. Liverpool: Department of Human Anatomy and Cell Biology, The University of Liverpool.
- FITTON, L., GROENING, F., COBB, S., FAGAN, M. & O'HIGGINS, P. Biomechanical Significance of Morphological Variation Between The Gracile *Australopithecus Africanus* (Sts5) and Robust *Australopithecus Boisei* (OH5). *Journal of Vertebrate Paleontology*, 2009. 96A-96A.
- FLANAGAN, S. P. 2014. *Biomechanics: A Case-based Approach*, Jones & Bartlett Publishers.
- FORD-HUTCHINSON, A. F., ALI, Z., SEERATTAN, R. A., COOPER, D. M. L., HALLGRÍMSSON, B., SALO, P. T. & JIRIK, F. R. 2005. Degenerative knee joint disease in mice lacking 3'-phosphoadenosine 5'-phosphosulfate synthetase 2 (Papss2) activity: a putative model of human PAPSS2 deficiency-associated arthrosis. *Osteoarthritis and Cartilage*, 13, 418-425.
- FREEMAN, P. W. & LEMEN, C. A. 2007. Using scissors to quantify hardness of insects: do bats select for size or hardness? *Journal of Zoology*, 271, 469-476.
- FREEMAN, P. W. & LEMEN, C. A. 2008a. Measuring bite force in small mammals with a piezo-resistive sensor. *Journal of Mammalogy*, 89, 513-517.
- FREEMAN, P. W. & LEMEN, C. A. 2008b. A simple morphological predictor of bite force in rodents. *Journal of Zoology*, 275, 418-422.
- FREITAS, T. R. O., LACEY, E. A. & MYERS, P. 2005. Analysis of skull morphology in 15 species of the genus *Ctenomys*, including seven karyologically distinct forms of *Ctenomys minutus* (Rodentia: Ctenomyidae). *Mammalian diversification: from chromosomes to phylogeography (a celebration of the career of James L. Patton)*(EA Lacey y P Myers, eds). *University of California Publications in Zoology*, 133, 131-154.
- FROMMER, J. & MARGOLIES, M. R. 1971. Contribution of Meckel's cartilage to ossification of the mandible in mice. *Journal of Dental Research*, 50, 1260-1267.
- FROST, H. 1990. Skeletal structural adaptations to mechanical usage (SATMU): 1. Redefining Wolff's law: the bone modeling problem. *The Anatomical Record*, 226, 403-413.
- FROST, H. M. 1987. Bone "mass" and the "mechanostat": A proposal. *The Anatomical Record*, 219, 1-9.
- GANS, C. 1982. Fiber architecture and muscle function. *Exercise and Sport Sciences Reviews*, 10, 160-207.
- GANS, C. & BOCK, W. J. 1965. The functional significance of muscle architecture-a theoretical analysis. *Ergebnisse der Anatomie und Entwicklungsgeschichte*, 38, 115.
- GANS, C. & DE VREE, F. 1987. Functional bases of fiber length and angulation in muscle. *Journal of Morphology*, 192, 63-85.
- GASSMANN, M. & HENNET, T. 1998. From genetically altered mice to integrative physiology. *Physiology*, 13, 53-57.
- GERBER, H.-P., VU, T. H., RYAN, A. M., KOWALSKI, J., WERB, Z. & FERRARA, N. 1999. VEGF couples hypertrophic cartilage remodeling, ossification and angiogenesis during endochondral bone formation. *Nature Medicine*, 5, 623-628.
- GERHARD, F. A., WEBSTER, D. J., VAN LENTHE, G. H. & MÜLLER, R. 2009. In silico biology of bone modelling and remodelling: adaptation.

- Philosophical Transactions of the Royal Society A: Mathematical, Physical and Engineering Sciences*, 367, 2011-2030.
- GILLESPIE, P. G. & WALKER, R. G. 2001. Molecular basis of mechanosensory transduction. *Nature*, 413, 194-202.
- GLASSTONE, S. 1971. Differentiation of the mouse embryonic mandible and squamo-mandibular joint in organ culture. *Archives of Oral Biology*, 16, 723-729.
- GOJO, K., ABE, S. & IDE, Y. 2002. Characteristics of myofibres in the masseter muscle of mice during postnatal growth period. *Anatomia, Histologia, Embryologia*, 31, 105-112.
- GÓMEZ-ROBLES, A. & POLLY, P. D. 2012. Morphological integration in the hominin dentition: evolutionary, developmental, and functional factors. *Evolution*, 66, 1024-1043.
- GONZÁLEZ-JOSÉ, R., VAN DER MOLEN, S., GONZÁLEZ-PÉREZ, E. & HERNÁNDEZ, M. 2004. Patterns of phenotypic covariation and correlation in modern humans as viewed from morphological integration. *American Journal of Physical Anthropology*, 123, 69-77.
- GONZÁLEZ-JOSÉ, R., VAN DER MOLEN, S., GONZÁLEZ-PÉREZ, E. & HERNANDEZ, M. 2003. Patterns of phenotypic covariation and correlation in modern humans as viewed from morphological integration. *American Journal of Physical Anthropology*, 123, 69-77.
- GOODALL, C. 1991. Procrustes methods in the statistical analysis of shape. *Journal of the Royal Statistical Society. Series B (Methodological)*, 285-339.
- GORDON, A., HUXLEY, A. F. & JULIAN, F. 1966. The variation in isometric tension with sarcomere length in vertebrate muscle fibres. *The Journal of Physiology*, 184, 170-192.
- GORNIK, G. C. 1977. Feeding in golden hamsters, *Mesocricetus auratus*. *Journal of Morphology*, 154, 427-458.
- GOSWAMI, A. 2006. Morphological integration in the carnivoran skull. *Evolution*, 60, 169-183.
- GOSWAMI, A. 2007. Phylogeny, diet, and cranial integration in australodelphian marsupials. *PLoS ONE*, 2, e995.
- GOSWAMI, A. & POLLY, P. D. 2010. The influence of modularity on cranial morphological disparity in Carnivora and Primates (Mammalia). *PLoS ONE*, 5, e9517.
- GOTTHARD, K. & NYLIN, S. 1995. Adaptive plasticity and plasticity as an adaptation: a selective review of plasticity in animal morphology and life history. *Oikos*, 3-17.
- GOVINDARAJAN, V. & OVERBEEK, P. A. 2006. FGF9 can induce endochondral ossification in cranial mesenchyme. *BMC Developmental Biology*, 6, 7.
- GOWER, J. C. 1975. Generalized procrustes analysis. *Psychometrika*, 40, 33-51.
- GREAVES, W. S. 1974. Functional implications of the mammalian jaw joint position. *Forma et Functio*, 7, 363-376.
- GREAVES, W. S. 1978. The jaw lever system in ungulates: a new model. *Journal of Zoology*, 184, 271-285.
- GREAVES, W. S. 1982. A mechanical limitation on the position of the jaw muscles of mammals: the one-third rule. *Journal of Mammalogy*, 261-266.
- GREAVES, W. S. 2000. Location of the vector of jaw muscle force in mammals. *Journal of Morphology*, 243, 293-299.

- GREENE, E. C. 1936. Anatomy of the Rat. *The American Journal of the Medical Sciences*, 191, 858.
- GRINE, F. E., JUDEX, S., DA EGLING, D. J., OZCIVICI, E., UNGAR, P. S., TEAFORD, M. F., SPONHEIMER, M., SCOTT, J., SCOTT, R. S. & WALKER, A. 2010. Craniofacial biomechanics and functional and dietary inferences in hominin paleontology. *Journal of Human Evolution*, 58, 293-308.
- GRISWOLD, C. K. 2006. Pleiotropic mutation, modularity and evolvability. *Evolution & Development*, 8, 81-93.
- GRODZINSKY, A. J., LEVENSTON, M. E., JIN, M. & FRANK, E. H. 2000. Cartilage tissue remodeling in response to mechanical forces. *Annual Review of Biomedical Engineering*, 2, 691-713.
- GRÖNING, F., FAGAN, M. J. & O'HIGGINS, P. 2011a. The effects of the periodontal ligament on mandibular stiffness: a study combining finite element analysis and geometric morphometrics. *Journal of Biomechanics*, 44, 1304-1312.
- GRÖNING, F., LIU, J., FAGAN, M. J. & O'HIGGINS, P. 2011b. Why do humans have chins? Testing the mechanical significance of modern human symphyseal morphology with finite element analysis. *American Journal of Physical Anthropology*, 144, 593-606.
- GRUBICH, J. R. & WESTNEAT, M. W. 2006. Four-bar linkage modelling in teleost pharyngeal jaws: computer simulations of bite kinetics. *Journal of Anatomy*, 209, 79-92.
- GUILAK, F. 1995. Compression-induced changes in the shape and volume of the chondrocyte nucleus. *Journal of Biomechanics*, 28, 1529-1541.
- GUILAK, F. & MOW, V. C. 2000. The mechanical environment of the chondrocyte: a biphasic finite element model of cell-matrix interactions in articular cartilage. *Journal of Biomechanics*, 33, 1663-1673.
- GUNZ, P. & HARVATI, K. 2007. The Neanderthal "chignon": variation, integration, and homology. *Journal of Human Evolution*, 52, 262-274.
- GUYTON, A. C. & HALL, J. E. 2006. *Textbook of Medical Physiology*, Philadelphia, Elsevier Saunders.
- HALL, B. K. 1999. *Evolutionary Developmental Biology*.
- HALL, B. K. 2005. *Bones and cartilage: developmental and evolutionary skeletal biology*, Access Online via Elsevier.
- HALL, J. E. 2010. *Guyton and Hall Textbook of Medical Physiology: Enhanced E-book*, Elsevier Health Sciences.
- HALLGRÍMSSON, B., BROWN, J. J. Y., FORD-HUTCHINSON, A. F., SHEETS, H. D., ZELDITCH, M. L. & JIRIK, F. R. 2006. The brachymorph mouse and the developmental-genetic basis for canalization and morphological integration. *Evolution & Development*, 8, 61-73.
- HALLGRÍMSSON, B., DORVAL, C. J., ZELDITCH, M. L. & GERMAN, R. Z. 2004a. Craniofacial variability and morphological integration in mice susceptible to cleft lip and palate. *Journal of Anatomy*, 205, 501-517.
- HALLGRÍMSSON, B., JAMNICZKY, H., YOUNG, N. M., ROLIAN, C., PARSONS, T. E., BOUGHNER, J. C. & MARCUCIO, R. S. 2009. Deciphering the palimpsest: studying the relationship between morphological integration and phenotypic covariation. *Evolutionary Biology*, 36, 355-376.

- HALLGRIMSSON, B. & LIEBERMAN, D. E. 2008. Mouse models and the evolutionary developmental biology of the skull. *Integrative and Comparative Biology*, 48, 373-384.
- HALLGRÍMSSON, B., LIEBERMAN, D. E., LIU, W., FORD-HUTCHINSON, A. F. & JIRIK, F. R. 2007. Epigenetic interactions and the structure of phenotypic variation in the cranium. *Evolution & Development*, 9, 76-91.
- HALLGRIMSSON, B., LIEBERMAN, D. E., YOUNG, N. M., PARSONS, T. & WAT, S. Evolution of covariance in the mammalian skull. Novartis Foundation Symposium, 2007. Chichester; New York; John Wiley; 1999, 164.
- HALLGRÍMSSON, B., WILLMORE, K., DORVAL, C. & COOPER, D. M. L. 2004b. Craniofacial variability and modularity in macaques and mice. *Journal of Experimental Zoology Part B: Molecular and Developmental Evolution*, 302B, 207-225.
- HAMILTON, D. L. & ABREMSKI, K. 1984. Site-specific recombination by the bacteriophage P1 lox-Cre system: Cre-mediated synapsis of two lox sites. *Journal of Molecular Biology*, 178, 481-486.
- HAMRICK, M. W. 1999. A chondral modeling theory revisited. *Journal of Theoretical Biology*, 201, 201-208.
- HANNAM, A. G., STAVNESS, I., LLOYD, J. E. & FELLS, S. 2008. A dynamic model of jaw and hyoid biomechanics during chewing. *Journal of Biomechanics*, 41, 1069-1076.
- HANSEN, T. & HOULE, D. 2008. Measuring and comparing evolvability and constraint in multivariate characters. *Journal of Evolutionary Biology*, 21, 1201-1219.
- HANSEN, T. F. 2003. Is modularity necessary for evolvability?: Remarks on the relationship between pleiotropy and evolvability. *Biosystems*, 69, 83-94.
- HAUTIER, L. 2010. Masticatory muscle architecture in the gundi *Ctenodactylus vali* (Mammalia, Rodentia). *Mammalia*.
- HAUTIER, L., LEBRUN, R. & COX, P. G. 2012. Patterns of covariation in the masticatory apparatus of hystricognathous rodents: Implications for evolution and diversification. *Journal of Morphology*.
- HAUTIER, L. & SAKSIRI, S. 2009. Masticatory muscle architecture in the Laotian rock rat *Laonastes aenigmamus* (Mammalia, Rodentia): new insights into the evolution of hystricognathy. *Journal of Anatomy*, 215, 401-410.
- HAWORTH, K. E., ISLAM, I., BREEN, M., PUTT, W., MAKRINO, E., BINNS, M., HOPKINSON, D. & EDWARDS, Y. 2001. Canine TCOF1; cloning, chromosome assignment and genetic analysis in dogs with different head types. *Mammalian Genome*, 12, 622-629.
- HEANEY, R. P. 1995. Bone mass, the mechanostat, and ethnic differences. *The Journal of Clinical Endocrinology and Metabolism*, 80, 2289.
- HERREL, A., DAMME, R. V., VANHOOYDONCK, B. & VREE, F. D. 2001. The implications of bite performance for diet in two species of lacertid lizards. *Canadian Journal of Zoology*, 79, 662-670.
- HERREL, A., DE SMET, A., AGUIRRE, L. F. & AERTS, P. 2008. Morphological and mechanical determinants of bite force in bats: do muscles matter? *Journal of Experimental Biology*, 211, 86-91.
- HERREL, A. & GIBB, A. C. 2006. Ontogeny of performance in vertebrates. *Physiological and Biochemical Zoology*, 79, 1-6.

- HERREL, A. & HOLANOVA, V. 2008. Cranial morphology and bite force in *Chamaeleolis* lizards—Adaptations to molluscivory? *Zoology*, 111, 467-475.
- HERREL, A., O'REILLY, J. & RICHMOND, A. 2002. Evolution of bite performance in turtles. *Journal of Evolutionary Biology*, 15, 1083-1094.
- HERREL, A., SPITHOVEN, L., VAN DAMME, R. & DE VREE, F. 1999. Sexual dimorphism of head size in *Gallotia galloti*: testing the niche divergence hypothesis by functional analyses. *Functional Ecology*, 13, 289-297.
- HERREL, A., VAN WASSENBERGH, S. & AERTS, P. 2003. Biomechanical studies of food and diet selection. *eLS*.
- HERRING, S. 1975. Adaptations for gape in the hippopotamus and its relatives. *Forma et Functio*, 8, 85-100.
- HERRING, S., ANAPOL, F. & WINESKI, L. 1991. Motor-unit territories in the masseter muscle of infant pigs. *Archives of Oral Biology*, 36, 867-873.
- HERRING, S. & LAKARS, T. C. 1981. Craniofacial development in the absence of muscle contraction. *Journal of Craniofacial Genetics and Developmental Biology*, 1, 341-357.
- HERRING, S. W. 1993. Formation of the vertebrate face epigenetic and functional influences. *American Zoologist*, 33, 472-483.
- HERRING, S. W. & HERRING, S. E. 1974. The superficial masseter and gape in mammals. *American Naturalist*, 561-576.
- HERRING, S. W. & WINESKI, L. E. 1986. Development of the masseter muscle and oral behavior in the pig. *Journal of Experimental Zoology*, 237, 191-207.
- HIEMAE, K. & HOUSTON, W. J. B. 1971. The structure and function of the jaw muscles in the rat (*Rattus norvegicus* L.). *Zoological Journal of the Linnean Society*, 50, 75-99.
- HIEMÄE, K. M. & ARDRAN, G. M. 1968. A cinefluorographic study of mandibular movement during feeding in the rat (*Rattus norvegicus*). *Journal of Zoology*, 154, 139-154.
- HILDEBRAND, M. 1988. *Analysis of Vertebrate Structure*, New York, John Wiley and Sons, Inc.
- HILDEBRAND, M. & GOSLOW, G. E. 2001. *Analysis of vertebrate structure*, J. Wiley.
- HILL, C. A., REEVES, R. H. & RICHTSMEIER, J. T. 2007. Effects of aneuploidy on skull growth in a mouse model of Down syndrome. *Journal of Anatomy*, 210, 394-405.
- HLUSKO, L. J. & MAHANEY, M. C. 2009. Quantitative genetics, pleiotropy, and morphological integration in the dentition of *Papio hamadryas*. *Evolutionary Biology*, 36, 5-18.
- HOFBAUER, L. C., KHOSLA, S., DUNSTAN, C. R., LACEY, D. L., BOYLE, W. J. & RIGGS, B. L. 2000. The roles of osteoprotegerin and osteoprotegerin ligand in the paracrine regulation of bone resorption. *Journal of Bone and Mineral Research*, 15, 2-12.
- HOFER, H. 1952. Des gestaltwandel des Schadels der Säugetiere und Vogel, mit besonderer Berücksichtigung der Knickungstypen und der Schadelbasiks. *Verh. Anat. Ges. Jena*, 50, 102-113.
- HOGAN, B. 1996. Bone morphogenetic proteins: multifunctional regulators of vertebrate development. *Genes & Development*, 10, 1580-1594.

- HOH, J. & HUGHES, S. 1988. Myogenic and neurogenic regulation of myosin gene expression in cat jaw-closing muscles regenerating in fast and slow limb muscle beds. *Journal of Muscle Research and Cell Motility*, 9, 59.
- HOLDEN, C. & VOGEL, G. 2002. Plasticity: time for a reappraisal? *Science*, 296, 2126-2129.
- HORI, A., ISHIHARA, A., KOBAYASHI, S. & IBATA, Y. 1998. Immunohistochemical classification of skeletal muscle fibers. *Acta Histochemica Et Cytochemica -Kyoto-*, 31, 375-384.
- HOSPITALECHE, C. A. & TAMBUSI, C. 2006. Skull morphometry of *Pygoscelis* (Sphenisciformes): inter and intraspecific variations. *Polar Biology*, 29, 728-734.
- HUBER, D. R., EASON, T. G., HUETER, R. E. & MOTTA, P. J. 2005. Analysis of the bite force and mechanical design of the feeding mechanism of the durophagous horn shark *Heterodontus francisci*. *Journal of Experimental Biology*, 208, 3553-3571.
- HUBER, D. R. & MOTTA, P. J. 2004. Comparative analysis of methods for determining bite force in the spiny dogfish *Squalus acanthias*. *Journal of Experimental Zoology Part A: Comparative Experimental Biology*, 301, 26-37.
- HUISKES, R. 2000. If bone is the answer, then what is the question? *Journal of Anatomy*, 197, 145-156.
- HUMPHREY, L., DEAN, M. & STRINGER, C. 1999. Morphological variation in great ape and modern human mandibles. *Journal of Anatomy*, 195, 491-513.
- HUNT, G. 2007. EVOLUTIONARY DIVERGENCE IN DIRECTIONS OF HIGH PHENOTYPIC VARIANCE IN THE OSTRACODE GENUS *POSEIDONAMICUS*. *Evolution*, 61, 1560-1576.
- HUXLEY, A. & NIEDERGERKE, R. 1954. Interference microscopy of living muscle fibres. *Nature*, 173, 13.
- HUXLEY, A. F. 1957. Muscle structure and theories of contraction. *Prog. Biophys. Biophys. Chem*, 7, 255-318.
- HUXLEY, H. & HANSON, J. 1954. Changes in the cross-striations of muscle during contraction and stretch and their structural interpretation. *Nature*, 173, 973-976.
- HUYGHE, K., VANHOOYDONCK, B., SCHEERS, H., MOLINA-BORJA, M. & VAN DAMME, R. 2005. Morphology, performance and fighting capacity in male lizards, *Gallotia galloti*. *Functional Ecology*, 19, 800-807.
- HYLANDER, W. L., JOHNSON, K. R. & CROMPTON, A. 1992. Muscle force recruitment and biomechanical modeling: an analysis of masseter muscle function during mastication in *Macaca fascicularis*. *American Journal of Physical Anthropology*, 88, 365-387.
- JACKSON-LABORATORY. 2013. *C57BL/6J; Strain Information* [Online]. The Jackson Laboratory. Available: <http://jaxmice.jax.org/strain/000664.html> [Accessed 03/12/2013 2013].
- JAMNICZKY, H. A. & HALLGRIMSSON, B. 2009. A comparison of covariance structure in wild and laboratory murid crania. *Evolution*, 63, 1540-1556.
- JAMNICZKY, H. A. & HALLGRIMSSON, B. 2011. Modularity in the skull and cranial vasculature of laboratory mice: implications for the evolution of complex phenotypes. *Evolution & Development*, 13, 28-37.

- JANIS, C. M. 1983a. Muscles of the masticatory apparatus in two genera of hyraxes (Procavia and Heterohyrax). *Journal of Morphology*, 176, 61-87.
- JANIS, C. M. 1983b. Muscles of the masticatory apparatus in two genera of hyraxes (Procavia and Heterohyrax). *Journal of Morphology*, 176, 61-87.
- JEFFERY, N., STEPHENSON, R., GALLAGHER, J. A., JARVIS, J. C. & COX, P. G. 2011. Micro-computed tomography with iodine staining resolves the arrangement of muscle fibres. *Journal of Biomechanics*, 44, 189-192.
- JIANG, X., ISEKI, S., MAXSON, R. E., SUCOV, H. M. & MORRISS-KAY, G. M. 2002. Tissue origins and interactions in the mammalian skull vault. *Developmental Biology*, 241, 106-116.
- JOJIC, V., BLAGOJEVIC, J., IVANOVIC, A., BUGARSKI-STANOJEVIC, V. & VUJOŠEVIC, M. 2007. Morphological integration of the mandible in yellow-necked field mice: The effects of B chromosomes. *Journal of Mammalogy*, 88, 689-695.
- JOJIĆ, V., BLAGOJEVIĆ, J. & VUJOŠEVIĆ, M. 2012. Two-module organization of the mandible in the yellow-necked mouse: a comparison between two different morphometric approaches. *Journal of Evolutionary Biology*.
- JONES, A. G., ARNOLD, S. J. & BÜRGER, R. 2007. The mutation matrix and the evolution of evolvability. *Evolution*, 61, 727-745.
- JUENGER, T., PURUGGANAN, M. & MACKAY, T. F. 2000. Quantitative trait loci for floral morphology in Arabidopsis thaliana. *Genetics*, 156, 1379-1392.
- KARDONG, K. V. 2002. *Vertebrates: comparative anatomy, function, evolution*, McGraw-Hill Boston.
- KAUFMAN, M. H. 1992. *The Atlas of Mouse Development* London, Academic Press.
- KAUFMAN, M. H. & BARD, J. B. L. 1999. *The Anatomical Basis of Mouse Development*, San Diego, Academic Press
- KAWAKAMI, M. & YAMAMURA, K.-I. 2008. Cranial bone morphometric study among mouse strains. *BMC Evolutionary Biology*, 8, 73.
- KENDALL, D. G. 1977. The diffusion of shape. *Advances in Applied Probability*, 9, 428-430.
- KENDALL, D. G. 1984. Shape manifolds, Procrustean metrics and complex projective spaces. *Bulletin of the London Mathematical Society*, 16, 81-121.
- KILTIE, R. A. 1982. Bite force as a basis for niche differentiation between rain forest peccaries (Tayassu tajacu and T. pecari). *Biotropica*, 188-195.
- KILTIE, R. A. 1984. Size ratios among sympatric neotropical cats. *Oecologia*, 61, 411-416.
- KINGSOLVER, J. G. & WIERNASZ, D. C. 1991. Development, function, and the quantitative genetics of wing melanin in pattern in Pieris butterflies. *Evolution*, 1480-1492.
- KLEIN-NULEND, J., BACABAC, R. & MULLENDER, M. 2005. Mechanobiology of bone tissue. *Pathologie Biologie*, 53, 576-580.
- KLEIN NULEND, J., PLAS, V. D. A., SEMEINS, C. M., FRANGOS, J. A., NIJWEIDE, P. J. & BURGER, E. H. 1995. Sensitivity of osteocytes to biomechanical stress in vitro. *Federation of American Societies for Experimental Biology Journal*, 9, 441 - 445.
- KLINGENBERG, C. P. 1998. Heterochrony and allometry: the analysis of evolutionary change in ontogeny. *Biological Reviews*, 73, 79-123.

- KLINGENBERG, C. P. 2002. Morphometrics and the role of the phenotype in studies of the evolution of developmental mechanisms. *Gene*, 287, 3-10.
- KLINGENBERG, C. P. 2003. Developmental instability as a research tool: using patterns of fluctuating asymmetry to infer the developmental origins of morphological integration. *Developmental instability: causes and consequences*, 427-442.
- KLINGENBERG, C. P. 2005a. Developmental constraints, modules and evolvability. *Variation: A central concept in biology*, 219-247.
- KLINGENBERG, C. P. 2005b. *Variation: A Central Concept in Biology*.
- KLINGENBERG, C. P. 2008. Morphological integration and developmental modularity. *Annual Review of Ecology, Evolution, and Systematics*, 39, 115-132.
- KLINGENBERG, C. P. 2009. Morphometric integration and modularity in configurations of landmarks: tools for evaluating a priori hypotheses. *Evolution & Development*, 11, 405-421.
- KLINGENBERG, C. P. 2012. MorphoJ. 1.05a ed.
- KLINGENBERG, C. P., BARLUENGA, M. & MEYER, A. 2002. Shape analysis of symmetric structures: quantifying variation among individuals and asymmetry. *Evolution*, 56, 1909-1920.
- KLINGENBERG, C. P. & LEAMY, L. J. 2001. Quantitative Genetics of Geometric Shape in the Mouse Mandible. *Evolution*, 55, 2342-2352.
- KLINGENBERG, C. P., LEAMY, L. J., ROUTMAN, E. J. & CHEVERUD, J. M. 2001. Genetic architecture of mandible shape in mice: effects of quantitative trait loci analyzed by geometric morphometrics. *Genetics*, 157, 785-802.
- KLINGENBERG, C. P. & MCINTYRE, G. S. 1998. Geometric Morphometrics of Developmental Instability: Analyzing Patterns of Fluctuating Asymmetry with Procrustes Methods. *Evolution*, 52, 1363-1375.
- KLINGENBERG, C. P., MEBUS, K. & AUFFRAY, J.-C. 2003. Developmental integration in a complex morphological structure: how distinct are the modules in the mouse mandible? *Evolution & Development*, 5, 522-531.
- KLINGENBERG, C. P. & ZAKLAN, S. D. 2000. Morphological integration between developmental compartments in the *Drosophila* wing. *Evolution*, 54, 1273-1285.
- KLINGENBERG, C. P. & ZIMMERMANN, M. 1992. Static, ontogenetic, and evolutionary allometry: a multivariate comparison in nine species of water striders. *The American Naturalist*, 140, 601-620.
- KLINTWORTH, G. K. 1968. The comparative anatomy and phylogeny of the tentorium cerebelli. *The Anatomical Record*, 160, 635-641.
- KOEHL, M. A. R. 1996. When does morphology matter? *Annual Review of Ecology and Systematics*, 27, 501-542.
- KOOLSTRA, J. H. & VAN EIJDEN, T. M. G. J. 1992. Application and validation of a three-dimensional mathematical model of the human masticatory system in vivo. *Journal of Biomechanics*, 25, 175-187.
- KOOLSTRA, J. H. & VAN EIJDEN, T. M. G. J. 2004. Functional significance of the coupling between head and jaw movements. *Journal of Biomechanics*, 37, 1387-1392.
- KOOLSTRA, J. H., VAN EIJDEN, T. M. G. J., WEIJS, W. A. & NAEIJE, M. 1988. A three-dimensional mathematical model of the human masticatory system

- predicting maximum possible bite forces. *Journal of Biomechanics*, 21, 563-576.
- KORFAGE, J., VAN WESSEL, T., LANGENBACH, G., AY, F. & VAN EIJDEN, T. 2006. Postnatal transitions in myosin heavy chain isoforms of the rabbit superficial masseter and digastric muscle. *Journal of Anatomy*, 208, 743-751.
- KOS, C. H. 2004. Methods in nutrition science: Cre/loxP system for generating tissue-specific knockout mouse models. *Nutrition Reviews*, 62, 243-246.
- KOYABU, D. B. & ENDO, H. 2009. Craniofacial variation and dietary adaptations of African colobines. *Journal of Human Evolution*, 56, 525-536.
- KULEMEYER, C., ASBAHR, K., GUNZ, P., FRAHNERT, S. & BAIRLEIN, F. 2009. Functional morphology and integration of corvid skulls—a 3D geometric morphometric approach. *Frontiers in Zoology*, 6.
- KÜNZEL, W., BREIT, S. & OPPEL, M. 2003. Morphometric investigations of breed-specific features in feline skulls and considerations on their functional implications. *Anatomia, histologia, embryologia*, 32, 218-223.
- KUPCZIK, K., DOBSON, C., CROMPTON, R., PHILLIPS, R., OXNARD, C. E., FAGAN, M. & O'HIGGINS, P. 2009. Masticatory loading and bone adaptation in the supraorbital torus of developing macaques. *American Journal of Physical Anthropology*, 139, 193-203.
- KUPCZIK, K., DOBSON, C., FAGAN, M., CROMPTON, R., OXNARD, C. & O'HIGGINS, P. 2007. Assessing mechanical function of the zygomatic region in macaques: validation and sensitivity testing of finite element models. *Journal of Anatomy*, 210, 41-53.
- KURIHARA, Y., KURIHARA, H., SUZUKI, H., KODAMA, T., MAEMURA, K., NAGAI, R., ODA, H., KUWAKI, T., CAO, W.-H. & KAMADA, N. 1994. Elevated blood pressure and craniofacial abnormalities in mice deficient in endothelin-1. *Nature*, 368, 703-710.
- KURIMA, K., WARMAN, M. L., KRISHNAN, S., DOMOWICZ, M., KRUEGER, R. C., DEYRUP, A. & SCHWARTZ, N. B. 1998. A member of a family of sulfate-activating enzymes causes murine brachymorphism. *Proceedings of the National Academy of Sciences of the United States of America*, 95, 8681-8685.
- KYRKANIDES, S., KAMBYLAFKAS, P., MILLER, J. H., TALLENTS, R. H. & PUZAS, J. E. 2007. The cranial base in craniofacial development: a gene therapy study. *Journal of Dental Research*, 86, 956-961.
- LA CROIX, S., HOLEKAMP, K. E., SHIVIK, J. A., LUNDRIGAN, B. L. & ZELDITCH, M. L. 2011a. Ontogenetic relationships between cranium and mandible in coyotes and hyenas. *Journal of Morphology*, 272, 662-674.
- LA CROIX, S., ZELDITCH, M. L., SHIVIK, J. A., LUNDRIGAN, B. L. & HOLEKAMP, K. E. 2011b. Ontogeny of feeding performance and biomechanics in coyotes. *Journal of Zoology*, 285, 301-315.
- LAILVAUX, S. P., HERREL, A., VANHOOYDONCK, B., MEYERS, J. J. & IRSCHICK, D. J. 2004. Performance capacity, fighting tactics and the evolution of life-stage male morphs in the green anole lizard (*Anolis carolinensis*). *Proceedings of the Royal Society of London. Series B: Biological Sciences*, 271, 2501-2508.
- LANE, P. W. & DICKIE, M. M. 1968. Three Recessive Mutations Producing Disproportionate Dwarfing in Mice: Aehondroplasia, brachymorphic, and stubby. Oxford University Press.

- LANGENBACH, G., VAN WESSEL, T., BRUGMAN, P., KORFAGE, J. & VAN EIJDEN, T. 2007. Is fiber-type composition related to daily jaw muscle activity during postnatal development? *Cells Tissues Organs*, 187, 307-315.
- LANGENBACH, G. E. J. & HANNAM, A. G. 1999. The role of passive muscle tensions in a three-dimensional dynamic model of the human jaw. *Archives of Oral Biology*, 44, 557-573.
- LANYON, L. 1984. Functional strain as a determinant for bone remodeling. *Calcified Tissue International*, 36, S56-S61.
- LANYON, L. & RUBIN, C. 1985. Functional adaptation in skeletal structures. *Functional Vertebrate Morphology*, 1-25.
- LANYON, L. E. 1993. Osteocytes, strain detection, bone modeling and remodeling. *Calcified Tissue International*, 53, S102-S107.
- LANYON, L. E. & RUBIN, C. T. 1984. Static vs dynamic loads as an influence on bone remodelling. *Journal of Biomechanics*, 17, 897-905.
- LAPPIN, A. K. & HUSAK, J. F. 2005. Weapon performance, not size, determines mating success and potential reproductive output in the collared lizard (*Crotaphytus collaris*). *The American Naturalist*, 166, 426-436.
- LEAMY, L. 1977. Genetic and environmental correlations of morphometric traits in randombred house mice. *Evolution*, 357-369.
- LEAMY, L. 1993. Morphological integration of fluctuating asymmetry in the mouse mandible. *Genetica*, 89, 139-153.
- LEAMY, L. & ATCHLEY, W. R. 1984. Morphometric integration in the rat (*Rattus* sp.) scapula. *Journal of Zoology*, 202, 43-56.
- LEAMY, L. J., KLINGENBERG, C. P., SHERRATT, E., WOLF, J. B. & CHEVERUD, J. M. 2008. A search for quantitative trait loci exhibiting imprinting effects on mouse mandible size and shape. *Heredity*, 101, 518-526.
- LEAMY, L. J., ROUTMAN, E. J. & CHEVERUD, J. M. 1999. Quantitative trait loci for early-and late-developing skull characters in mice: a test of the genetic independence model of morphological integration. *The American Naturalist*, 153, 201-214.
- LEVINS, R. 1968. *Evolution in Changing Environments: Some Theoretical Explorations*. (MPB-2), Princeton University Press.
- LEWONTIN, R. C. 1978. Adaptation. *Scientific American*, 239, 212-230.
- LI, S. 2011. Concise formulas for the area and volume of a hyperspherical cap. *Asian Journal of Mathematics & Statistics* 4., 4, 66-70.
- LIEBER, R. L. 2002. *Skeletal muscle structure, function, and plasticity*, Wolters Kluwer Health.
- LIEBER, R. L. & BOAKES, J. L. 1988. Sarcomere length and joint kinematics during torque production in frog hindlimb. *American Journal of Physiology-Cell Physiology*, 254, C759-C768.
- LIEBERMAN, D. E. 1997. Making behavioural and phylogenetic inferences from hominid fossils: considering the developmental influence of mechanical forces. *Annual Review of Anthropology*, 26, 185-210.
- LIEBERMAN, D. E., HALLGRÍMSSON, B., LIU, W., PARSONS, T. E. & JAMNICZKY, H. A. 2008. Spatial packing, cranial base angulation, and craniofacial shape variation in the mammalian skull: testing a new model using mice. *Journal of Anatomy*, 212, 720-735.

- LIEBERMAN, D. E., MCBRATNEY, B. M. & KROVITZ, G. 2002. The evolution and development of cranial form in *Homo sapiens*. *Proceedings of the National Academy of Sciences*, 99, 1134-1139.
- LIEBERMAN, D. E., PEARSON, O. M. & MOWBRAY, K. M. 2000a. Basicranial influence on overall cranial shape. *Journal of Human Evolution*, 38, 291-315.
- LIEBERMAN, D. E., ROSS, C. F. & RAVOSA, M. J. 2000b. The Primate Cranial Base: Ontogeny, Function and Integration. *Yearbook of Physical Anthropology*, 43, 269-280.
- LINDAUER, S., GAY, T. & RENDELL, J. 1993. Effect of jaw opening on masticatory muscle EMG-force characteristics. *Journal of Dental Research*, 72, 51-51.
- LOBE, S. L., BERNSTEIN, M. C. & GERMAN, R. Z. 2006. Life-long protein malnutrition in the rat (*Rattus norvegicus*) results in altered patterns of craniofacial growth and smaller individuals. *Journal of Anatomy*, 208, 795-812.
- LORENSEN, W. E. & CLINE, H. E. Marching cubes: A high resolution 3D surface construction algorithm. ACM Siggraph Computer Graphics, 1987. ACM, 163-169.
- LORENZO, J., HOROWITZ, M. & CHOI, Y. 2008. Osteoimmunology: interactions of the bone and immune system. *Endocrine Reviews*, 29, 403-440.
- LOZANOFF, S., JURECZEK, S., FENG, T. & PADWAL, R. 1994. Anterior cranial base morphology in mice with midfacial retrusion. *Cleft Palate Craniofacial Journal*, 31, 417-428.
- LYONS, G. E., ONTELL, M., COX, R., SASSOON, D. & BUCKINGHAM, M. 1990. The expression of myosin genes in developing skeletal muscle in the mouse embryo. *The Journal of Cell Biology*, 111, 1465-1476.
- MACHOLÁN, M. 2008. The mouse skull as a source of morphometric data for phylogeny inference. *Zoologischer Anzeiger - A Journal of Comparative Zoology*, 247, 315-327.
- MACHOLÁN, M., MIKULA, O. & VOHRALÍK, V. 2008. Geographic phenetic variation of two eastern-Mediterranean non-commensal mouse species, *Mus macedonicus* and *M. cypriacus* (Rodentia: Muridae) based on traditional and geometric approaches to morphometrics. *Zoologischer Anzeiger - A Journal of Comparative Zoology*, 247, 67-80.
- MACKENNA, B. & TÜRKER, K. 1978. Twitch tension in the jaw muscles of the cat at various degrees of mouth opening. *Archives of Oral Biology*, 23, 917-920.
- MACKENNA, B. R. 1983. Jaw separation and maximum incising force. *The Journal of Prosthetic Dentistry*, 49, 726-730.
- MACLEOD, N. & FOREY, P. L. 2004. *Morphology, shape and phylogeny*, CRC Press.
- MAEDAA, N. K., TSUYOSHI.; OSAWAC, KOICHI.; YAMAMOTOB, YOSHIRO.; SUMIDAB, HOSAKU.; MASUDAC, TAMURO.; KUMEGAWAA, MASAYOSHI. 1987. Effects of long-term intake of a fine-grained diet on the mouse masseter muscle. *Acta Anatomica*, 128, 326-333.
- MAKEDONSKA, J., WRIGHT, B. W. & STRAIT, D. S. 2012. The effect of dietary adaption on cranial morphological integration in capuchins (order primates, genus *cebus*). *PLoS ONE*, 7, e40398.

- MANLY, B. F. J. 2007. *Randomization, Bootstrap and Monte Carlo Methods in Biology*, Boca Raton, FL, Chapman & Hall/CRC.
- MANNING, A., MIRALLES, R. & PALAZZI, C. 1979. EMG, bite force, and elongation of the masseter muscle under isometric voluntary contractions and variations of vertical dimension. *The Journal of Prosthetic Dentistry*, 42, 674-682.
- MAO, J. 2002. Mechanobiology of craniofacial sutures. *Journal of Dental Research*, 81, 810-816.
- MAO, J. J. & NAH, H.-D. 2004. Growth and development: hereditary and mechanical modulations. *American Journal of Orthodontics and Dentofacial Orthopedics*, 125, 676-689.
- MARCUS, L. F., CORTI, M., LOY, A., NAYLOR, G. J. P. & SLICE, D. 1996. *Advances in morphometrics*, New York, Plenum.
- MARDIA, K. V., BOOKSTEIN, F. L. & MORETON, I. J. 2000. Statistical assessment of bilateral symmetry of shapes. *Biometrika*, 87, 285-300.
- MARROIG, G. & CHEVERUD, J. M. 2001. A comparison of phenotypic variation and covariation patterns and the role of phylogeny, ecology, and ontogeny during cranial evolution of New World monkeys. *Evolution*, 55, 2576-2600.
- MARROIG, G., VIVO, M. & CHEVERUD, J. 2003. Cranial evolution in sakis (Pithecia, Platyrrhini) II: evolutionary processes and morphological integration. *Journal of Evolutionary Biology*, 17, 144-155.
- MARTÍNEZ-ABADÍAS, N., ESPARZA, M., SJØVOLD, T., GONZÁLEZ-JOSÉ, R., SANTOS, M. & HERNÁNDEZ, M. 2009. Heritability of human cranial dimensions: comparing the evolvability of different cranial regions. *Journal of Anatomy*, 214, 19-35.
- MARTÍNEZ-ABADÍAS, N., ESPARZA, M., SJØVOLD, T., GONZÁLEZ-JOSÉ, R., SANTOS, M., HERNÁNDEZ, M. & KLINGENBERG, C. P. 2012. Pervasive genetic integration directs the evolution of human skull shape. *Evolution*.
- MATHWORKS Matlab. Natick, MA, USA.
- MAXWELL, L. C., CARLSON, D. S., MCNAMARA, J. A. & FAULKNER, J. A. 1979. Histochemical characteristics of the masseter and temporalis muscles of the rhesus monkey (*Macaca mulatta*). *The Anatomical Record*, 193, 389-401.
- MAYNE, R. 1990. Collagen Types and Chondrogenesis. *Annals of the New York Academy of Sciences*, 599, 39-44.
- MCCALL, G., BYRNES, W., DICKINSON, A., PATTANY, P. & FLECK, S. 1996. Muscle fiber hypertrophy, hyperplasia, and capillary density in college men after resistance training. *Journal of Applied Physiology*, 81, 2004-2012.
- MCLEOD, K. J., RUBIN, C. T., OTTER, M. W. & QIN, Y.-X. 1998. Skeletal cell stresses and bone adaptation. *The American Journal of the Medical Sciences*, 316, 176-183.
- MEASEY, G., REBELO, A., HERREL, A., VANHOOYDONCK, B. & TOLLEY, K. 2011. Diet, morphology and performance in two chameleon morphs: do harder bites equate with harder prey? *Journal of Zoology*, 285, 247-255.
- MELORO, C., RAIÁ, P., CAROTENUTO, F. & COBB, S. N. 2011. Phylogenetic signal, function and integration in the subunits of the carnivoran mandible. *Evolutionary Biology*, 38, 465-475.

- MENDEZ, J. & KEYS, A. 1960. Density and composition of mammalian muscle. *Metabolism*, 9, 184.
- MENG, J., HU, Y. & LI, C. 2003. The osteology of *Rhombomylus* (Mammalia, Glires): implications for phylogeny and evolution of Glires. *Bulletin of the American Museum of Natural History*, 1-247.
- METZGER, K. A. & HERREL, A. 2005. Correlations between lizard cranial shape and diet: a quantitative, phylogenetically informed analysis. *Biological Journal of the Linnean Society*, 86, 433-466.
- MEYERS, J., HERREL, A. & BIRCH, J. 2002. Scaling of morphology, bite force, and feeding kinematics in an iguanian and a sclerosglossan lizard. In: AERTS, P., D'AOUT, K., HERREL, A. & VAN DAMME, R. (eds.) *Topics in Functional and Ecological Vertebrate Morphology*. Maastricht: Shaker Publishing.
- MEZEY, J. G., CHEVERUD, J. M. & WAGNER, G. P. 2000. Is the Genotype-Phenotype Map Modular?: A Statistical Approach Using Mouse Quantitative Trait Loci Data. *Genetics*, 156, 305-311.
- MIETTINEN, P. J., CHIN, J. R., SHUM, L., SLAVKIN, H. C., SHULER, C. F., DERYNCK, R. & WERB, Z. 1999. Epidermal growth factor receptor function is necessary for normal craniofacial development and palate closure. *Nature Genetics*, 22, 69-73.
- MITTEROECKER, P. & BOOKSTEIN, F. 2007. The conceptual and statistical relationship between modularity and morphological integration. *Systematic Biology*, 56, 818-836.
- MITTEROECKER, P. & BOOKSTEIN, F. 2008. The evolutionary role of modularity and integration in the hominoid cranium. *Evolution*, 62, 943-958.
- MITTEROECKER, P. & GUNZ, P. 2009. Advances in geometric morphometrics. *Evolutionary Biology*, 36, 235-247.
- MITTEROECKER, P., GUNZ, P., BERNHARD, M., SCHAEFER, K. & BOOKSTEIN, F. L. 2004. Comparison of cranial ontogenetic trajectories among great apes and humans. *Journal of Human Evolution*, 46, 679-698.
- MOAZEN, M., CURTIS, N., EVANS, S. E., O'HIGGINS, P. & FAGAN, M. J. 2008. Combined finite element and multibody dynamics analysis of biting in a *Uromastix hardwickii* lizard skull. *Journal of Anatomy*, 213, 499-508.
- MOAZEN, M., CURTIS, N., O'HIGGINS, P., EVANS, S. E. & FAGAN, M. J. 2009a. Biomechanical assessment of evolutionary changes in the lepidosaurian skull. *Proceedings of the National Academy of Sciences*, 106, 8273-8277.
- MOAZEN, M., CURTIS, N., O'HIGGINS, P., JONES, M. E. H., EVANS, S. E. & FAGAN, M. J. 2009b. Assessment of the role of sutures in a lizard skull: a computer modelling study. *Proceedings of the Royal Society B: Biological Sciences*, 276, 39-46.
- MONTEIRO, L. R. 1999. Multivariate regression models and geometric morphometrics: the search for causal factors in the analysis of shape. *Systematic Biology*, 48, 192-199.
- MONTEIRO, L. R., BONATO, V. & DOS REIS, S. F. 2005. Evolutionary integration and morphological diversification in complex morphological structures: mandible shape divergence in spiny rats (Rodentia, Echimyidae). *Evolution & Development*, 7, 429-439.

- MONTEIRO, L. R., LESSA, L. G. & ABE, A. S. 1999. Ontogenetic variation in skull shape of *Thrichomys apereoides* (Rodentia: Echimyidae). *Journal of Mammalogy*, 80, 102-111.
- MOORE, S. W. 2003. Scrambled eggs: mechanical forces as ecological factors in early development. *Evolution & Development*, 5, 61-66.
- MOORE, W. 1967. Muscular function and skull growth in the laboratory rat (*Rattus norvegicus*). *Journal of Zoology*, 152, 287-296.
- MORENO, K., WROE, S., CLAUSEN, P., MCHENRY, C., D'AMORE, D. C., RAYFIELD, E. J. & CUNNINGHAM, E. 2008. Cranial performance in the Komodo dragon (*Varanus komodoensis*) as revealed by high-resolution 3-D finite element analysis. *Journal of Anatomy*, 212, 736-746.
- MORRIS-KAY, G. M. & WILKIE, A. O. M. 2005. Growth of the normal skull vault and its alteration in craniosynostosis: insights from human genetics and experimental studies. *Journal of Anatomy*, 207, 637-653.
- MOSLEY, J. R. 2000. Osteoporosis and bone functional adaptation: mechanobiological regulation of bone architecture in growing and adult bone, a review. *Journal of Rehabilitation Research and Development*, 37, 189-199.
- MOSLEY, J. R. & LANYON, L. E. 1998. Strain rate as a controlling influence on adaptive modeling in response to dynamic loading of the ulna in growing male rats. *Bone*, 23, 313-318.
- MOSS, M. L. & SALENTIJN, L. 1971. Differences between the functional matrices in anterior open-bite and in deep overbite. *American Journal of Orthodontics*, 60, 264-280.
- MULLENDER, M. & HUISKES, R. 1997. Osteocytes and bone lining cells: Which are the best candidates for mechano-sensors in cancellous bone? *Bone*, 20, 527-532.
- MÜLLER, G. B. 2003. Embryonic motility: environmental influences and evolutionary innovation. *Evolution & Development*, 5, 56-60.
- MÜLLER, G. B. & WAGNER, G. P. 1996. Homology, Hox genes, and developmental integration. *American Zoologist*, 36, 4-13.
- MURPHY, R. A. & BEARDSLEY, A. C. 1974. Mechanical properties of the cat soleus muscle in situ. *American Journal of Physiology*, 227, 1008-1013.
- MURRAY, P. D. F. 1936. *Bones, a study of the development and structure of the vertebrate skeleton.*, Cambridge, Cambridge University Press.
- MURRAY, P. D. F. & HUXLEY, J. S. 1925. Self-differentiation in the grafted limb-bud of the chick. *Journal of Anatomy*, 59, 379-384.
- NAGY, A. 2000. Cre recombinase: The universal reagent for genome tailoring. *Genesis*, 26, 99-109.
- NAKASHIGE, M., SMITH, A. L. & STRAIT, D. S. 2011. Biomechanics of the macaque postorbital septum investigated using finite element analysis: implications for anthropoid evolution. *Journal of Anatomy*, 218, 142-150.
- NAKASHIMA, T., HAYASHI, M. & TAKAYANAGI, H. 2012. New insights into osteoclastogenic signaling mechanisms. *Trends in Endocrinology & Metabolism*, 23, 582-590.
- NICHOLSON, E. K., STOCK, S. R., HAMRICK, M. W. & RAVOSA, M. J. 2006. Biomineralization and adaptive plasticity of the temporomandibular joint in myostatin knockout mice. *Archives of Oral Biology*, 51, 37-49.
- NIES, M. & YOUNG RO, J. 2004. Bite force measurement in awake rats. *Brain Research Protocols*, 12, 180-185.

- NIVEN, J. S. F. 1933. The development in vivo and in vitro of the avian patella. *Development Genes and Evolution*, 128, 480-501.
- NODEN, D. M. & TRAINOR, P. A. 2005. Relations and interactions between cranial mesoderm and neural crest populations. *Journal of Anatomy*, 207, 575-601.
- NORDSTROM, S., BISHOP, M. & YEMM, R. 1974. The effect of jaw opening on the sarcomere length of the masseter and temporal muscles of the rat. *Archives of Oral Biology*, 19, 151-155.
- NORDSTROM, S. & YEMM, R. 1974. The relationship between jaw position and isometric active tension produced by direct stimulation of the rat masseter muscle. *Archives of Oral Biology*, 19, 353-359.
- NOWAK, R. M. & PARADISO, J. L. 1991. *Walker's Mammals of the World*, Cambridge Univ Press.
- O'CONNOR, C. F., FRANCISCUS, R. G. & HOLTON, N. E. 2005. Bite force production capability and efficiency in Neandertals and modern humans. *American Journal of Physical Anthropology*, 127, 129-151.
- O'HIGGINS, P. 1997. Methodological issues in the description of forms. In: LESTREL, P. E. (ed.) *Fourier Descriptors and their Applications in Biology*. Cambridge: Cambridge University Press
- O'HIGGINS, P. & JONES, N. 1998. Facial growth in *Cercocebus torquatus*: an application of three-dimensional geometric morphometric techniques to the study of morphological variation. *Journal of Anatomy*, 193, 251-272.
- O'HIGGINS, P., COBB, S. N., FITTON, L. C., GRÖNING, F., PHILLIPS, R., LIU, J. & FAGAN, M. J. 2011. Combining geometric morphometrics and functional simulation: an emerging toolkit for virtual functional analyses. *Journal of Anatomy*, 218, 3-15.
- OFFERMANS, M. & DE VREE, F. 1989. Morphology of the masticatory apparatus in the springhare, *Pedetes capensis*. *Journal of Mammalogy*, 70, 701-711.
- OLIVARES, A. I., VERZI, D. H. & VASSALLO, A. I. 2004. Masticatory morphological diversity and chewing modes in South American caviomorph rodents (family Octodontidae). *Journal of Zoology*, 263, 167-177.
- OLSON, E. C. & MILLER, R. L. 1958. *Morphological Integration*.
- ONAR, V. & GÜNEŞ, H. L. 2003. On the variability of skull shape in German shepherd (Alsatian) puppies. *The Anatomical Record Part A: Discoveries in Molecular, Cellular, and Evolutionary Biology*, 272, 460-466.
- OPPERMAN, L. A. 2000. Cranial sutures as intramembranous bone growth sites. *Developmental Dynamics*, 219, 472-485.
- ORBAN, P. C., CHUI, D. & MARTH, J. D. 1992. Tissue- and site-specific DNA recombination in transgenic mice. *Proceedings of the National Academy of Sciences*, 89, 6861-6865.
- ORKIN, R. W., PRATT, R. M. & MARTIN, G. R. 1976. Undersulfated chondroitin sulfate in the cartilage matrix of brachymorphic mice. *Developmental Biology*, 50, 82-94.
- ORR, H. A. 2000. Adaptation and the cost of complexity. *Evolution*, 54, 13-20.
- OVCHINNIKOV, D. A., DENG, J. M., OGUNRINU, G. & BEHRINGER, R. R. 2000. Col2a1-directed expression of Cre recombinase in differentiating chondrocytes in transgenic mice. *Genesis*, 26, 145-146.
- OYEN, O., WALKER, A. & RICE, R. 1979. Craniofacial growth in olive baboons (*Papio cynocephalus anubis*): browridge formation. *Growth*, 43, 174-187.

- PADILLA, D. K. & ADOLPH, S. C. 1996. Plastic inducible morphologies are not always adaptive: the importance of time delays in a stochastic environment. *Evolutionary Ecology*, 10, 105-117.
- PANAGIOTOPOULOU, O., KUPCZIK, K. & COBB, S. N. 2011. The mechanical function of the periodontal ligament in the macaque mandible: a validation and sensitivity study using finite element analysis. *Journal of Anatomy*, 218, 75-86.
- PAPHANGKORAKIT, J. & OSBORN, J. W. 1997. Effect of jaw opening on the direction and magnitude of human incisal bite forces. *Journal of Dental Research*, 76, 561-567.
- PARFITT, A. 1997. Genetic effects on bone mass and turnover-relevance to black/white differences. *Journal of the American College of Nutrition*, 16, 325-333.
- PARSONS, T. E., KRISTENSEN, E., HORNUNG, L., DIEWERT, V. M., BOYD, S. K., GERMAN, R. Z. & HALLGRÍMSSON, B. 2008. Phenotypic variability and craniofacial dysmorphology: increased shape variance in a mouse model for cleft lip. *Journal of Anatomy*, 212, 135-143.
- PATEL, N. G. 1978. Functional morphology of the masticatory muscles of *Mus musculus*. *Proceedings of the Indian Academy of Sciences*, 87b (Animal Sciences), 51-57.
- PECK, C. C., LANGENBACH, G. E. J. & HANNAM, A. G. 2000. Dynamic simulation of muscle and articular properties during human wide jaw opening. *Archives of Oral Biology*, 45, 963-982.
- PÉREZ-BARBERÍA, F. J. & GORDON, I. J. 1999. The functional relationship between feeding type and jaw and cranial morphology in ungulates. *Oecologia*, 118, 157-165.
- PERLYN, C. A., DELEON, V. B., BABBS, C., GOVIER, D., BURELL, L., DARVANN, T., KREIBORG, S. & MORRISS-KAY, G. 2006. The craniofacial phenotype of the crouzon mouse: analysis of a model for syndromic craniosynostosis using three-dimensional microCT. *The Cleft Palate-Craniofacial Journal*, 43, 740-748.
- PERRY, J. M. & WALL, C. E. 2008. Scaling of the chewing muscles in prosimians. In: VINYARD, C. J., RAVOSA, M. J. & WALL, C. E. (eds.) *Primate craniofacial function and biology*. New York: Springer.
- PERRY, J. M. G. 2008. *The anatomy of mastication in extant strepsirrhines and Eocene adapines*, ProQuest.
- PETTE, D. & STARON, R. S. 1990. *Cellular and molecular diversities of mammalian skeletal muscle fibers*, Springer.
- PIGLIUCCI, M. 2001. *Phenotypic plasticity: beyond nature and nurture*, Johns Hopkins University Press.
- PIGLIUCCI, M. 2003. Phenotypic integration: studying the ecology and evolution of complex phenotypes. *Ecology Letters*, 6, 265-272.
- PIGLIUCCI, M. & PRESTON, K. 2004. *Phenotypic integration: studying the ecology and evolution of complex phenotypes*, Oxford, Oxford University Press.
- POLANSKI, J. M. 2011. Morphological integration of the modern human mandible during ontogeny. *International Journal of Evolutionary Biology*, 2011.

- POLANSKI, J. M. & FRANCISCUS, R. G. 2006. Patterns of craniofacial integration in extant Homo, Pan, and Gorilla. *American Journal of Physical Anthropology*, 131, 38-49.
- POMIKAL, C. & STREICHER, J. 2010. 4D-analysis of early pelvic girdle development in the mouse (*Mus musculus*). *Journal of Morphology*, 271, 116-126.
- POWELL, P. L., ROY, R. R., KANIM, P., BELLO, M. A. & EDGERTON, V. R. 1984. Predictability of skeletal muscle tension from architectural determinations in guinea pig hindlimbs. *Journal of Applied Physiology*, 57, 1715-1721.
- PREUSCHOFT, H. & WITZEL, U. 2002. Biomechanical investigations on the skulls of reptiles and mammals. *Senckenbergiana Lethaea*, 82, 207-222.
- RAADSHEER, M., VAN EIJDEN, T., VAN GINKEL, F. & PRAHL-ANDERSEN, B. 1999. Contribution of jaw muscle size and craniofacial morphology to human bite force magnitude. *Journal of Dental Research*, 78, 31-42.
- RADINSKY, L. 1985a. Patterns in the evolution of ungulate jaw shape. *American Zoologist*, 25, 303-314.
- RADINSKY, L. B. 1981a. Evolution of skull shape in carnivores: 1. Representative modern carnivores. *Biological Journal of the Linnean Society*, 15, 369-388.
- RADINSKY, L. B. 1981b. Evolution of skull shape in carnivores: 2. Additional modern carnivores. *Biological Journal of the Linnean Society*, 16, 337-355.
- RADINSKY, L. B. 1982. Evolution of skull shape in carnivores. 3. The origin and early radiation of the modern carnivore families. *Paleobiology*, 8, 177-195.
- RADINSKY, L. B. 1985b. Approches in Evolutionary Morphology: A Search for Patterns. *Annual Review of Ecology and Systematics*, 16, 1-14.
- RAFF, E. C. & RAFF, R. A. 2000. Dissociability, modularity, evolvability. *Evolution & Development*, 2, 235-237.
- RAFF, R. A. 1996. The shape of life: genes, development, and the evolution of animal form.
- RAFF, R. A. & KAUFMAN, T. C. 1991. *Embryos, genes, and evolution: the developmental-genetic basis of evolutionary change*, Indiana University Press.
- RAFF, R. A. & SLY, B. J. 2000. Modularity and dissociation in the evolution of gene expression territories in development. *Evolution & Development*, 2, 102-113.
- RAJEWSKY, K., GU, H., KUHN, R., BETZ, U. A., MULLER, W., ROES, J. & SCHWENK, F. 1996. Conditional gene targeting. *The Journal of Clinical Investigation*, 98, 600-3.
- RAMAESH, T. & BARD, J. B. L. 2003. The growth and morphogenesis of the early mouse mandible: a quantitative analysis. *Journal of Anatomy*, 203, 213-222.
- RAUCH, F. & SCHOENAU, E. 2001. The developing bone: slave or master of its cells and molecules? *Pediatric Research*, 50, 309-314.
- RAVOSA, M. 1991. The ontogeny of cranial sexual dimorphism in two old world monkeys: *Macaca fascicularis* (Cercopithecinae) and *Nasalis larvatus* (Colobinae). *International Journal of Primatology*, 12, 403-426.
- RAVOSA, M., NING, J., COSTLEY, D., DANIEL, A., STOCK, S. & STACK, M. 2010. Masticatory biomechanics and masseter fiber-type plasticity. *Journal of Musculoskeletal & Neuronal Interactions*, 10, 46-55.

- RAVOSA, M. J. 1990. Functional assessment of subfamily variation in maxillomandibular morphology among old World monkeys. *American Journal of Physical Anthropology*, 82, 199-212.
- RAVOSA, M. J. 1996. Jaw morphology and function in living and fossil Old World monkeys. *International Journal of Primatology*, 17, 909-932.
- RAVOSA, M. J. & DANIEL, A. N. 2010. Ontogeny and phyletic size change in living and fossil lemurs. *American Journal of Primatology*, 72, 161-172.
- RAVOSA, M. J. & HYLANDER, W. L. 1994. Function and fusion of the mandibular symphysis in primates: stiffness or strength. *Anthropoid origins*, 447-468.
- RAVOSA, M. J., JOHNSON, K. R. & HYLANDER, W. L. 2000. Strain in the galago facial skull. *Journal of Morphology*, 245, 51-66.
- RAVOSA, M. J., LOPEZ, E. K., MENEGAZ, R. A., STOCK, S. R., STACK, M. S. & HAMRICK, M. W. 2008a. Adaptive plasticity in the mammalian masticatory complex: you are what, and how, you eat. *Primate Craniofacial Function and Biology*. Springer.
- RAVOSA, M. J., LÓPEZ, E. K., MENEGAZ, R. A., STOCK, S. R., STACK, M. S. & HAMRICK, M. W. 2008b. Using “Mighty Mouse” to understand masticatory plasticity: myostatin-deficient mice and musculoskeletal function. *Integrative and Comparative Biology*, 48, 345-359.
- REDUKER, D. W. 1983. Functional analysis of the masticatory apparatus in two species of *Myotis*. *Journal of Mammalogy*, 277-286.
- REED, D. A., PORRO, L. B., IRIARTE-DIAZ, J., LEMBERG, J. B., HOLLIDAY, C. M., ANAPOL, F. & ROSS, C. F. 2011. The impact of bone and suture material properties on mandibular function in *Alligator mississippiensis*: testing theoretical phenotypes with finite element analysis. *Journal of Anatomy*, 218, 59-74.
- RENAUD, S., AUFFRAY, J. & DE LA PORTE, S. 2010. Epigenetic effects on the mouse mandible: common features and discrepancies in remodeling due to muscular dystrophy and response to food consistency. *BMC Evolutionary Biology*, 10, 1471-2148.
- RENAUD, S. & MICHAUX, J. R. 2007. Mandibles and molars of the wood mouse, *Apodemus sylvaticus*: integrated latitudinal pattern and mosaic insular evolution. *Journal of Biogeography*, 34, 339-355.
- RENAUD, S., PANTALACCI, S., QUÉRÉ, J.-P., LAUDET, V. & AUFFRAY, J.-C. 2009. Developmental constraints revealed by co-variation within and among molar rows in two murine rodents. *Evolution & Development*, 11, 590-602.
- RICHARD, B. & WAINWRIGHT, P. 1995. Scaling the feeding mechanism of largemouth bass (*Micropterus salmoides*): kinematics of prey capture. *Journal of Experimental Biology*, 198, 419-433.
- RICHTSMEIER, J. T., ZUMWALT, A., CARLSON, E. J., EPSTEIN, C. J. & REEVES, R. H. 2002. Craniofacial phenotypes in segmentally trisomic mouse models for Down syndrome. *American Journal of Medical Genetics*, 107, 317-324.
- RIEDL, R. 1977. A systems-analytical approach to macro-evolutionary phenomena. *Quarterly Review of Biology*, 351-370.
- RINKER, G. C. 1954. The comparative myology of the mammalian genera *Sigmodon*, *Oryzomys*, *Neotoma*, and *Peromyscus* (Cricetinae), with remarks

- on their intergeneric relationships. *Miscellaneous Publications Museum Zoology University of Michigan*, 83, 1-124.
- RINKER, G. C. & HOOPER, E. T. 1950. Notes on the cranial musculature in two subgenera of *Reithrodontomys* (harvest mice). *Occasional Papers of the Museum of Zoology, University of Michigan*, 528, 1-11.
- ROBERTS, L. H. 1975. The functional anatomy of the rodent larynx in relation to audible and ultrasonic cry production. *Zoological Journal of the Linnean Society*, 56, 255-264.
- ROBINS, M. W. 1977. Biting loads generated by the laboratory rat. *Archives of Oral Biology*, 22, 43-47.
- ROHLF, F. J. 1996. Morphometric spaces, shape components and the effects of linear transformations. In: MARCUS, L. F. (ed.) *Advances in morphometrics* New York: Plenum Press.
- ROHLF, F. J. & CORTI, M. 2000. Use of two-block partial least-squares to study covariation in shape. *Systematic Biology*, 49, 740-753.
- ROHLF, F. J. & SLICE, D. 1990. Extensions of the Procrustes method for the optimal superimposition of landmarks. *Systematic Biology*, 39, 40-59.
- ROSEMAN, C. C., WEAVER, T. D. & STRINGER, C. B. 2011. Do modern humans and Neandertals have different patterns of cranial integration? *Journal of Human Evolution*, 60, 684-693.
- ROSS, C. & HENNEBERG, M. 1995. Basicranial flexion, relative brain size, and facial kyphosis in *Homo sapiens* and some fossil hominids. *American Journal of Physical Anthropology*, 98, 575-593.
- ROSS, C. F., PATEL, B. A., SLICE, D. E., STRAIT, D. S., DECHOW, P. C., RICHMOND, B. G. & SPENCER, M. A. 2005. Modeling masticatory muscle force in finite element analysis: sensitivity analysis using principal coordinates analysis. *The Anatomical Record Part A: Discoveries in Molecular, Cellular, and Evolutionary Biology*, 283, 288-299.
- ROSS, C. F. & RAVOSA, M. J. 1993. Basicranial flexion, relative brain size, and facial kyphosis in nonhuman primates. *American Journal of Physical Anthropology*, 91, 305-324.
- ROSSANT, J. & MCMAHON, A. 1999. "Cre"-ating mouse mutants—a meeting review on conditional mouse genetics. *Genes & Development*, 13, 142-145.
- ROTH, V. L. 1996. Cranial integration in the Sciuridae. *American Zoologist*, 14-23.
- SACCO, T. & VAN VALKENBURGH, B. 2004. Ecomorphological indicators of feeding behaviour in the bears (Carnivora: Ursidae). *Journal of Zoology*, 263, 41-54.
- SANGER, T. J., MAHLER, D. L., ABZHANOV, A. & LOSOS, J. B. 2012. Roles for modularity and constraint in the evolution of cranial diversity among *Anolis* lizards. *Evolution*.
- SANSAL, I. & SELLERS, W. R. 2004. The biology and clinical relevance of the PTEN tumor suppressor pathway. *Journal of Clinical Oncology*, 22, 2954-2963.
- SANTANA, S. & DUMONT, E. 2009. Connecting behaviour and performance: the evolution of biting behaviour and bite performance in bats. *Journal of Evolutionary Biology*, 22, 2131-2145.
- SANTANA, S. E., DUMONT, E. R. & DAVIS, J. L. 2010. Mechanics of bite force production and its relationship to diet in bats. *Functional Ecology*, 24, 776-784.

- SATOH, K. 1997. Comparative functional morphology of mandibular forward movement during mastication of two murid rodents, *Apodemus speciosus* (Murinae) and *Clethrionomys rufocanus* (Arvicolinae). *Journal of Morphology*, 231, 131-142.
- SATOH, K. 1998. Balancing function of the masticatory muscles during incisal biting in two murid rodents, *Apodemus speciosus* and *Clethrionomys rufocanus*. *Journal of Morphology*, 236, 49-56.
- SATOH, K. 1999. Mechanical advantage of area of origin for the external pterygoid muscle in two murid rodents, *Apodemus speciosus* and *Clethrionomys rufocanus*. *Journal of Morphology*, 240, 1-14.
- SATOH, K. & IWAKU, F. 2004. Internal architecture, origin-insertion, and mass of jaw muscles in Old World hamsters. *Journal of Morphology*, 260, 101-116.
- SATOH, K. & IWAKU, F. 2006. Jaw muscle functional anatomy in northern grasshopper mouse, *Onychomys leucogaster*, a carnivorous murid. *Journal of Morphology*, 267, 987-999.
- SATOH, K. & IWAKU, F. 2009. Structure and direction of jaw adductor muscles as herbivorous adaptations in *Neotoma mexicana* (Muridae, Rodentia). *Zoomorphology*, 128, 339-348.
- SCHAERLAEKEN, V., HOLANOVA, V., BOISTEL, R., AERTS, P., VELENSKY, P., REHAK, I., ANDRADE, D. V. & HERREL, A. 2012. Built to bite: feeding kinematics, bite forces, and head shape of a specialized durophagous lizard, *Dracaena guianensis* (teiidae). *Journal of Experimental Zoology Part A: Ecological Genetics and Physiology*, 317, 371-381.
- SCHEINER, S. M. 1993. Genetics and evolution of phenotypic plasticity. *Annual Review of Ecology and Systematics*, 35-68.
- SCHIAFFINO, S. & REGGIANI, C. 1996. Molecular diversity of myofibrillar proteins: gene regulation and functional significance. *Physiological Reviews*, 76, 371-423.
- SCHIAFFINO, S. & REGGIANI, C. 2011. Fiber types in mammalian skeletal muscles. *Physiological reviews*, 91, 1447-1531.
- SCHLICHTING, C. D. & PIGLIUCCI, M. 1998. *Phenotypic evolution: a reaction norm perspective*, Sinauer Associates Incorporated.
- SCHLOSSER, G. & WAGNER, G. P. 2004. *Modularity in Development and Evolution*, Chicago, University of Chicago Press.
- SCHLUTER, D. 1996. Adaptive radiation along genetic lines of least resistance. *Evolution*, 1766-1774.
- SCIOTE, J. J. & MORRIS, T. J. 2000. Skeletal muscle function and fibre types: the relationship between occlusal function and the phenotype of jaw-closing muscles in human. *Journal of Orthodontics*, 27, 15-30.
- SEARS, K., GOSWAMI, A., FLYNN, J. & NISWANDER, L. 2007. The correlated evolution of Runx2 tandem repeats, transcriptional activity, and facial length in Carnivora. *Evolution & Development*, 9, 555-565.
- SEEMAN, E. & DELMAS, P. D. 2006. Bone quality—the material and structural basis of bone strength and fragility. *New England Journal of Medicine*, 354, 2250-2261.
- SHARON, B. E. & RADINSKY, L. 1980. Functional analysis of Sabertooth cranial morphology. *Paleobiology*, 6, 295-312.

- SHELTON, G. D., CARDINET, G. H. & BANDMAN, E. 1988. Expression of fiber type specific proteins during ontogeny of canine temporalis muscle. *Muscle & Nerve*, 11, 124-132.
- SHIDA, T., ABE, S., SAKIYAMA, K., AGEMATSU, H., MITARASHI, S., TAMATSU, Y. & IDE, Y. 2005. Superficial and deep layer muscle fibre properties of the mouse masseter before and after weaning. *Archives of Oral Biology*, 50, 65-71.
- SHIRAI, L. T. & MARROIG, G. 2010. Skull modularity in neotropical marsupials and monkeys: size variation and evolutionary constraint and flexibility. *Journal of Experimental Zoology Part B: Molecular and Developmental Evolution*, 314, 663-683.
- SILBERMANN, M. & FROMMER, J. 1972. The nature of endochondral ossification in the mandibular condyle of the mouse. *The Anatomical Record*, 172, 659-667.
- SINGH, N., HARVATI, K., HUBLIN, J.-J. & KLINGENBERG, C. P. 2011. Morphological evolution through integration: A quantitative study of cranial integration in *Homo*, *Pan*, *Gorilla* and *Pongo*. *Journal of Human Evolution*.
- SKERRY, T., O'HIGGINS, P. & COHN, M. Biomechanical influences on skeletal growth and development. Linnean Society Symposium Series, 2000. 29-40.
- SLICE, D. E. 2001. Landmark coordinates aligned by Procrustes analysis do not lie in Kendall's shape space. *Systematic Biology*, 61, 157-171.
- SLICE, D. E. 2007. Geometric morphometrics. *Annual Review of Anthropology*, 36, 261-281.
- SMITH, J. M. & SAVAGE, R. J. G. 1956. Some locomotory adaptations in mammals. *Journal of the Linnean Society of London, Zoology*, 42, 603-622.
- SMITH, M. M. & HALL, B. K. 1990. Development and evolutionary origins of vertebrate skeletogenic and odontogenic tissues. *Biological Reviews*, 65, 277-373.
- SMITH, R. J. 1984. Comparative functional morphology of maximum mandibular opening (gape) in primates. *Food Acquisition and Processing in Primates*. Springer.
- SOMMERFELDT, D. & RUBIN, C. 2001. Biology of bone and how it orchestrates the form and function of the skeleton. *European Spine Journal*, 10, S86-S95.
- SPECTOR, J. A., GREENWALD, J. A., WARREN, S. M., BOULETREAU, P. J., DETCH, R. C., FAGENHOLZ, P. J., CRISERA, F. E. & LONGAKER, M. T. 2002. Dura mater biology: Autocrine and paracrine effects of fibroblast growth factor 2. *Plastic and Reconstructive Surgery*, 109, 645-654.
- SRINIVASAN, S., WEIMER, D. A., AGANS, S. C., BAIN, S. D. & GROSS, T. S. 2002. Low-magnitude mechanical loading becomes osteogenic when rest is inserted between each load cycle. *Journal of Bone and Mineral Research*, 17, 1613-1620.
- STAYTON, C. T. 2006. Testing hypotheses of convergence with multivariate data: morphological and functional convergence among herbivorous lizards. *Evolution*, 60, 824-841.
- STORCH, G. 1968. Funktionsmorphologische Untersuchungen an der Kaumuskulatur und an korrelierten Schaedelstrukturen der Chiropteren. *Abhandlungen der Senckenbergischen Naturforschenden Gesellschaft*, 517, 1-92.

- STRAIT, D. S. 2001. Integration, phylogeny, and the hominid cranial base. *American Journal of Physical Anthropology*, 114, 273-297.
- STRAIT, D. S., RICHMOND, B. G., SPENCER, M. A., ROSS, C. F., DECHOW, P. C. & WOOD, B. A. 2007. Masticatory biomechanics and its relevance to early hominid phylogeny: an examination of palatal thickness using finite-element analysis. *Journal of Human Evolution*, 52, 585.
- STRAIT, D. S., WEBER, G. W., NEUBAUER, S., CHALK, J., RICHMOND, B. G., LUCAS, P. W., SPENCER, M. A., SCHREIN, C., DECHOW, P. C. & ROSS, C. F. 2009. The feeding biomechanics and dietary ecology of *Australopithecus africanus*. *Proceedings of the National Academy of Sciences*, 106, 2124-2129.
- SWIDERSKI, D. & ZELDITCH, M. 2010. Morphological diversity despite isometric scaling of lever arms. *Evolutionary Biology*, 37, 1-18.
- TAKAYANAGI, H. 2007. Osteoimmunology: shared mechanisms and crosstalk between the immune and bone systems. *Nature Reviews Immunology*, 7, 292-304.
- TANNER, J. B., ZELDITCH, M. L., LUNDRIGAN, B. L. & HOLEKAMP, K. E. 2010. Ontogenetic change in skull morphology and mechanical advantage in the spotted hyena (*Crocuta crocuta*). *Journal of Morphology*, 271, 353-365.
- TAYLOR, A. 2006. Feeding behavior, diet, and the functional consequences of jaw form in orangutans, with implications for the evolution of Pongo. *Journal of Human Evolution*, 50, 377-393.
- TAYLOR, A. B., ENG, C. M., ANAPOL, F. C. & VINYARD, C. J. 2009. The functional correlates of jaw-muscle fiber architecture in tree-gouging and nongouging callitrichid monkeys. *American Journal of Physical Anthropology*, 139, 353-367.
- TAYLOR, A. B., JONES, K. E., KUNWAR, R. & RAVOSA, M. J. 2006. Dietary consistency and plasticity of masseter fiber architecture in postweaning rabbits. *The Anatomical Record Part A: Discoveries in Molecular, Cellular, and Evolutionary Biology*, 288A, 1105-1111.
- TAYLOR, A. B. & VINYARD, C. J. 2004. Comparative analysis of masseter fiber architecture in tree-gouging (*Callithrix jacchus*) and non-gouging (*Saguinus oedipus*) callitrichids. *Journal of Morphology*, 261, 276-285.
- THEXTON, A. & HIIEMAE, K. M. 1975. The twitch-contraction characteristics of opossum jaw musculature. *Archives of Oral Biology*, 20, 743-748.
- THOMAS, R. D. 2005. Hierarchical integration of modular structures in the evolution of animal skeletons. *Modularity: Understanding the Development and Evolution of Natural Complex Systems*, 239-258.
- THOMASON, J. 1991a. Cranial strength in relation to estimated biting forces in some mammals. *Canadian Journal of Zoology*, 69, 2326-2333.
- THOMASON, J., RUSSELL, A. & MORGELI, M. 1990. Forces of biting, body size, and masticatory muscle tension in the opossum *Didelphis virginiana*. *Canadian Journal of Zoology*, 68, 318-324.
- THOMASON, J. J. 1991b. Cranial strength in relation to estimated biting forces in some mammals. *Canadian Journal of Zoology*, 69, 2326-2333.
- THORINGTON, R. K. & DARROW, K. 1996. Jaw muscles of Old World squirrels. *Journal of Morphology*, 230, 145-165.
- THOROGOOD, P. 1993. Differentiation and morphogenesis of cranial skeletal tissues. *The Skull*, 1, 112-152.

- THROCKMORTON, G. S., FINN, R. A. & BELL, W. H. 1980. Biomechanics of differences in lower facial height. *American Journal of Orthodontics*, 77, 410-420.
- THROCKMORTON, G. S. & THROCKMORTON, L. S. 1985. Quantitative calculations of temporomandibular joint reaction forces—I. The importance of the magnitude of the jaw muscle forces. *Journal of Biomechanics*, 18, 445-452.
- TOBIN, J. L., DI FRANCO, M., EICHERS, E., MAY-SIMERA, H., GARCIA, M., YAN, J., QUINLAN, R., JUSTICE, M. J., HENNEKAM, R. C., BRISCOE, J., TADA, M., MAYOR, R., BURNS, A. J., LUPSKI, J. R., HAMMOND, P. & BEALES, P. L. 2008. Inhibition of neural crest migration underlies craniofacial dysmorphology and Hirschsprung's disease in Bardet-Biedl syndrome. *A*, 105, 6714-6719.
- TOYE, A., LIPPIAT, J., PROKS, P., SHIMOMURA, K., BENTLEY, L., HUGILL, A., MIJAT, V., GOLDSWORTHY, M., MOIR, L. & HAYNES, A. 2005. A genetic and physiological study of impaired glucose homeostasis control in C57BL/6J mice. *Diabetologia*, 48, 675-686.
- TSAI, H. P. & HOLLIDAY, C. M. 2011. Ontogeny of the Alligator *Cartilago transiliens* and its significance for sauropsid jaw muscle evolution. *PLoS ONE*, 6, e24935.
- TSENG, Z. J. 2009. Cranial function in a late Miocene *Dinocrocuta gigantea* (Mammalia: Carnivora) revealed by comparative finite element analysis. *Biological Journal of the Linnean Society*, 96, 51-67.
- TSUMAKI, N. & YOSHIKAWA, H. 2005. The role of bone morphogenetic proteins in endochondral bone formation. *Cytokine & Growth Factor Reviews*, 16, 279-285.
- TURKAWSKI, S. & VAN EIJDEN, T. 2001. Mechanical properties of single motor units in the rabbit masseter muscle as a function of jaw position. *Experimental Brain Research*, 138, 153-162.
- TURNBULL, W. D. 1970. Mammalian masticatory apparatus. *Fieldiana: Geology*, 18, 149-356.
- TURNER, C., ROBLING, A., DUNCAN, R. & BURR, D. 2002. Do bone cells behave like a neuronal network? *Calcified Tissue International*, 70, 435-442.
- TUXEN, A. & KIRKEBY, S. 1990. An animal model for human masseter muscle: Histochemical characterization of mouse, rat, rabbit, cat, dog, pig, and cow masseter muscle. *Journal of Oral and Maxillofacial Surgery*, 48, 1063-1067.
- UL HAQUE, M. F., KING, L. M., KRAKOW, D., CANTOR, R. M., RUSINIAK, M. E., SWANK, R. T., SUPERTI-FURGA, A., HAQUE, S., ABBAS, H., AHMAD, W., AHMAD, M. & COHN, D. H. 1998. Mutations in orthologous genes in human spondyloepimetaphyseal dysplasia and the brachymorphic mouse. *Nature Genetics*, 20, 157-62.
- USAMI, A., ABE, S. & IDE, Y. 2003. Myosin heavy chain isoforms of the murine masseter muscle during pre-and post-natal development. *Anatomia, Histologia, Embryologia*, 32, 244-248.
- VAN CAKENBERGHE, V., HERREL, A. & AGUIRRE, L. 2002. Evolutionary relationships between cranial shape and diet in bats (Mammalia: Chiroptera). *In: AERTS, P., D'AOUT, K., HERREL, A. & VAN DAMME, R. (eds.) Topics in functional and ecological vertebrate morphology*. Maastricht: Shaker Publishing.

- VAN DER MEULEN, M. C. & HUISKES, R. 2002. Why mechanobiology?: A survey article. *Journal of Biomechanics*, 35, 401-414.
- VAN RUIJVEN, L. & WEIJS, W. 1990. A new model for calculating muscle forces from electromyograms. *European Journal of Applied Physiology and Occupational Physiology*, 61, 479-485.
- VANHOODYDONCK, B., BOISTEL, R., FERNANDEZ, V. & HERREL, A. 2011. Push and bite: trade-offs between burrowing and biting in a burrowing skink (*Acontias percivali*). *Biological Journal of the Linnean Society*, 102, 91-99.
- VANHOODYDONCK, B., HERREL, A., VAN DAMME, R., MEYERS, J. J. & IRSCHICK, D. J. 2005. The relationship between dewlap size and performance changes with age and sex in a green anole (*Anolis carolinensis*) lizard population. *Behavioral Ecology and Sociobiology*, 59, 157-165.
- VECCHIONE, L., BYRON, C., COOPER, G. M., BARBANO, T., HAMRICK, M. W., SCIOTE, J. J. & MOONEY, M. P. 2007. Craniofacial morphology in myostatin-deficient mice. *Journal of Dental Research*, 86, 1068-1072.
- VELHAGEN, W. A. & ROTH, V. L. 1997. Scaling of the mandible in squirrels. *Journal of Morphology*, 232, 107-132.
- VINCENT, S. E., MOON, B. R., HERREL, A. & KLEY, N. J. 2007. Are ontogenetic shifts in diet linked to shifts in feeding mechanics? Scaling of the feeding apparatus in the banded watersnake *Nerodia fasciata*. *Journal of Experimental Biology*, 210, 2057-2069.
- VINYARD, C., YAMASHITA, N. & TAN, C. 2004. Maximum bite forces among three sympatric Haplemur species at Ranomafana National Park, Madagascar. *Journal of Morphology*, 260, 338.
- VINYARD, C. J. 2008. Putting shape to work: making functional interpretations of masticatory apparatus shapes in primates. *Primate Craniofacial Function and Biology*. Springer.
- VINYARD, C. J. & RAVOSA, M. J. 1998. Ontogeny, function, and scaling of the mandibular symphysis in papionin primates. *Journal of Morphology*, 235, 157-175.
- VINYARD, C. J., WALL, C. E., WILLIAMS, S. H. & HYLANDER, W. L. 2003. Comparative functional analysis of skull morphology of tree-gouging primates. *American Journal of Physical Anthropology*, 120, 153-170.
- VISAGEIMAGING 2008. Amira 5.2.0. Berlin.
- WAGNER, G. 1990. A comparative study of morphological integration in *Apis mellifera* (Insecta, Hymenoptera). *Journal of Zoological Systematics and Evolutionary Research*, 28, 48-61.
- WAGNER, G. P. 1996. Homologues, natural kinds and the evolution of modularity. *American Zoologist*, 36, 36-43.
- WAGNER, G. P. & ALTENBERG, L. 1996. Perspective: Complex adaptations and the evolution of evolvability. *Evolution*, 967-976.
- WAGNER, G. P., BOOTH, G. & BAGHERI-CHAICHIAN, H. 1997. A population genetic theory of canalization. *Evolution*, 329-347.
- WAGNER, G. P. & MEZEY, J. 2004. The role of genetic architecture constraints in the origin of variational modularity. *Modularity in Development and Evolution*, 338-358.
- WAGNER, G. P., PAVLICEV, M. & CHEVERUD, J. M. 2007a. The road to modularity. *Nat Rev Genet*, 8, 921-931.

- WAGNER, G. P., PAVLICEV, M. & CHEVERUD, J. M. 2007b. The road to modularity. *Nature Reviews Genetics*, 8, 921-931.
- WAINWRIGHT, P. C., BELLWOOD, D. R., WESTNEAT, M. W., GRUBICH, J. R. & HOEY, A. S. 2004. A functional morphospace for the skull of labrid fishes: patterns of diversity in a complex biomechanical system. *Biological Journal of the Linnean Society*, 82, 1-25.
- WAINWRIGHT, P. C. & REILLY, S. M. 1994. *Ecological morphology: integrative organismal biology*, University of Chicago Press.
- WAINWRIGHT, P. C. & RICHARD, B. A. 1995. Predicting patterns of prey use from morphology of fishes. *Ecomorphology of fishes*. Springer.
- WALKER, D. G. 1972. Enzymatic and electron microscopic analysis of isolated osteoclasts. *Calcified Tissue Research*, 9, 296-309.
- WANG, Q., WRIGHT, B. W., SMITH, A., CHALK, J. & BYRON, C. D. 2010. Mechanical impact of incisor loading on the primate midfacial skeleton and its relevance to human evolution. *The Anatomical Record*, 293, 607-617.
- WANG, X. & MAO, J. 2002a. Chondrocyte proliferation of the cranial base cartilage upon in vivo mechanical stresses. *Journal of Dental Research*, 81, 701-705.
- WANG, X. & MAO, J. J. 2002b. Accelerated chondrogenesis of the rabbit cranial base growth plate by oscillatory mechanical stimuli. *Journal of Bone and Mineral Research*, 17, 1843-1850.
- WAYNE, R. K. 1986. Cranial morphology of domestic and wild canids: the influence of development on morphological change. *Evolution*, 40, 243-261.
- WEBER, G. W. & BOOKSTEIN, F. L. 2011. *Virtual anthropology: a guide to a new interdisciplinary field*, Springer.
- WEIJS, W. & DANTUMA, R. 1975a. Electromyography and mechanics of mastication in the albino rat. *Journal of Morphology*, 146, 1-33.
- WEIJS, W. A. 1973. Morphology of the muscles of mastication in the Albino Rat, *Rattus norvegicus* (Berkenhout, 1769). *Acta Morphol Neerl-Scand*, 11, 321-340.
- WEIJS, W. A. 1975. Mandibular movements of the albino rat during feeding. *Journal of Morphology*, 145, 107-124.
- WEIJS, W. A. & DANTUMA, R. 1975b. Electromyography and mechanics of mastication in the albino rat. *Journal of Morphology*, 146, 1-33.
- WEST-EBERHARD, M. J. 1989. Phenotypic plasticity and the origins of diversity. *Annual Review of Ecology and Systematics*, 20, 249-278.
- WEST-EBERHARD, M. J. 2003. *Developmental Plasticity and Evolution*, New York, Oxford University Press.
- WEST-EBERHARD, M. J. 2005. Phenotypic accommodation: adaptive innovation due to developmental plasticity. *Journal of Experimental Zoology Part B: Molecular and Developmental Evolution*, 304, 610-618.
- WESTNEAT, M. 1994. Transmission of force and velocity in the feeding mechanisms of labrid fishes (Teleostei, Perciformes). *Zoomorphology*, 114, 103-118.
- WESTNEAT, M. W. 2003. A biomechanical model for analysis of muscle force, power output and lower jaw motion in fishes. *Journal of Theoretical Biology*, 223, 269-281.
- WESTNEAT, M. W. 2004. Evolution of levers and linkages in the feeding mechanisms of fishes. *Integrative and Comparative Biology*, 44, 378-389.

- WILEY, D. F. 2005. Landmark. 3.0.0.6 ed.: Institute for Data Analysis and Visualisation.
- WILEY, D. F., AMENTA, N., ALCANTARA, D. A., GHOSH, D., KIL, Y. J., DELSON, E., HARCOURT-SMITH, W., ROHLF, F. J., ST JOHN, K. & HAMANN, B. Evolutionary morphing. *Visualization*, 2005. VIS 05. IEEE, 23-28 Oct. 2005 2005. 431-438.
- WILKIE, A. O. & MORRISS-KAY, G. M. 2001. Genetics of craniofacial development and malformation. *Nature Reviews Genetics*, 2, 458-468.
- WILLIAMS, P. & GOLDSPINK, G. 1978. Changes in sarcomere length and physiological properties in immobilized muscle. *Journal of Anatomy*, 127, 459.
- WILLIAMS, P. E. & GOLDSPINK, G. 1971. Longitudinal growth of striated muscle fibres. *Journal of Cell Science*, 9, 751-767.
- WILLIAMS, S. H., PEIFFER, E. & FORD, S. 2009. Gape and Bite Force in the Rodents *Onychomys leucogaster* and *Peromyscus maniculatus*: Does Jaw-Muscle Anatomy Predict Performance? . *Journal of Morphology*, 270, 1338-1347.
- WILLMORE, K. E., LEAMY, L. & HALLGRÍMSSON, B. 2006a. Effects of developmental and functional interactions on mouse cranial variability through late ontogeny. *Evolution & Development*, 8, 550-567.
- WILLMORE, K. E., ROSEMAN, C. C., ROGERS, J., CHEVERUD, J. M. & RICHTSMEIER, J. T. 2009. Comparison of mandibular phenotypic and genetic integration between baboon and mouse. *Evolutionary Biology*, 36, 19-36.
- WILLMORE, K. E., ZELDITCH, M. L., YOUNG, N., AH-SENG, A., LOZANOFF, S. & HALLGRÍMSSON, B. 2006b. Canalization and developmental stability in the Brachyrrhine mouse. *Journal of Anatomy*, 208, 361-372.
- WIRKNER, C. S. & PRENDINI, L. 2007. Comparative morphology of the hemolymph vascular system in scorpions—A survey using corrosion casting, MicroCT, and 3D-reconstruction. *Journal of Morphology*, 268, 401-413.
- WIRKNER, C. S. & RICHTER, S. 2004. Improvement of microanatomical research by combining corrosion casts with MicroCT and 3D reconstruction, exemplified in the circulatory organs of the woodlouse. *Microscopy Research and Technique*, 64, 250-254.
- WOLD, H. 1966. Estimation of principal components and related models by iterative least squares. *Multivariate analysis*, 1, 391-420.
- WOOD, A. E. 1965. Grades and clades among rodents. *Evolution*, 19, 115-130.
- WOODS, C. A. 1972. Comparative myology of jaw, hyoid, and pectoral appendicular regions of New and Old world hystricomorph rodents. *Bulletin of the American Museum of Natural History*, 147, 115-198.
- WOODS, C. A. & HERMANSON, J. W. 1985. Myology of hystricognath rodents: an analysis of form, function, and phylogeny. In: LUCKETT, E. W. O. & HARTENBERGER, J. L. (eds.) *Evolutionary relationships among rodents*. New York: Plenum Press.
- WOODS, C. A. & HOWLAND, E. B. 1979. Adaptive radiation of capromyid rodents: anatomy of the masticatory apparatus. *Journal of Mammalogy*, 60, 95-116.

- WROE, S., FERRARA, T. L., MCHENRY, C. R., CURNOE, D. & CHAMOLI, U. 2010. The craniomandibular mechanics of being human. *Proceedings of the Royal Society B: Biological Sciences*, 277, 3579-3586.
- WROE, S., MCHENRY, C. & THOMASON, J. 2005. Bite club: comparative bite force in big biting mammals and the prediction of predatory behaviour in fossil taxa. *Proceedings of the Royal Society B: Biological Sciences*, 272, 619-625.
- WROE, S. & MILNE, N. 2007. Convergence and remarkably consistent constraint in the evolution of carnivore skull shape. *Evolution*, 61, 1251-1260.
- WROE, S., MORENO, K., CLAUSEN, P., MCHENRY, C. & CURNOE, D. 2007. High-resolution three-dimensional computer simulation of Hominid cranial mechanics. *The Anatomical Record*, 290, 1248-1255.
- WUTZL, A., BROZEK, W., LERNBASS, I., RAUNER, M., HOFBAUER, G., SCHOPPER, C., WATZINGER, F., PETERLIK, M. & PIETSCHMANN, P. 2006. Bone morphogenetic proteins 5 and 6 stimulate osteoclast generation. *Journal of Biomedical Materials Research Part A*, 77, 75-83.
- YAMADA, M., KOGA, Y., OKAYASU, I., SANEFUJI, K., YAMADA, Y., OI, K. & YOSHIDA, N. 2006. Influence of soft diet feeding on development of masticatory function. *The Journal of Japanese Society of Stomatognathic Function*, 12, 118-125.
- YOON, B. S. & LYONS, K. M. 2004. Multiple functions of BMPs in chondrogenesis. *Journal of Cellular Biochemistry*, 93, 93-103.
- YOSHIKAWA, T. & SUZUKI, T. 1969. The comparative anatomical study of the masseter of the mammal (3). *Anatomischer Anzeiger*, 125, 363-387.
- YOUNG, A. & BANNASCH, D. 2006. Morphological variation in the dog. *Cold Spring Harbor Monograph Archive*, 44, 47-65.
- YOUNG, R. L. & BADYAEV, A. V. 2007. Evolution of ontogeny: linking epigenetic remodeling and genetic adaptation in skeletal structures. *Integrative and Comparative Biology*, 47, 234-244.
- YOUNG, R. L., HASELKORN, T. S. & BADYAEV, A. V. 2007. Functional equivalence of morphologies enables morphological and ecological diversity. *Evolution*, 61, 2480-2492.
- YOUNG, R. L., SWEENEY, M. J. & BADYAEV, A. V. 2010. Morphological diversity and ecological similarity: versatility of muscular and skeletal morphologies enables ecological convergence in shrews. *Functional Ecology*, 24, 556-565.
- YU, J. C., LUCAS, J. H., FRYBERG, K. & BORKE, J. L. 2001. Extrinsic tension results in FGF-2 release, membrane permeability change, and intracellular Ca⁺⁺ increase in immature cranial sutures. *Journal of Craniofacial Surgery*, 12, 391-398.
- ZELDITCH, M., SWIDERSKI, D., SHEETS, D. H. & FINK, W. 2004a. *Geometric Morphometrics for Biologists: A Primer*, San Diego, Academic Press
- ZELDITCH, M. L. 1987. Evaluating models of developmental integration in the laboratory rat using confirmatory factor analysis. *Systematic Biology*, 36, 368-380.
- ZELDITCH, M. L. 1988. Ontogenetic variation in patterns of phenotypic integration in the laboratory rat. *Evolution*, 28-41.

- ZELDITCH, M. L. & CARMICHAEL, A. C. 1989. Ontogenetic variation in patterns of developmental and functional integration in skulls of *Sigmodon fulviventer*. *Evolution*, 43, 814-824.
- ZELDITCH, M. L., LUNDRIGAN, B. L. & GARLAND, T. 2004b. Developmental regulation of skull morphology. I. Ontogenetic dynamics of variance. *Evolution & Development*, 6, 194-206.
- ZELDITCH, M. L., STRANEY, D. O., SWIDERSKI, D. L. & CARMICHAEL, A. C. 1990. Variation in developmental constraints in *Sigmodon*. *Evolution*, 44, 1738-1747.
- ZELDITCH, M. L., WOOD, A. R., BONETT, R. M. & SWIDERSKI, D. L. 2008. Modularity of the rodent mandible: integrating bones, muscles, and teeth. *Evolution & Development*, 10, 756-768.
- ZOLLIKOFER, C. P. E. & PONCE DE LEON, M. S. 2002. Visualizing patterns of craniofacial shape variation in *Homo sapiens*. *Proceedings of the Royal Society of London. Series B: Biological Sciences*, 269, 801-807.